CELL METABOLISM IN RESPONSE TO BIOMATERIAL MECHANICS

Enateri Vera Alakpa

(BSc (Hons), MRes)

Submitted in fulfilment of requirements for the degree of Doctor of Philosophy

Centre for Cell Engineering

Institute of Molecular, Cell and Systems Biology

School of Medical, Veterinary and Life Sciences

University of Glasgow

October 2013.

ABSTRACT

This project assessed the use of short chain peptide (F_2/S) hydrogel biomaterial substrates as an instructional tool for driving stem cell differentiation through fine-tuning of the substrate mechanical properties (altered elasticity or stiffness) to mimic that of naturally occurring tissue types. By doing this, differentiation of mesenchymal stem cells (MSCs) into neuronal cells on a 2 kPa (soft) substrate, chondrocytes on 6 kPa (medium) substrate and osteoblasts on 38 kPa (rigid) substrates was achieved.

This non-invasive procedure of influencing stem cell behaviour allows a means of exploring innate cell behaviour as they adopt different cell lineages on differentiation. As such, an LC-MS based metabolomics study was used to profile differences in cell behaviour. Stem cells were observed as having increased metabolic activity when undergoing differentiation compared to their 'resting' state when they are observed as metabolically quiescent or relatively inactive. As such, the metabolome, as a reflection of the current state of cell metabolism, was used to illustrate the observed divergence of phenotypes as differentiation occurs on each substrate F_2/S type.

The project further investigated the potential of endogenous small molecules (metabolites) identified using metabolomics, as effective compounds in driving or supporting cell differentiation *in vitro*. From this, the compounds cholesterol sulphate and sphinganine were found to induce MSC differentiation along the osteogenic and neurogenic routes respectively. A third compound, GP18:0, was observed to have influence on promoting both osteo- and chondrogenic development. These results highlight the potential role a broad based metabolomics study plays in the identification of endogenous metabolites and ascertaining the role(s) they play in cellular differentiation and subsequent tissue development. Lastly, the use of F_2/S substrates as a potential clinical scaffold for the regeneration of cartilage tissue was explored. Long term differentiation of pericytes into chondrocytes cultured in 20 kPa F_2/S substrates was assessed and the cellular phenotype of the resultant chondrocytes compared to the more conventionally used induction media method. Pericytes cultured within the biomaterial alone showed a balanced expressed of type II collagen and aggrecan with lessened type X collagen expression compared to the coupled use of induction media which showed a bias towards collagen (both type II and type X) gene expression. This observation suggests that in order to mimic native hyaline cartilage tissue *in vitro*, the use of biomaterial mechanics is potentially a better approach in guiding stem cell differentiation than the use of chemical cues.

CONTENTS

LIST OF FIGURES

LIST OF TABLES

ACKNOWLEDGEMENTS

My Papi, Mami and my little big family - for their patience and the freedoms given me to dare wherever and whenever I care. There is no better gift.

I half expected the sun would come out today, or the rain would come down in droves. Perhaps my mood would be lighter and the ever-scowling postman might crack a smile. Something, no matter how small, unusual would happen to mark today. As it turned out, it was cloudy all day with rain lingering in the shadows. My mood is no lighter and the postmans face is stuck that way. It is, unsurprisingly, the epitome of an average day. So instead of lauding something special, I will be grateful for all that contributes to my perception of an average day. Because it is the built in steadfastness and dependency that has made them days on which I can completely and utterly rely.

My supervisors: Matthew Dalby, Karl Burgess and Rein Ulijn. I am particularly grateful to Matt for a lot but especially for tempering my uncertainty and cynism with huge doses (probably now almost exhausted) of 'Dalby optimism'. I feel obliged to explain my bouts of sudden silences and strange looks were mostly due to me wondering if a human being is truly that optimistic or if it's just a job requisite. Thank you for not being like me.

My non-supervisory mentors: Vineetha Jayawarna, Monica Tsimbouri, Mathis Riehle and Carol-Anne Smith; you have saved my bacon more times than I care to admit - so you'll never know. Thank you all the same.

To everyone at CCE, I am particularly grateful that I managed to be comfortable enough with each and every one of you to not worry if the next sentence that came out of my mouth made me sound like a two-headed alien. Especially to the few I shared an office with - I don't envy you having to put up with my face.

I have to say thank you to Thomas Macartney for holding me together, literally sometimes, making sure I was never too far gone and having more than enough faith to give when mine own was spent.

Jojo for lunches and brunches spent moaning, grumbling and realising that we're on the road to crazyville. How well we'll fit in there!!! It was definitely time away that was desperately needed. We should do lunch soon.

.

AUTHORS' DECLARATION

The work presented in this thesis was performed solely by the author except where the assistance of others has been acknowledged.

Enateri Alakpa, October 2013

ABSTRACTS AND PUBLICATIONS

Poster presentations

Tissue & cell engineering society annual meeting. 4th – 6th July, 2012. University of Liverpool, UK.*
E., V., Alakpa, V., Jayawarna, K., Burgess, R., Ulijn & M., J., Dalby. Characterisation of peptide biomaterials & innate metabolites that direct stem cell differentiation in vitro. European Cell & Materials Journal. 2012; 23 (supplement 4); 50.

EuPA/BSPR proteomics congress. 9th – 12th July, 2012. Glasgow Royal Concert Hall, Glasgow, UK.
E., V., Alakpa, V., Jayawarna, K., Burgess, R., Ulijn & M., J., Dalby. Characterisation of peptide biomaterials & innate metabolites that direct stem cell differentiation *in vitro.*

3rd TERMIS world congress. 5th – 8th September 2012. Hofburg congress centre. Vienna, Austria.
E., V., Alakpa, V., Jayawarna, K., Burgess, R., Ulijn & M., J., Dalby. Development of biomaterials for cellular differentiation using a metabolomics approach. Journal of tissue engineering & regenerative medicine. 2012; 6 (Supplement 1); 238.

Oral presentations

Tissue & cell engineering society annual meeting. 19th – 21st July 2011. University of Leeds, UK.
E., V., Alakpa, V., Jayawarna, K., Burgess, R., Ulijn & M., J., Dalby. Elucidating cellular reaction to biomaterial substrates using a metabolomics approach. European Cell & Materials Journal. 2011; 22 (supplement 3);18.

Glasgow Orthopaedic Research Initiative (GLORI). 22nd October 2012. Southern General Hospital, Glasgow, UK.
E., V., Alakpa. Mesenchymal stem cell differentiation in hydrogels.

Doctoral Training Centre (DTC) Symposium. 7th December 2012. University of Glasgow, UK.
E., V., Alakpa. Effect of substrate mechanics on cellular behaviour.

European Materials Research Society (E-MRS). 27th – 31st May 2013. Congress centre. Strasbourg, France.
E., V., Alakpa. Combining hydrogels with tuned stiffness and metabolomics to identify small molecules that drive mesenchymal stem cell differentiation.

Publications

Using nanotopography and metabolomics to identify biochemical effectors of multipotency.
P. Monica Tsimbouri, Rebecca J. McMurray, Karl V. Burgess, Enateri V. Alakpa, Paul M. Reynolds, Kate Murawski, Emmajayne Kingham, Richard O.C. Oreffo, Nikolaj Gadegaard & Matthew J. Dalby.
ACS Nano. 2012 Nov 27;6 (11):10239-49. doi: 10.1021/nn304046m.

* *Winner – best poster presentation.*

* Preparation procedures for reagents & buffers made in house are detailed in the appendix

ABBREVIATION DEFINITIONS

ACAN	Aggrecan
ADAM	A disintegrin and metalloprotease
ADAMT	A disintegrin and metalloprotease with thrombospondin motifs
ADP	Adenosine diphosphate
ANOVA	Analysis of Variance
ATP	Adenosine triphosphate
BMP	Bone morphogenic protein
BSA	Bovine serum albumin
C3 - C18	Carbon-x, where x is the number of carbons
Cdc42	Cell division control protein 42
cDNA	Complementary DNA
COL10A1	Type X collagen
COL2A1	Type II collagen
DAPI	4’6-diaminodino-2-phenylindole
DMEM	Dulbecco's modified eagles medium
DMSO	Dimethyl sulfoxide
DNA	Deoxyribonucleic acid
ECM	Extracellular matrix
ERK	Extracellular signal regulated kinases
F_2/S	Fmoc-diphenylalanine/serine
FAD	Flavin adenine dinuclotide
FAK	Focal adhesion kinase
FBS	Foetal bovine serum
FITC	Fluorescein isothiocyanate
FMN	Flavin mononucleotide
Fmoc	9-fluorenylmethoxy carbonyl
Fmoc-F_2	Fmoc-diphenylalanine
Fmoc-S	Fmoc-Serine
GAG	Glycosaminoglycans
GAPDH	Glyceraldehyde-3-phosphate dehydrogenase
GFAP	Glial fibrillary acidic protein
GLUT-4	Glucose transporter type 4
GP18:0	1-octadecanoyl-sn-glycero-3-phosphate
GTP	Guanidine triphosphate
HILIC	Hydrophilic liquid interaction chromatography
HMDB	Human metabolome database
KEGG	Kyoto encyclopedia of genes and genomes
kPa	Kilopascal
LC	Liquid chromatography
LC-MS	Liquid chromatography-mass spectrometry
LINC	Linking the nucleus to the cytoskeleton

LPA	Lysophosphatidic acid
MAPK	Mitogen activated protein kinase
MLCK	Myosin light chain kinase
MMP	Matrix metalloproteinase
MS	Mass spectrometry
MSC	Mesenchymal stem cell
NAD/NADH	Nicotine adenine dinucleotide
NADPH	Nicotinamide adenine dinucleotide phosphate
NMM-II	Non-muscle myosin II
OCN	Osteocalcin
OPN	Osteopontin
PBS	Phosphate buffered saline
PCA	Principal component analysis
PCR	Polymerase chain reaction
PEG	Polyethylene glycol
PPAR-γ	Peroxisome proliferator activating receptor-γ
QC	Quality control
qRT-PCR	Quantitative real time polymerase chain reaction
RGD	Arginine-glycine-aspartate
RNA	Ribonucleic acid
ROCK	Rho-associated protein kinase
RUNX-2	Runt related transcription factor 2
SEM	Standard error from the mean
SLRP	Small leucine rich proteoglycan
SOX-9	Sex determining region Y – box 9
StDev	Standard deviation
TGF-β	Transforming growth factor-β
TRITC	Trimethylrhodamine isothiocyanate
UV	Ultraviolet
v/v	Volume per volume
w/v	Weight per volume

1 GENERAL INTRODUCTION

1.1 Regenerative medicine & tissue engineering

Surgical transplantation and reconstruction of damaged tissues and organs due to trauma or disease currently presents a heavy strain on healthcare in terms of both cost and patient aftercare (Kamolz et al., 2013). An increase in life expectancies over the last thirty years and its extrapolation to continue over the immediate future has led to a concomitant rise (and continued anticipation) of the occurrences of tissue trauma such as knee and hip replacements for example (Vaupel, 2010). The subsequent increase in tissue degeneration places high pressure on expectant development of surgical procedures and technologies, which can effectively lead to an understanding and treatment of such traumas.

Current treatment protocols involve the use of autogeneic and allogeneic transplant procedures of either similar or different tissue types to act as scaffolds for would healing. Examples of these are dermal replacements in burn patients and the use of colon to rebuild the oesophagus respectively (Kamolz et al., 2013). Xenogeneic transplant procedures are also widely used, typically employing the use of porcine intestinal mucosa for arterial and venous grafts as well as the use of urinary bladder matrix for reconstruction of urinary tract defects (Badylak, 2004, Benders et al., 2013). Alternatively, non-biological components as scaffolding are also used extensively in orthopaedics, ophthalmology, cardiovascular and reconstructive surgeries in the form of stents and prosthetics.

While surgical procedures for healing or regenerating lost tissue from disease or trauma have brought on significant advances in the field, they are not without their limitations. These are inclusive of lack of biocompatibility, infection, added injury sites from autogenic implantations and scaffold durability. Strategies in tissue engineering aim to find new or improved applications and techniques that overcome the above stated limitations with the design and implementation of efficient biological scaffolds that better integrate with the human body to assist the healing process. And thus, subsequently, alleviate some of the strain compounded by healthcare demands. To do this, a number of different disciplines encompassing engineering, chemistry and the life sciences are integrated in order to enable an understanding of native tissue cells and their interaction with the biomaterial design(s) in order to restore, maintain or enhance tissue integrity and function (Fisher and Mauck, 2013).

1.2 Stem cells

Stem cells are progenitor cells that undergo self-renewal and differentiation into a number of specialised cell lineages. These cell lineages are inclusive of cell types that

make up and sustain functional tissues and organs such as muscle, tendons or bone. Generally, stem cells are categorised either as embryonic or adult. Embryonic stem (ES) cells are derived from the inner cell mass of a blastocyst embryo (Figure 1-1). Adult stem cells originate from already differentiated postnatal tissue and are functional as a regenerative intermediary in cell aging and wound healing (Mimeault and Batra, 2008).

The ability of a stem cell to differentiate into specialised cell types, however, has limitation depending on the cell type and its stage in maturity, inferring a degree of 'plasticity'. These restrictions are also used to classify stem cells according to their differentiation capabilities (Figure 1-1). A morula; early stage embryo, typically consisting of 16 – 32 cells, has the ability to develop into all three human germ layers (ectoderm, mesoderm and endoderm) and the trophoblast which later develops into the placenta. As such, these cells are termed totipotent. Subsequently, the cells of the morula begin to specialise forming the blastocyst; a hollow cellular sphere containing the inner cell mass from which the embryo develops. The cells from the inner cell mass that constitute the embryo and give rise to ES cells are referred to as pluripotent, that is, these cells are able to give rise to most (germ layers) but not all (trophoblast) cells supporting development.

Further down in the hierarchy are adult stem cells, which have a limited scope of differentiation capabilities and are termed multipotent. The differentiation capabilities of these cells are more or less classed further with regards to their originating tissue. For example, neuronal stem cells give rise to neurons, astrocytes & oligodendrocytes; mesenchymal stem cells typically develop into cells of the musculoskeletal system and intestinal stem cells give rise to goblet and enteroendocrine cells. This nomenclature restriction on the multipotent capabilities of adult stem stems however, may not be a true reflection on differentiation competence of most adult stem cells as research over the past years have noted cross-over behaviour of certain stem cells, an ability to form cell types which are not off their native germ layer (transdifferentiation). Examples of these include the ability of mesenchymal stem cells to form endothelial (Petersen et al., 1999, Wong et al., 2007) and neuronal cell types (Sanchez-Ramos et al., 2000, Woodbury et al., 2000), and the development of neural stem cells into early hematopoietic progenitor cells (Bjornson et al., 1999). These observations have led to the argument that a defined hierarchy of stem cell plasticity and niche restriction is not necessarily the case but that stem cells adopt a state or number of states between being an uncommitted and committed cell arguing that stem cell progeny is not a strict lineage but a range of capabilities of a cell based on its stage of commitment (Minguell et al., 2001).

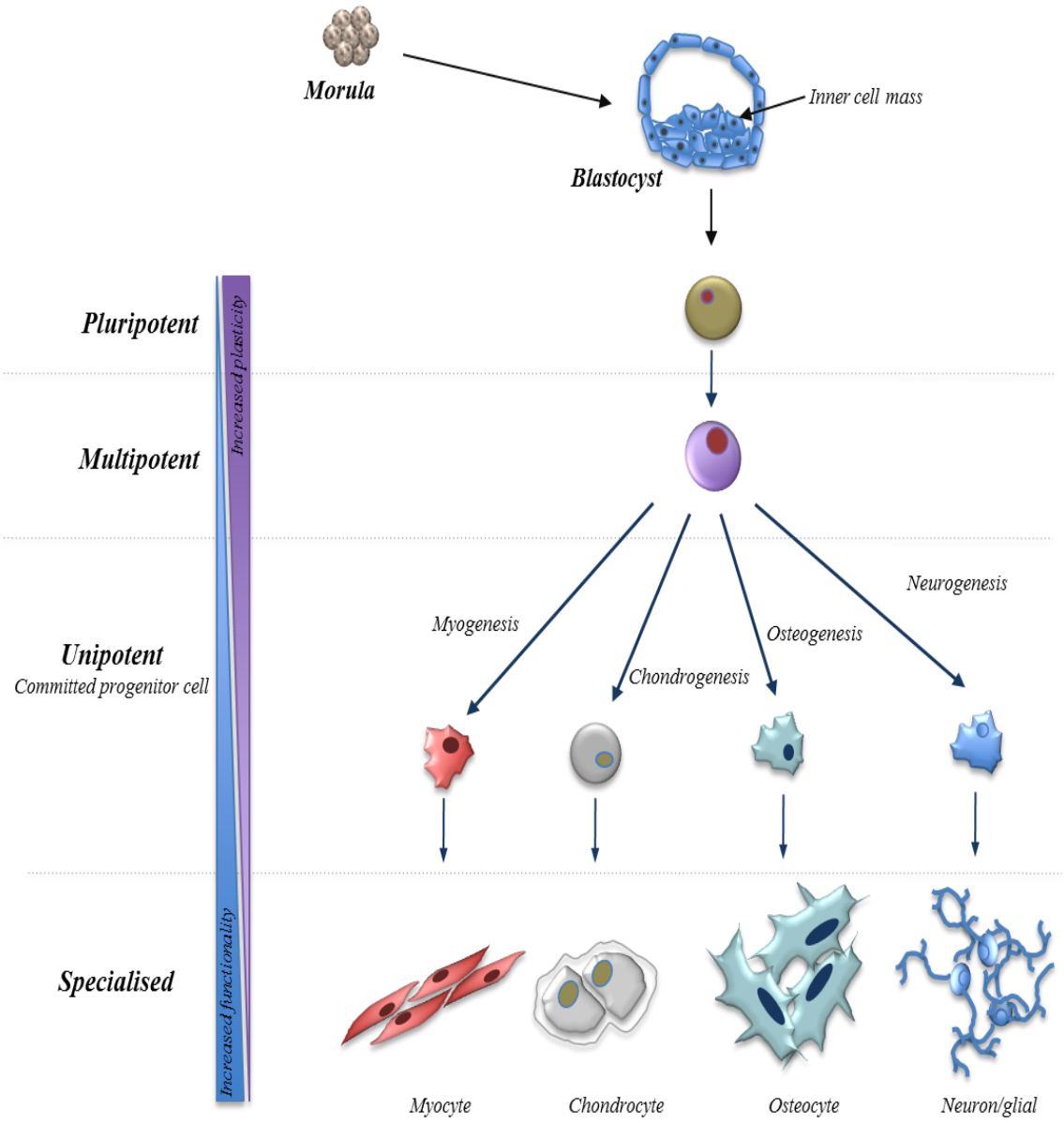

Figure 1-1 Illustration depicting the differentiation potential of stem cells. *The 16-cell morula is capable of differentiating into all cells in the body and is generally referred to as totipotent. Pluripotent cells are embryonic stem cells, which originate from the inner cell mass of the blastocyst and go on to form the cells that make up the 3 germ layers. Adult stem cells are multipotent and differentiation capabilities are more restricted than toti- or pluripotent cell types. As development progresses the relative plasticity of each cell decreases until a specialised cell type is developed.*

The use of adult stem cells in research is of particular attraction as there are less ethical issues surrounding their use, immunomodulatory with the advantage of performing autogeneic implants and they are readily available in comparison to ES cells. Of these, mesenchymal stem cells (typically derived from bone marrow) are an attractive therapeutic tool owing to their relative ease of isolation and expansion in culture as well as their potentially wide application range in tissue engineering strategies.

Nomenclature and identification criteria of mesenchymal stem cells are an element that is somewhat plagued with ambiguity. The former due to the evolving nature of research in the field and the latter due to an incomplete understanding of what exactly a stem cell can be defined by in a physical sense. The observation of colony forming fibroblasts which had osteogenic potential identified by Friedenstein *et al* (Friedenstein et al., 1970, Friedenstein et al., 1987) led to the original name of colony forming unit fibroblasts (CFU-F). This has since evolved into the currently used mesenchymal stem cell (MSC) with a few other connotations still in circulation such as marrow stromal cell (MSC), multipotent adult progenitor cell (MAPC), marrow stromal fibroblasts (MSF) and mesenchymal progenitor cells (MPC). This, however, assumed the primary sources of MSCs were typically from bone marrow and as such, recent use of mesenchyme derived stem cells tend to refer primarily to their origin source, that is, adipose derived stem cells (ASC) or bone marrow derived stem cells (BMSC). This project makes use of bone marrow derived stem cell and is here on referred to in the broad term mesenchymal stem cell or MSC unless stated otherwise.

Undefined characteristics, variation in tissue sources and types have been known to cause some ambiguity in research results using MSC populations. To standardise research findings a minimum requirement for characterising MSCs were put forward by the international society for stem cell therapy (Dominici et al., 2006). These were to define MSC using three main characteristics; adherence to plastic, an ability to differentiate into adipose, cartilage and bone cells (typical mesenchyme lineages) and lastly the expression of the surface antigens CD105, CD73 and CD90 as well as the lack of the surface markers CD45, CD34, CD14 and CD79α. The list of surface markers are by no means restrictive and a number of surface markers in addition to the ones mentioned, reviewed by Tare *et al*, are routinely used to characterise MSC (Tare et al., 2008).

1.2.1 The stem cell niche

The steady state turnover of stem cells, that is, its ability to undergo self renewal or asymmetric division to ensure population survival as opposed to just symmetric division into differentiated cell progeny, is thought to be regulated by the interaction of stem cells with intrinsic properties of its microenvironment leading to the proposal of a stem cell niche by Schofield (Schofield, 1978). In this sense, niche is essentially referred to as the components of the cells surrounding matrix in addition to the emitted signals from supporting cells as opposed to its spatial location (Figure 1-2). These, in cohort, essentially regulate stem cell behaviour determining whether the cells undergo self-renewal or differentiation.

This hypothesis was supported by the subsequent identification of a niche for germ line stem cells in the apical tip of drosophila ovariole (Xie and Spradling, 2000). Studies in mammalian systems resulted in the suggestion of a stem cell niche in the bulge region of hair follicles for epithelial cells (Cotsarelis et al., 1990) and the bottom crypt of the intestine for intestinal stem cells (Sancho et al., 2004). The stem cell niche for mesenchymal stem cells, so far, still remains an unanswered question with regards to both matrix structure and spatial location. Options put forward for the MSC niche include the endosteal of the bone marrow where extrinsic communication between native cells (Calvi et al., 2003, Chow, 2011) and the sinusoidal vessels in the marrow (Katayama et al., 2006) contribute to regulating stem cell phenotype (Bianco, 2011, Ehninger and Trumpp, 2011). An alternative is a perivascular location as a niche *in vivo* where were resident pericyte cells (considered to be a predecessor of MSCs) not only act a cell source for repair but also play functional roles inclusive of regulating blood vessel contraction (Caplan, 2008, Crisan et al., 2008, Meirelles et al., 2008).

A particularly important function of the stem cell niche is also to act as a hub or anchorage point where cell adhesion molecules such as integrins or syndecans couple adhesion states adapted through matrix properties and developmental signalling to tightly regulate stem cell behaviour (Simmons et al., 1997). The regulation of stem cell behaviour by its microenvironment is an important factor in tissue engineering as studies to maintain stem cell multipotency as well as driving differentiation along defined lineages have shown that physical properties such as surface patterning and substrate elasticity (Engler et al., 2006, McMurray et al., 2011) in addition to chemical signalling have considerable consequence on stem cell behaviour *ex vivo,* and as a consequence, the manner and precision in which biomaterials are designed are therefore of vital importance in maintaining or differentiating stem cells (Curran et al., 2010, Gilbert et al., 2010).

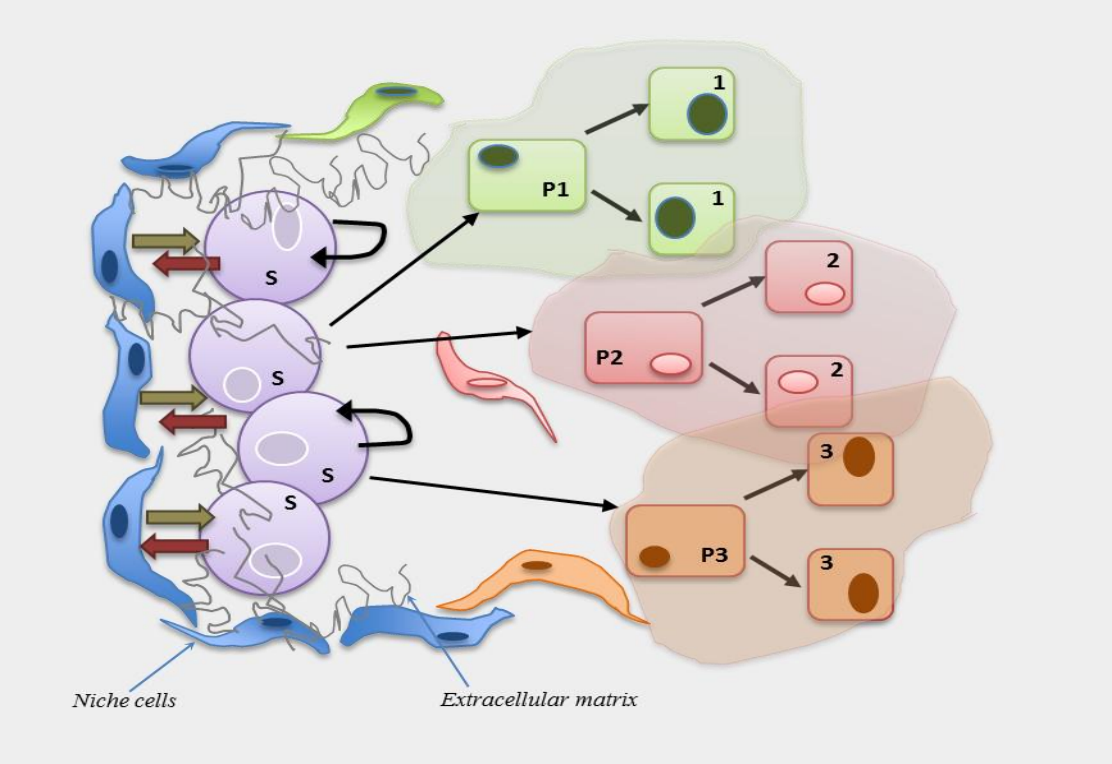

Figure 1-2 Depiction of a stem cell niche. *The stem cell niche is thought to regulate stem cell (S) phenotype through a combination of extrinsic signalling cues (block arrows) between itself, niche cells and the extracellular matrix. Changes in signalling events causes stem cells to undergo self-renewal, symmetrical or asymmetrical division into progenitor cells (P), which subsequently develop into specialised cell types (1 – 3). Image adapted from Watt & Hogan, Science 287. 2000.*

1.3 The extracellular matrix

The extracellular matrix (ECM) is the non-cellular component of all tissues and organs within a system and is referred to as the cellular microenvironment, albeit within in this text the term microenvironment is used in the context in which cells are resident, that is, it is inclusive of the substrate used for cell culturing. The ECM is invariably responsible for the morphological attributes of different tissue types, playing a major role in imparting mechanical strength and scaffolding for cell anchorage and migration (Badylak, 2007, Frantz et al., 2010, Gullberg and Ekblom, 1995).

The design and modelling of the ECM by native cells is a precisely controlled and constantly regulated process to continually support tissue homeostasis in response to changing external conditions. Impairments in this process can result in a number of pathologies such as multiple sclerosis (van Horssen et al., 2007), osteogenesis imperfecta (Bateman et al., 2009) and chronic asthma (Bai et al., 2000).

1.3.1 Architecture

The ECM constitutes mainly a loose meshwork of fibrous proteins, proteoglycans and a host of regulatory molecules such as cytokines and proteolytic enzymes. While these three components are the main facets of the ECM, their design, distribution and architecture are tissue specific facilitated by different cell types resulting in the varied morphology of resultant tissue types. The makeup is designed to withstand the demands of the microenvironment in order to maintain tissue homeostasis, this demand changes at various stages in cell and tissue development and as such the ECM becomes a dynamic entity undergoing constant remodelling and reorganisation by its denizen. To cope with such pressures means that the nature of the ECM is not only tissue specific but possess a degree of heterogeneity within tissues themselves to facilitate proper functionality (Hunziker et al., 2002, Hwang et al., 1992)

1.3.1.1 Fibrillary proteins

Of the fibrous proteins found in the ECM, collagen makes up the major constituent. They comprise a triple helical structure that has high numbers of the polypeptide repeats Gly-X-Y, where X and Y are typically proline and hydroxyproline. Collagen currently has 28 known isoforms (Gordon and Hahn, 2010) resulting mainly from a number of post translational modifications (Gordon and Hahn, 2010, Myllyharju and Kivirikko, 2004) and although in many tissues types, the collagen populations are heterogeneous, usually one form is prevalent, such as type I collagen in bone tissue and type II collagen in cartilage. Type II collagen is also definitive of cartilage type being specific to hyaline cartilage tissue (Responte et al., 2007). The collagens, as a whole, serve to impart tensile and mechanical strength to the tissue as well as directing a number of cell behaviours such as cell polarity (Izu et al., 2011, Thery et al., 2006), adhesion and migration (Rozario et al., 2009).

While collagen is capable of forming supramolecular structures through self-assembly, organisation and assembly is often undertaken by the cell itself thorough integrin interaction and fibronectin cross-linking (Myllyharju and Kivirikko, 2004). This reorganisation causes the arrangement of collagen into sheets or bundled cables significantly affecting the overall tertiary structure and integrity of the tissue.

Fibronectin is another fibrillary element of the ECM and contemporarily acts as a bridge between collagen and cell surface integrins. Fibronectin is secreted from the cell as a loosely folded globular dimer and is unfurled through interaction with the ECM (Engvall et al., 1978), the cell (Friedland et al., 2009) or other fibronectin molecules (Frantz et al., 2010) allowing assembly of fibronectin filaments. Fibronectin repeats contain arginine-

glycine-aspartate (RGD) binding motifs specific to integrin interaction allowing cell adhesion and spreading. Changes in its tensile state, due to constant cellular traction indicate that fibronectin has a fair degree of elasticity (Ohashi et al., 1999). This force dependent extension of fibronectin is thought to expose cryptic cellular binding sites, which can trigger mechanosensory responses (Friedland et al., 2009) mediated through the cytoskeleton.

Elastin is another fibrous ECM protein that is located mainly within tissue types that undergo extensive deformation such as the skin, lungs, arteries and elastic cartilage (located in the external ear and epiglottis) where they ensure recovery imparting a naturally elastic function to the tissue. Elastin is formed from the self-assembly of individual tropoelastin molecules through coacervation. This results in the alignment of lysine residues on tropoelastin, which subsequently undergo conversion by lysyl oxidase (LOX) enzymes to form reactive aldehydes that then form spontaneous desmosine cross-links forming a deformable meshwork (Gosline et al., 2002, Mithieux et al., 2013).

Like fibronectin, elastin also associates with collagen regulating the extent of stretch the filament experiences (Wise and Weiss, 2009) as well as interacting directly with cells via $\alpha_v\beta_3$ integrins (Rodgers and Weiss, 2004).

1.3.1.2 Proteoglycans

Proteoglycans consist of a chain of repeating disaccharide units (glycosaminoglycans, GAGs) covalently linked to a protein core. The GAGs are invariably sulphated moieties: keratin sulphate, chondrotin sulphate and heparin sulphate, with the exception of hyaluronate, which is not sulphated. The high number of sugar groups within GAGs promotes interaction with water molecules making proteoglycans hydrophilic molecules. The attraction of water fills the spaces between collagen fibrils, adopting a hydrogel conformation and allows tissue the ability to resist compressive loads.

ECM proteoglycans are broadly classed into 1) small leucine rich proteoglycan (SLRPs); as well as a structural role, SLRPs are known to be integral in cell signalling events influencing inflammatory responses (Nastase et al., 2012). Experiments using mice having a double gene knockout of the SLRPs biglycan and decorin had shown extensive deformation in bone and dental development (Young et al., 2003) implicating that these proteoglycans have an influential role in functional bone development. This observation has also been confirmed in a number of similar studies (Bianco et al., 1990, Kimoto et al., 1994, Xu et al., 1998). 2) Cell surface proteoglycans such as CD44 and syndecans which act as co-receptors for a wide variety of ligands increasing binding affinity and the strength of adhesion (Carey, 1997, Mythreye and Blobe, 2009) and 3) structural or

modular proteoglycans which regulate physical interactions such as cell adhesion, migration and proliferation.

While the above named components occur extensively throughout the ECM, they are by no means the only components present in the ECM. Laminins and tenascin are also well known ECM components known to play an important role in the structural and functional integrity of the ECM. These are reviewed in papers by the following authors: (Daley et al., 2008, Frantz et al., 2010, Hynes and Naba, 2012).

1.3.2 Dynamics and homeostasis

The molecular components that make up the tissue specific ECM act not only as structural cell support for migration and anchorage but also as signalling cues inducing change in cellular behaviour in order to adapt to the environment and through this, tissue homeostasis (Frantz et al., 2010)

Exposure of the ECM to the 'external', whether chemical or physical factors such as shear, compression or stretch means that the ECM is by no means a static entity and is constantly weathered by external forces and remodelled by native cells making it a highly changeable and dynamic substrate (Colige et al., 1999, Ruangpanit et al., 2002). In cells, ECM production is tempered by proteinase enzyme activity inclusive of matrix metalloprotinases (MMPs) and 'a disintegrin and metalloproteinase with thrombospondin motif' (ADAMTs). MMPs are broad acting degradation proteins which act as collagenases (Ruangpanit et al., 2002, Tocchi and Parks, 2013) but also acts on a number of cell membrane proteins and receptors (Tocchi and Parks, 2013) recycling and remodelling cell surface properties. ADAMTs, on the other hand, tend to act specifically where isoforms like ADAMT2 promote the formation of collagen from procollagen and ADAMTS4 specifically cleaves the GAG aggrecan found in cartilage tissue (Colige et al., 1999, Tortorella et al., 1999).

SLRPs, through their hydrogel properties typically act as a reserve for sequestered growth factors and cytokines immobilising them into the matrix and cleavage of these proteins by MMPs release them to bind with cell receptors. Matrix proteinase activity is tightly regulated and, in general, occurs in response to tissue injury and repair (Chen and Parks, 2009, Gill and Parks, 2008), effectively playing an overall regenerative role in ECM modulation. Albeit, some MMPs are consistently expressed by cells (Tocchi and Parks, 2013), suggesting that they also play a role in general tissue maintenance and homeostasis.

The constant turnover of the ECM through continual probing by the cells has a profound effect on the innate composition of the resultant matrix defining its chemical,

topographical and elastic nature. As the ECM interacts with the cells cytoskeleton via transmembrane integrins (Maniotis et al., 1997) these ECM characteristics have been shown to be powerful instructional cues, eliciting cell responses with regards to polarisation (Thery et al., 2006), alignment (Wood, 1988), migration (Korpos et al., 2010, Wood, 1988), adhesion formation (Schiller, 2013) and differences in stem cell differentiation states (McBeath et al., 2004).

1.3.3 Biomaterial design to emulate the ECM

In order to ascertain the intricacies of cell behaviour and capabilities in tissue engineering, an understanding of cell interactions with the ECM is of fundamental importance. With the intention of replicating innate cell behaviour *ex vivo*, a number of naturally occurring and synthetic substrates have been developed for use in tissue engineering. These aim to cater for a range of demands from being able to support adherence and viability to the more intricately tailored designs geared towards researching a particular hypothesis. These substrates are generally of an instructional nature and include both modifiable and patterned substrates.

The most obvious and convenient source of a cellular scaffold or biomaterial for culturing cells *in vitro* is the use of the ECM itself. The material is designed and produced by cells and by this link, guarantee the primary requisite of biocompatibility. Being designed by the cells, it is also amenable to vascularisation and diffusion of small molecules, which act as a nutrient source to the seeded cells. The use of naturally derived ECM substrate in regenerative medicine has garnered considerable success with most being commercially available, some examples of these are listed in reviews by Badylak (Badylak, 2007) and Dawson (Dawson et al., 2008). Success rates with the use of natural ECM as surgical stents, however, do present with mixed results and this is thought to be due to an averaging effect of use of an efficient, but not necessary optimal, biomaterial.

In addition, reconstituted ECM gels are also widely used in cell culture, materials such as Matrigel and type I collagen, which can be assembled into a fibrillary meshwork with tuneable mechanics that readily supports cell adhesion and proliferation (Kleinman et al., 1982, Levental et al., 2009, Sawkins et al., 2013). The above examples tend to make use of cell culture in three dimensions; surface or two dimensional cell culture, however, has allowed the widespread use of a natural/synthetic hybrid by way of ECM adsorbed polymer surfaces (Dawson et al., 2008). The use of fibronectin, laminin or vitronectin coated surfaces have found widespread use in research applications but are not without their idiosyncrasies. While the three mentioned ECM proteins are able to support cell

adhesion and activity on synthetic surfaces, protein interaction with the biomaterial polymer can develop their own interactions which can lead to changes in protein conformational state and adsorption properties leading to differential cellular interactions both between biomaterial types and from that observed *in vivo* (Bale et al., 1989, Lewandowska et al., 1992).

While these biomaterials have great usefulness in comparative cell studies, their heterogeneity, chemical complexity and alteration in their organisation presents a number of difficulties in providing an instructional tool in the form of a substrate. To achieve a particular outcome from the cell, like directed wound healing for example, it is important that the biomaterial used is able to bias the cell activity towards achieving this aim with minimal interference.

The differential behaviour of protein types used to coat polymer surfaces lead to the characterisation studies where binding kinetics showed that there is an optimal concentration at which cells interact with ECM proteins to facilitate cell adhesion and spreading (Akiyama and Yamada, 1985, Underwood and Bennett, 1989). Studies by Bale *et al* (Bale et al., 1989) had shown that the ECM protein/polymer composition has the tendency to affect the type of proteolytic cleavage that occurs during adsorption. This effect may also account for the varied expression of cellular integrins when cells seeded onto ECM coated polymers (Rezania and Healy, 1999, Sinha and Tuan, 1996).

These noted differential behaviourisms led to strategies to improve the specificity with which cells interact with their ECM, some of these presented in the form of the development and use of biological adhesion motifs on biomaterial surfaces. The identification of specific cell-ECM binding motifs such as the RGD peptide motif present on fibronectin, VPGVG on elastin, IKVAV from laminin and GFOGER from collagen are now commonly used in cell culture studies (Huang et al., 2009, Silva et al., 2004, Zhang et al., 2003a). Immobilisation of these adhesive sites on other inert synthetic polymers allows for precise patterning of the substrate surface, which has enabled studies to show the considerable effect ligand conformation and spatial orientation has on cell behaviour such as integrin clustering (Schiller, 2013), cell polarisation (Thery et al., 2006), migration (Cavalcanti-Adam et al., 2007, Maheshwari et al., 2000) and differentiation (Kilian et al., 2010, McBeath et al., 2004).

In addition to density and spatial orientation of surface ligands, the topographical detail of the cell substrate is known to act as a recognisable instructional cue to elicit specific cell responses. Tissue structures in themselves possess varied topologies from smooth or striated muscle to the roughened surface of trabecular bone. It is likely therefore that

mimicking these patterns *in vitro* can cause behavioural changes in the cells placed within these defined microenvironments to closely match that which occurs *in vivo*.
Integrins, the means by which cells sense their environment, are typically in the size range of 9 – 12 nm in length (Xiong et al., 2001, Xiong et al., 2002) and as such, changes in topographical detail at the nanometre scale can be detected by cells and subsequently elicit powerful cell responses. Examples include the use of near ordered (controlled disorder) nanopits to prompt osteogenesis (Dalby et al., 2007c) and highly ordered nanopits to maintain stem cell phenotype (McMurray et al., 2011), myoblasts cultured on grooved polyacrylamide surfaces were particularly influential in promoting their eventual fusion and striation (Choi et al., 2012b) and MSCs cultured on 15 nm nanopillared titanium surface were observed to optimally promote osteogenic development (McNamara et al., 2011).

While these materials are particularly effective at unravelling the intricacies of the cell-ECM interface, they do not, however, emulate the structure and orientation properties of naturally occurring ECM as a complete entity. Of recent, the use of hydrogels as biomaterials for cell culture has garnered increasing popularity. The use of a cross-linker molecule interspersed in water to create a gel medium is symptomatic of the ECM composition. Cross-linkers include the use of synthetic polymers such as polyacrylamide and polyethylene glycol (PEG) but also the use of peptide moieties that self-assemble to form nanofibres likened to collagen fibres (Gerecht et al., 2007, Jayawarna et al., 2006, Orbach et al., 2009). Relative stiffness of the hydrogel biomaterials can subsequently be tuned by restricting the extent of cross-linking using alterations in pH, temperature or concentration during fabrication. This allows the researcher to maintain a constant chemistry while properties that relate to elasticity can be used to investigate effects on cellular behaviour. Studies employing this approach have shown that the rigidity of a substrate has consequences on properties such as cell survival (Flanagan et al., 2002, Saha et al., 2008), optimal function (Engler et al., 2008, Gilbert et al., 2010, Hoerning et al., 2012) and differentiation lineages adopted by stem cells (Engler et al., 2006, Huebsch et al., 2010, Trappmann et al., 2012).

1.4 Mechanotransduction

Mechanotransduction is the process by which cells sense and convert mechanical stimuli into biochemical activity, resulting in an adaptive response. Cells are exposed to a number of tissue specific physical forces, which range from the shear stress and stretch experienced in blood vessels to compressive loads on skin and bone tissue. In addition

to these external forces, cells themselves exert their own forces acting as probes on their surrounding ECM (Harris et al., 1980). This section focuses on known processes and effects of mechanotransduction as instigated through innate cellular activity.

The phenomenon is initiated at the cell-ECM interface with integrins; transmembrane receptors that facilitate cell adhesion and play an important role in cell sensing and subsequent regulatory behaviour, making them an important link in translating outside information into the cell. This incidence is referred to in some cases as mechanosensing (del Rio et al., 2009, Sawada and Sheetz, 2002, Sawada et al., 2006, Galbraith et al., 2002)

Transductive effects, in some measure, can be immediate such as the activation of ion channels and second messenger activation through mechanical deformation of a number of transmembrane receptors (Evans et al., 1976, Martinac and Hamill, 2002). Others, like integrin clustering, focal adhesion maturation and cytoskeletal contraction and reorganisation occur on a comparatively delayed timescale, which subsequently results in 'larger' changes in cell adaptation such as gene expression and differentiation (Iyer et al., 2012).

Mechanotranductive effects not only instigate particular change(s) in cell behaviour but are also known to contribute to maintaining homeostasis (continuous feedback) on load bearing tissues. Examples include the regulation of bone mass where mechanical loading triggers the release of signalling molecules by osteocytes which in turn regulates osteoblast and osteoclast activity (Klein-Nulend et al., 2013) and in the alignment of collagen fibres, proteoglycan content and cell distribution from the superficial to deep zone of articular cartilage (Hunziker et al., 1997, Hunziker et al., 2002, Responte et al., 2007).

The following sections look into the form and function of constituent parts involved in mechanotransduction and aims to elucidate how these then relate together bringing about a unified response in cell conduct, such as differentiation or migration.

1.4.1 Integrins: form & function

Integrins are heterogeneous transmembrane glycoproteins that comprise α and β subunits. Together they initiate cell-cell and cell-matrix interactions facilitating functions inclusive of anchorage, migration and morphology in adherent cells.

Each subunit comprises a short ovoid cytoplasmic domain and an elongated extracellular domain (tail). The α and β tail units adopt two main conformations; a low affinity state, which is characterised by a folding of the external tail and a high affinity state, where on binding with a ligand, the tail is then extended and the cytoplasmic domains pull apart to

allow binding of focal adhesion proteins (Figure 1-3) (Takagi et al., 2002, Xiao et al., 2004, Xiong et al., 2001, Xiong et al., 2002).

Integrins are tethered to localised focal adhesions via the association of the β subunit with vinculin and α-actinin (Chen et al., 1985, Damsky et al., 1985) providing an extracellular link to the intracellular domain, influencing eventual behavioural outcomes such as cell polarisation (Prager-Khoutorsky et al., 2011, Thery et al., 2006), spreading (Cavalcanti-Adam et al., 2008, Cavalcanti-Adam et al., 2007), migration and cytoskeletal reorganisation (Jiang et al., 2006, Prager-Khoutorsky et al., 2011).

In mammalian cells, integrins comprise 18 α and 8 β subunits (that are known), which can assemble to form 24 different receptors (Hynes, 2002). The variety of these integrin subunits and their diverse range of known interactions with extracellular components make them major players in terms of cell adhesion dynamics, in particular, the role they play in facilitating mechanotransduction where force dependent responses brought on by sensing mechanical stress is a characteristic particular to integrin receptors (Wang and Ingber, 1994, Wang and Ingber, 1995), making them complicit in mechanotransductive events.

These interactions, in turn, have effects on the overall development of the cell as physical matrix characteristics such as substrate elasticity or stiffness are conveyed through force induced contacts. For example, myocytes are able to survive on substrates ranging from relatively soft to hard but only form striated myotubes when cultured on substrates bearing mechanical stiffness resembling its native tissue (Engler et al., 2004b). This cell-ECM interaction also has bearing on the functionality of cells such as myocyte contraction (Engler et al., 2004b), neurite branching (Flanagan et al., 2002, Saha et al., 2008) and hepatocyte aggregation and albumin secretion (Semler, 1999).

At the intracellular domain, individual proteins are recruited to the sight of integrin adhesion where they are known collectively as a focal adhesion. It is at this point where integrins are bridged with the cytoskeleton, the focal adhesion effectively acting as a ‘signalling sensor’ regulating the extent of tensile strength experienced at the transmembrane end (integrin clustering leading to subsequent adhesion strengthening) or within the cytoplasmic domain (cytoskeletal contractility) (Kanchanawong et al., 2010).

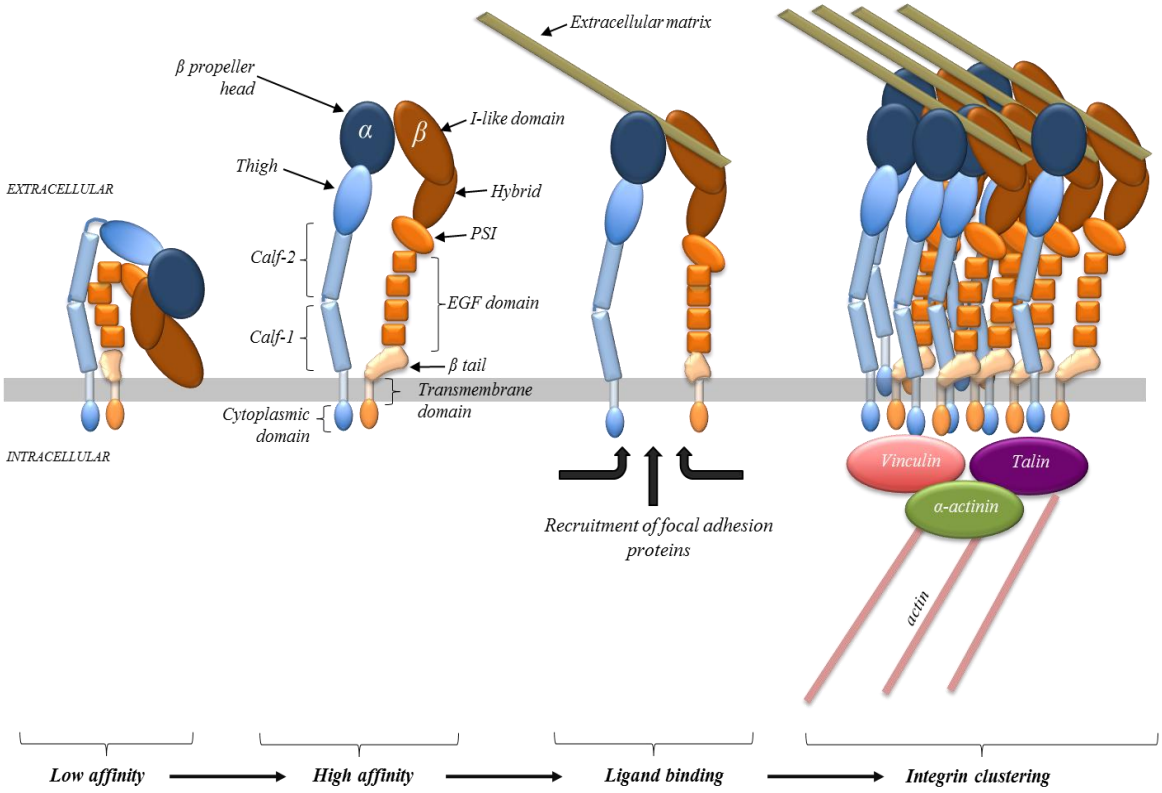

Figure 1-3 Schematic illustrating the transmembrane structure of integrin molecules. *The image shows an integrin pair in its inactive or otherwise low affinity state and active (high affinity) conformation. Activation causes the cytoplasmic α and β subunits to separate facilitating docking of early focal adhesion proteins from which a link between the external and internal is made via the cytoskeleton.*

1.4.2 Focal adhesions

Focal adhesions are protein clusters that form a macro molecular signalling hub, localising with cellular integrins to convey ECM signals intracellularly. Focal adhesions recruit a large number of proteins – currently up to 180+ have been identified (Wolfenson et al., 2013) to perform this function. The numbers of proteins that interact within a focal adhesion suggest that they interpret and regulate a broad range of functions inclusive of migration, cell spreading, proliferation, cell cycle and differentiation.

The diverse functional output means that focal adhesions maintain a state of fluidity where they assemble and disassemble at a high turnover rate with regards to the needs of the cell (Choi et al., 2008, Yu et al., 2011, Zaidel-Bar et al., 2003, Wolfenson, 2009b).

The sizes of focal adhesions depend on a number of factors, such as the cluster of integrins formed from interaction with the substrate and their current state in development as they approach maturity. Nascent focal complexes are small in size (~ 1μm long) and relatively short lived as they are subsequently subjected to further growth

or disassembly (Choi et al., 2008). They are located mainly in the lamellipodia and their formation plays an important role in the leading edge of cell migration while focal adhesion disassembly occurs at the tail end of the cell resulting in polarisation. Focal adhesions by comparison, are larger structures with a longer life span (Beningo et al., 2001) and is generally characterised by the presence of the protein zyxin, as it is present only in mature focal adhesions (Zaidel-Bar et al., 2003).

The influence of external forces or forces applied by the cell to the ECM via integrins induces the growth and eventual maturation of focal adhesions (Figure 1-4). While the exertion of force induces focal adhesion maturation, this process is able to take place over a tensional gradient (Oakes et al., 2012) suggesting a degree of flexibility in cell anchorage. Relative stability and subsequent strengthening of focal adhesions, however, is very much dependent on the tensile strength in actin fibres (Alexandrova et al., 2008) showing that even in stable focal adhesions, structures are constantly turned over to maintain a balanced tensional force in response to external stimuli. A phenomenon that occurs on a time scale spanning seconds (Wolfenson, 2009b, Wolfenson, 2009a).

The network of focal adhesion proteins that interact with cell integrins are classified broadly into two groups: a) Structural proteins – these are proteins that are tethered to integrins, the cytoskeleton or allow docking for the recruitment of subsequent focal adhesion proteins and b) Regulatory proteins – these comprise proteins that are mainly associated with signalling and modulating the activity that occurs within the cell such as GTPases, kinases and phosphatases. However, like most biological systems, these proteins rarely perform a singular function and a degree of overlap exists between both classification groups (Zaidel-Bar, 2009, Zaidel-Bar et al., 2007).

The interaction of α and β integrin subunits with an extracellular ligand brings about a change in conformation to its active state separating the cytoplasmic domains of both subunits exposing binding sites to allow the subsequent assembly of the adhesion network of proteins currently referred to as the adhesome illustrated in Figure 1-5 (Kim et al., 2003, Zaidel-Bar et al., 2007).

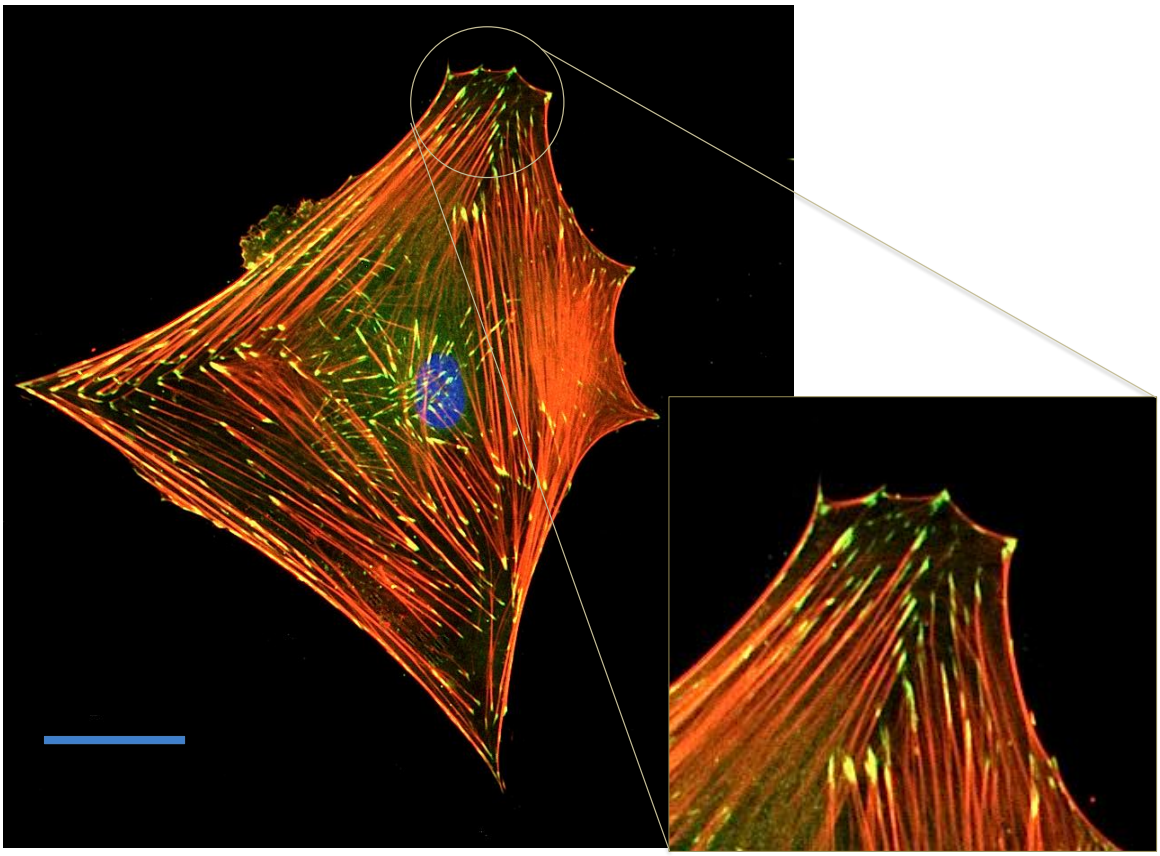

Figure 1-4 Immunofluorescent image of MSCs on glass coverslip showing focal adhesion localisation of vinculin. *Focal adhesions (shown in green) are observed as small projections throughout the cell at the periphery of actin bundles (shown in red). The inset figure shows a close up of the cell edge where smaller focal complexes manifest at the periphery of the cell. Mature adhesions throughout the cell are larger and elongated in comparison. The cell nucleus is also shown in blue. Image courtesy of J. Roberts. Scale bar – 50 µm*

The fluidity of a focal adhesion compounded with the large population of adhesome proteins associated makes its exact mode of assembly and recycling something of an enigma. Nonetheless, focal adhesions have their tell-tale signs and primary constituents such as focal adhesion kinase (FAK), Src and paxillin are ever present in an assembled focal adhesion.

Some, but not all focal adhesion proteins are discussed in the following text, the examples are used to illustrate the dynamic nature of a focal adhesion initiated through the multiple functions and interactions that can be sustained by a single protein molecule. It also, perhaps, gives an insight into the increasing complexity brought on by the aforementioned 180 strong adhesome population; most, if not all, of which are capable of the same functional and structural diversity (Figure 1-5).

Recruitment of FAK, Src and paxillin are needed prior to tyrosine phosphorylation of FAK at the adhesion site initiating ‘activation’ and thus, recruiting further

kinases/phosphatases to the adhesion site (Kirchner et al., 2003). FAK, as well as acting as a signalling protein, also functions as a docking site for other proteins such as paxillin, Src and p130Cas. The presence of FAK within the adhesome plays an important role in the static nature of focal adhesions as its inclusion in a focal adhesion is further enhanced by autophosphorylation (Kwong et al., 2003).

Studies in FAK -/- cells have exhibited enhanced focal adhesions and reduced migration ability (Ilic et al., 1995), implicating a role in adhesion maturity. Contradictorily, phosphorylation of FAK by Src is known to lead to its exclusion from the adhesome (Katz et al., 2003). Reasons put forward for this build up and breakdown by phosphorylation events is that it is thought to be regulated by the specific tyrosine residue that is subject to phosphorylation events ensuring continuous recycling of FAK in and out of a focal adhesion (Wozniak et al., 2004) regulating adhesion strength.

Src acts as a docking protein for FAK and paxillin as well as having catalytic activity on binding with FAK. Loss of Src function showed impaired regulation of focal adhesions likely through lessened tyrosine phosphorylation events (Cary et al., 2002), implicating Src in adhesion co-ordination.

Paxillin, while exhibiting similar phosphorylation and docking activity, is implicit in the activation of small GTPases like Rac, which are active in actin assembly (Lamorte et al., 2003). FAK, FAK-Src and paxillin bind directly to the cytoplasmic domain of either integrin subunit and, in the case of paxillin, inhibit migratory behaviour when bound to an α4 subunit (Arias-Salgado et al., 2003, Cooper et al., 2003, Liu et al., 2002). Their function as a docking point for other proteins also facilitates an indirect link between integrins and the cytoskeleton among other cytoplasmic domains (Kuo, 2013).

Other focal adhesion proteins within the adhesome, however, provide a direct link between integrins and actin filaments. Inclusive of these are filamin, α-actinin and talin. All three proteins are known to bind to β integrin (Calderwood et al., 2001, Greenwood et al., 2000, Pfaff et al., 1998) as well as being implicated in force sensing and adhesion strengthening through integrin clustering (Giannone et al., 2003, von Wichert et al., 2003, Yamazaki et al., 2002). Filamin, through integrin-cytoskeletal interactions has been shown to modulate cell migratory behaviour (Calderwood et al., 2001) while talin is also implicated in protein docking as its presence within a focal adhesion acts as a recruiting site for vinculin (Izard et al., 2004). α-actinin is present in nascent focal adhesions suggesting a role in focal adhesion genesis as well as maintaining cross-links between actin filaments (Greenwood et al., 2000).

Force induced focal adhesion assembly or disassembly regulates the type of adhesion that is eventually adopted (Geiger and Bershadsky, 2002). That is, the size, strength and adhesome of a focal adhesion as a mechanosensor act to maintain the isomeric tensile

state a cell adopts in conjunction with the mechanics of its microenvironment. The formation of focal adhesions in response to mechanical stimulus, inclusive of ECM rigidity, has been chronicled in a number of studies (Balaban et al., 2001, Katz et al., 2000, Riveline et al., 2001).

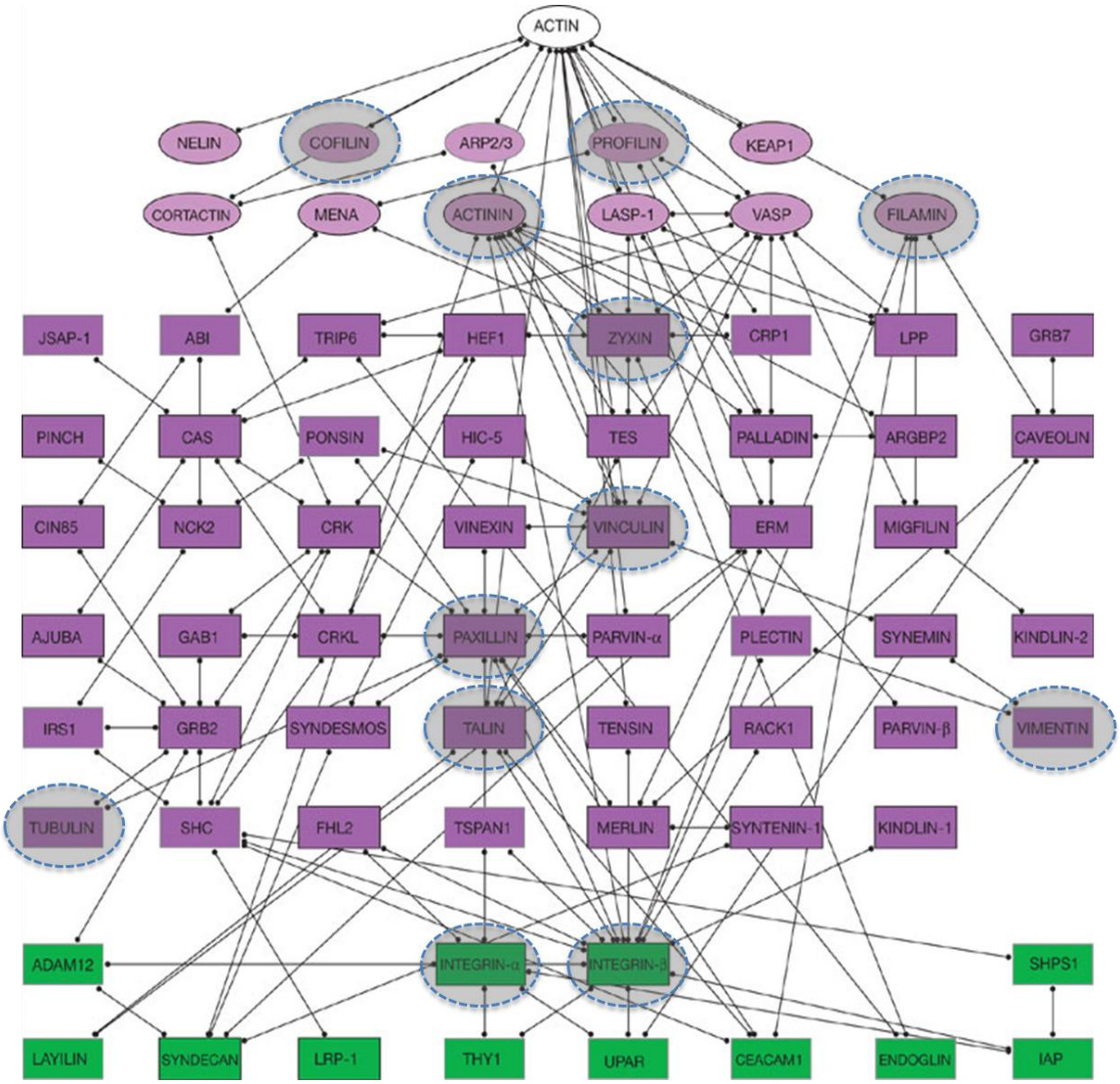

Figure 1-5 Actin-integrin interconnections formed within a focal adhesion. *The illustration shows known physical interacts connecting the cell membrane to the cytoskeleton. The population comprises transmembrane proteins (green), adaptor proteins (purple rectangles), actin modulators (purple ovals) and actin itself at the apex. A chronicle of molecules associated with focal adhesions can be found at www.adhesome.org or referring to (Zaidel-Bar et al., 2007). Molecules mentioned within this thesis are highlighted in dashed ovals. Image adapted from Zaidel-Bar et al., 2007.*

1.4.3 The cytoskeleton

The cytoskeleton is an intricately linked network of fibres that radiate throughout the cell body. It plays a number of diverse functions within the cell from determining structural integrity and withstanding mechanical stresses to facilitating the organisation of the cell acting as a scaffold and trafficking system for transport of small molecules. The cytoskeleton also plays an important role in relaying feed back to the cell eliciting a plethora of adaptive responses that include migration, differentiation and overall metabolism. The cytoskeleton comprises three main features known as microtubules, intermediate filaments and microfilaments.

1.4.3.1 Cytoskeletal elements

Microtubules

Microtubules are hollow filaments made up of polymerized α and β tubulin dimers. Structurally, microtubules radiate outwards from the microtubule organising centre (centrosome) adjacent to the nucleus toward the periphery of the cell (Figure 1-6A). The tubules facilitate the movement of intracellular vesicles and organelles around the cell body as well as acting as a central axis during cell division as the mitotic spindle. Microtubule polymerisation and depolymerisation is a dynamic process facilitated by GTP hydrolysis of both α and β tubulin. As a cytoskeletal component, microtubules also regulate cell shape and play an influential role in facilitating cell migration where they play a role focal adhesion disassembly (Kirchner et al., 2003).

Intermediate filaments

Intermediate filaments, aside from being named for size, differ from the other two cytoskeletal components (microtubules and microfilaments) in that they are not globular assembled filaments but fibrous peptide chains. They are broadly sorted into five categories based on their primary peptide sequences. Type I & II comprise acidic and basic keratin and are localized in epithelial and hair cells, type III constitute vimentin, desmin and glial fibrillary acidic protein (GFAP), type IV are neurofilaments and type V are the nuclear lamins.

Vimentin is the main cytosolic intermediate filament found in cells of mesenchyme lineage (Figure 1-6B). Vimentin maintains the mechanical integrity of the cell forming a mesh like structure whose cross-link density can by altered in the presence of divalent ions (Koester et al., 2010, Qin et al., 2009a, Qin et al., 2009b). For this function, it also exhibits a degree of viscoelasticity and dynamism as it undergoes extensive remodeling under stress as well as showing varied expression patterns during differentiation and at

different stages in cell development (Ivaska et al., 2007). In addition, vimentin serves as a scaffold for other cell organelles and maintain membrane traffic inclusive of transporting integrins to the cell membrane (Ivaska et al., 2007).

Lamins are intermediate filaments that are located at the periphery of the cell nucleus where, along with their associated proteins, are referred to as the nuclear lamina or nucleoskeleton (Figure 1-6C). Lamins provide structural support to the nucleus and regulate its shape and mechanical loading. They are also implicated in chromatin organisation, DNA repair and in replication and transcriptional activity (Zuela et al., 2012). Lamins are intricately linked with cytosolic filaments via the LINC (linking nucleus to the cytoskeleton) complex (Crisp et al., 2006, Lombardi et al., 2011) providing a connection between the nucleus and the external environment, which has profound effects on consequential cell behaviour.

Microfilaments (Actin)

Cytoskeletal microfilaments are made up from polymerised globular actin monomers (G-actin) to form filamentous actin (F-actin) (Figure 1-6D). Polymerisation of F-actin occurs in both directions but at different rates giving rise to fast (+) and slow (-) growing ends orientated toward the cell membrane and into the cytoplasm respectively (Begg et al., 1978, Stossel, 1984) (Figure 1-7B).

Actin in its globular and filamentous form co-exists in equilibrium. At a critical concentration of G-actin, the + end of actin grows constantly while the – end undergoes a degree of decay, an effect known as treadmilling (Bonder et al., 1983). Treadmilling is ATPase driven brought on from ATP hydrolysis of the conversion of G-actin to F-actin (Bonder et al., 1983, Oda et al., 2009).

The regulation of actin polymerization and depolymerisation is carried out by a number of proteins inclusive of villin, cofilin, profilin & gelsolin, which function to keep actin filaments of a certain length. Others such as fimbrin & filamin facilitate cross linking of f-actin and subsequent formation of filament bundles, while vinculin, talin and α-actinin integrate f-actin with the cell membrane. The cross linking properties of these proteins are also implicated in the formation of stress fibres which are usually a bundle of 10 to 30 actin filaments. These assemble to form ventral stress fibres located at the base of the cell and attached to focal adhesions at both ends (Figure 1-4), dorsal stress fibres that emanate from the cell periphery (anchored to focal adhesions) toward the cell centre and transverse arcs located mainly in the lamella. α-actinin cross-linked stress fibres are subsequently displaced by myosins, which are intertwined within the filaments. Movement or contraction of f-actin is consequently brought about by its association with myosins, in particular myosin II.

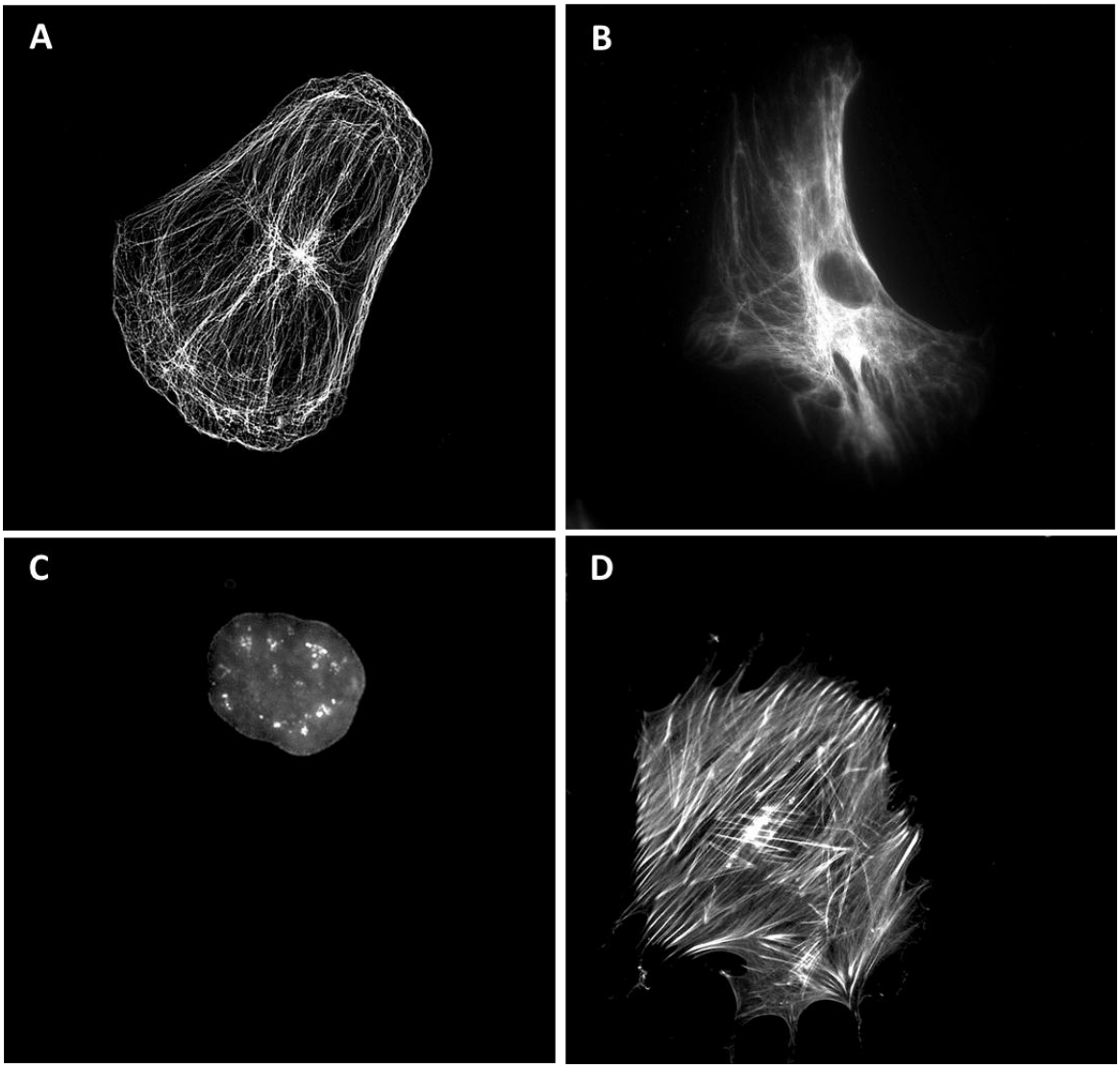

Figure 1-6 Images illustrating cytoskeletal forms. *Fluorescence images of β-tubulin for localisation of microtubule network radiating from the centrosome (A), of intermediate filaments vimentin (B) and lamin B (C) localised within the cell nucleus and actin microfilaments (D). Image A was courtesy of J. Roberts, images B & C – P. Tsimbouri and image D – Alakpa unpublished data.*

Myosin II

Myosins are motor proteins that play a major role in general cell motility. They occur widely in eukaryotic organisms, organized into 24 classes based on their head domain sequence and organisation (Syamaladevi, 2012). Myosin II is found mainly in muscle and the cell cytoplasm (non-muscle myosin II) where they interact with f-actin fibres promoting cytoskeletal contraction and influencing a number of cell functions such as cell shape, division, polarization, adhesion and migration (Syamaladevi, 2012, Vicente-Manzanares, 2009).

Non-muscle myosin II (NMM-II) comprises two heavy chains that form a α-helical coiled tail, a regulatory light chain that regulates its activity and an essential light chain, which forms a complex with the globular actin binding head (Figure 1-7A). Actin contraction by myosin II is dependent on ATP hydrolysis where the energy produced by the release of an inorganic phosphate drive a conformational change in the actin bound globular myosin head resulting in cytoskeletal contraction (Vicente-Manzanares, 2009).

The regulatory light chain of NMM-II can be phosphorylated by a number of kinases triggering activation or inactivation of NMM-II. These are also inclusive of focal adhesion GTPases RhoA and Rac, which promote and inhibit NMM-II activation respectively (Geiger et al., 2009, Vicente-Manzanares, 2009, Vicente-Manzanares et al., 2009). As focal adhesions mature, Rac signalling is modulated and RhoA activation increases mediating actin filament formation and increasing NMM-II activity (Beningo et al., 2001, Galbraith et al., 2002, Vicente-Manzanares et al., 2009) resulting in enhanced actomyosin bundles. The contractile forces generated in these bundles, in turn, exert forces on the distal focal adhesions affecting further maturation and adhesion dynamics.

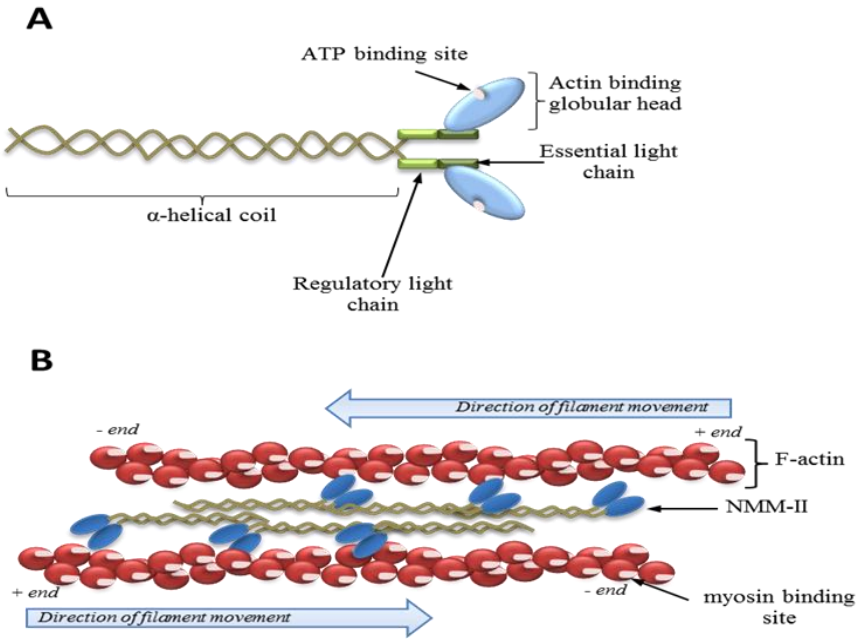

Figure 1-7 Structural orchestration of non-muscle myosin type II (NMM-II). *A) Structural domains of NMM-II showing the α-helical coiled rod which ends in a dimerised globular head containing an actin binding site adjacent to an ATP motor domain. B) The organisation of NMM-II with filamentous actin; an interaction that drives acto-mysin contraction. The α-helical rods are arranged to form the myosin thick filament allowing the globular head domain to bind with actin and facilitate the formation of stress fibres. On binding to actin, ATP hydrolysis causes a change in the head domain of NMM-II resulting in filament movement (contraction).*

1.4.4 Cytoskeletal reorganisation in response to external stimuli

The association of F-actin with the cell membrane through focal adhesion proteins such as vinculin and talin means that actin organization throughout the cell is sensitive to changes or the activity of membrane bound receptors inclusive of integrins. The continuous treadmilling of actin filaments is a constant dynamic process and as such affected by the properties of the external microenvironment mediated through these receptors, which subsequently brings about changes in cell activity, morphology and behaviour (McBeath et al., 2004, Papakonstanti et al., 2000) (Figure 1-8).

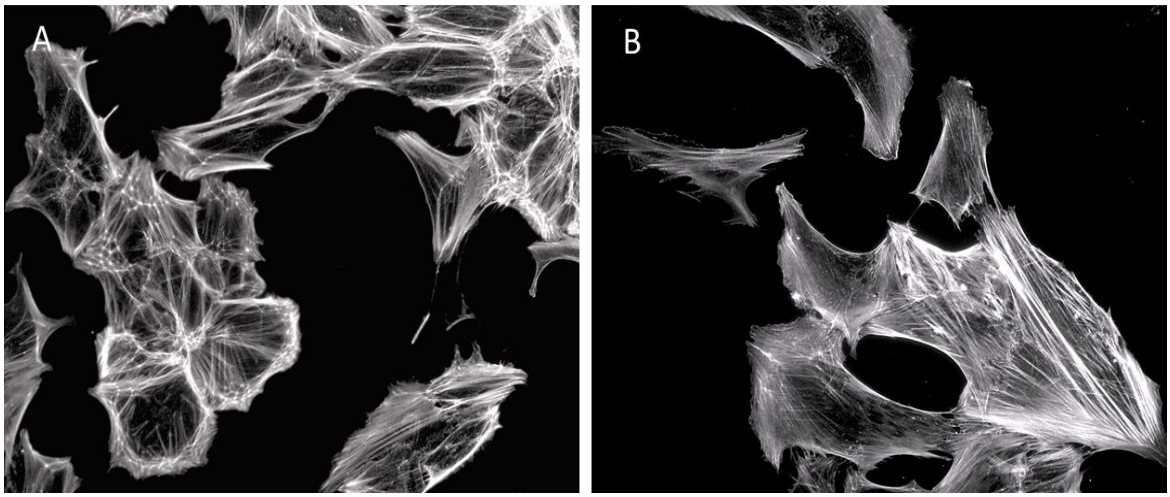

Figure 1-8 Cytoskeletal organisation in response to external stimulus. *Fluorescence images of the actin cytoskeleton of MSCs undergoing early stage adipogenic differentiation (A) and early stage osteogenic differentiation (B). Cells undergoing adipogenesis are rounded and actin fibres largely localised at the periphery of the cell body. Cells undergoing osteogenesis in comparison are more spread and form thicker stress fibres that span the length of the cell (Alakpa, unpublished data).*

Exploration of the immediate extracellular space is facilitated by a number of projections - the lamellipodia, a broad sheet like extension that is characterized by a rapid turnover of focal complexes and actin flow which play a major role in the leading progression of cell migration (Alexandrova et al., 2008). And filopodia, which are finger like projections that extend beyond the lamellipodium due to the presence of rapid actin polymerisation (Pollard and Borisy, 2003).

Actin filaments associate with a number of proteins that regulate its polymerization, depolymerisation and branching processes. Of these Cdc42 actively regulates polymerisation in filopodia and Rac in lamellipodia, both of which inherently inhibits NMM-II activity while RhoA promotes it, driving acto-myosin contractility and giving rise to stress fibres (Burridge and Wennerberg, 2004, Sander et al., 1999). Regulation of these

G-proteins is mainly via the activation of a host protein kinases or phosphatases regulating phosphorylation states of the cytoskeletal associated proteins. The balance created between these three proteins; Rho, Rac and Cdc42 are the main factors that drive cell polarisation and migration (Sander et al., 1999), and in cell types such as neurons regulate the outgrowth of dendrites (Kuhn et al., 1998, Swetman et al., 2002).

Mechanosensing however, is based on generating intracellular tensile forces to counteract that experienced extracellularly. As such, transductive effects are significantly influenced by the contractile properties exerted by the cytoskeleton.

The importance of the Rho family GTPases in stress fibre formation was initially shown by the inability of Vero cells to form microfilaments when treated with clostridium botulinum C3, a toxin known to inhibit Rho protein activity (Chardin et al., 1989), as well as the observation of increased stress fibre formation when cells are overexposed to recombinant RhoA (Paterson et al., 1990). Although all three Rho isoforms (A, B and C) are implicated in stress fibre formation (Giry et al., 1995), most research performed involves RhoA, which is implicated as the foremost regulator of stress fibre assembly.

Stress fibre formation and its subsequent contractile activity involves the activity of the RhoA downstream effector Rho-associated kinase (ROCK), which directly phosphorylates myosin light chain kinase (MLCK) (Amano et al., 1996, Somlyo and Somlyo, 2003). MLCK in turn phosphorylates myosin II light chain causing an increase in myosin ATPase activity resulting in actin contraction (Katoh et al., 2001). While it is known that MLCK can also induce stress fibre contraction in the absence of ROCK through its activation by calcium/calmodulin activity, inhibition of ROCK activity leads to the disassembly of focal adhesions, actin stress fibres and overall loss of cellular tension, indicating that Rho/ROCK mediated activity is important for continuous cell contraction that is required for mechanotransduction (Katoh et al., 2001). In addition, ROCK, as well as being able to instigate actin contraction via MLCK, also plays a role in regulating this function as it is known to indirectly inhibit myosin phosphatase activity resulting in sustained contractility (Koyama et al., 2000, MacDonald et al., 2001, Murata-Hori et al., 1999).

The cytoskeletal organisation and contractile strength generated dependent on the mechanical properties, as previously mentioned, affects overall adapted cell morphology. Morphological changes brought on by differences in cellular tension have been shown to act as a regulator of cell differentiation lineages. For example, studies done using mice which were p190B Rho GTPase activating protein negative (RhoGAP -/-); a suppressor of RhoA activity had shown impaired adipogenesis (formation of low tensile state cells) and enhanced myogenesis (Sordella et al., 2003). Similarly, inhibition of NMM-II in MSCs blocking actin contractility was shown to affected adopted differentiation lineages (Engler

et al., 2006). Cytoskeletal contractility therefore plays an important role in cells 'sensing' their matrix properties, having significant consequences with regards to directing stem cell differentiation *in vitro* (Engler et al., 2006, McBeath et al., 2004, Wozniak et al., 2003, Bhadriraju et al., 2007, Kilian et al., 2010).

1.4.5 Nuclear deformation due to mechanical stress

Observed differences in the rate of cell division in fibroblast cells when mechanical stress was applied suggested that mechanical stresses or loading is able to affect the nuclear activity of cells (Curtis and Seehar, 1978). Reorganisation of the cytoskeleton, nucleus and its nucleoli in the direction of an applied tensional force, through manipulation of microbeads attached to the cell surface, confirmed an innate link between the cell surface actuators and the cell nucleus (Maniotis et al., 1997). As nucleoli occupy specific spatial locations, reorganisation brought about by mechanical forces is thought to affect gene regulation, associating biophysical cues as causality for gene expression. While it is known that the nucleus of a cell is generally stiffer than the cytoplasmic space suggesting greater propensity for resistance to mechanical stress, small displacements on the cell surface are still significantly 'felt' at the nucleus causing a degree of distortion, a phenomenon that is dependent on the pre-stressed levels of the cytoskeleton (Hu et al., 2005). This, in addition to the time dependent changes in actin reorganisation, chromatin assembly and nuclear translocation of cytoskeletal associated cofactors (Iyer et al., 2012), suggest that the feedback mechanism is highly sensitive and does not simply rely on general microenvironmental pressures but active input by the cell itself.

Indeed, changes in cell and nuclear morphology due to adaptation of biophysical cues have subsequently been shown to have an effect on cellular transcription turnover and in turn protein translation altering cell behaviour (Dalby et al., 2003, Prajapati et al., 2000, Dalby et al., 2007a, Dalby et al., 2007b, Gupta et al., 2012).

Such sensitive propagation of mechanical stimulus to the nucleus is thought to occur via the LINC proteins nesprin and SUN as well as their associated adaptor proteins, which traverse the perinuclear space of the nuclear envelope providing a bridge between the cytoskeleton and nuclear lamins (Crisp et al., 2006, Lombardi et al., 2011, Padmakumar et al., 2005). As such, changes in cytoskeletal tension, contractility and reorganisation as instigated from integrins at the cell-ECM interface can alter states in gene expression and effect changes in cell behaviour.

1.5 Cell phenotype as a consequence of metabolism

1.5.1 Metabolites as a reflection of organism physiology

According to the National institute of Health, metabolism is defined as a physical or chemical process that converts or uses energy. A metabolite is therefore any substance that is produced as a result of metabolism. These compounds encompass a diverse range of physical, chemical and structural properties carrying out numerous functions within the body. For this reason, it is not surprising that metabolism and metabolites are generally at the forefront in most research and diagnostic applications, as anomalies in known metabolic patterns are often a very telling sign in gauging an individuals' health status. A classic example of this is glucose concentrations for monitoring and diagnosis of diabetes mellitus, urine pH tests for kidney function and alkaline phosphatase for liver function. With the latter two examples, the biomarkers focused on to assess organ function are generally proteins but it is also their metabolic activity that contributes to the malaise.

The body's ability to metabolise any given compound is also of considerable importance in the field of drug design, screening and toxicology. Often, the potency of a particular drug is dependent on the rate and manner in which the body acts on a particular drug (pharmacokinetics). Administered drugs need to have the ability for the body to neutralise and excrete the substance to prevent accumulation and toxification. This is an inherent process that is not only restricted to administered drugs but a broad acting process that maintains stasis and keeps the system going or allowing it to adapt to change.

Metabolic behaviour, however, is not an isolated process and from the examples mentioned above it is very much an interactive process with the external environment. As such the so-called stasis a system achieves is very much influenced by the state of its immediate surroundings and how they affect it. While in some cases the effect is transient or malady as those seen with drug screening and diabetes, in others it can bring about change in physiology, adapting to exist within a changed environment. This leads to divergence in metabolic character between individuals where certain stresses can be handled without any due effects in one person but another can result in severe repercussions. An example of this can be seen in human polymorphism of the cytochrome P450 enzyme 2D6 (CYP2D6) that metabolises codeine into morphine.

On a cellular level, however, metabolites and metabolism create a similar effect in terms of maintaining cell stasis or altering cell states for adaptability. These changes, however, occur on a much quicker time scale and activity is influenced by subtler environmental changes such as topographical detail and substrate rigidity in addition to chemical composition. These environmental properties existing at the nano- and microscale are

known to have diverse effects metabolic processes resulting in cell migration, growth, adhesion, proliferation and differentiation

In an analytical context and within this thesis, metabolites as measured using a metabolomics study is defined as the range of detectable small mass molecules (70 – 1400 Da) within a study sample.

1.5.2 Metabolomics

In terms of an analytical approach, metabolomics has been referred to as a non-biased identification and quantification of all metabolites present within a biological system (Fiehn, 2002). Due in part, to the infancy of metabolomics, an exact execution of this is limited by the available analytical techniques against the range of metabolites that are produced by a cellular organism which vary widely in their physicochemical, functional and structural properties. Metabolomics in the aforementioned sense has been argued as too vast and varied a task to be actualised in reality and so proposals are put forward to define it as the study of the metabolome under a given set of physiological conditions (Hollywood et al., 2006, Villas-Boas et al., 2005). As such, given the amount of debate on defining metabolomics, these criteria often coincide with studies referred to as metabonomics, albeit individual authors make their distinctions. Titling a study as either metabolomics or metabonomics is seemingly influenced to a degree by personal opinion rather than the application of stringent qualifying criterion.

The metabolite composites of a system are generally the substrate or product of active protein components, mostly through enzymatic activity. They are therefore considered to be downstream of the full protein compliment of a cell. As such, they are placed downstream in the ‘omics hierarchy (Figure 1-9). They also occupy this space due to the effect the metabolome represents in comparison to the genome or proteome for example. The metabolome represents the actions performed by a cell and is therefore a definitive snapshot of what process or processes have occurred. In this manner, it is less speculative than studying the other ‘omics sectors.

Study of the metabolome, however, has the added complexity in the sense that, the metabolome is not only a result of gene expression and protein activity but also acts as a regulatory system, which in turn influences gene expression and protein activity. As such, because metabolites are not simply an end point or product, the metabolome has the potential to give information on processes that have occurred in the cell due to its interaction with external stimuli, and on the flipside, it also gives an insight to its influence on activities that may also alter or continually drive/inhibit a particular cell behavioural process. This unique position as an entry/exit point means that the metabolome is closely

reflective of the physiology or phenotype of the cell or organism at that particular point in time.

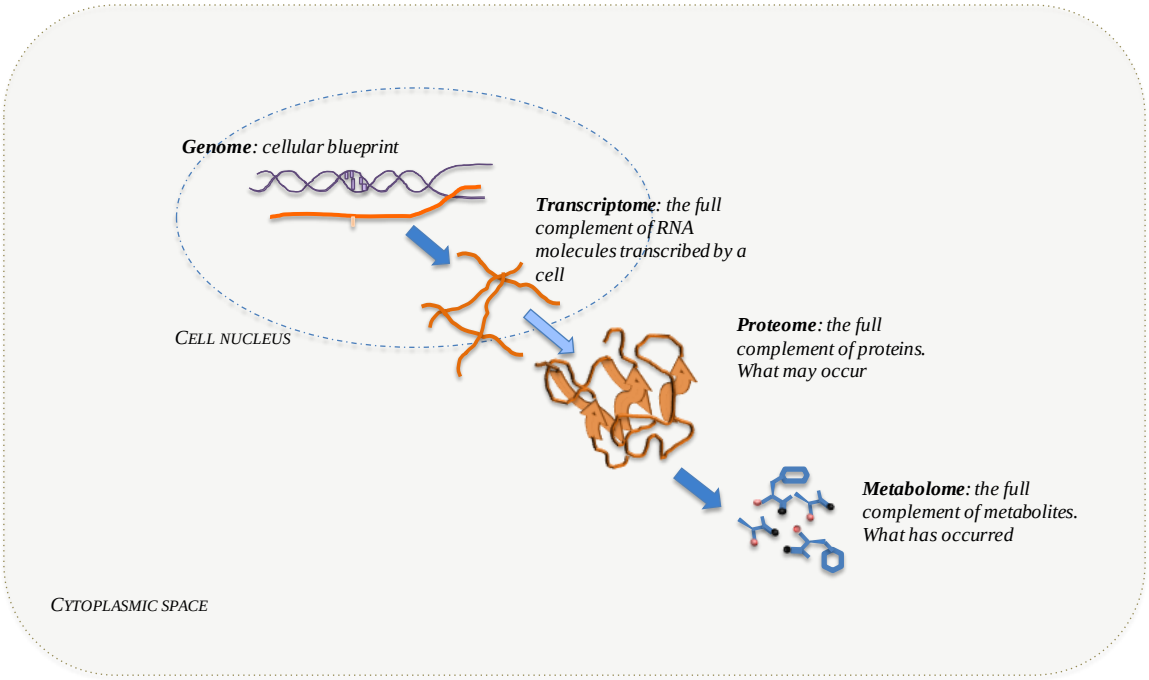

Figure 1-9 Simplified schematic illustrating the cellular functional lineage. *Each stage produces a full complement of classified molecules (suffixed –ome as indicated on diagram) to which their study is dedicated (suffixed –omics). This starts at the genome for genes through their expression (transcriptome), translation (proteome) to inherent activity (metabolome). This process is in no way singular however, as each stage provides regulatory feedback to the other.*

In this sense, the metabolome and the proteome bear the analytical advantage in that their makeup is particularly sensitive to the context in which the cells are placed. That is, their makeup is far more sensitive to changes in their microenvironment. This close proximity to altering events at the interface means that activity that occurs at this scale is highly dynamic. Compared to the genome and its transcription, where processes are relatively inflexible, proteins are subject to a number of post translation modifications altering structure and function. Activity by most proteins requires initiation of an 'on switch' (usually by phosphorylation), an action which is not gene regulated but for the most part is brought on by the affectations of cellular metabolites. The resultant sequestering, depletion or synthesis of metabolites also depend on a number of outwith factors such as enzyme specificity, kinetics and the effect they ultimately have on the cells regulatory mechanisms (Higuera et al., 2012, Khan and Sheetz, 1997, Wolfenson et al., 2011).

A lot of activity at this level is also non-dependent on gene transcription taking its cue from the cells own intricate signalling system to regulate intracellular activity. This allows for reaction time turnover to occur at rates of milliseconds in response to stimuli rather than over longer time scales (Oakes et al., 2012, Wolfenson et al., 2011). Non-gene dependent cell activity that rely on such feedback processes which can then eventually lead to gene expression are inclusive of focal adhesion turnover and cytoskeletal contractility which have been discussed earlier in this chapter.

Metabolomics requires the integration of a number disciplines (inclusive of biological, chemistry, computational and mathematical) to realise its definition. Even if you are of a pedantic disposition, and do not necessarily agree with the commonly used definition as the analysis of the full complement of metabolites within a system, it is clear, however, that this very analogy drives the continued evolution of the methods geared specifically at studying the metabolome. The broad net cast for metabolite information means that metabolomics itself demands methods and techniques with the capability of reflecting what is caught in the net, so to speak. For this reason, amongst others, nuclear magnetic resonance (NMR) and mass spectrometry (MS) have become the more popular means of metabolite detection. While NMR is able to perform broad range detections, its lessened sensitivity makes MS the more attractive option. The flexibility of MS not only allows molecular detection by direct infusion (DI-MS) but it can also be coupled with a number of separation techniques for quantification such as capillary electrophoresis (CE-MS), gas chromatography (GC-MS), liquid chromatography (LC-MS) and supercritical fluid chromatography (SFC-MS).

Because this type of study inevitably provides a large amount of data for any one experiment, or indeed sample, computational analysis then becomes the workhorse of metabolomics in order to transform raw data into an understandable and user friendly format that allows meaningful assessments to be made.

1.5.3 A place in regenerative medicine

From wound healing to organogenesis, an understanding of cell interactions with its ECM and their elicited responses to specific cues is an important factor in tissue engineering. A first step towards these goals however, requires an understanding of cell interactions on a much smaller scale.

While it has been shown that cytoskeletal and morphological reorganisation leads to signalling events that inhibit or initiate a number of cell functions inclusive of differentiation (Bhadriraju et al., 2007, Engler et al., 2004a, Ingber, 1991, Kilian et al., 2010, McBeath et al., 2004), most of the small molecule biochemistry that facilitates

mechanotransductive effects are lesser known. A single event may be able to access behavioural changes within a cell but a single event altering a single signalling route is rarely the case with regards to holistic cell events.

One such means of gaining an insight into the entire orchestration is to make use of a metabolomics based approach to investigate the whole over the individual. In other words, to gain an understanding of how molecular interactions carried out within the cell occurs in response to their microenvironment resulting in a singular specific behaviour such as migration, growth, proliferation and differentiation.

Of recent, a number of studies, such as the investigation of the influence of unsaturated molecules on embryonic stem cell pluripotency (Yanes et al., 2010), topographical maintenance of MSC phenotype (McMurray et al., 2011) and identification of biochemical signalling pathways that affect differentiation (Tsimbouri et al., 2012) have all made use of metabolomics to support their findings. These examples highlight the increasing role(s) the metabolome and metabolomics plays in furthering cell and tissue engineering.

Lastly, it is also worthy of mention that while metabolomics can provide a broad insight into cell activity, it is still confined to the restraints of its definition. In order to understand cell behaviour wholly, the integration of genomics, transcriptomics, proteomics and metabolomics is a necessity.

1.6 Project aims/objectives

The cell-material interface is known to have considerable effect on stem cell function and differentiation properties. These interactions are inclusive of the material chemical properties through surface functionalisation using functional groups such as alcohols, peptide motifs or the use of whole proteins to coat or pattern surfaces (Bhadriraju and Hansen, 2002, Kilian et al., 2010, McBeath et al., 2004), nanotopographical detailing through lithography or embossing processes (Bettinger et al., 2009, Biggs et al., 2009, Chen et al., 1998) and variation in the elasticity or stiffness of the material which can be tuned through manipulation of ligand cross-linking (Engler et al., 2006, Saha et al., 2008).

The design of materials for targeted differentiation of stem cells aim to fulfil a number of requirements inclusive of its ease of manufacture and implementation, ability to support cell adhesion and expansion as well as acting as an instructional tool to direct differentiation, ideally producing a homogenous cell population.

This project assesses the use of hydrogel biomaterials made using self-assembling N-terminal capped (Fmoc) peptides (diphenylalanine and serine, F_2/S) as an instructional tool for driving stem cell differentiation through fine tuning of the relative elasticity of the

hydrogels to mimic that of naturally occurring tissue types as previously shown (Engler et al., 2006), (Chapter 2).

The comprehensive investigation of cell activity such as gene and proteomic expression have allowed the discovery of a number of gene and protein level expressions that are of particular relevance to stem cell biology. These include genomic sequences correlating to histone methylation as a regulatory mechanism in embryonic stem cell pluripotency which are distinct from their differentiated progeny (Azuara et al., 2006). Graumann *et al* also showed that these changes in chromatin states correlated with changes in protein expression profiles in ES cells (Graumann et al., 2008). Although these represent important findings in researching stem cell pluripotency, it is known that due to post translational modifications and altered activity states, gene expression and protein expression do not provide a complete insight into how a cell adapts and controls it altered phenotype (Gygi et al., 1999).

Metabolites, on the other hand, offer an insight into the protein activity of cells bypassing the ambiguity brought on through altered protein states and reflect function over mere expression. The metabolites represent a snapshot of the cell in its currently active state and therefore its current phenotypical state. Studies have shown measured altered metabolic states that characterise the pluripotent state of stem cells (McMurray et al., 2011, Tsimbouri et al., 2012, Yanes et al., 2010). The use of mechanically tuned F_2/S biomaterials has the ability to alter the conformation adopted by a number of biochemical molecules under differential stress states, in turn altering their kinetics (Ingber, 2006, Khan and Sheetz, 1997). This alteration in kinetics and activity states are likely to have an effect on the overall metabolic states of the cell(s) driving change such as differentiation in stem cells. This being the case, investigating the global metabolome of stem cells under such stresses can give an insight into altered cell activity, which lead to adoption of different phenotypes on differentiation. A facet, which is explored in this project (Chapter 3).

The use of a global unbiased metabolomics study to investigate stem cell behaviour inevitably gives information on a host of naturally occurring molecules that exist within the cell which may be implicated in signalling events leading up to differentiation. This is considered possible as the cells are coaxed into differentiation using the biomaterial elasticity as the sole instructional tool leaving the system free from chemical interference (use of tailor made differentiation media). From the information garnered, metabolites that are likely to play an influential role in driving differentiation were singled out and investigated in further detail under the hypothesis that currently experienced problems such as population heterogeneity observed with synthetic chemicals used in *in vitro* differentiation protocols (Bujalska et al., 2008, Ding and Schultz, 2004, Klemm et al.,

2001, Zuk et al., 2001) can be reduced by researching the effect of lesser known metabolites or small molecules on differentiation (Chapter 4).

The project concludes by encompassing the study scope (stem cell biology, metabolism and material interactions) and focusing on potential applications in regenerative medicine as well as looking into the efficacy of substrate tuned biomaterials to be used as an instructional differentiating tool toward a singular cell line. Chapter 5 investigates the ability of F_2/S hydrogel biomaterials to act as means of optimising chondrogenic development of pericyte cells *in vitro* in the longer term for use in cartilage tissue engineering either for use as a cell source or as a potential transplant material.

Summary of project objectives

- Ascertain the suitability of F_2/S hydrogels as a substrate for cell culture and the ability of the substrate to guide MSC differentiation along a number distinct cell lineages based on their mechanical properties
- To investigate whether the use of an unbiased metabolomics study is able to distinguish between different behavioural patterns as MSCs undergo differentiation on the F_2/S substrates
- To make use of a metabolomics based approach to investigate the effect or role of lesser known or researched metabolites may have in inducing or guiding lineage commitment on differentiation.
- To combine biomaterial design and metabolomics as an exploratory tool for the potential use of F_2/S as a clinical scaffold for use in cartilage regeneration and repair.

2 MSC DIFFERENTIATION USING PEPTIDE HYDROGEL SUBSTRATES WITH TUNED MECHANICAL PROPERTIES

2.1 Introduction

2.1.1 Substrate mechanics & stem cell differentiation

While the mechanics of a substrate is known to affect the physical qualities of specialised cell types, in stem and progenitor cells, these physical states have a large influence on lineage commitment whilst driving differentiation. Naturally, these observed effects have garnered much interest in the way that biomaterials are designed and developed for use in regenerative medicine (Engler et al., 2006, Gilbert et al., 2010).

For example, the relative deformability or elasticity (measured as the Young's modulus in the unit Pascal) of tissue types within the human body show considerable variation from the soft adipose and brain tissue with a Young's modulus of around 1 kPa (Elkin et al., 2007) at one extreme to the less flexible likeness of calcified bone at the opposite extreme measuring in the range of 6 – 10 GPa (Discher et al., 2005, Reilly and Burstein, 1974). These qualities bear considerable importance to tissue functionality and specialised cells housed within these niches are adapted to exist as such. Stem cells, having the propensity to form a number of any of these specialised cell types that exist within these very different niches need to be able to interpret the mechanical properties of the extracellular matrix in order to undergo development into a fully functional specialised cell type.

As part of the cohort to reduce the occurrence of randomised events or spontaneous differentiation *in vivo* that can be observed with the formation of teratomas for example, it is considered that physical characteristics of the ECM inclusive of its elastic properties have substantial influence on inherent tissue assembly and functionality (Evans et al., 2009, Krieg et al., 2008, Rozario et al., 2009). In order to maintain such organisation, cellular sensing of changes in ECM stiffness is mediated through a constant cycle of mechanosensing and responses mediated through focal adhesions that generate intracellular cytoskeletal tensional states (Choquet et al., 1997, Yamada and Geiger, 1997).

Increased intracellular tension resulting from cells cultured on substrates able to withstand high cytoskeletal contractility have been shown to influence changes in broad signalling events culminating in the up regulation of transcription factors such as RUNX-2 and bone morphogenic proteins leading to the osteogenic development of MSCs cultured on these substrates (Engler et al., 2006).

On the other hand, MSCs cultured on deformable substrates mean that less tension is generated within the cell, modulating contractility and in turn influencing certain physical characteristics such as cell morphology and spreading. These changes are also related to the expression of transcription factors such as peroxisome proliferator-activated

receptor gamma (PPARγ) and neuronal cell adhesion molecule 1 (NCAM1) associated with the development of cell types associated with the softer adipose and neuronal tissue types respectively (Engler et al., 2006, Kilian et al., 2010, McBeath et al., 2004, McMurray et al., 2011, Tsimbouri et al., 2012).

As well as influencing the production of particular transcription factors that promote the formation of certain cell types, the optimised functional state of the cell(s) are also affected by their native tissue physical characteristics. For example, studies have shown that neural cells survive better with cultured *in vitro* on soft substrates as opposed to more rigid surfaces (Flanagan et al., 2002, Saha et al., 2008) and optimal differentiation of MSCs into naïve osteoblasts occurs when cells are cultured on substrates that measure a Young's modulus of approximate 40 kPa, an elasticity measurement that is similar to non-mineralised bone tissue (Engler et al., 2006, Place et al., 2009, Rowlands A., 2008, Trappmann et al., 2012, Wang et al., 2012).

In addition, studies involving differentiation along the myocardial route not only echo the trends of the previously mentioned examples (Engler et al., 2008, Engler et al., 2006), but also noted that increased functionality is also due to an innate mechanical coupling of the cells mechano-sensory adhesions to that of its surrounding microenvironment (Hoerning et al., 2012).

In light of these, the importance of designing biological mimics for cell culture needs to take into consideration the manner in which cells 'feel' and response to certain cues, making the mechanical integrity of the substrate a highly important factor with regards to guiding specific behavioural responses *in vitro*.

2.1.2 The substrate

Preceding sections in this thesis have highlighted the importance substrate mechanics, specifically elasticity, have on eliciting particular behavioural responses in stem cells. The influence of which is such that mechanical substrate properties can promote phenotypical changes rather than resort to use of soluble factors and chemical formulations (Curtis and Wilkinson, 1997, Engler et al., 2006).

Hydrogels, in a general context, are cross-linked polymer networks of which water is the main dispersion media. They represent an excellent biomaterial choice as they offer flexibility - being able to incorporate a host of different chemistries and topographical design. Also, their high hydration and viscoelastic property renders their make up very close to that of native tissue. The given ability to mimic the latter property means that cell behaviour on these biomaterials is a close approximation of their *in vivo* likeness (Discher et al., 2009).

The use of supramolecular hydrogels have of recent allowed the formation of biomaterials with flexible elasticity, nanoscale features and simple chemical functionalisation (Benoit et al., 2008, Jayawarna et al., 2009), which are of particular importance to cell interpretation. The added quality of these biomaterials to self-assemble is also of the advantage in the sense that contamination issues from external handling during fabrication is eliminated.

This project makes use of short chain self-assembling peptides to comprise a hydrogel biomaterial. The primary function of the material is to direct lineage commitment on differentiation by cell interpretation of the biomaterial mechanical properties as the sole instruction. Prof R. Ulijns group at Applied Chemistry at the University of Strathclyde have developed the hydrogel biomaterials used for this thesis.

Short chain peptides capped at the N-terminus with a 9-fluorenylmethoxycarbonyl moiety (Fmoc) have been shown previously to have the tendency to form hydrogels through formation of filamentous micelles (Vegners et al., 1995) that also have the ability to undergo liquid-solid phase transitions by tailoring pH and temperature (Tang et al., 2009, Zhang et al., 2003b). Specifically, Fmoc capped diphenylalanine (Fmoc-F_2) is known to form cytocompatible hydrogels at physiological pH, which are formed by π-π stacking between aromatic groups (Jayawarna et al., 2006, Smith et al., 2008, Tang et al., 2009, Zhou et al., 2009). This interaction also enables the use of small peptide molecules to impart functionality to the hydrogel (Jayawarna et al., 2009).

The substrate used within this project comprises the short chain peptides Fmoc-F_2 in equimolar concentrations with Fmoc-Serine (Fmoc-S). This results in a nanofibrous hydrogel with surfactant properties (F_2/S). As separate entities, Fmoc-F_2 forms nanofibres in solution while Fmoc-S form aggregated spheres. In conjunction with one another, the fibres remain present in solution while the aggregates are lost as Fmoc-S acts as a surface coating, imparting functionality to the resultant structure (Figure 2-1).

The physical characteristics of hydrogels can be controlled in a number of ways, through careful manipulation of factors such as temperature, pH and concentration. The changes of which facilitate the extent of fibre formation as well as influencing the cross linking capabilities of the polymer resulting in elasticity variability.

The Youngs' modulus or rigidity of the F_2/S hydrogels have been tailored successfully through either sole manipulation of the peptide solution pH or in conjunction with careful management of F_2/S concentrations within the solution which give rise to the hydrogels finished characteristics (Figure 2-2).

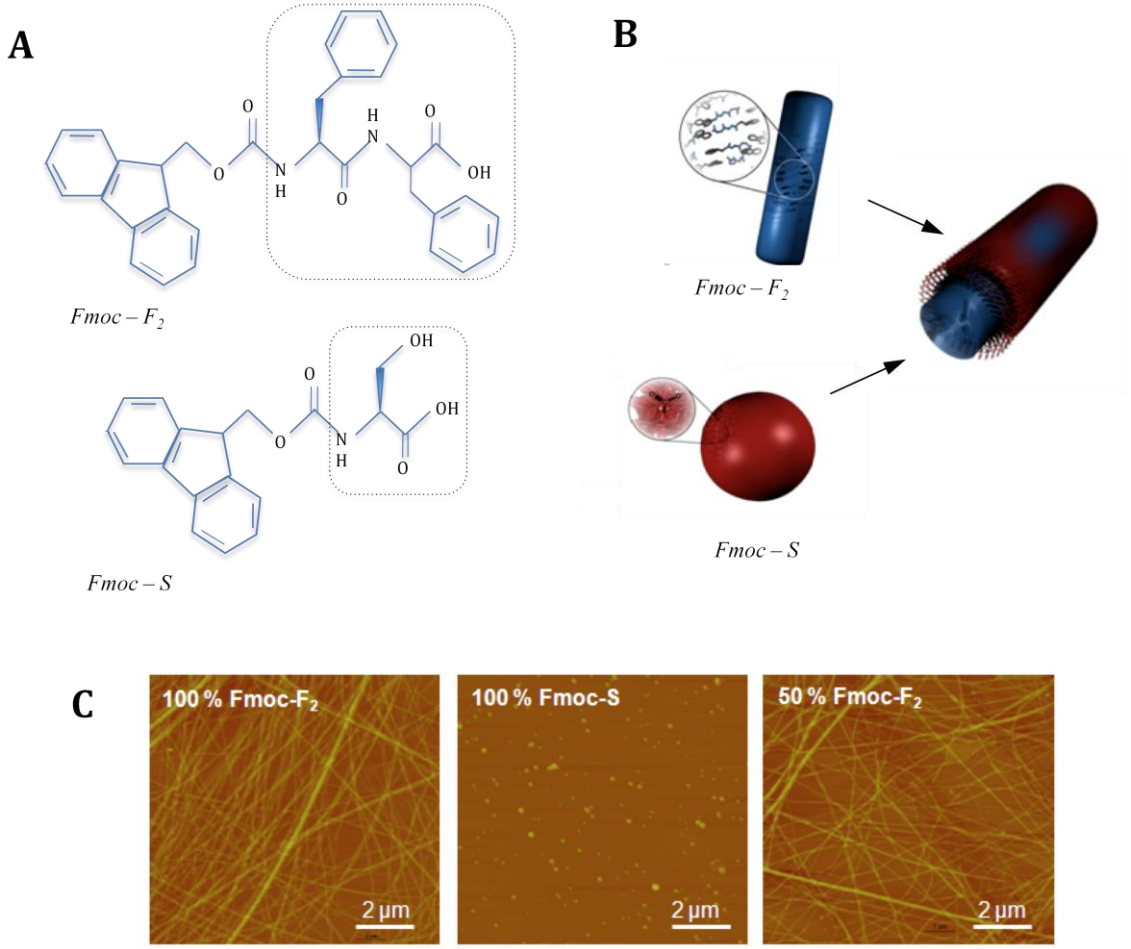

Figure 2-1 Components of self-assembled peptide hydrogel, F_2/S. *(A) Chemical structures of Fmoc-diphenylalanine (F_2) and Fmoc-serine (S); the peptide moieties are highlighted as that within the dashed enclosure. (B) Illustration of the proposed interaction between Fmoc-F_2 and Fmoc-S when together in solution. (C) AFM images of Fmoc-F_2, Fmoc-S and 1:1 F_2/S. Images B & C were kindly provided by R. Ulijn.*

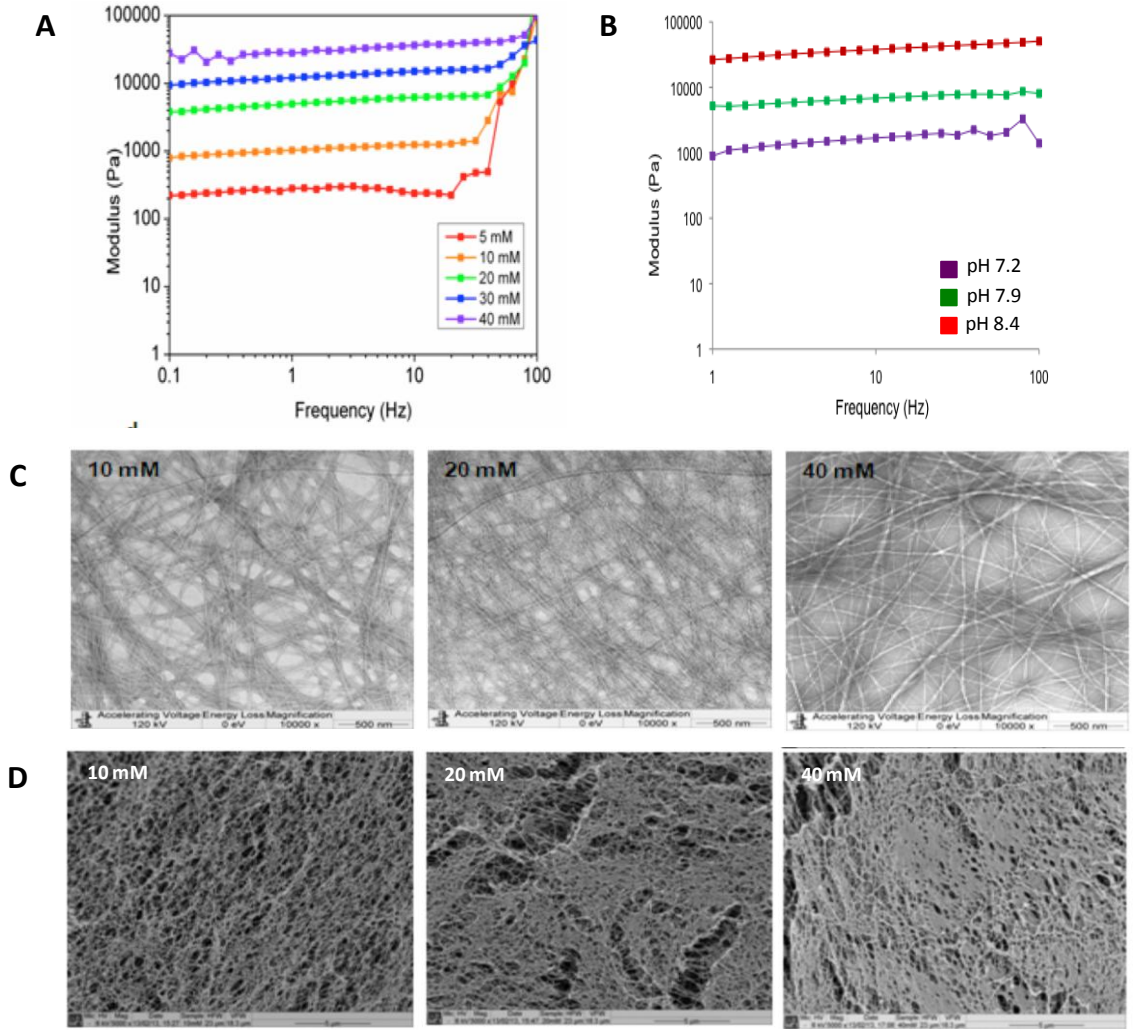

Figure 2-2 Characterisation of F_2/S hydrogels. *Oscillatory rheology analysis of F_2/S hydrogel stiffness fabricated by tailored concentration (A) and pre-gelation pH manipulation of a 20 mM F_2/S solution (B). Approximate modulus of 10mM and pH 7.2 is 2 kPa, 20mM and pH 7.9 is 7 kPa and 40mM and pH 8.4 is 36 kPa respectively. TEM and SEM images of pre-gelation solutions are shown in (C) & (D) respectively. Images were kindly provided by V. Jayawarna and R. Ulijn.*

2.1.3 Objectives

This study aims to answer a number of questions that deal with biomaterial properties on the behavioural patterns of mesenchymal stem cells. In the first instance, it shows that the F_2/S substrate supports cell attachment and growth and as such is a suitable material for cell culture. Secondly, to show that mesenchymal stem cells cultured on F_2/S hydrogel biomaterials at differing elasticity instruct these cells to undergo differentiation into specialised cell types. Thirdly, to ascertain what differentiation lineages are adopted by the stem cells on each of the substrates and whether these lineages are particular to those of innate tissue types as observed in previous studies.

2.2 Materials & methods

2.2.1 Materials

Materials/reagents	**Supplier(s)**
Human bone marrow mesenchymal stem cells	Promocell GmBH, Germany.
Fmoc-diphenylalanine	Bachem, UK
Fmoc-serine	Bachem, UK
Sodium hydroxide	Fisher chemicals, UK
Water	Invitrogen, UK
Dulbeccos modified eagle medium (DMEM)	Sigma Aldrich, UK
Foetal bovine serum (FBS)	Sigma Aldrich, UK
Penicillin streptomycin	Sigma Aldrich, UK
Trypsin	Sigma Aldrich, UK
Calcein acetoxymethyl ester	Invitrogen, UK
Propidium iodide	Vector laboratories, USA
Phosphate buffered saline (PBS)*	In-house
Fixative*	In-house
Permeability buffer*	In-house
1% BSA in PBS*	In-house
Vectashield-DAPI	Vector laboratories, USA
Rhodamine-phalloidin	Invitrogen, USA
Primary antibodies	Abcam, UK & Santa Cruz biotechnologies, USA
Biotinylated secondary antibodies	Vector laboratories, USA
Streptavidin-FITC	Vector laboratories, USA
0.5% Tween 20 in PBS*	In-house
Trizol	Life technologies, UK
Chloroform	Sigma Aldrich, UK
Glycoblue	Ambion, UK
Isopropanol	Sigma Aldrich, UK
Ethanol	VWR Chemicals, France
RNase free water	Qiagen, UK
Quantitech reverse transcription kit	Qiagen, UK
Quantifast SYBR green PCR kit	Qiagen, UK

* Preparation procedures for reagents & buffers made in house are detailed in the appendix

2.2.2 Cell culture

Human mesenchymal stem cells obtained from purified bone marrow were cultured and maintained at 37˚C and 5% CO_2 atmosphere in DMEM culture media supplemented with 100 µM sodium pyruvate, 0.8 mM L-glutamine, 10% foetal bovine serum (FBS) and 1% of penicillin streptomycin (10 mg/ml solution) of the total volume. This supplemented DMEM culture mix was used for all cell culture procedures unless defined otherwise.

Cells were sub-cultured when approximately 80 – 90% confluent by incubating with trypsin for approximately 5 minutes to detach the adherent cells from the culture flask. The action of trypsin was then halted by the addition of an equal volume of culture media and the resulting cell suspension transferred into 20 ml flasks and centrifuged for 5 minutes at 1400 g to sediment the cells. The trypsin/media supernatant was then decanted to waste and the cells resuspended in an appropriate volume of fresh media (cell numbers used in subsequent experiments were maintained between 1 and 2 x 10^5 cells unless otherwise stated). Cells were then either seeded into another culture well flask and allowed to grow confluent as the subsequent passage or used for pending experiments. Cells used for all ensuing experiments were between passage 1 and 3 and media changes were performed twice weekly.

2.2.3 Substrate fabrication

Prior to use, all compounds were sterilised under ultraviolet light for 40 minutes. 0.0214 g of peptide powders Fmoc-diphenylalanine and 0.0138 g of Fmoc-serine (Bachem Ltd, UK) were weighed and dissolved in 4 ml distilled water and 0.5 M sodium hydroxide (Sigma-Aldrich, UK) by alternate sonication and vortexing to make a 20 mM Fmoc-diphenylalanine/serine (F_2/S) peptide solution. The end physical characteristic (rigidity) of the resulting hydrogel was varied by altering the pH of each peptide solution with sodium hydroxide. The rigidity, expressed as the Young's modulus of the hydrogel and pH of each peptide solution as determined from previous optimisation experiments, is shown in Table 2-4.

The dissolved peptide solutions were then incubated at 4˚C for a minimum of 1 hr before being warmed to 37˚C in a water bath or incubator. Hydrogels were made by dispensing 0.3 ml of each peptide solution into a 12-well culture plate insert and 1.4 ml of DMEM culture medium dispensed into the well itself so that the media comes in contact with the membrane at the base of the insert. The culture plates were then incubated at 37˚C for at least 1.5 hrs to allow hydrogel formation. Following incubation, the culture medium in each well was decanted to waste and replaced with fresh medium. 0.2 ml of culture medium was then added onto the formed hydrogels in the well inserts. The culture plate

was then returned to incubate at 37˚C overnight to allow the gels to equilibrate to physiological pH for cell culturing.

2.2.3.1 Cell culture using F_2/S hydrogels

Human bone marrow mesenchymal stem cells expanded in cell culture flasks were detached from the flasks by incubating with trypsin for 3 – 5 minutes and then quenching by the addition of culture media after time had elapsed. The tripsinised cell-media mix was centrifuged for 4 minutes at 1500 g to pellet the cells from the culture medium and the supernatant decanted to waste. The pellet was re-suspended in an appropriate amount of cell culture media to give a cell number of approximately 2 x 10^5 cells per ml.

The medium in the well insert holding the hydrogels was carefully aspirated to waste and 0.1 ml of the cell suspension was added onto the hydrogel. 1.4 ml of DMEM was added to the culture well plate and the samples incubated for 2 hours to allow cell adherence. Following this, the media on each hydrogel was carefully removed and replaced with 0.3 ml of fresh media. The media within the wells were also replaced during this time. Cells were then maintained at 37˚C and 5% CO_2 atmosphere changing the media twice weekly until required for assay.

2.2.4 Cell viability

Cell viability was assessed using the fluorescent dyes calcein acetoxymethyl ester (calcein AM) and propidium iodide (Invitrogen, UK).

Calcein acetoxymethyl ester is a non-fluorescent compound that is cell permeable. On transportation into cells, the acetoxymethyl group is cleaved by cellular esterases causing the resulting molecule (calcein) to give off a strong green fluorescence signal ($\lambda_{ext/em}$ 495/515) indicating an active cell population. Propidium iodide is a membrane impermeable dye that binds to nucleic acids to give a red fluorescence. Cells emitting red fluorescence therefore have compromised cell membranes and are thus considered dead.

Culture medium was carefully aspirated from each culture well and from the well inserts holding the hydrogels then decanted to waste. Hydrogel discs were then removed from the insert and placed into clean well plates. 0.4 ml of a solution containing 2 μM calcein AM and 2 μM propidium iodide in phosphate buffered saline (PBS) was added to each well and then allowed to incubate at 37˚C in the dark for approximately 25 minutes.

Fluorescence microscopy images of live and dead cells were taken on days 1, 3 and 7 of culturing to ascertain viable cell populations on the hydrogels.

2.2.5 Immunocytochemistry

Cell samples or material substrates were rinsed once in PBS and fixed at 37˚C for 15 minutes. They were then permeabilised and blocked using 1% BSA in PBS. Following this, cells were then incubated at 37˚C for an hour with rhodamine conjugated phalloidin and the required primary antibody (Table 2-1). After 1 hr, cells were washed three times for 5 minutes with 0.5% tween in PBS (cells cultured within substrates were washed for 15 minutes to ensure removal of excess antibody from the hydrogels) and incubated for an hour at 37˚C with the corresponding secondary antibody. Cells were again washed thrice with 0.5% tween in PBS as required, incubated at 4˚C for 30 minutes with streptavidin conjugated FITC and washed again as before after the incubation time elapsed.

Samples were then mounted onto a drop of vectashield-DAPI (a glycerol based mounting medium for preserving fluorescence containing DAPI for nucleic acid staining) on a microscope slide. For biomaterial substrates, vectashield-DAPI was diluted in PBS and added to the well plates. All samples were stored at 4˚C wrapped in foil to protect from photobleaching until ready for viewing under a microscope.

Table 2-1 Biomarkers used for detection of cellular differentiation

<table>
<tr><th>Differentiation lineage</th><th>Biomarker</th><th>Primary antibody</th><th>Secondary antibody</th><th>Fluorophore</th></tr>
<tr><td>Neurogenesis</td><td>Nestin</td><td>Mouse monoclonal IgG</td><td>Biotinylated anti mouse</td><td rowspan="6">Stretavidin conjugated FITC</td></tr>
<tr><td>Adipogenesis</td><td>PPAR-γ</td><td>Goat polyclonal IgG</td><td>Biotinylated anti goat</td></tr>
<tr><td>Myogenesis</td><td>MyoD</td><td rowspan="3">Mouse monoclonal IgG</td><td rowspan="3">Biotinylated anti mouse</td></tr>
<tr><td>Osteogenesis</td><td>RUNX-2</td></tr>
<tr><td>Chondrogenesis</td><td>SOX-9</td></tr>
<tr><td>Cytoskeleton</td><td>F-actin</td><td></td><td></td><td>Phalloidin conjugated rhodamine</td></tr>
<tr><td>Nucleus</td><td></td><td></td><td></td><td>DAPI</td></tr>
</table>

2.2.6 Microscopy & Imaging

Epifluorescence and phase contrast images were taken using an inverted Axiovert 200 microscope (Carl Zeiss, Jena, Germany) equipped with a charge coupled devive (CCD) camera (QImaging, Canada).

Greyscale fluorescence images obtained using ImagePro software were converted to RGB format and coloured overlays made using Adobe Photoshop Creative Suite (Adobe Inc. Ireland), version 8.0 to reflect the fluorescence colour emission of the fluorophores used in experiments (Table 2-2).

To represent scale, 1000 µm rule images were taken using the appropriate objective lens. Number of pixels was then converted into the equivalent distance in µm as measured on the ruler. Conversion of pixel to distance was done using ImageJ software (National Institute of Health, USA) and used as scale reference in all microscopy images. Final images were then compiled for representation using Microsoft power point.

Table 2-2 Excitation and emission wavelengths of fluorophores used for microscopy

FITC	λ_{ext}: 494 λ_{em}: 525	Green
TRITC	λ_{ext}: 557 λ_{em}: 576	Red
DAPI	λ_{ext}: 358 λ_{em}: 461	Blue

2.2.7 RNA extraction & reverse transcription

Hydrogels were removed from the culture well plate and placed into 500 µl of trizol reagent. The samples were allowed to stand at room temperature for approximately 10 minutes to allow the hydrogel biomaterials to fully dissolve within the reagent.

0.1 ml of chloroform was added to each tube, shaken vigorously and allowed to incubate at room temperature for 2 minutes. Samples were then centrifuged at 12000 g for 5 minutes at 4°C to separate each sample mixture into a lower phenol-chloroform and an upper aqueous phase.

The aqueous phase was carefully aspirated from each sample and placed into a clean eppendorf tube to carry out RNA isolation. The phenol-chloroform phase was stored at 4°C for protein extraction.

To the aqueous phase 5 µl of a 3mg/ml glycoblue solution was added to each sample followed by 250 µl of isopropanol. Glycoblue is a blue dye conjugated to glycogen. Glycogen is precipitated with RNA in alcohol and its addition serves as a means of visualising RNA by way of producing a blue pellet during the extraction procedure. Samples were mixed by inverting each tube lightly and then incubated at room temperature for approximately 10 minutes. After incubation, samples were centrifuged at 12000g for 10 minutes at 4°C. The supernatant was aspirated to waste and the pellet washed in 500 µl of 75% ethanol solution. Samples were then centrifuged at 7500g for 5

minutes at 4°C to draw down the pellet. The supernatant was aspirated to waste and the pellet allowed to air dry. The pellet was then resuspended in 20 µl of RNase free water and incubated for 10 minutes on a heat block set to 55°C. to dissolve the RNA. Samples were stored at – 80°C until ready for use.

Reverse transcription was carried out using the QuantiTect reverse transcription kit (Qiagen) as per the manufacturers' instructions. Resultant cDNA samples were then stored at -20°C or used immediately for qRT-PCR experiments.

2.2.8 QRT-PCR analysis

Human specific primers designed to detect a number of differentiation biomarkers (Table 2-3) was done using the universal probe library assay design centre available from Roche Applied Sciences (RocheAppliedSciences). PCR was carried out using a 7500 Real time PCR system & corresponding software (Applied Biosystems, UK). Samples had a total reaction volume of 20 µl containing 2 µl of cDNA, each reverse and forward primer at a final concentration of 100 µM and analysed using SYBR green chemistry. Samples were held at 50°C for 2 minutes then 95°C for 10 minutes then amplified using 95°C for 15 seconds and 60°C for 1 minute for 40 cycles. The specificity of the PCR amplification was checked with a heat dissociation curve (measured between 60 – 95°C) performed subsequent to the final PCR cycle. Gene expression levels were standardised using glyceraldehyde-3-phosphate dehydrogenase (GAPDH) as an internal control. Quantification analysis was performed using the comparative ΔΔCt method (Schefe et al., 2006) and gene expression calculated as fold change relative to the defined control sample. Details of the PCR primers used within this chapter are given in Table 2-3

Table 2-3 PCR primers designed for human genes

Gene		
PPAR-γ	Forward	5'-TGT GAA GCC CAT TGA AGA CA-3'
	Reverse	5'-CTG CAG TAG CTG CAC GTG TT-3'
GLUT-4	Forward	5'-ATG TTG CGG AGG CTA TGGG-3'
	Reverse	5'-AAA GAG AGG GTG TCC GGT GG-3'
RUNX-2	Forward	5'-GGT CAG ATG CAG GCG GCC-3'
	Reverse	5'-TAC GTG TGG TAG CGC GTC-3'
OPN	Forward	5'-AGC TGG ATG ACC AGA GTG CT- 3'
	Reverse	5'-TGA AAT TCA TGG CTG TGG AA -3'

SOX-9	Forward	5'-AGA CAG CCC CCT ATC GAC TT-3'
	Reverse	5'-CGG CAG GTA CTG GTC AAA CT-3'
Collagen type II (COL2A1)	Forward	5'-GTG AAC CTG GTG TCT CTG GTC-3'
	Reverse	5'-TTT CCA GGT TTT CCA GCT TC-3'
Nestin	Forward	5'-GTG GGA AGA TAC GGT GGA GA-3'
	Reverse	5'-ACC TGT TGT GAT TGC CCT TC-3'
β3-tubulin	Forward	5'-CAG ATG TTC GAT GCC AAG AA -3'
	Reverse	5'-GGG ATC CAC TCC ACG AAG TA-3'
GAPDH	Forward	5'-ACC CAG AAG ACT GTG GAT GG-3'
	Reverse	5'-TTC TAG ACG GCA GGT CAG GT-3'

2.2.9 Statistical Analysis

Suitable statistical tests were applied where warranted. Unpaired student t-tests were carried out using Microsoft excel for comparisons between two test groups. Analysis of variance (ANOVA) and Bonferroni post hoc tests were performed using GraphPad prism software to compare more than two study groups. One-way ANOVA was used when tests present with a single variant and two-way ANOVA for sample sets with more than one variable. Statistical significance is noted where the calculated probability that the null hypothesis is true (p-value) is less than 5% confident (0.05) using four biological replicates unless otherwise stated.

Mean values for replicate experiments, standard deviations (StDev) and standard error from the mean (SEM) were calculated using Microsoft excel.

2.3 Results & discussion

2.3.1 Hydrogel fabrication

The elastic properties of equimolar concentrations of Fmoc-F_2 and Fmoc-S (F_2/S) were tailored by pH manipulation of the peptide solution prior to formation of the hydrogels. Changes in the pH at time of gelation (range 7 – 8) gives rise to network cross-linking and fibre thickening resulting in differential hydrogel elasticity. Pre-gelation solutions where prepared at pH values of 7.2, 7.9 and 8.1. The cross linking and gel formation process was then stabilised at physiological pH by immersion in culture media. Immersion in culture also facilitates cross-linking of the peptide fibres due to the presence of divalent ion sourced from the culture media. An account of the step taken to

fabricate the F_2/S hydrogels is illustrated in Figure. Elastic properties of the substrate determined previously by Jayawarna *et al* using rheology are given in Table 2-4.

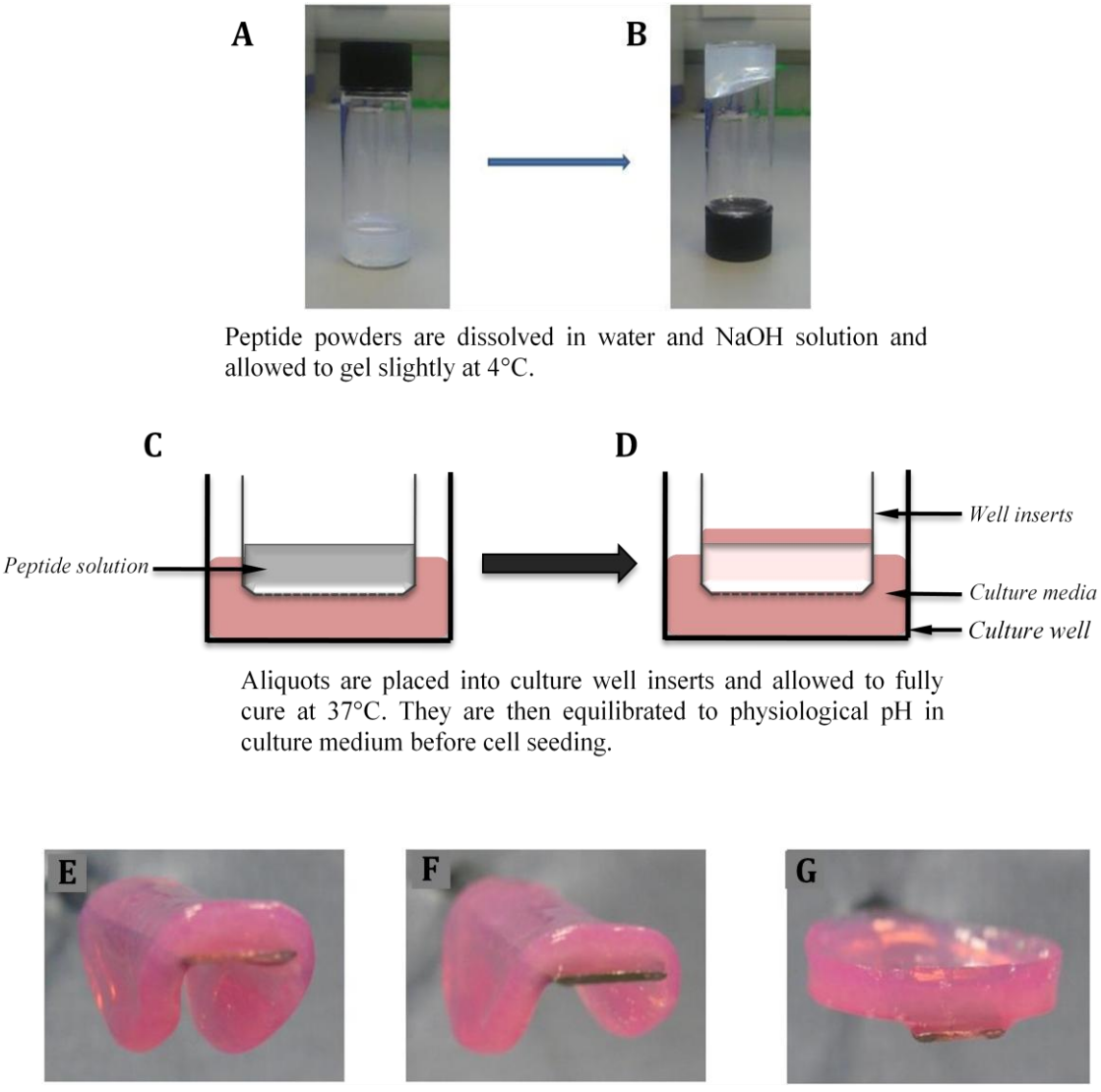

Figure 2-3 Schematic illustrating the process by which F_2/S hydrogel biomaterials are prepared prior to cell culture. *The rigidity or elastic moduli of the resultant hydrogel discs were determined by careful pH control of the peptide solutions prior to full gel formation. Fmoc-F_2 and Fmoc-S powders are first dissolved into solution and the pH of the peptide mixture tailored with NaOH (A). On standing, the solution then forms a highly viscous solution (B). This is then transferred to culture well inserts and allowed to gel fully at 37°C (C). The fully formed F_2/S hydrogels are then immersed in culture media and allowed to equilibrate to physiological pH prior to seeding (D). Representative images of the fully formed F_2/S hydrogel used for cell culture are shown in E – G. Approximate modulus for each F_2/S hydrogel was 2, 6 and 38 kPa respectively.*

Table 2-4 Hydrogel properties

	Soft Hydrogel	Stiff Hydrogel	Hard Hydrogel
0.5 M NaOH	130 µl	145 µl	155 µl
Peptide solution pH	7.2	7.9	8.1
Young's Modulus of resulting hydrogel	1.7 ± 0.45 kPa	6.36 ± 1.02 kPa	38.3 ± 0.86 kPa

2.3.2 Cell adhesion, viability & morphology

Phase contrast images of MSCs cultured on the hydrogel biomaterials differed morphologically from those cultured on the more conventionally used tissue culture plastic. Cells cultured on the hydrogels were observed as smaller in size and rounded compared to wider spread and flatter cells on culture well plastic (Figure 2-4). This is thought to be due to the nature of the biomaterial itself. When compared with tissue culture plastic, the substrates of all three hydrogels are orders of magnitude softer. Cells cultured on relatively soft substrates are known to inherently produce less focal adhesions than those on relatively harder surfaces (Bershadsky et al., 2003).

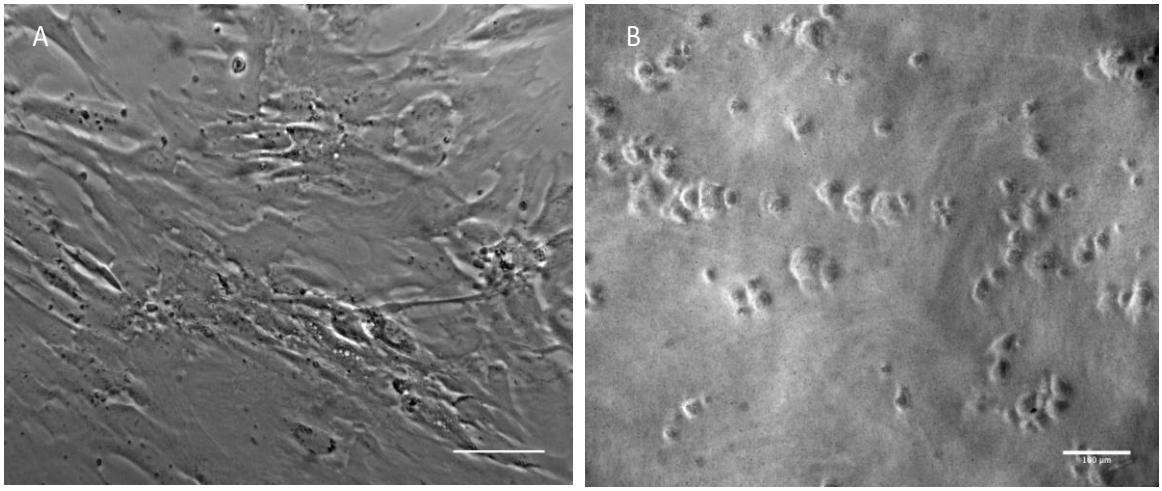

Figure 2-4 Phase contrast images showing the morphology of human mesenchymal stem cells seeded onto culture well polystyrene (A) and onto a 2 kPa F_2/S hydrogel surface (B). *The images illustrate the two distinctive morphologies that MSCs adopt when seeded on to each substrate. Cells seeded on well plates are flatter and widely spread compared to those on the hydrogels which are less spread and rounded in shape. Scale bar - 100µm.*

As the viability of the cells cultured on the F_2/S hydrogels cannot be determined by simply viewing under a light microscope, they were assessed for viability by monitoring fluorescence activity of calcein and propidium iodide. Using this method it was ascertained that cells cultured on each hydrogel were found to have a healthy population of live cells at each observed time point and as such, were deemed suitable for use within this duration (Figure 2-5).

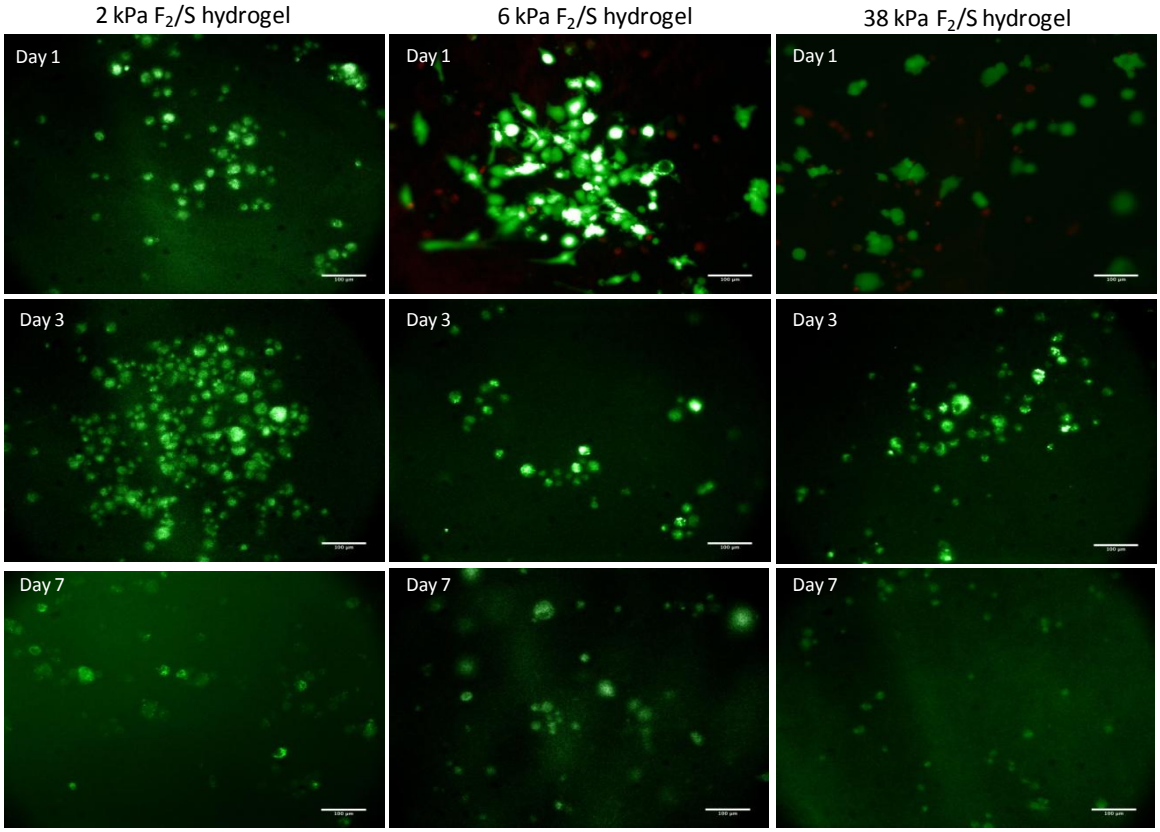

Figure 2-5 Fluorescence images showing viable cell populations of MSCs cultured on F_2/S hydrogel substrates. *Cells were cultured on 2, 6 and 38 kPa F_2/S hydrogels and assessed using live (green)/dead (red) viability staining. Fluorescence staining was carried out after cells had been in culture for 1, 3, and 7 days. MSCs showed good viability on all three F_2/S substrates indicating that they are suitable for cell culture. Scale bar - 100µm.*

Further investigation into the morphological characteristics of MSCs cultured on the F_2/S hydrogels were performed by assessing the substrate effects on cell spreading and cytoskeletal arrangement using fluorescence staining of f-actin (Figure 2-6). Measurements taken from distal tips of cells showed that cells on the 2 kPa hydrogel were generally longer than the remaining two hydrogels. There was no statistically significant difference in cell lengths between the 6 kPa and 38 kPa hydrogels. Examination of f-actin showed that cells cultured on the 2 kPa F_2/S surface form

cytoplasmic extensions similar to dendrites. Although it is not claimed that the cells form dendrites, dendrite out growth is characteristically driven by actin polymerisation via the Rho GTPases RhoA, Rac1 and Cdc42 (Hall, 1998, Swetman et al., 2002). It is however likely that the activation of Rac1 and Cdc42 (known to promote filopodia outgrowth) over RhoA produces the same type of effect observed with cells cultured on the 2 kPa hydrogel and to a lesser extent on the 6 kPa, a phenomenon that is also noted to be dependent on substrate property (Engler et al., 2006, Kuhn et al., 1998, Swetman et al., 2002). It is a feature that may, however, be related to constrictions the cells experience due to differences in the physical cross-links formed in each hydrogel type.

While this type of cytoskeletal arrangement is not typically observed of MSCs *in vitro*, this type of conformation; filopodial outgrowth that extends over several micrometers through the extracellular matrix, is one that has been noted in MSCs monitored in chick embryo limb buds *in vivo* (Boehm et al., 2010, Kelley and Fallon, 1978, Sanders, 2013). Experiments performed by Sanders et al reported MSCs *in vivo* that possess actin based cytoskeletal protrusions that play an active role in cellular communication, facilitating the transport of sonic hedgehog protein into the extracellular space along long distances.

Rho contractility of the cytoskeleton for cells on the F_2/S substrates does not produce stress fibres like those typically seen on substrates such as glass cover slips but active rigidity sensing by the cell mean that they maintain their rounded morphology as they lose tension to the substrate (Schiller, 2013).

2.3.3 Cellular differentiation on substrate surfaces

The elasticity of the hydrogel biomaterials were tuned to mimic certain tissue types; adipose at 2 kPa, muscle at 6 kPa and osteoid (demineralised bone tissue) at 38 kPa (Engler et al., 2006) with the hypothesis that MSCs will interpret these properties and differentiate accordingly. As such, cells were stained for formation of cell types of typical mesenchyme lineage. In addition, cells were also checked for neuronal development as development along this lineage by MSCs has been observed on rigidity-tuned hydrogels (Kopen et al., 1999, Mareschi et al., 2006, Woodbury et al., 2002).

Immunofluorescent-labelled biomarkers showed that differential behaviour of cells on the F_2/S hydrogels were not as clear-cut as suggested by the aforementioned hypothesis. Cells showed a heterogeneous mix of lineages on the substrates staining positively for more than one cell lineage.

Cells cultured on the soft (2 kPa) F_2/S hydrogel surface stained positively for the early neurological biomarker nestin, adipogenic marker PPAR-γ and the chondrogenic marker SOX-9. There was no observed production of the osteogenic biomarker RUNX-2 (Figure 2-7).

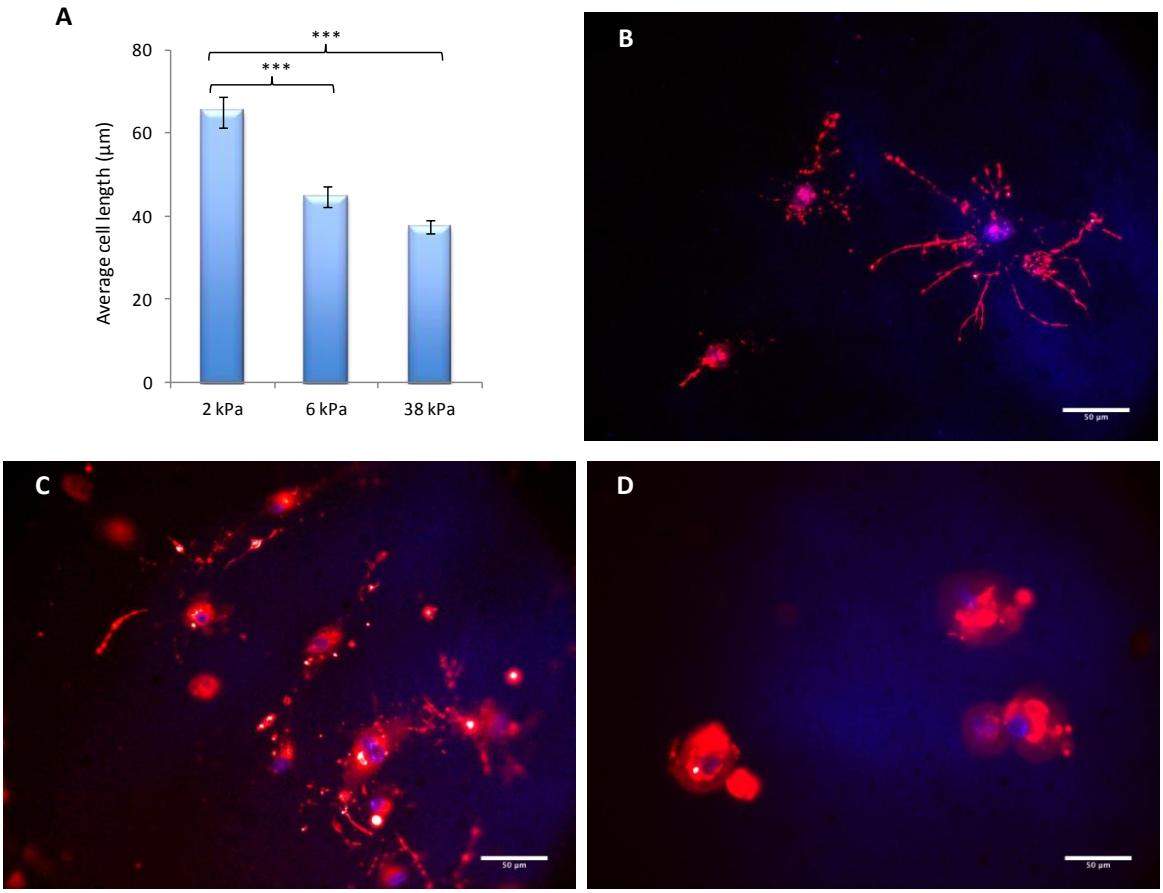

Figure 2-6 Analysis of morphological properties of MSCs cultured on 2 kPa, 6 kPa and 38 kPa F_2/S substrates. *Cells were analysed for degree of cell spreading (cell lengths measured from distal tips) on each substrate (A) and cytoskeletal properties (F-actin, shown in red and cell nucleus shown in blue) were also investigated (B-D). Cells cultured on 2 kPa F_2/S hydrogels (B) showed the presence of filopodia like out growths emanating from the cell body. Shorter processes were observed on the 6 kPa substrate (C) while cells on the 38 kPa substrate were lacking in the outgrowths showing a diffused actin composition (D). Error bars in (A) denote standard error; *** indicates statistical significance where $p < 0.001$ as calculated using one way ANOVA; $n > 40$; Scale bar – 50 µm.*

Cells cultured on the stiff (6 kPa) F_2/S hydrogel surface stained positively for nestin, PPAR-γ, SOX-9 and RUNX-2 with the highest population observed for PPAR-γ and SOX-9 (Figure 2-8). Cells cultured on the rigid (38 kPa) F_2/S hydrogel surface stained positively for nestin, PPAR-γ, SOX-9 and RUNX-2 with the highest population observed for SOX-9 and RUNX-2 (Figure 2-9).

Cells stained for myoblast formation (MyoD), as was expected for the stiff (6 kPa) hydrogel, did not give any positive results. As such it was concluded that the hydrogels did not support cell differentiation along the myogenic lineage.

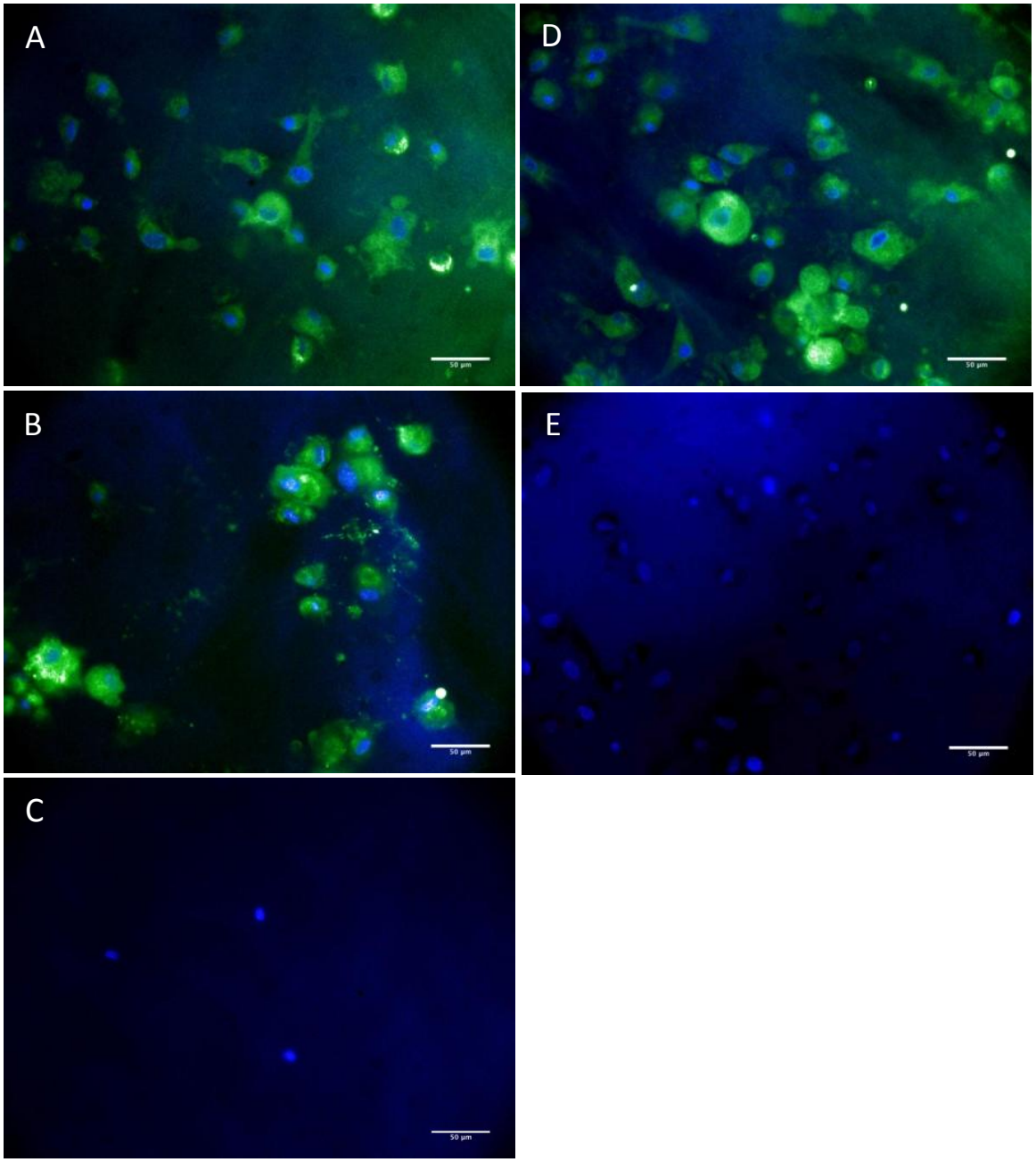

Figure 2-7 Immunofluorescence microscopy images to ascertain phenotypical development of MSCs cultured on 2 kPa F_2/S hydrogel surfaces. *Cells were cultured on 2 kPa F_2/S surfaces and maintained for 1 week. Fluorescence staining was carried out for detection of the differentiation biomarkers (shown in green) nestin, for neurogenesis (A), PPAR-γ for adipogenesis (B), MyoD for myogenesis (C), SOX-9 for chondrogenesis (D) and RUNX-2 for osteogenesis (E). Cells had stained positively for neurogenic, adipogenic and chondrogenic development but were negative for myogenesis and osteogenesis. Cell nuclei are shown in blue (DAPI). Scale bar – 50 µm.*

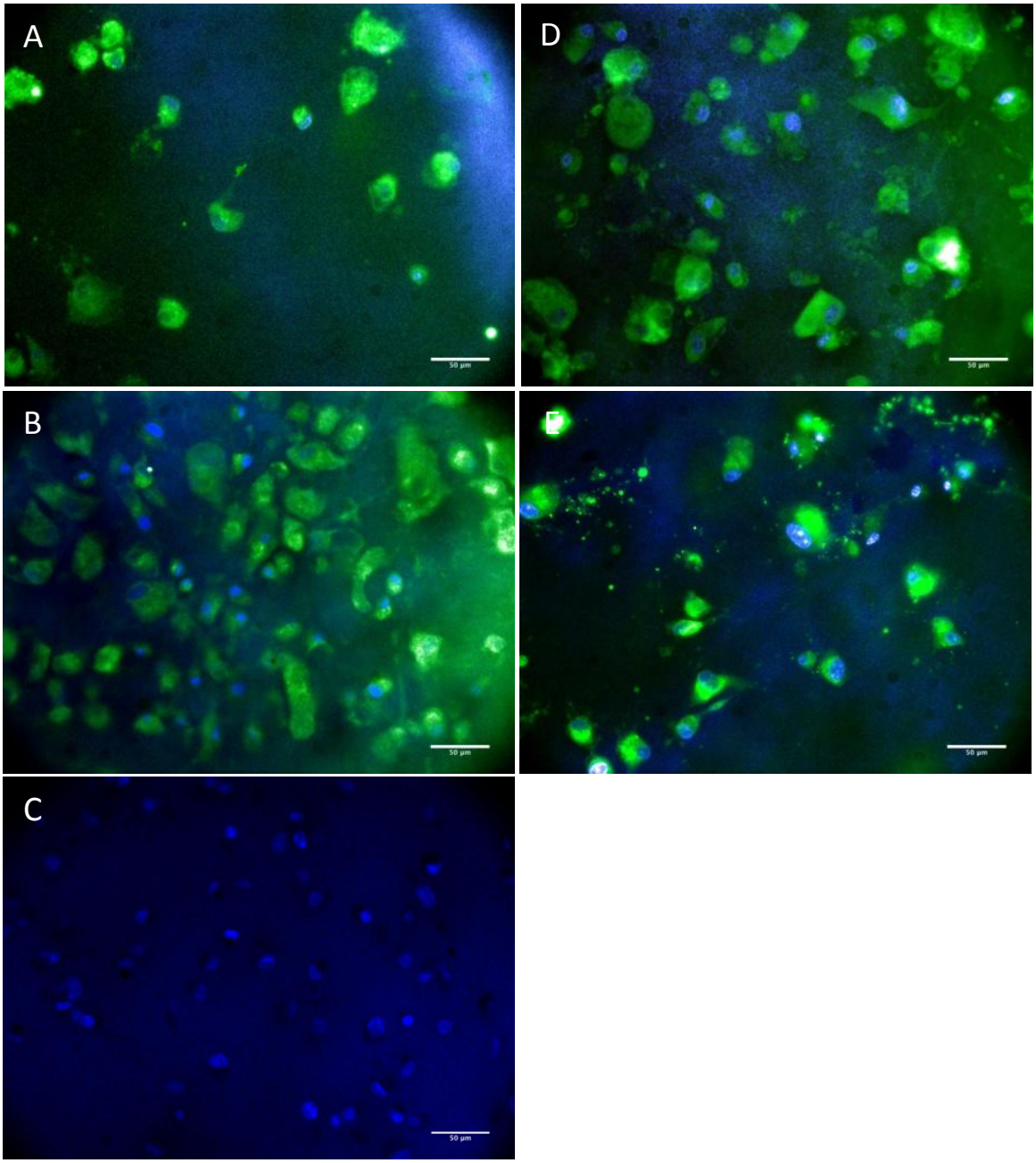

Figure 2-8 Immunofluorescence microscopy images to ascertain phenotypical development of MSCs cultured on 6 kPa F_2/S hydrogel surfaces. *Cells were cultured on 6 kPa F_2/S surfaces and maintained for 1 week. Fluorescence staining was carried out for detection of the differentiation biomarkers (shown in green) nestin, for neurogenesis (A), PPAR-γ for adipogenesis (B), MyoD for myogenesis (C), SOX-9 for chondrogenesis (D) and RUNX-2 for osteogenesis (E). Cells had stained positively for all tested lineages with the exception of myogenesis. Cell nuclei are shown in blue (DAPI). Scale bar – 50 µm.*

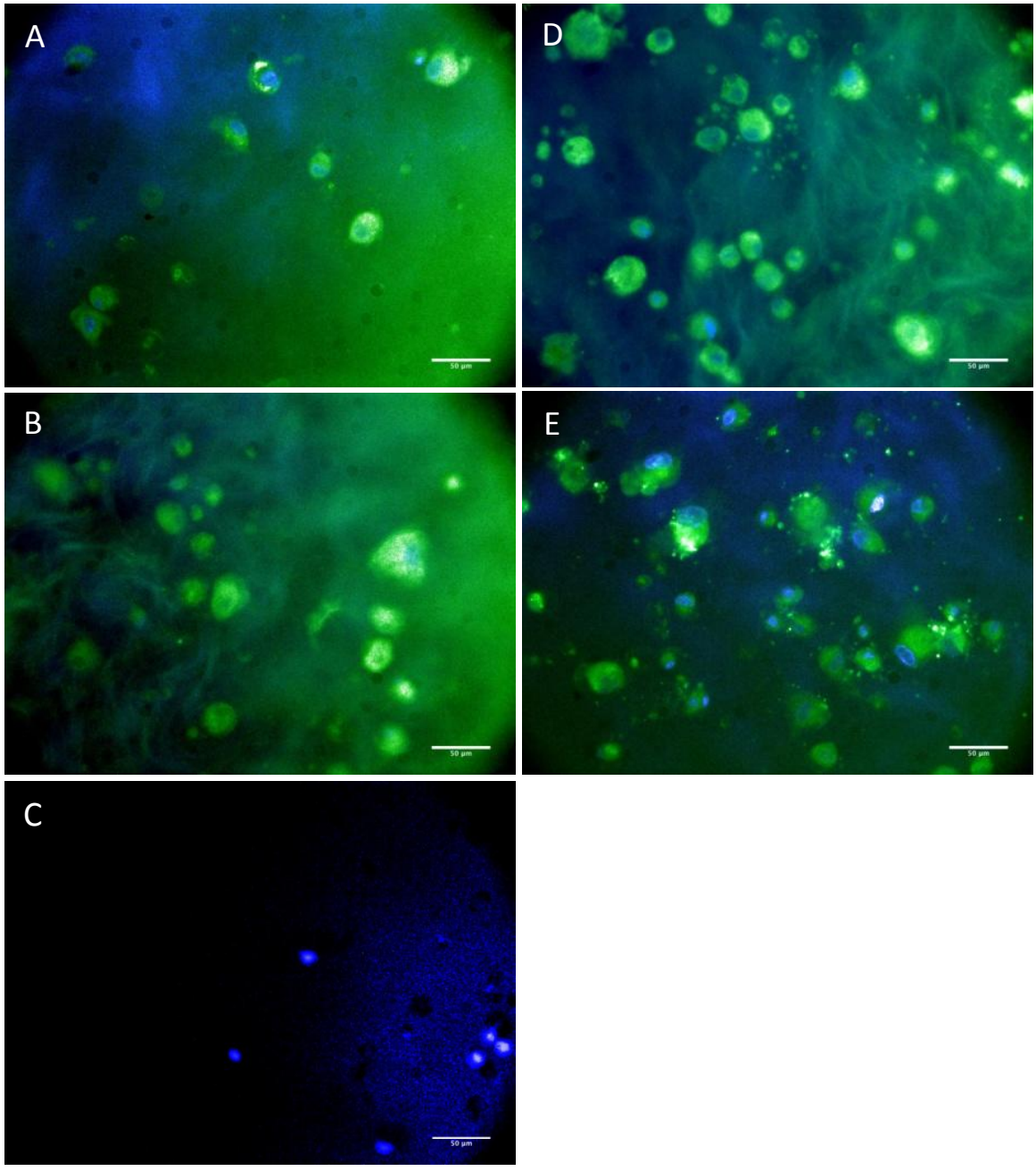

Figure 2-9 Immunofluorescence microscopy images to ascertain phenotypical development of MSCs cultured on 38 kPa F_2/S hydrogel surfaces. *Cells were cultured on 38 kPa F_2/S surfaces and maintained for 1 week. Fluorescence staining was carried out for detection of the differentiation biomarkers (shown in green) nestin, for neurogenesis (A), PPAR-γ for adipogenesis (B), MyoD for myogenesis (C), SOX-9 for chondrogenesis (D) and RUNX-2 for osteogenesis (E). Cells had stained positively for all tested lineages with the exception of myogenesis. Cell nuclei are shown in blue (DAPI). Scale bar – 50 µm.*

As the cells cultured on each of the F_2/S substrates had stained positively for a number of cell lineages using immunocytochemistry techniques, the degree to which the observed population heterogeneity had occurred was then ascertained by quantifying biomarker gene expression on each of the substrate types using qRT-PCR.

Cells were analysed for expression of early and subsequently expressed biomarkers particular to neuronal, adipogenic, chondrogenic and osteogenic development after 1 week in culture.

While also reflecting the heterogeneity observed using immunofluorescence, quantitative results obtained by qRT-PCR was able to give a more defined picture of the adopted differentiation lineages of cell populations cultured on the hydrogels. From this, primary differentiation lineages on each F_2/S were determined.

Cells on the 2 kPa substrate showed high expression of nestin compared to the other two hydrogels suggesting initial differentiation along the neuronal route. Elevated levels of β3-tubulin were also observed for cells cultured on this substrate albeit not statistically significant (Figure 2-10). A statistically significant increase in GLUT-4 expression was also noted on this hydrogel illustrating adipogenic development. Levels however, were far less compared to that observed for nestin and β3-tubulin (approximately 900 and 8 times respectively). On the 6 kPa substrate, type II collagen was observed to have the highest expression of all tested genes (Figure 2-11). In addition, SOX-9 levels were also observed to be highest on the 6 kPa hydrogels compared to the 2 kPa and 38 kPa substrates – expression levels of SOX-9 were approximately 17 times greater on 6 kPa than on 38 kPa F_2/S and 194 times higher than measured on 2 kPa F_2/S.

Cells cultured on the 38 kPa substrate showed highest expression of osteopontin (Figure 2-12). The earlier expressed RUNX-2 was also observed as showing higher expression on the 38 kPa hydrogel compared to the remaining two substrates – expression levels of RUNX-2 were approximately 5 times greater on 38 kPa than on 6 kPa F_2/S and 14 times higher than measured on 2 kPa F_2/S.

Although there is some underlying overlap, these results suggest that the stiff (6 kPa) and rigid (38 kPa) substrates are best adept at influencing chondrogenic and osteogenic development respectively.

Relative to the control, expression of adipogenic markers PPAR-γ and GLUT-4 were found to be elevated on all three substrates but did not show any preference to any one substrate in particular.

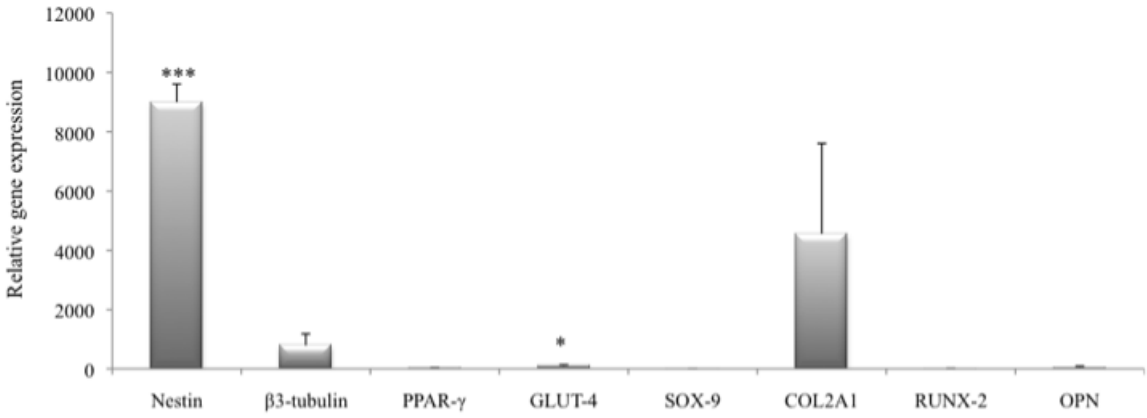

Figure 2-10 Gene expression analysis of MSCs undergoing phenotypical development on 2 kPa F_2/S hydrogel surfaces. *Cells were cultured for 1 week on 2 kPa F_2/S hydrogels and samples subsequently analysed for expression of early and latterly expressed differentiation specific biomarkers. Cells were analysed for production of nestin & β3-tubulin for neurogenesis, PPAR-γ & GLUT-4 for adipogenesis, SOX-9 & COL2A1 for chondrogenesis and RUNX-2 & OPN for osteogenesis. Gene expression was measured as fold change compared to cells maintained on plain surfaces as a negative control (held nominally at 1). Error bars denote standard error from the mean; n = 4 replicates; * notes statistical significance compared to the control where $p < 0.05$ and *** where $p < 0.001$ as calculated using one way ANOVA followed by Bonferroni post hoc tests.*

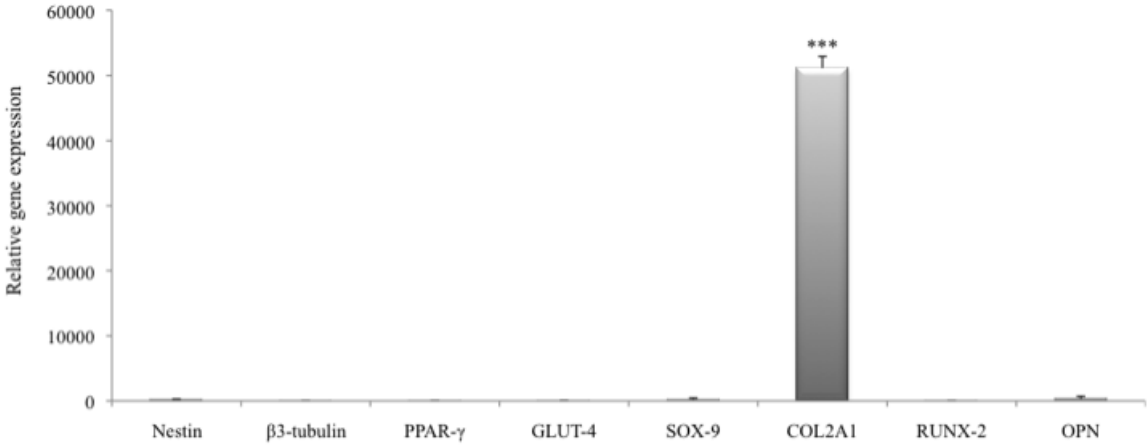

Figure 2-11 Gene expression analysis of MSCs undergoing phenotypical development on 6 kPa F_2/S hydrogel surfaces. *Cells were cultured for 1 week on 6 kPa F_2/S hydrogels and samples subsequently analysed for expression of early and latterly expressed differentiation specific biomarkers. Cells were analysed for production of nestin & β3-tubulin for neurogenesis, PPAR-γ & GLUT-4 for adipogenesis, SOX-9 & COL2A1 for chondrogenesis and RUNX-2 & OPN for osteogenesis. Gene expression was measured as fold change compared to cells maintained on plain surfaces as a negative control (held nominally at 1). Error bars denote standard error from the mean; n = 4 replicates; *** notes statistical significance compared to the control where $p < 0.001$ as calculated using one way ANOVA followed by Bonferroni post hoc tests.*

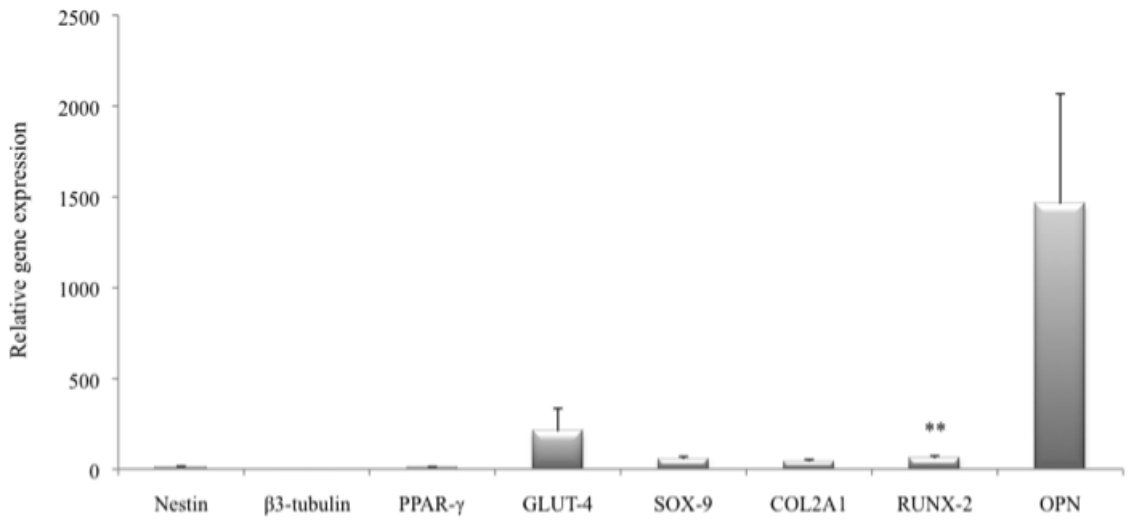

Figure 2-12 Gene expression analysis of MSCs undergoing phenotypical development on 38 kPa F_2/S hydrogel surfaces. *Cells were cultured for 1 week on 38 kPa F_2/S hydrogels and samples subsequently analysed for expression of early and latterly expressed differentiation specific biomarkers. Cells were analysed for production of nestin & β3-tubulin for neurogenesis, PPAR-γ & GLUT-4 for adipogenesis, SOX-9 & COL2A1 for chondrogenesis and RUNX-2 & OPN for osteogenesis. Gene expression was measured as fold change compared to cells maintained on plain surfaces as a negative control (held nominally at 1). Error bars denote standard error from the mean; n = 4 replicates; ** notes statistical significance compared to the control where $p < 0.01$ as calculated using one way ANOVA followed by Bonferroni post hoc tests.*

2.4 Summary

Mesenchymal stem cells were found to be viable on all three F_2/S hydrogel types (2, 6 and 38 kPa) over the time period tested (1 week). It was also noted that cells did not adopt the spread morphology as when maintained on culture well plastic but adopted a rounded morphology. This difference is thought to be due mainly to the structural properties and the tensile strength offered by the substrate itself as the cells perform a 'balancing act' to achieve a state of equilibrium with their microenvironment.

When tested for expression of specific differentiation markers, MSCs were found to be positive for a number of lineages using immunocytochemistry inferring that although the cells do undergo differentiation, the cells tend to adopt a heterogeneous population suggesting that interpretation of mechanical properties of the substrate is of a transcendent nature. That is, a degree of overlap exists in cell interpretation on differentiation as opposed to the substrate having a restrictive or defined effect on what differentiation lineage is permissible.

However, in order to determine what primary differentiation lineages were adopted by MSCs on each hydrogel type, a quantitative approach was used measuring relative gene

expression of each biomarker from cells cultured on each hydrogel. From this, it was ascertained that the 2 kPa hydrogels promoted neurological development, the 6 kPa hydrogel chondrogenesis and osteogenesis on the 38 kPa hydrogel. The variations in cell processes or activity that occurs as MSCs begin to develop into the determined phenotypes will be further explored in the following chapter.

3 METABOLOMICS AS A TOOL FOR ILLUSTRATING DIFFERENCES IN CELL PHENOTYPE

3.1 Introduction

The breadth of metabolomics has enabled the development of a number of structured approaches in its continuous efforts at unravelling the metabolome. These options require a preformed idea of what it is the researcher is pursuing and available options are then tailored toward achieving the aim as best possible. Selective methods for studying the metabolome are considered at every stage; from experimental design through to analysis of the results. This introduction makes mention of some but not necessarily all available analytical routes with particular focus on those that are used within this thesis.

3.1.1 Metabolite analysis

3.1.1.1 The targeted and untargeted approach

Targeted analysis encompasses the measurement or quantitation of a single or small number of known metabolites affected within a certain pathway and is more or less the method of choice for carrying out metabolite/metabolic analysis of specific pathways or classes of biomolecules. Metabolites investigated are of a known interest and analysis is focused around the behaviour of the molecule(s) in question. Compounds within certain metabolic pathways usually bear related chemistries and methodologies are concentrated around optimisation for these classes of molecules.

While consideration is given to sample extract and clean up methods, it depends mostly on chromatographic separation of metabolite moieties and the specificity of detection. Targeted analysis is generally employed where specificity and accuracy in quantitation are of particular importance such as drug screening, design, toxicology or enzyme kinetics.

Untargeted analysis, on the other hand, is closer to metabolomics in the defined sense and utilises the entirety of small mass molecules that can be detected or measured within the restriction of the chosen methodology. As this method bears less constraints on metabolite detection compared with using a targeted approach, its means for investigation include a broad, if not the entire range of extraction, separation and detection methods that best suit the study.

3.1.1.2 Fingerprinting & footprinting

Both fingerprinting and footprinting can be done using targeted or untargeted measurements coupled with high throughput methodologies. Analysis is performed by way of semi-quantitation of detectable metabolites within the system which may or not be wholly identified (Dunn et al., 2005). Fingerprinting is referred to general analysis of

sample extracts, focussing on the intracellular complement of metabolites - also referred to as the endometabolome (Nielsen and Oliver, 2005, Oldiges et al., 2007). Footprinting, on the other hand, refers to the analysis of metabolites expelled or exhausted by the cells into the culture system, termed the exometabolome (Allen et al., 2003, Nielsen and Oliver, 2005). This method in some respects is particularly advantageous as it is non-invasive, negates the need for rapid quenching techniques to preserve the cell metabolome accurately, as is required for fingerprinting and measurement variations brought about through sample handling is lessened.

This chapter makes use of an untargeted fingerprint approach. It aims to measure the metabolome, incorporating as wide a range of chemistries possible to acquire as much information as the method allows for investigating cell behaviour. Fingerprinting was favoured over footprinting as it is thought better suited to stem cell culture. It is thought that footprinting will not provide any discernible information due to the fact that early stage differentiation is generally characterised by internal changes in cell activity (Salti et al., 2013). Also, changes occur on a less rapid timescale compared to yeast cultures for example (Hojer-Pedersen et al., 2008, Raamsdonk et al., 2001), measuring accurate changes in media composition are therefore inevitably hampered by cell maintenance over time through constant media changes for the duration of the experiment.

3.1.2 Analytical methodology

To collect reliable metabolome datasets, uniformity of culture and sampling conditions, as well as the cellular metabolic state are crucial. For this reason, method standardisation becomes important (Oldiges et al., 2007). There is no set standard protocol for sample preparation, as samples subject to metabolomic analyses tend to vary widely from microbes to plants and human samples (Hojer-Pedersen et al., 2008, Raamsdonk et al., 2001, Maharjan and Ferenci, 2003, Tsimbouri et al., 2012). It is also dependent on the fraction of the sample to be investigated. For example, samples to be processed come in a variety of forms; from urine and whole blood to tissue samples. Each of these is handled differently in order to extract metabolites in as efficient a manner possible. As such, the first port of call is deciding on what type of extraction procedure is suited to the experimental demands.

3.1.2.1 Metabolite extraction

For global untargeted metabolite analysis, extraction methods ideally should be non-specific, able to recover the largest population of metabolites possible and have little or non-detrimental effects on the metabolite by elimination or modification. The rapid

turnover of some cell processes, like glycolysis for example, requires that cell-quenching methods are particularly effective and the use of appropriate controls compensate for any differences experienced from the native state.

Traditionally, quenching and extraction is performed using methanol (although ethanol is also widely used) in a variety of ways, ranging from 100% - 50% content either as a cold or hot solution (Dietmair et al., 2010, Maharjan and Ferenci, 2003, Paglia et al., 2012). Methanol also is of added advantage for metabolic fingerprinting, as it is known to cause protein denaturation, damaging the cell membrane and allowing the expulsion of intracellular metabolites. A number of studies looking into the extraction efficiencies of a number of solvents have shown that extraction solvents tend to be more favourable for a certain class of compounds over another dependent of their make up (Dietmair et al., 2010, Maharjan and Ferenci, 2003). For example, the extraction efficiency and total abundance of polar metabolites are best in solution like methanol or perchloric acid but is lowered when extracted in the less polar 1:1 v/v solution of methanol:chloroform (Maharjan and Ferenci, 2003). On the whole, tempering one extraction solvent with another can affect the extraction efficiencies, as solubility of some metabolites are duly affected but it broadens the range of metabolite species contained within the sample as it no longer caters for the extraction of a single class of compounds (Dietmair et al., 2010, Maharjan and Ferenci, 2003, Tokuoka et al., 2010).

The wide range of chemistries of metabolites makes this a difficult task to incorporate every species in its entirety, and inevitably, some metabolites are compromised (through low or null extraction efficiencies) for the sake of the majority.

3.1.2.2 Metabolite separation

On acquisition of a pool of metabolite species, the next step in isolating individual metabolites is their separation from one another. Separation is generally performed based on the physicochemical properties of each compound, enabling exclusion based on characteristics such as size and polarity amongst others.

A number of separation methods are widely used in metabolomics, these are inclusive of capillary electrophoresis, gas chromatography and liquid chromatography.

Separation by liquid chromatographic methods conventionally employ the use of a two phase system; a stationary and mobile phase. Metabolite separation is dependent on optimisation of the interplay between the stationary phase (usually C8 or C18 columns) as the retentive agent interacting with the metabolite and the mobile phase (which consists of aqueous and organic solvent phases) as the eluting agent prior to introduction to the detection system.

For studying the metabolome, the use of Hydrophilic Interaction Liquid Chromatography (HILIC) has become widely popular, its main attraction being that it is particularly effective at the separation and elution of small polar molecules (Paglia et al., 2012). As cells constitute a high degree of water, it can be put forward that a high population of its metabolome are very likely polar molecules, a system that can make distinctions within the majority therefore such as HILIC makes it a highly desirable tool for metabolomics.

HILIC combines a number of characteristics employed by the three mainstream chromatographic methods; reverse phase for mobile phase eluent, allows organic solvents for molecules to stay in solution (> 50% organic), this less viscous composition also allows for better separation of strongly polar compounds compared to other available LC methods (Gritti et al., 2010); ion exchange, allowing the analysis of charged species and the adsorption stationery phase properties of normal phase LC.

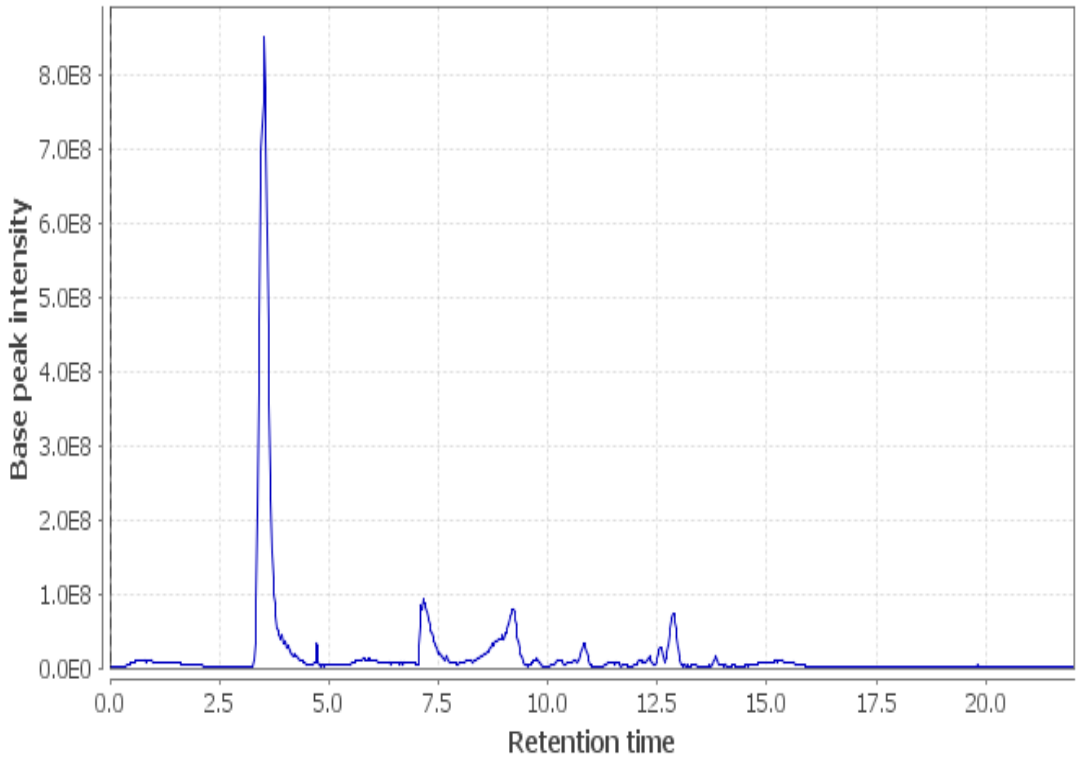

Figure 3-1 Total ion chromatogram (TIC) showing separation of extracted stem cell metabolites. *The chromatogram shows the separation of the entire metabolite population obtained from cell sample extraction using HILIC. Metabolites elute from the column in order of increasing polarity, allowing increased retention of polar molecules while non-polar metabolites are eluted earlier (Alakpa, unpublished data).*

3.1.2.3 Detection

There are a number of options that can be used for detection of separated metabolite species within a sample, these are generally spectrometric methods inclusive of ultraviolet (UV), fluorescence, Raman, nuclear magnetic resonance (NMR) and by mass analysis; typically mass spectroscopy (MS). Both NMR and MS allows detection based on a broad scope of properties inclusive physical, chemical and structural characteristics using separation & mass analysis in MS or chemical shifts due to magnetic resonance in NMR. Due to the reduced sensitivity of NMR spectroscopy however, it is often used in conjunction with MS, or MS can be utilised as the sole detection resource.

Mass spectrometry in itself, allows the analysis of the principal composition of a sample by measuring the presence and abundance of ionised molecules in the form of a single spectrum of the charged (ionised) species relative to its molecular weight (mass to charge ratio, m/z). As such, broad analysis of the constituents of a system is best described by this method. Information garnered by mass spectrometry can sometimes involve the use of multiple mass analysis stages in time or space (MS/MS or MS^n), typically referred to as tandem mass spectrometry. Structural information of a singular ion of interest detected on first mass analysis (MS) can be obtained by fragmentation of that specific mass, producing daughter ions, which are subsequently re-analysed (MS/MS). Fragmentation patterns of a parent ion offer high specificity in distinguishing it from others of similar mass, as fragmentation patterns are often specific to its parent ion aiding molecule identification.

Mass spectrometry itself incorporates a broad range of mass analysers – quadrupole, ion trap, Fourier transform (FT) and time of flight (TOF) based on the physics that is used to build each mass analyser.

The orbitrap mass spectrometer is based on the phenomenon of orbital trapping of ions around a central dielectric (Kingdon, 1923, Makarov et al., 2006) and integrates a number of features from the previously mentioned mass analysers (Figure 3-2). The orbitrap mass analyser allows for measurements with high mass accuracy and resolution, enabling distinction between a number of molecules that have similar descriptive masses, typically to less than 1 part per million (ppm) with use of locked mass internal calibration.

Mass spectrometry, typically coupled to liquid chromatography separation and in tandem is referred to as liquid chromatography-mass spectrometry (LC-MS). Typical data acquisition file obtained from an LC-MS sample injection is shown in Figure 3-3.

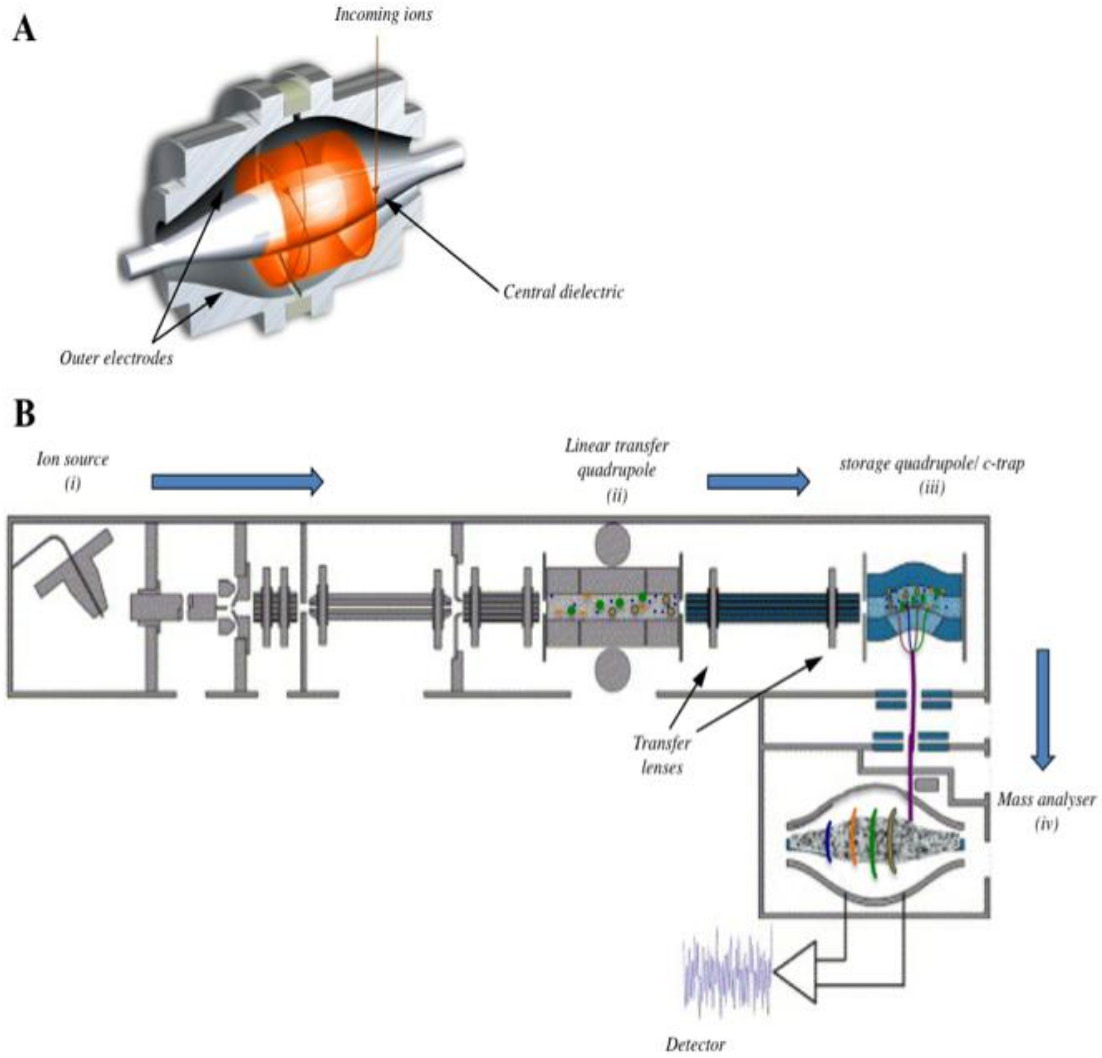

Figure 3-2 Illustration of a cross section through an orbitrap mass analyser (A) and schematic of a linear transfer quadrupole (LTQ) orbitrap mass spectrometer*. (A) Ions sequestered in the storage quadrupole are injected perpendicular to the long axis. Tailored voltage parameters between the central and outer electrodes create a radial electric field and centrifugal force, which holds the ions in a near circular trajectory about the central electrode. Image adapted from Scigelova & Krusel, Thermo Fisher scientific. (B) Ions are produced at the electrospray ion source where the samples are introduced into the MS (i). Ions then pass through the LTQ (ii) into the storage quadrupole (iii) where they are sequestered facilitating a link between a continuous electrospray ion source and a pulsed orbitrap mass analyser (iv). The central electrode also acts as a receiver digitised current detection of oscillating ions, which is ultimately represented as a time acquired mass spectra. Image B adapted from Makarov et al, 2006.*

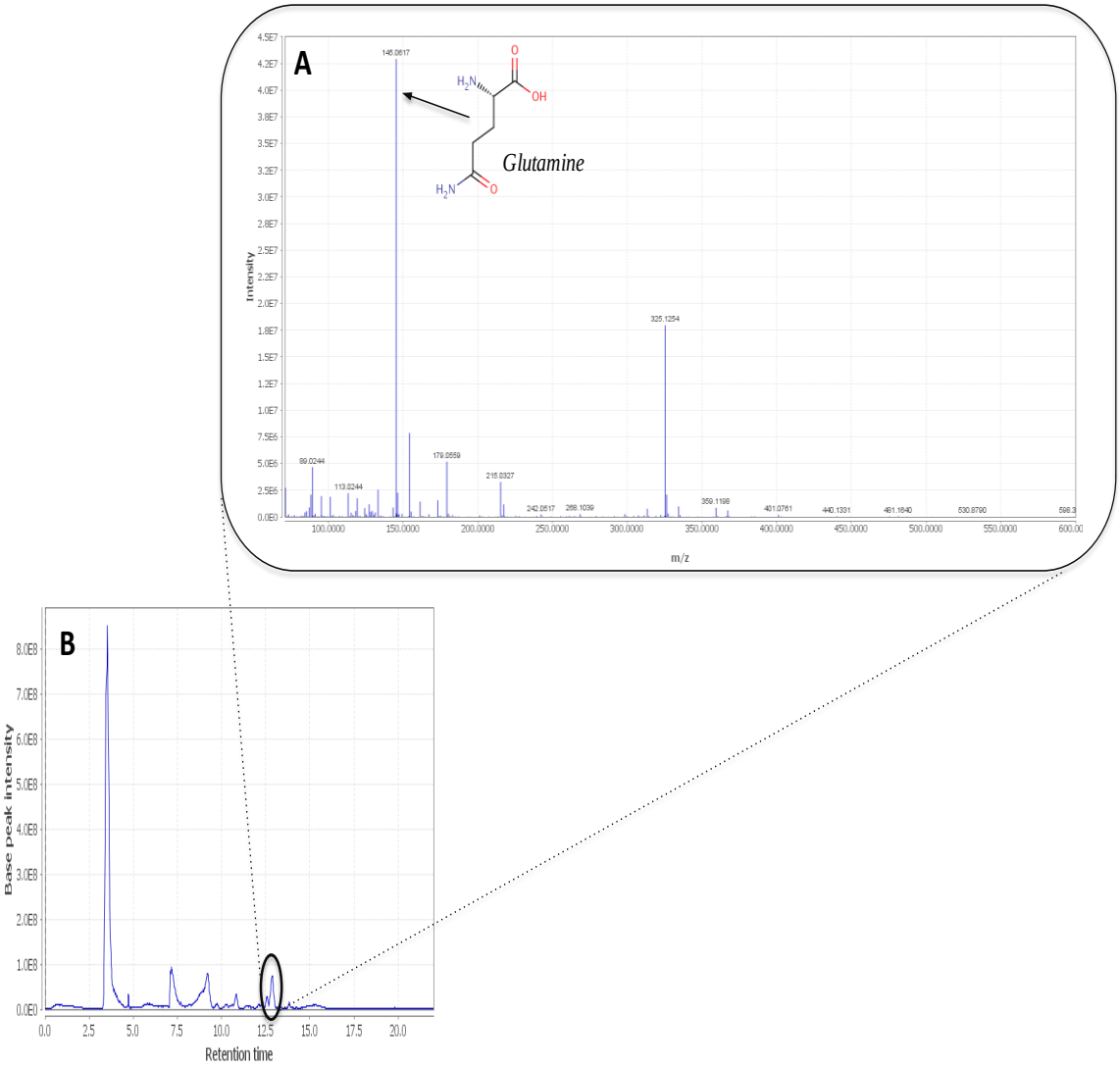

Figure 3-3 Diagram illustrating a mass spectrum obtained from a TIC. *The spectrum shows the array of metabolite masses detected by MS between m/z 70 – 600 (A) at the chromatogram peak retention time of 13 minutes (B). Putative identification of the amino acid glutamine (m/z – 145.0617) is also highlighted on the spectrum (A). Alakpa, unpublished data.*

3.1.3 Bioinformatics

The process of extraction, separation and detection, especially with regards to a global metabolomics study, typically generates a large volume of numerical output. How then to handle all this data and morph it into something which describes the system as a whole inevitably becomes an important focus. To do this, pattern analysis models are generated to analyse linear or non-linear correlation patterns, and in this manner different biological systems are elucidated using a data driven process (Hogeweg, 2011).

It is not surprising then that of all the steps in the metabolomics work flow, data analysis and interpretation is the most time consuming. Garnering information relies heavily on good visualisation of numerical output for comparisons and conclusions to be made. Prior knowledge of various biochemical processes also allows the integration with transcriptome and proteome data to create network pathways, putting interconnected biological activity into context.

This chapter incorporates the use of several bioinformatics platforms to analyse, visualise and interpret the data generated (Creek et al., 2011, Creek et al., 2012, Leader et al., 2011, Scheltema et al., 2011, Xia et al., 2009), inclusive of metabolite mass identification by cross referencing a number of available databases, uni- and multivariate statistics, correlation analysis and pathway networking.

A comprehensive list for software on pathway and interactome resources can be found at www.pathguide.org.

3.1.4 Objective

Being able to influence the differentiation behaviour of mesenchymal stem cells through substrate mechanics is a non-invasive means of effecting cellular changes. That is, cells are not pushed into differentiation by interfering directly with signalling pathways but are directed through the action of micro-environmental interpretation by the cells themselves. By effecting phenotypical changes without chemical means, naturally occurring cellular activity reflects innate behaviour as the cells undergo initial differentiation. By employing the earlier described metabolomics workflow adapted to fit the experimental objective (Figure 3-4), obtaining a snapshot of the metabolome should give insight into cell activity as it undergoes initial differentiation, reflecting changes that occur in its metabolite pool to alter phenotype.

This chapter aims to ascertain whether the use of an unbiased global metabolomics approach can detect metabolic changes that occur as MSCs adopt a newly acquired phenotype on differentiation.

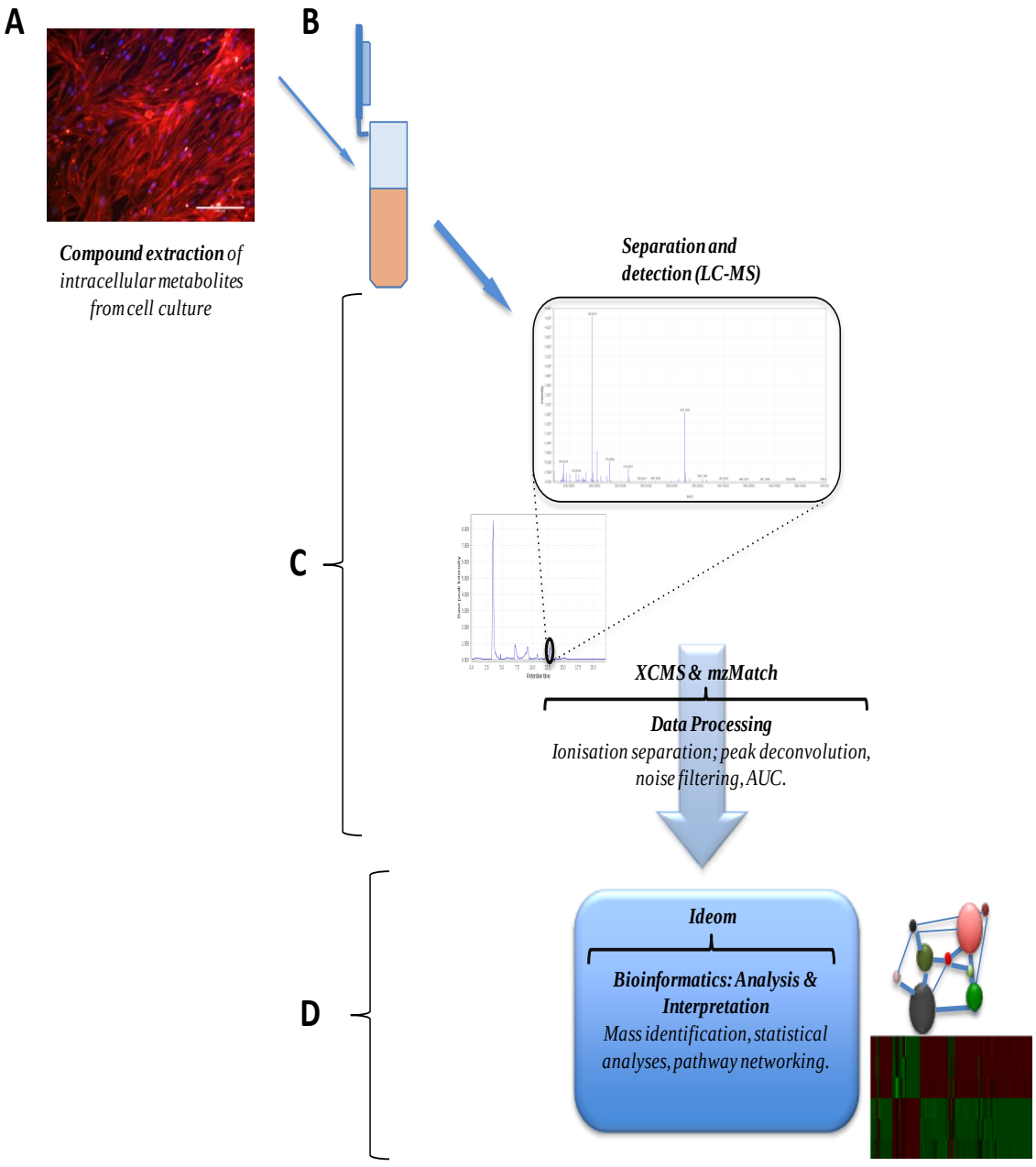

Figure 3-4 Schematic summarising the metabolomics workflow. *The figure illustrates the working protocol undertaken for this chapter. Cells cultured on biomaterial substrates (A) had their intracellular metabolite content extracted and pooled (B) then separated and detected using LC-MS (C) and the obtained data subject to identification analysis and interpretation (D). The metabolite information garnered gives an insight into the physiological state of the cell(s) at the time of extraction*

3.2 Materials & methods

3.2.1 Materials

Materials/reagents	Supplier(s)
Mesenchymal stem cells	Promocell GmBH, Germany.
Fmoc-diphenylalanine	Bachem, UK
Fmoc-serine	Bachem, UK
0.5 M sodium hydroxide	Fisher chemicals
Distilled water	Invitrogen, UK
Dulbeccos modified eagle medium (DMEM)	Sigma Aldrich, UK
Foetal bovine serum (FBS)	Sigma Aldrich, UK
Penicillin streptomycin	Sigma Aldrich, UK
Trypsin	Sigma Aldrich, UK
Isopropanol	Sigma Aldrich, UK
Ethanol	VWR Chemicals, France
Guanidine hydrochloride	Sigma Aldrich, UK
Sodium dodecyl sulphate (SDS)	Sigma Aldrich, UK
Bio-rad protein assay kit	Bio-Rad, UK
Tecan GENios microplate reader	Tecan Group, Switzerland
Chloroform	Sigma Aldrich, UK
Methanol	Sigma Aldrich, UK
Phosphate buffered saline (PBS) *	In-house
ZIC-HILIC pre column, sulfobetaine functional group, 20 x 2mm	Merck Sequant, Sweden
ZIC-HILIC chromatography column, sulfobetaine functional group, 150 x 4.6mm	Merck Sequant, Sweden
Acetonitrile	Sigma Aldrich, UK
Formic acid	Sigma Aldrich, UK
Ultimate 3000 RSLC LC system	Thermo Finnigan, UK
Orbitrap Exactive mass spectrometer	Thermo Finnigan, UK
Xcalibur, version 2.1 (acquisition software)	Thermo Finnigan, UK

* Preparation procedures for reagents and buffers made in house are detailed in the appendix

3.2.2 Hydrogel fabrication & cell culture

Hydrogel substrates (2, 6 & 38 kPa) were fabricated and used for culturing MSCs as described earlier in sections 2.2.3. Cells were cultured for up to 1 week before harvesting for use in metabolomics experiments.

3.2.3 Protein extraction and measurements

Protein extracts were obtained from the same samples used to generate RNA extracts in the previous chapter using the phenol-chloroform extract.

750 µl of isopropanol was added to each phenol-chloroform extract and the mixture incubated at room temperature for 10 minutes. Samples were next centrifuged at 12000 g for 10 minutes at 4°C and the supernatant aspirated to waste. Pellets were then incubated for 20 minutes and washed three times with 1 ml of a 0.3 M guanidine hydrochloride solution made up in 95% ethanol. Samples were then centrifuged at 7500 g for 5 minutes at 4°C to draw down the pellet. The supernatant was aspirated to waste and the pellet washed thrice using 0.5 ml of a 0.3 M guanidine hydrochloride solution in 95% ethanol, incubated for 20 minutes at room temperature and then centrifuged at 4˚C, 7500 g for 5 minutes. The pellets were washed in 1ml of 100% ethanol by vortexing briefly and re-sedimented by centrifuging at 4˚C, 7500 g for 5 minutes. The ethanol was aspirated to waste and the pellets allowed to air dry for 10 minutes, the pellets were re-suspended in a 0.01% sodium dodecyl sulphate (SDS) solution by pipetting the solution up and down a number of times. The tubes were then incubated on a heating block at 55˚C for 10 minutes to dissolve proteins and centrifuged at 13000 g for 10 minutes to sediment any insoluble material. The supernatant was transferred into clean eppendorf tubes and used for subsequent protein assays.

Relative amounts of protein were determined using the Bio-Rad microassay procedure according to the manufacturers' protocol.

3.2.4 Metabolomics

3.2.4.1 Metabolite extraction assay

Metabolite extraction from samples were done using a solvent comprising chloroform:methanol:water (1:3:1, v/v). The methanol serves to disrupt cellular integrity and denature proteins. As a solvent for metabolites, the composition acts to incorporate a broad range of compounds from non-polar metabolites such a lipids on the one extreme (dissolved in chloroform) to more polar components on the other extreme contained within the methanol.

Hydrogel substrates were washed once with warm PBS solution and placed in clean culture well plates and 0.5ml of ice-cold extraction solvent (chloroform: methanol: water, 1:3:1 v/v) added. The culture well plates were then wrapped in parafilm and kept on ice (to minimise evaporation) and agitated gently on a shaker for one hour in a cold room (4°C). Samples were subsequently centrifuged at 13,000 g for 5 minutes to sediment cell debris and the supernatant transferred into vials to be analysed by LC-MS. Otherwise samples were aspirated into clean eppendorf tubes and stored at -80˚C until ready for LC-MS analysis.

A set of 'zeroes' (biomaterial with no cells seeded) was also taken through the methodology detailed above to act as a zero sample for mass spectrometric analysis.

3.2.4.2 LC-MS

5 µl of each sample used within a batch were pooled into a single aliquot to be used as a quality control (pooled QC). These were injected several times over the duration it took to run a single batch of samples to monitor metabolite quality and stability. Batches were also run with three standard samples; these contain a number of known metabolites used for identification and LC retention time predictions. 10 µl of each sample was injected onto the LC-MS system for analysis.

High performance liquid chromatography

Chromatographic separation of metabolites was done routinely using a zwitterionic hydrophilic interaction liquid chromatography (ZIC-HILIC) 150 x 4.6mm, 100Å column as the stationary phase, acetonitrile containing 0.08% formic acid as the organic mobile phase and water containing 0.1% formic acid as the aqueous mobile phase. The mobile phase was run as a gradient over 46 minutes, the details of which are given in Table 3-1.

A ZIC-HILIC 20 x 2.0 100A was also used as a guard column to protect the main column from impurities that may be strongly retentive or cause blockages on the main column. Chromatography columns were maintained at 25°C.

Mass Spectrometry

Mass spectrometry was performed using an Orbitrap Exactive accurate mass orbitrap mass spectrometer. Scans were performed at 50,000 resolution at 100 m/z in alternating positive and negative ion modes within the mass range 70 – 1400 m/z for the duration of the LC gradient.

Prior to acquisition, mass calibration was performed in both positive and negative modes using a calibration mix that contains a number of compounds with masses spanning the acquisition range.

Table 3-1 Gradient elution conditions used for chromatographic separation

Time (min)	Aqueous (%)	Organic (%)	Flow rate	Curve
0	20	80	0.3ml/min	1
30	20	80	0.3ml/min	6
32	80	20	0.3ml/min	6
40	95	5	0.3ml/min	6
42	95	5	0.3ml/min	6
46	20	80	0.3ml/min	6

3.2.4.3 Data processing

Raw data file conversion, chromatographic peak selection and metabolite identification were done using IDEOM/MzMatch Excel interface (Creek et al., 2012, Scheltema et al., 2011) and measured chromatographic peak intensities (area under the curve) by LC-MS were normalised against calculated protein content. Identification was done using a set of known standards to define mass and chromatographic retention times, as mentioned previously. Putative metabolites were also identified on this basis using predicted retention times as described by Creek *et al* (Creek et al., 2011).

3.2.5 Statistical analyses

Statistical analysis was carried out as detailed in 2.2.9. Multivariate, correlation and hierarchical cluster analyses were performed using Metaboanalyst 2.0 (Edmonton, Canada) (Xia et al., 2009, Xia and Wishart, 2010).

3.3 Results & discussion

3.3.1 Protein expression profiles

The phenol phase from cell samples used to acquire RNA samples for PCR experiments in the previous chapter were also used to determine the total amount of protein present in each sample set. These were calculated as fold change from the control sample (cells cultured on plain substrate) after 24 hours in culture as a baseline (Figure 3-5).

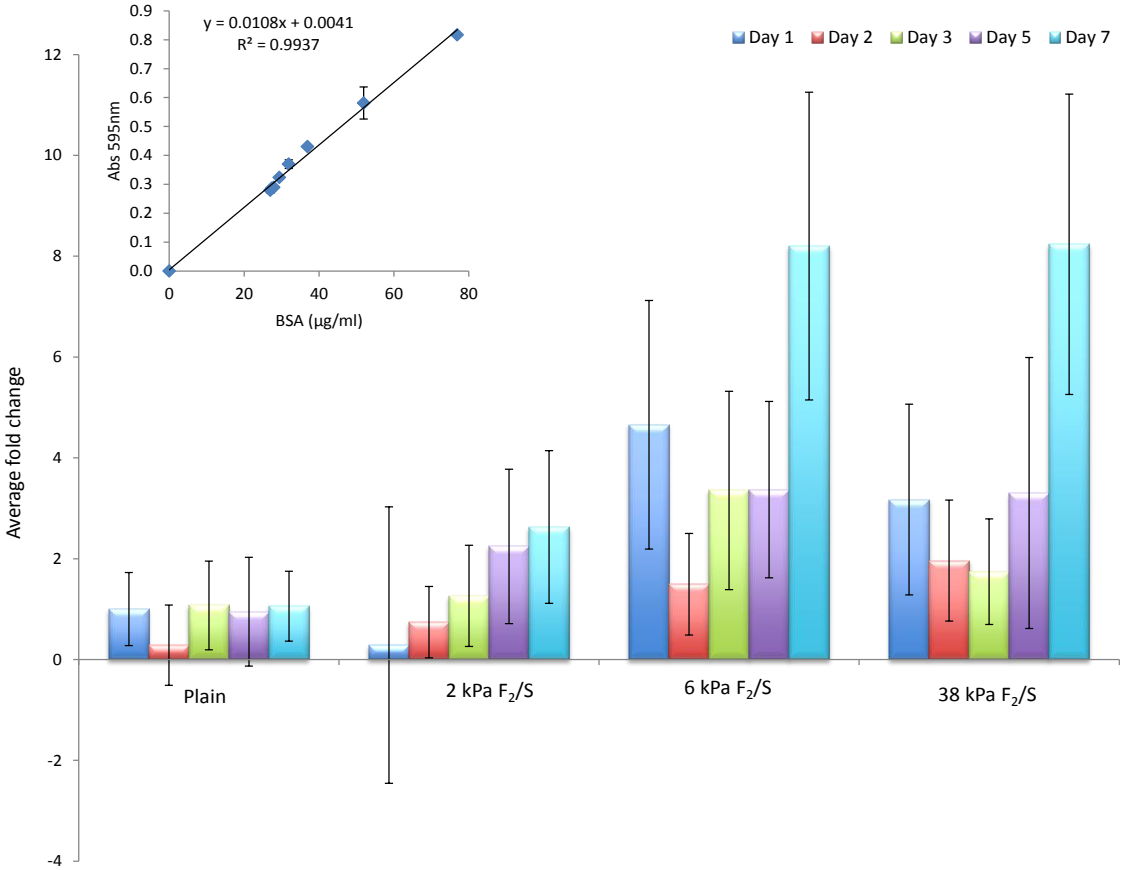

Figure 3-5 Protein content analysis for MSCs cultured on F_2/S hydrogel substrates. *Protein concentrations were observed to be generally higher for cells cultured on the F_2/S hydrogels with a steady increase occurring from day 2 to 7. Fold change in protein content was normalised against negative control, set nominally at 1. Negative control set is annotated as 'Plain'; these are MSCs that are maintained normally on planar culture well plastic. Inset is a representative graph of BSA standards used to measure protein abundance in each sample. Error bars denote standard deviations; n = 6 replicates.*

General protein abundance was noted to be higher for cells cultured on the F_2/S substrates compared to the plain. A dip in protein quantities was observed at 48 hours (2 days) after which the protein abundance increased steadily over 1 week for all substrates with the exception of 2 kPa F_2/S. Levels for cells on the plain substrate more or less

remain uniform for the entire experimental duration. Whether or not this observed effect (dip in concentrations at 48 hrs) is real cannot be said with any real certainty due in part to the large variation in biological replicates. One plausible explanation however, would be the effect of the substrates initiating a flurry of activity as the cells adhere and settle in their microenvironment. The same effect, albeit much subtler, is also noted for cells cultured on the plain substrate. The highest change was measured at 1 week (Day 7) for cells cultured on the 6 and 38 kPa F_2/S hydrogel substrates.

The acquired protein profiles were then used to normalise identified metabolite peak intensities subsequently detected by LC-MS.

3.3.2 Total metabolite activity: illustrating the metabolome as a whole

The total metabolite abundance measured by LC-MS was approximated for each sample by averaging the measured peak intensities of all detected masses. This is intended to give an idea into the overall activity the cells adapt in comparison to the plain substrate which does not harbour actively differentiating cell populations (Figure 3-6). LC-MS noise filtering and removal of irreproducible peaks were also done in IDEOM prior to averaging peak intensities.

No significant change is noted for cells cultured on the plain substrates at 24 and 168 hrs (1 week). The measurements reflect metabolic quiescence of MSCs inferring stability of the cells metabolic processes.

Cells cultured on the F_2/S substrates however, showed a different effect. Total metabolite amounts were significantly lower for all three F_2/S hydrogels at 24 hrs compared to the plain, an effect that may be due to the cells undergoing drastic changes as they interpret their microenvironment. Features such as cell attachment, spreading morphology and phenotype all undergo an extent of change on the F_2/S hydrogels (Figure 2-4) and these naturally make a high demand of the cells.

By one week however, metabolite amounts increase for the cells on the F_2/S substrates returning to levels that are comparable to the ‘basal’ activity seen with the plain substrate.

To better envisage the metabolome as a whole, metabolite dispersions were visualised using volcano plots. The volcano plots maps out the fold change calculated for each metabolite relative to that observed at 24 hours on the plain substrate against its corresponding p-value (calculated using unpaired students t-test) enabling visualisation of changes in metabolite populations that are of statistical significance.

After one week (168 hrs) in culture, cells on the plain substrate reflect the measurements observed in Figure 3-6, showing very little dispersion from those measured after 24 hrs

(Figure 3-7D). Cells cultured on the F_2/S hydrogels however showed very broad dispersion from the control sample as the subsequent depletion and increase in metabolite amounts is also reflected (Figure 3-7A - C). Worthy of note, is the overall patterning adopted by the metabolite dispersion on each of the graphs. Each substrate adopts its own unique imprint; a by product that is thought to manifest from the degree of difference in cell activity on each of the hydrogel substrates giving rise to different cell lineages as they undergo differentiation. The volcano plots (Figure 3-7) also illustrate that which cannot be represented by the bar graph. That is, although at 168 hrs, total metabolite abundance reaches comparable levels between all four substrates as a whole, the metabolic 'arrangements' contributing towards this overall stasis is very different between substrate types.

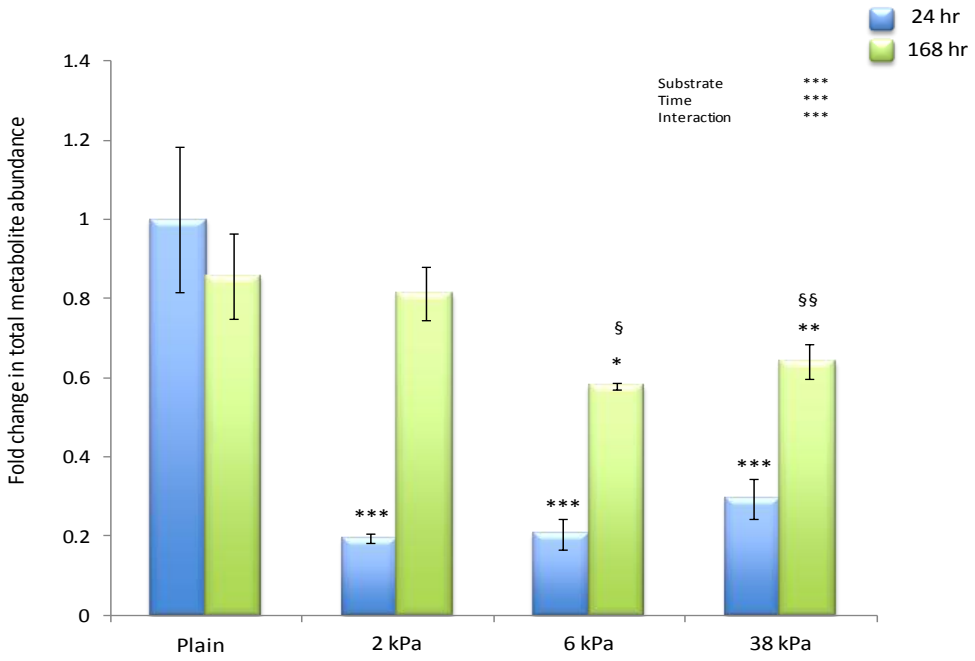

Figure 3-6 Averaged peak intensities of identified metabolite masses detected using LC-MS. *The graph depicts a general overview of the metabolome of MSCs cultured on plain, 2 kPa, 6 kPa and 38 kPa F_2/S hydrogels after 24 hrs and 168 hrs (1 week) in culture. Average peak intensities remain unchanged for MSCs maintained on the plain substrate (control), while MSCs on the F_2/S substrates show significant deviation from both the plain substrate and each other indicating differences in overall cell behaviour between substrates. Error bars denote standard deviations from the mean; n = 3. Statistical significance is noted as *** where $p < 0.001$, as calculated using two way ANOVA ascertaining whether the observed effect is due to time in culture, substrate type or the interaction between both variables (inset). Bonferroni post hoc tests were also performed and significance noted as * where $p < 0.05$, ** where $p < 0.01$ and *** where $p < 0.001$ on the graph compared to the plain substrate. § where $p < 0.05$ and §§ where $p < 0.01$ compared to 2 kPa F_2/S substrate*

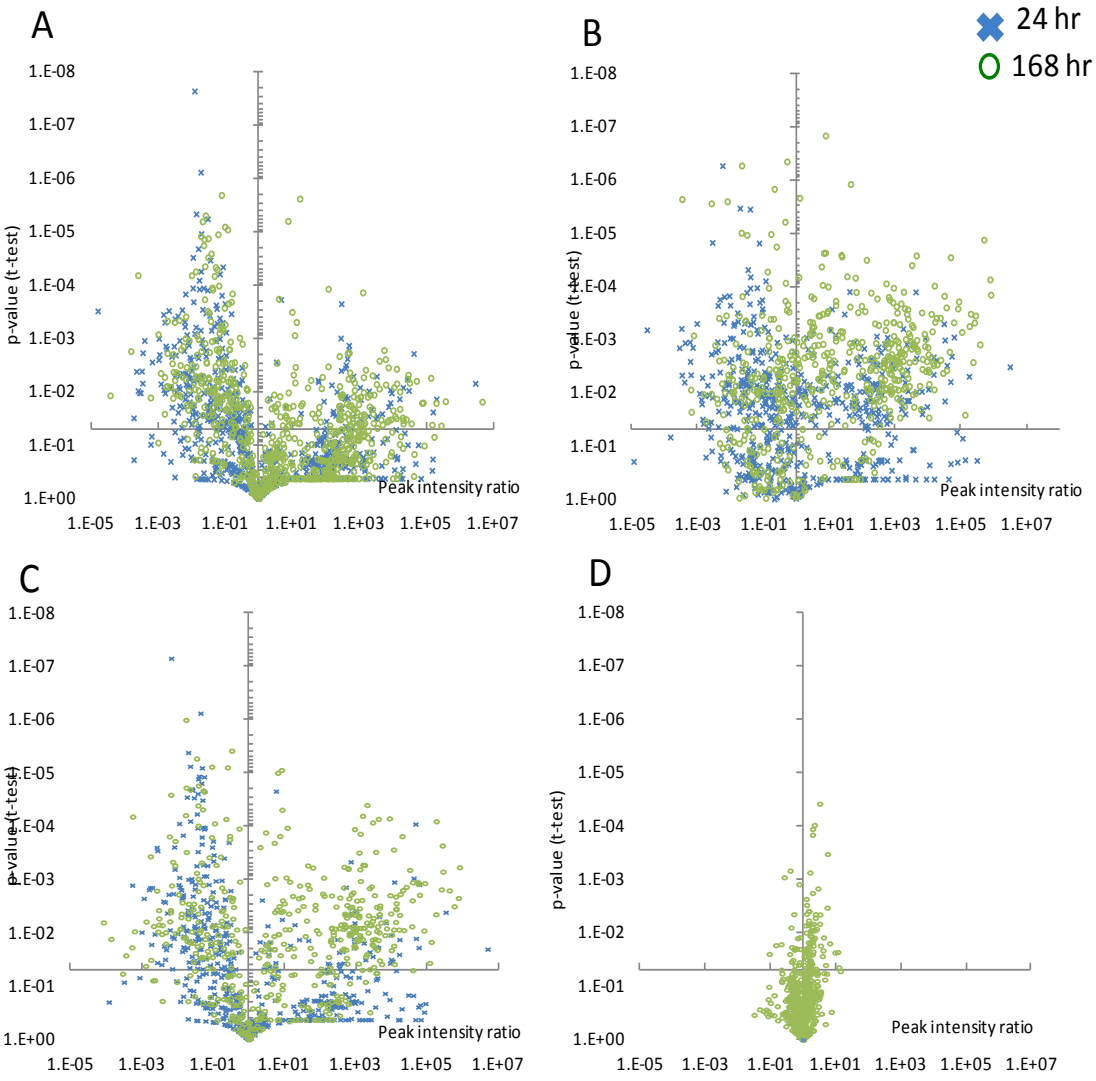

Figure 3-7 Volcano plots illustrating the metabolome of MSCs cultured on F_2/S hydrogel substrates. *Cells were seeded onto F_2/S hydrogels with elastic moduli of approximately 2 kPa (A), 6 kPa (B) and 38 kPa (C) and their metabolome ascertained after 24 and 168 hrs in culture. Each hydrogel gave a widely dispersed pattern compared to MSCs maintained on plain culture well plastic as a control (D). By 168hrs, the dispersion patterns manifest in each volcano plot is unique to each F_2/S hydrogel as the cells adopt varying differentiation lineages reflected in their cellular activities.*

3.3.3 Metabolic pathways: assessing differential behaviour as a consequence of substrate properties.

Having determined the overall metabolic activity on each hydrogel substrate, a more intricate scrutiny of cell activity was undertaken. To do this, cell activity was examined for differential behaviour between substrates by performing a series of multivariate statistical tests (Xia et al., 2009) on smaller subsets of the acquired data. In the first instance, putative metabolites identified using Ideom were classified into broadly recognised metabolic pathways; carbohydrate, amino acid, vitamin and lipid metabolism and analysed as such. From this, it was noted that these groups could be classed based on their observed overall activity. These were anabolic metabolism, where activity showed a general increase on the hydrogel substrates and catabolic metabolism where the opposite effects were observed.

Anabolic metabolism was noted for metabolites classed under vitamin & cofactor metabolism and amino acid metabolism while lipid and carbohydrate metabolism was observed to be catabolic (Figure 3-8). This observation compliments each other nicely as catabolism of carbohydrates and lipids generally produce energy for anabolic reactions (Dressel et al., 2003, Tozzi et al., 2006). The observed increase (anabolism) of amino acids inherently leads to the formation of functional and structural proteins that are pivotal to altering cell phenotype as the increase in cofactor metabolism indicate the need to drive a number of cellular reactions greater than when the cell is in a ‘restive’ state (plain substrate) (Figure 3-8).

3.3.3.1 Total metabolic activity

Of the two catabolic pathways, carbohydrate metabolism showed the most constant degree of depletion over time, the differences from the plain substrate being of greater significance at 168 hrs compared to lipid metabolism (Figure 3-8).

The observed pattern/outlier with this particular pathway could be attributed to the fact that these metabolites are primarily driven to meet the energy demands of the entire cell and it’s continuous catabolism provides for the changes in phenotypes as the cells undergo differentiation.

Although energy requirements of the cell can be met by other means (lipid & amino acid metabolism), carbohydrate metabolism mainly involves the breakdown of complex sugars to simpler molecules (glucose), which is the basic substrate for glycolysis (Lunt and Vander Heiden, 2011). As such, the metabolism of carbohydrates to form glucose is

a more readily available and less complex process when compared to lipid metabolism for example. It follows that the observed lessened activity at day 7 is in line with meeting the cells energy demands as carbohydrate metabolism is a preferred route over lipid metabolism.

Overall lipid metabolism was observed to be particularly active at 24 hours and less so by 168 hrs. In a similar manner to carbohydrate metabolism cells cultured on the F_2/S hydrogels at 168 hrs were still significantly active compared to the plain substrate. Overall activity between F_2/S substrate types also become apparent at this point as differences between the 2 kPa and 38 kPa are also noted.

Putative metabolites classified as participating in amino acid metabolism were observed as having no overall change after 24 hrs for MSCs cultured on all four substrates. At 168 hrs, however, amino acid metabolism showed significant increase in activity on all three hydrogel substrates compared to the plain surface, where metabolite abundance remained unchanged from that observed at 24 hrs (Figure 3-8). Divergent behaviour between F_2/S hydrogels is also noted here as activity on the 2 kPa F_2/S hydrogel was generally higher than the 6 and 38 kPa substrates.

These results suggest an inclination toward the synthesis of structural and functional proteins that are geared towards supporting differentiation on each of the hydrogels. The theory is further supported by the fact that most stem cells undergoing differentiation are known to show up regulation in gene expression early on in culture and have a more established presence by 1 week (168 hrs) when they become sensitive to most detection methods.

Total activity of putative metabolites identified as those involved in vitamin and cofactor metabolism were observed as, albeit not significantly, having increased activity at 24 hrs on the F_2/S hydrogel substrates (average metabolite abundance on the 2 kPa substrate was 2x the plain substrate while 6 kPa measured a 1.7x increase). The exception to this being the cells cultivated on the 38 kPa hydrogel substrate (on average 3.7x fold change), which was statistically significant. Cells cultured on the 2 kPa surface showed highest activity after 168 hrs in culture while those on the 6 kPa and 38 kPa hydrogel peaked at 24 hours. Overall behaviour shows a distinction on the soft hydrogel substrate whilst the general trend between the 6 kPa and 38 kPa hydrogels are similar.

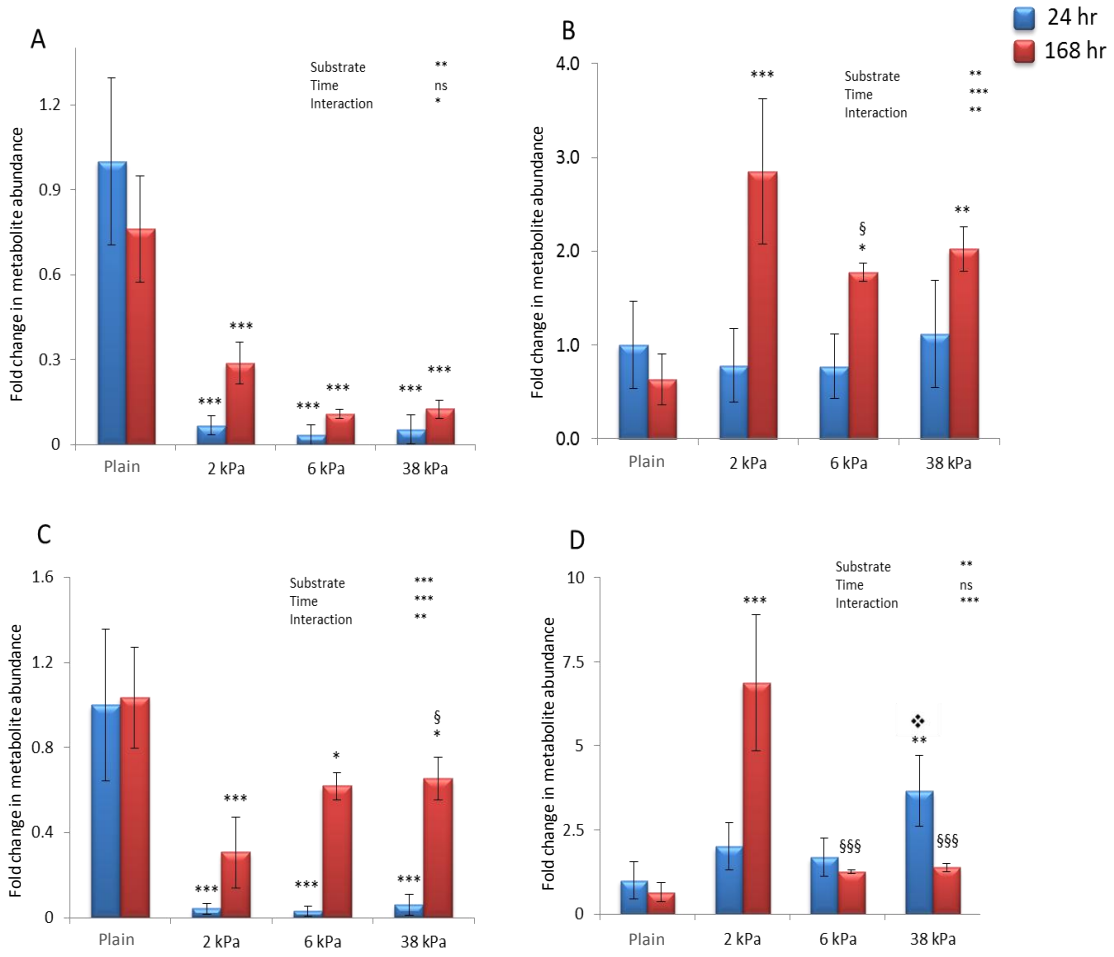

Figure 3-8 Average metabolite abundance illustrating metabolic pathway activity in cells cultured on plain, 2 kPa, 6 kPa and 38 kPa F_2/S hydrogel substrates. *Total metabolite abundance was averaged from peak areas of all putatively identified metabolites classified into carbohydrate (A), amino acid (B), lipid (C) and vitamin & cofactor (D) metabolism after 24 and 168 hrs in culture. Distinct catabolic (A & C) and anabolic (B & D) behaviour was noted for cells cultured on the F_2/S substrates while those on the plain substrate remain unchanged. Error bars denote standard deviations from the mean; n = 3. Statistical significance is noted as * where $p < 0.05$, ** where $p < 0.01$ and *** where $p < 0.001$, as calculated using two way ANOVA, ascertaining whether the observed effect is due to time in culture, substrate type or the interaction between both variables (inset). Bonferroni post hoc tests were also performed and significance noted as * where $p < 0.05$, ** where $p < 0.01$ and *** where $p < 0.001$ on the graph compared to the plain substrate. § where $p < 0.05$ and §§§ where $p < 0.001$ compared to 2 kPa F_2/S substrate. ❖ where $p < 0.05$ compared to the 6 kPa F_2/S substrate.*

Principal component analysis (PCA)

Principal component analyses were performed on data sets obtained from each time point (24 hr and 168 hr). The factor scores of each principal component was used to generate scatter plots to best describe the variance within the data sets. The separation of clusters in the scatter plots therefore represents the existence of distinct differences

between each sample set (Fiehn, 2001, Robinson et al., 2005, Roessner and Bowne, 2009), in this case, by way of its metabolic arrangement or differences.

Illustrated in Figure 3-9 and Figure 3-10 are the scatter plots generated from combining the first two principal components, that is, the components that best describe sample variances. Details of variance description accounted for by PCA are shown in Table 3-2. The high percentage of combined variables accounted for (greater than 73%), is suggestive of the presence of strong relationships between the data sets (Robinson et al., 2005). This is explored in more detail using hierarchical cluster analysis in the following section.

Table 3-2 Amount of variance explained using principal component analysis. *The table describes the percentage variance described in each dataset using metaboanalyst 2.0 for individual and combined principal components.*

	24 hours			168 hours		
	PC1	PC2	Combined	PC1	PC2	Combined
Carbohydrate metabolism	73.2%	9.5%	82.7%	71.8%	14.9%	86.8%
Amino acid metabolism	48.3%	24.8%	73.1%	69.3%	17.4%	86.7%
Vitamin & cofactor	72.7%	14.2%	86.9%	67.6%	19.5%	87.1%
Lipid metabolism	60.9%	21.5%	82.5%	51.2%	31.6%	82.7%

Metabolite behaviour of cells cultured on the plain substrate remained distinct from those on the F_2/S hydrogel for all pathways and at both time points, indicating that cell activity on this substrate is markedly different from that on the F_2/S substrates.

At 24 hours, cells cultured on all three F_2/S surfaces showed an appreciable degree of overlap implying that there is very little dissimilarity between cell activities for all three substrates at this point in time. By 1 week in culture (168 hrs) cells on the 2 kPa hydrogels developed behaviour that is largely distinct in all four assessed pathways from the 6 and 38 kPa F_2/S surfaces. The 6 and 38 kPa substrates however, exhibited a very close relationship with considerable overlap occurring in amino acid and lipid metabolism (Figure 3-9 & Figure 3-10 C & D).

Interestingly, the pathway with the most distinct activity across all four substrate types was seen with vitamin and cofactor metabolism at 168 hrs (Figure 3-10B). Metabolites classed within this group are responsible for facilitating a large number of redox reactions as building blocks for coenzymes (Depeint et al., 2006a, Depeint et al., 2006b) and as such, are likely to have an insurmountable impact on specific cellular function and behaviour.

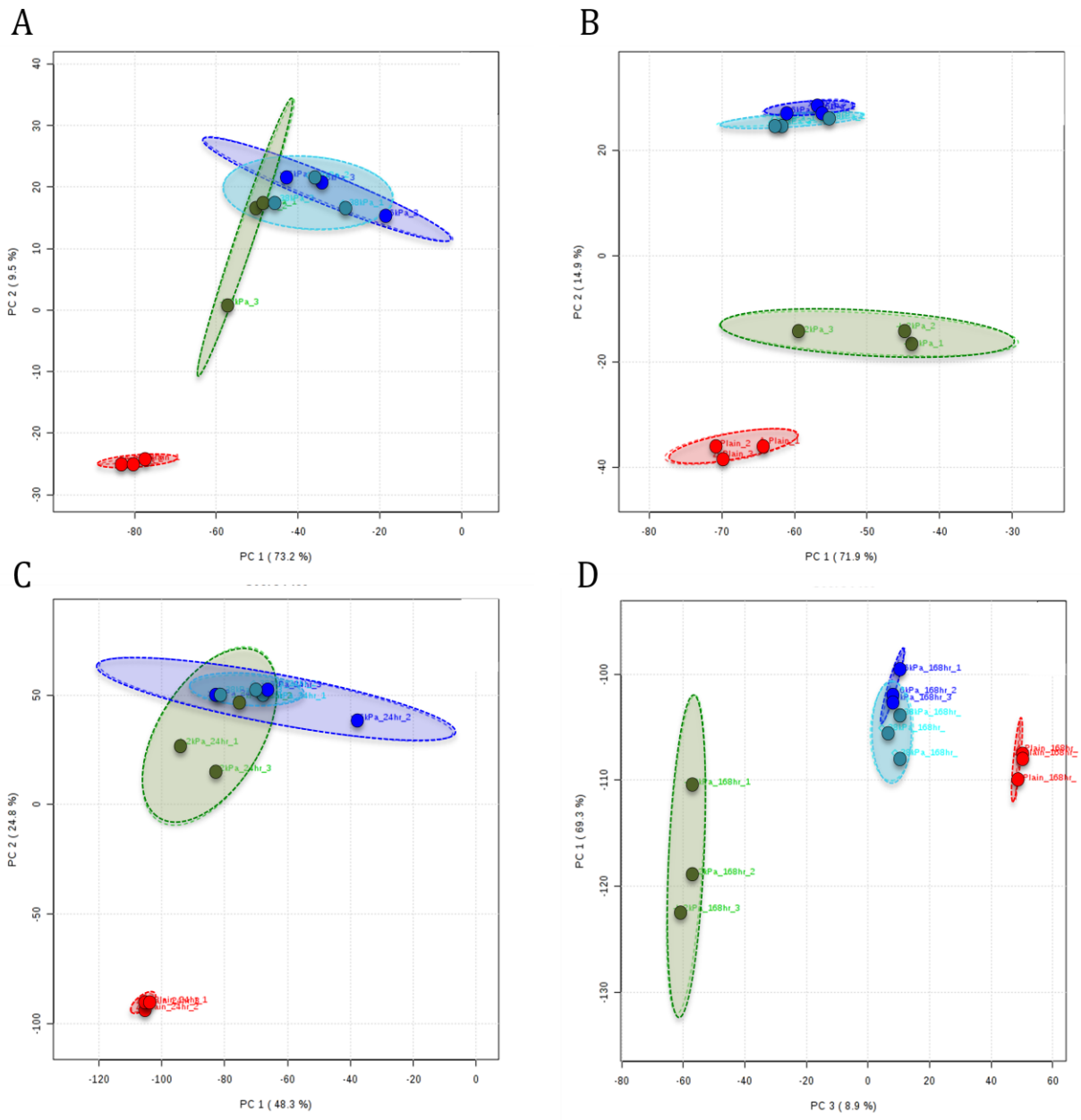

Figure 3-9 Principal component analysis (PCA) of metabolites detected in MSCs cultured on plain, 2 kPa, 6 kPa and 38 kPa F_2/S hydrogel substrates. *Data sets were obtained from putative metabolites identified from cells that were analysed after 24 hrs and 168 hrs in culture classed within carbohydrate metabolism (A & B respectively) and amino acid metabolism (C & D respectively). Plot points represent individual samples from each substrate set (n =3) for plain (red), 2 kPa (green), 6 kPa (blue) and 38 kPa (cyan) F_2/S hydrogels. Cell metabolism on the F_2/S substrates for both pathways remains distinct from the plain substrate at both time points. The observed overlap of the F_2/S hydrogels at 24 hrs is diminished as cells on the 2 kPa F_2/S adopts distinctive behaviour from the 6 and 38 kPa F_2/S substrates, which remain similar. Coloured ellipses illustrate spatial borders of each sample set calculated to 95% confidence.*

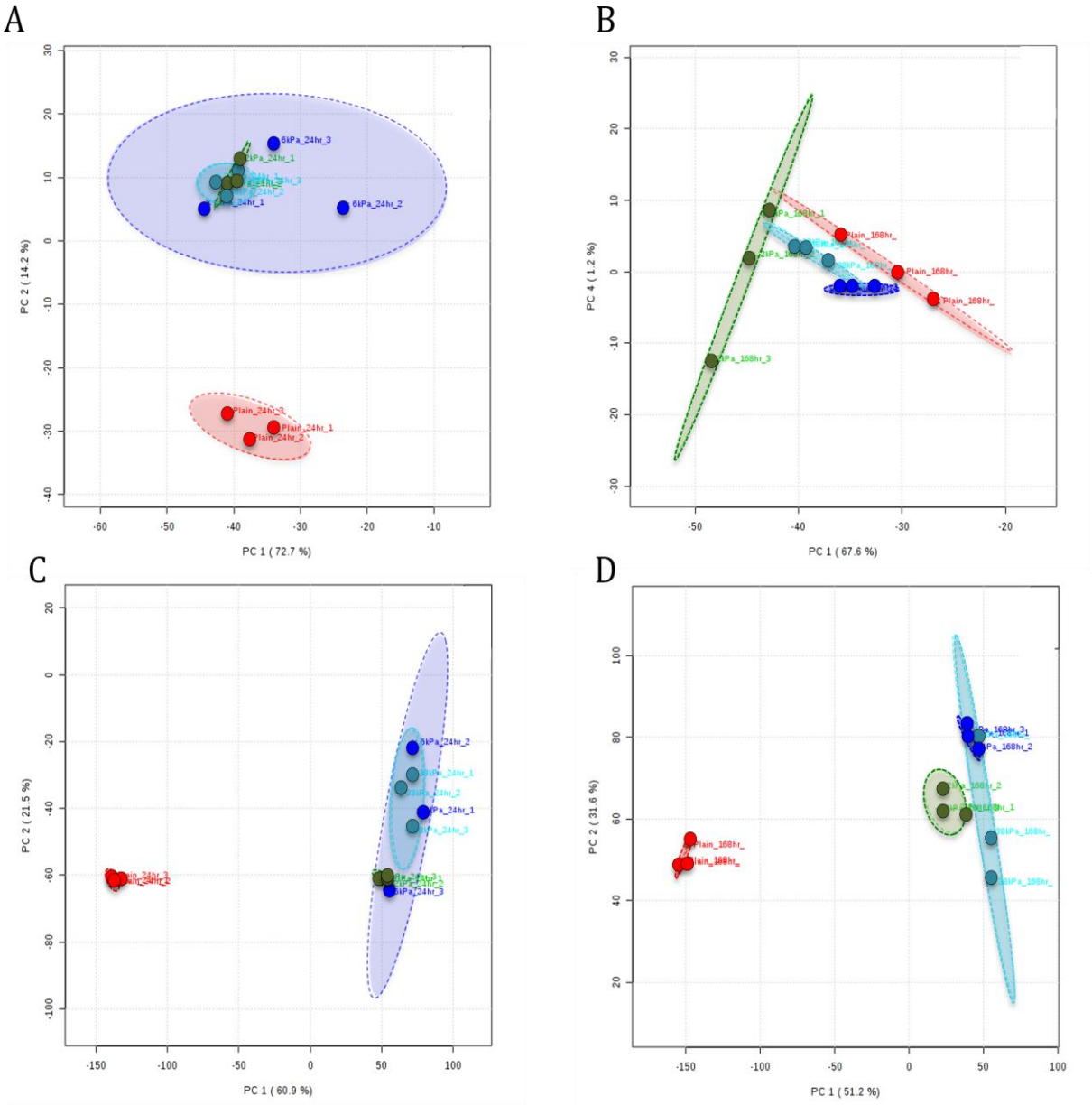

Figure 3-10 Principal component analysis (PCA) of metabolites detected in MSCs cultured on plain, 2 kPa, 6 kPa and 38 kPa F_2/S hydrogel substrates. *Data sets were obtained from putative metabolites identified from cells that were analysed after 24 hrs and 168 hrs in culture classed within vitamin & cofactor metabolism (A & B respectively) and lipid metabolism (C & D respectively). Plot points represent individual samples from each substrate set (n =3) for plain (red), 2 kPa (green), 6 kPa (blue) and 38 kPa (cyan) F_2/S hydrogels. Cell metabolism on the F_2/S substrates for both pathways remains distinct from the plain substrate at both time points. The observed overlap of the F_2/S hydrogels at 24 hrs is diminished as cells on all four substrates adopt distinctive behaviour from one another for vitamin metabolism at 168 hrs (B). Lipid metabolism at 168hrs remains similar for the 6 and 38 kPa substrates with a small distinction observed for the cells on the 2 kPa F_2/S (D). Coloured ellipses illustrate spatial borders of each sample set calculated to 95% confidence.*

3.3.3.2 Hierarchical cluster analysis

Cluster analysis groups metabolites together by measuring sample similarity using correlation analysis. Numerical data are then represented in colour scales (heat map) allowing sample dissimilarities to be easily observed.
It is noteworthy that although heat maps are good at spotlighting highly contrasting behaviour, some measurements, especially where data populations are very high, make changes that occur on a subtle scale difficult to single out in cluster analysis.

For the most part, the cluster analysis echo the observations derived by principal component analysis. That is, the noted general likeness in cellular activity between F_2/S substrates at 24 hours and the more obvious distinction of cell activity on the 2 kPa hydrogel at 168 hrs. Profiles for the 6 and 38 kPa hydrogels were also perceived as very similar to each other in all instances (Figure 3-11, Figure 3-13, Figure 3-17 & Figure 3-16). The principal component analysis also indicated however, that there is some amount of distinction between the 6 and 38 kPa F_2/S hydrogel sets, the likes of which may be considered in some instances too subtle to be represented on a colour gradient heat map.
Irrespective, what the cluster analyses enable is the isolation of areas of divergence within each metabolic pathway allowing the data to be whittled down to more specific modes of action within the subset. To assess this, regions of interest were restricted to three main facets; metabolites that showed the most change (up and down regulated) between the plain and F_2/S substrates, together representing regions where the most active change occurs and regions where contrasting change is particular to a certain F_2/S hydrogel type.
Performed searches for these distinct points, pertain only to the 168 hr data set as they show the most polarised change in cell behaviour.

Carbohydrates
Although for the most part, there was active catabolism for MSCs cultured on all three F_2/S hydrogels compared to the plain substrate. At 168 hrs, there were occurrences that are contrary to the observed general trend where higher activity on the F_2/S hydrogels was noted (Figure 3-11).
Masses of the compounds isolated as described previously were analysed using Pathos; a web based facility which allows for detected MS masses to be allocated and mapped using the Kyoto Encyclopaedia for Genes and Genomes (KEGG) to the metabolic pathways in which they may occur (Kanehisa and Goto, 2000, Leader et al., 2011).

Metabolites tend not to participate wholly within a single pathway, playing a number of diverse functions and as such a single metabolite cannot be attributed to a sole purpose. By combining the entire population, an idea of which specific pathway(s) may be of importance in cell differentiation is highlighted by the number of hits gained from the total population. For pathway mapping, the population consists of those metabolite masses that showed a considerable amount of change, defined earlier as regions of interest and by the annotations used on the cluster heat maps.

The pathways that gave the most number of hits for metabolites considered the most active compared to the plain substrate were pentose & glucuronate interconversion, ascorbate & aldarate metabolism, pentose phosphate metabolism and amino & nucleotide sugar metabolism respectively. Contrasting behaviour particular to a F_2/S substrate was observed for the 2 kPa hydrogel only, and pathway mapping prioritised the same as those named previously.

Of these, the pentose phosphate pathway was of considerable note as it is the primary source of NADPH for use in a number of biosynthetic reactions. It is also the source of the five carbon sugar ribose-5-phosphate and its derivatives for DNA and RNA synthesis. The pentose phosphate pathway also recycles C3 to C7 sugars for reincorporation into glycolysis (Figure 3-12) as well as entry points in pentose and glucuronate interconversion.

Glucuronate is a component of proteoglycan and as such occurs in high concentrations in the extracellular matrix. It is also a known precursor of ascorbate (Bublitz et al., 1958, Grollman and Lehniger, 1957), which is required for the degradation of procollagen into collagen by hydroxylation of proline residues into hydroxyproline (Eleftheriades et al., 1995, Rosenblat et al., 1999, Sullivan et al., 1994).

These observations; glucuronate and ascorbate metabolism being 2 of the pathways having the most contrasting change between the plain and F_2/S substrates coupled with the fact that ascorbate is widely used to promote cell differentiation *in vitro* (Lin et al., 2005, Mirmalek-Sani, 2006, Pittenger et al., 1999, Sekiya et al., 2002), suggest that these processes may, in part at least, drive the synthesis of extracellular matrix components.

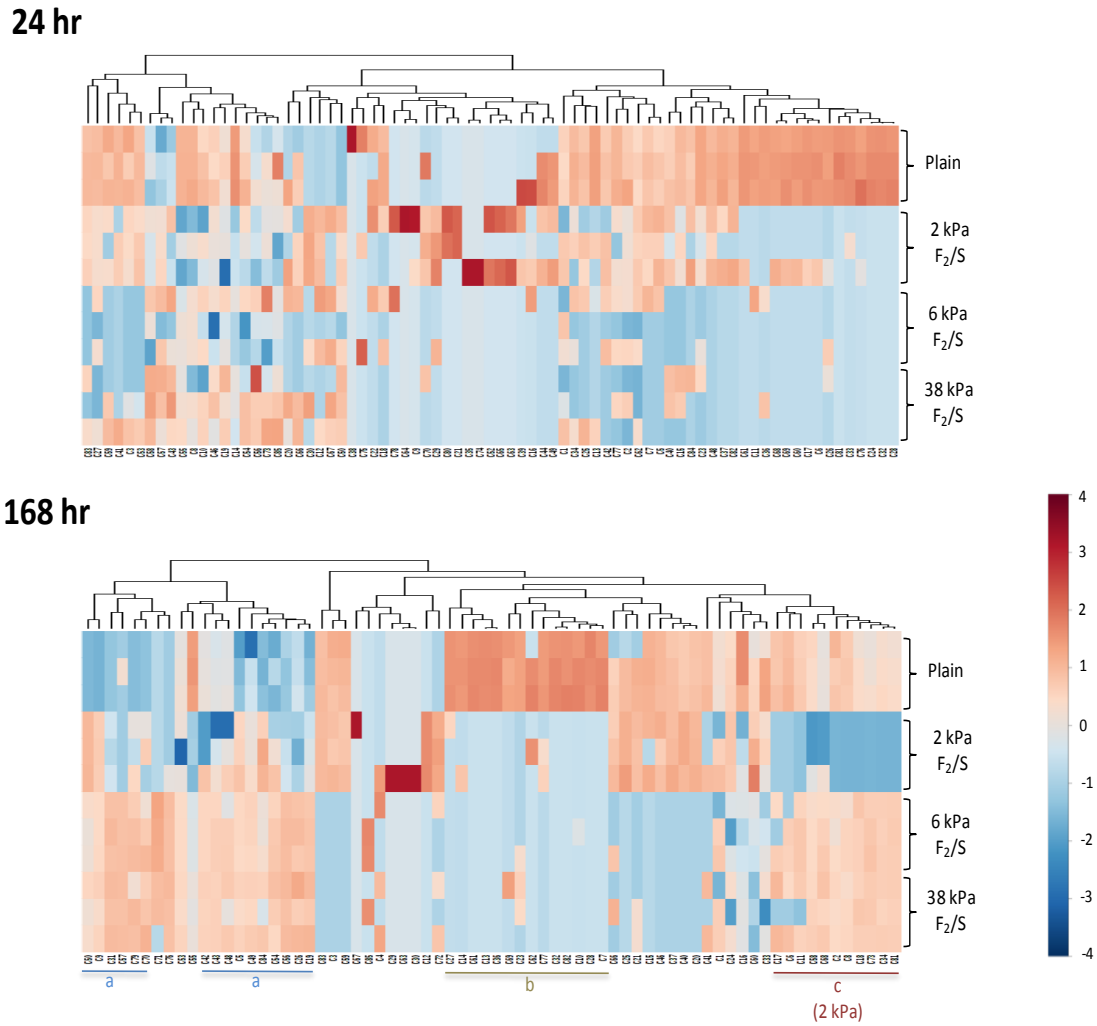

Figure 3-11 Hierarchical cluster analysis performed for cells cultured on plain, 2 kPa, 6 kPa and 38 kPa F_2/S hydrogel substrates. *Data sets were obtained from putative metabolites that were classed within carbohydrate metabolism and analysed at 24 and 168 hours from each substrate set. The image shows the heat maps generated from individual samples (n=3) cultured on each substrate type. At 168 hrs (considered to be the time point where the most divergent activity lies), regions are annotated that show the most contrasting change where metabolites were most up regulated on the F_2/S hydrogels (a) and most up regulated on the plain substrate (b). Together, these both highlight regions of most activity brought on by substrate change. Region (c) is defined by areas that are particular to a certain F_2/S hydrogel type as indicated on the image.*

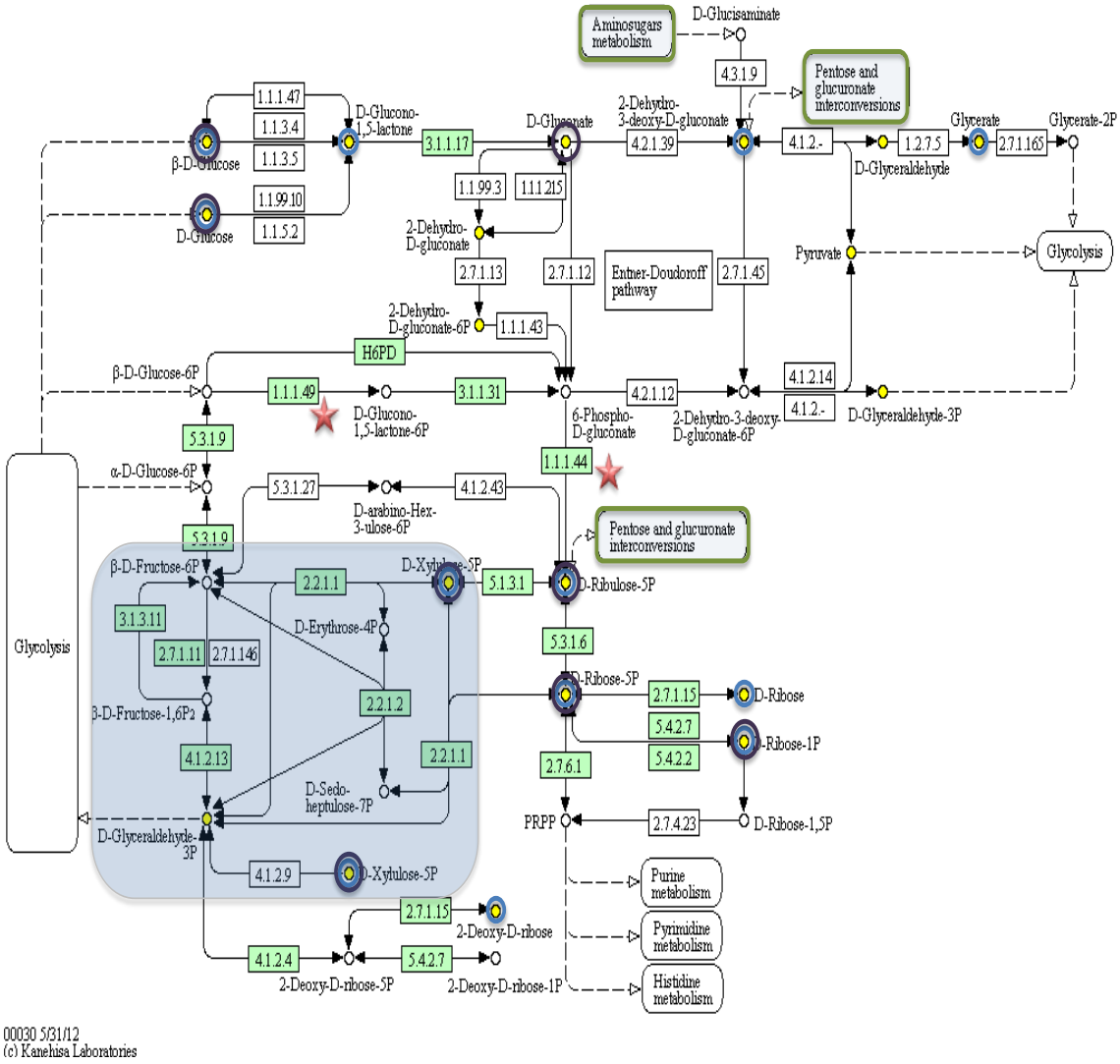

Figure 3-12 KEGG metabolite map illustrating the pentose phosphate pathway. *Detected metabolite masses are highlighted in yellow. Masses that showed considerable change from the plain substrate when seeded on F_2/S hydrogels are circled in blue. Masses that showed particular change on the 2 kPa hydrogel are circled in purple. Most of the circled masses lead into pentose & glucuronate interconversions or DNA/RNA synthesis. This pathway also primarily provides NADPH to drive biosynthetic reactions. The points in the pathway where NADPH is produced are denoted with a red asterix. The shaded box singles out non-oxidative inteconversions of sugars.*

Amino acids

Due to the large population of putative metabolites detected within this pathway, only the 100 most significantly changed features were included in this analysis. Features were selected using one way ANOVA analysis in Metaboanalyst and discriminatory behaviour assessed from these before investigation in Pathos.

Within this population, pathways that gave the most number of hits were for metabolites involved in arginine & proline metabolism, aminoacyl tRNA biosynthesis and phenylalanine metabolism. Like the previous, contrasting behaviour particular to a F_2/S substrate was observed for the 2 kPa hydrogel only, and pathway mapping prioritised as the same.

Arginine & proline metabolism plays an essential role in the production of nitric oxide, which acts as a powerful signalling molecule in a number of regulatory pathways (Pegg, 2009). It is also responsible for the biosynthesis of polyamines through the interconversion of ornithine by ornithine decarboxylase (ODC). Polyamines are ubiquitous cationic molecules that play an essential role in the regulation of a number of cell functions inclusive of gene expression (Childs et al., 2003, Pegg, 2009). The net positively charged polyamines are known to bind to acidic site of molecules characteristically found in cells such as DNA, RNA, proteins and the phospholipid membrane. As such, they have a vast effect on the regulation of gene expression and a number of other cellular functions such as cell proliferation, stem cell self-renewal (Zhao et al., 2012) and differentiation (Childs et al., 2003, Igarashi and Kashiwagi, 2010, Ishii et al., 2012, Tjabringa et al., 2008).

Intriguingly, within this pathway, metabolites that show considerable changes between the plain and F_2/S substrates have a high number of detected masses clustered around proline interconversions (Figure 3-14). Proline through interconversion between it cis and trans conformations, plays an important role in defining the secondary and tertiary structure of proteins (Wedemeyer et al., 2002).

Considerable activity observed for aminoacyl tRNA synthesis, suggests increased proteinogenic activity of cells cultured on the F_2/S hydrogels compared to the plain substrate. An observation that is also supported by the overall behaviour in amino acid metabolism observed in Figure 3-8.

Analysis of individual amino acids showed a varied composition, with the cells cultured on the 2 kPa F_2/S substrate having the highest abundance levels of all the substrates. This was followed by the 38 kPa F_2/S, then the 6 kPa F_2/S and lastly the plain substrate (Figure 3-15). Interestingly, levels of the amino acid leucine were observed to be highest on the 38 kPa F_2/S hydrogel where the most amount of osteogenic development was

observed (Figure 2-12). Increased levels of leucine associated with osteogenic development of MSCs have also been noted in studies assessing the osseointegrative properties of cell substrate topographies in orthopaedic medicine (McNamara et al., 2011). Metabolomic analysis of MSCs differentiating into osteoblasts on nanopatterned titanium pillars of various heights by McNamara *et al* had shown that the optimal osteoinductive pillar height of 15 nm also resulted in the highest abundance of the amino acid leucine during cellular differentiation (McNamara et al., 2011).

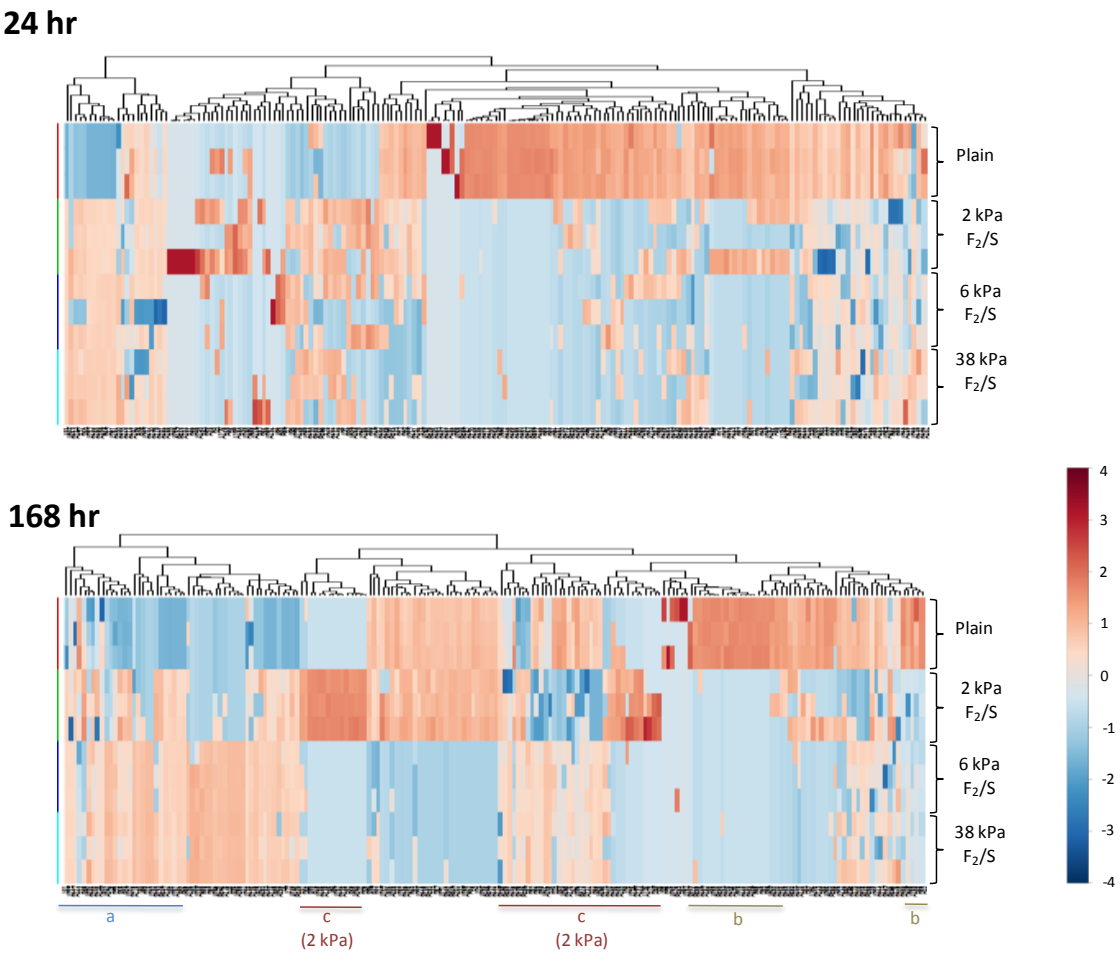

Figure 3-13 Hierarchical cluster analysis performed for cells cultured on plain, 2 kPa, 6 kPa and 38 kPa F_2/S hydrogel substrates. *Data sets were obtained from putative metabolites that were classed within amino acid metabolism and analysed at 24 and 168 hours from each substrate set. The image shows the heat maps generated from individual samples (n=3) cultured on each substrate type. At 168 hrs (considered to be the time point where the most divergent activity lies), regions are annotated that show the most contrasting change where metabolites were most up regulated on the F_2/S hydrogels (a) and most up regulated on the plain substrate (b). Together, these both highlight regions of most activity brought on by substrate change. Region (c) is defined by areas that are particular to a certain F_2/S hydrogel type as indicated on the image.*

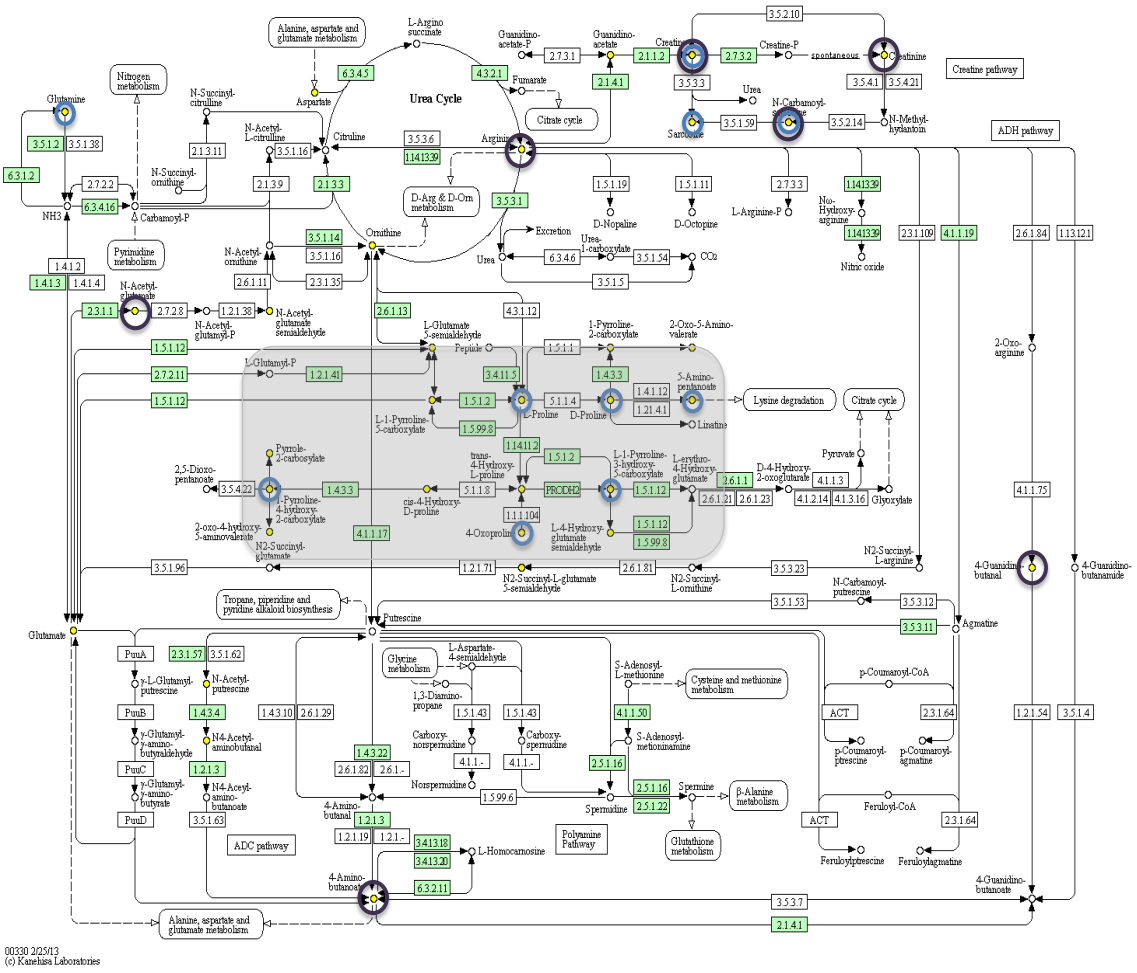

Figure 3-14 KEGG metabolite map illustrating arginine & proline metabolism. *Detected metabolite masses are highlighted in yellow. Masses that showed considerable change from the plain substrate when seeded on F_2/S hydrogels are circled in blue. Masses that showed particular change on the 2 kPa hydrogel are circled in purple. Most metabolites that showing considerable change from the plain substrate are clustered around proline metabolism (shaded box).*

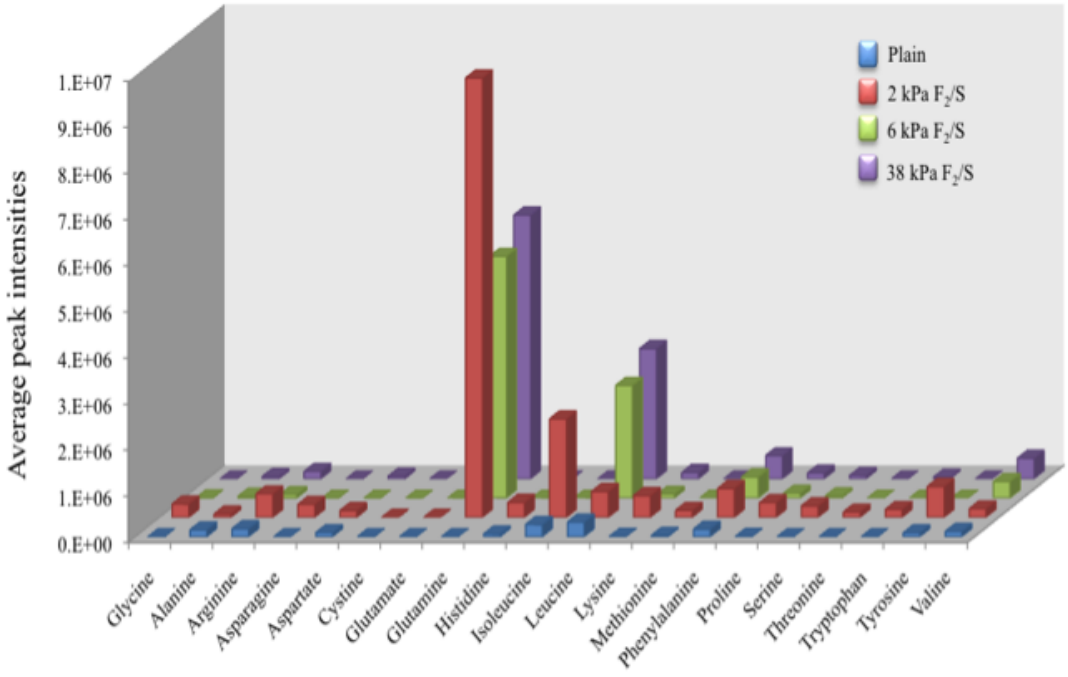

Figure 3-15 Average peak intensities of amino acid as detected using LC-MS, for cells cultured on plain, 2 kPa F_2/S, 6 kPa F_2/S and 38 kPa F_2/S substrates. *In general, amino acid abundances were higher for cells cultured of the F_2/S substrates when compared to the plain substrate. Cells cultured on the 2 kPa F_2/S hydrogels show the highest abundance for most of the amino acids with the exception of leucine, phenylalanine and valine. Measurements were averaged from 3 replicate injections.*

Lipids

The cluster profiles for lipids have the most contrast of all four pathways between the plain substrate and the F_2/S substrates. They also represent the bulk of the metabolites identified. Most of the lipids are present in appreciable quantities on the plain substrate of which little or none are detected on the F_2/S substrates (Figure 3-16). Mapping in Pathos had revealed that the pathways with the highest number of hits for the population were for arachidonate metabolism. Arachidonate is a cell membrane lipid and plays a role in second messenger cell signalling processes (Janmey and Lindberg, 2004, Merrill and Schroeder, 1993). The lack of detection of most of these masses on the F_2/S hydrogels could suggest a redesign or redistribution in the cell membrane composition on substrate change (Kellam et al., 2003).

The approach used with amino acids for sample comparison (100 most changed metabolites by ANOVA) could not be applied here, so a different tack was taken.

Metabolites with little or no information on the F_2/S substrate were removed from the compound list and only those present in at least 3 of the 4 substrates as 'functional' metabolites were analysed further. This process reduced the metabolite population from 260 to 71 and the cluster analysis of the truncated list is shown in Figure 3-16.

An underrepresentation of most lipids, and a general lack of understanding about their principal function(s), does not allow straightforward mapping in most integrated software tools and only a small number of these were represented in Pathos (less than 16%, with the most number of hits per pathway being 3). Use of the human metabolome database (HMDB) (Wishart et al., 2009) identifiers were mapped using Metaboanalyst but were only slightly better compared to Pathos. Given this result, a reasonable assessment of the role of identified metabolites in known biochemical pathways could not be made.

The results from attempted lipid mapping are summarised in Table 3-3.

Table 3-3 Summary of detected LC-MS masses putatively identified as lipids. *Masses were mapped using metaboanalyst and the top four pathways listed*

	Pathway	Hits	p-value
Mapped (43 masses)	1. Sphingolipid metabolism	6/25	3.12e-6
	2. Glycerophospholipid metabolism	4/39	0.0046
	3. Propanoate metabolism	3/35	0.023
	4. Butanoate metabolism	3/40	0.033
Unmapped (382 masses)			

Propanoate and Butanoate metabolism are not endogenous cell processes and are thought to occur through extracellular acquisition of these short chain fatty acids, mostly likely from the culture media. Research into sphingolipid metabolism is mainly centred on its two key active molecules; sphingosine-1-phosphate and ceramide-1-phosphate. Both compounds are known to act as cell membrane components imparting stasis and fluidity to the membrane as well as acting as intracellular signalling molecules (Pyne and Pyne, 2000, Spiegel and Milstien, 2002).

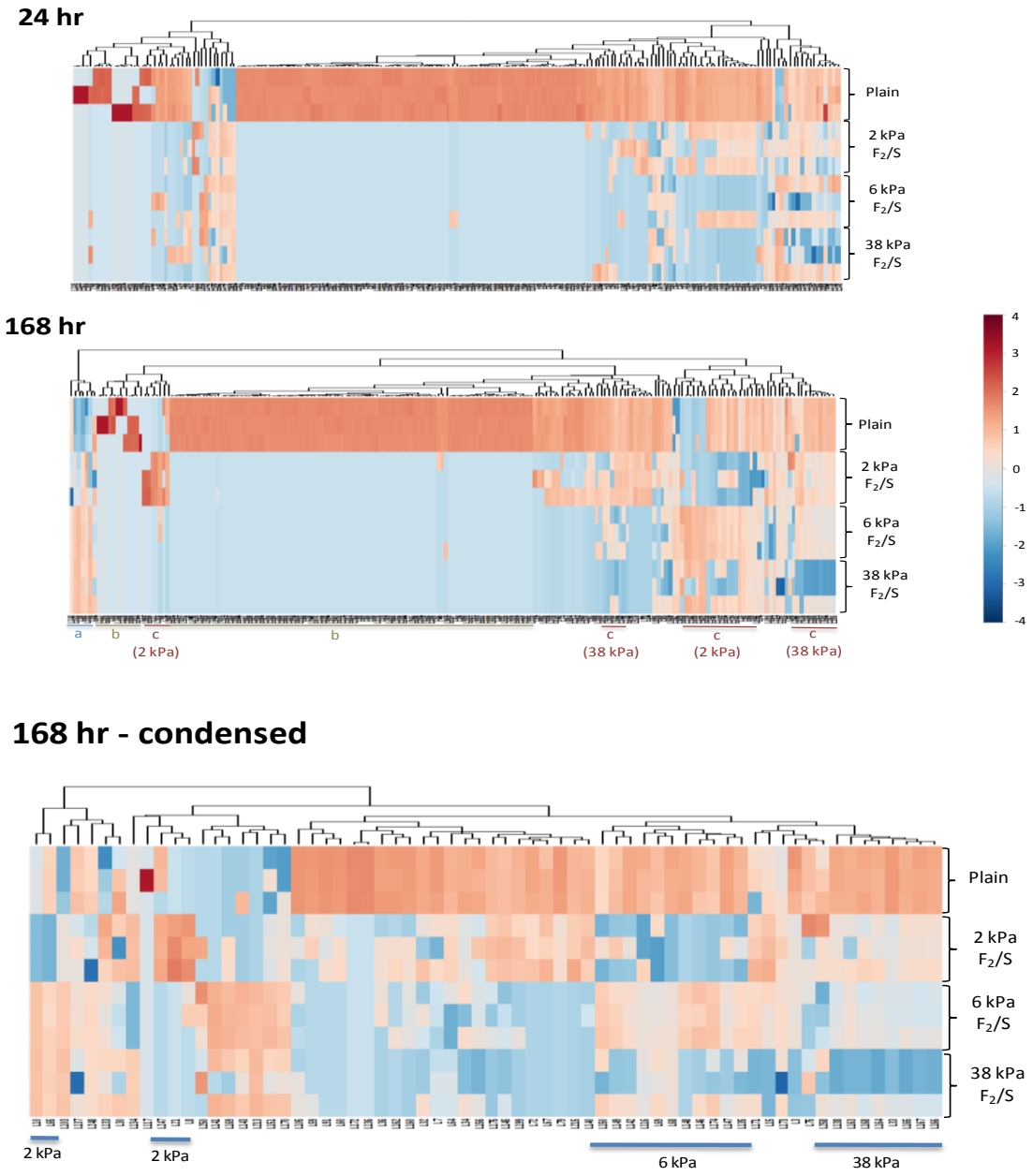

Figure 3-16 Hierarchical cluster analysis performed for cells cultured on plain, 2 kPa, 6 kPa and 38 kPa F_2/S hydrogel substrates. *Data sets were obtained from putative metabolites that were classed within lipid metabolism and analysed at 24 and 168 hours from each substrate set. The image shows the heat maps generated from individual samples (n=3) cultured on each substrate type. The top two traces show the profiles for the complete population of detected lipids at each time point. The bottom trace shows a truncated version of 168hr having restricted the population to only those detected in the majority of substrates. At 168 hrs (considered to be the time point where the most divergent activity lies), regions are annotated that show the most contrasting change where metabolites were most up regulated on the F_2/S hydrogels (a) and most up regulated on the plain substrate (b). Together, these both highlight regions of most activity brought on by substrate change. Region (c) is defined by areas that are particular to a certain F_2/S hydrogel type as indicated on the image. These are also annotated on the condensed heat map.*

Sphingosine-1-phosphate, however, is also known to act as a mediator of extracellular signals (Spiegel and Milstien, 2002) and is of particular influence in the adaption of cell morphology (Harma et al., 2012).

Glycerophopholipids are the major constituent of the cell membrane. The name encompasses a vast host of molecules comprising a glycerol moiety with variations occurring at their head groups, producing phosphatidylinositols, phosphatidylcholines or phosphatidylglycerols to name a few. All of which incorporate an added degree of complexity through variations in fatty acid chain length and degree of saturation. Although most known functions of glycerophospholipids are as structural components promoting cell integrity, a number of studies have shown that these compounds in their own right carry out signalling and regulatory functions (Kilpinen et al., 2013, Li et al., 2007, Sims et al., 2013).

Vitamins & cofactors

The small numbers of metabolites detected within this group make it hard to postulate with any degree of certainty where the bulk of cell activity specifically lies. Analysis of detected masses in Pathos broadly distributes these into a number of pathways not necessarily known to overlap. That is the number of hits per pathway were no higher than 3 lending little confidence about making assessments attributed to a specific process.

Nevertheless, differential behaviour between substrate for specific compounds can be observed (Figure 3-17). In a general sense, the bulk of the total population can be placed within B-vitamin metabolism (80%). The difficulty to pin point areas of particular interest may also be due to the fact that these metabolites deal with functional molecules that have a high degree of recyclability; B3 vitamins are precursor to nicotinamide adenine dinucleotide (NAD/NADH) and adenosine triphosphate (ATP), B2 vitamins are precursors to flavin mononucleotide (FMN) and flavin adenine dinucleotide (FAD). The nature of these molecules and the roles they play in facilitating reactions mean that they are in constant and rapid flux; therefore their activities may not be wholly captured by the currently employed methodologies.

One such pathway of interest is nicotinate and nicotinamide metabolism which plays a major role in the synthesis of NAD and NADH as well as ensuring the cell maintains these in optimal proportions (Stein and Imai, 2012). The ratios of NAD/NADH maintained by the cells are differential, and observed to be specific to particular cell types (Alano, 2007).

As such, it could be postulated that demands of such a specific nature, can be taken into account when considering differences in phenotype adopted by MSCs cultured on each

of the substrate surfaces. This also likely goes some way to influencing the effect seen in **Error! Reference source not found.**F where substrate properties produce the differential effects observed by principal component analysis.

Although they do not form mature cell types within the 24 hr time frame it is likely that early adopted behaviour to meet energy demands reflect the intentions of the cells as they develop on the substrates.

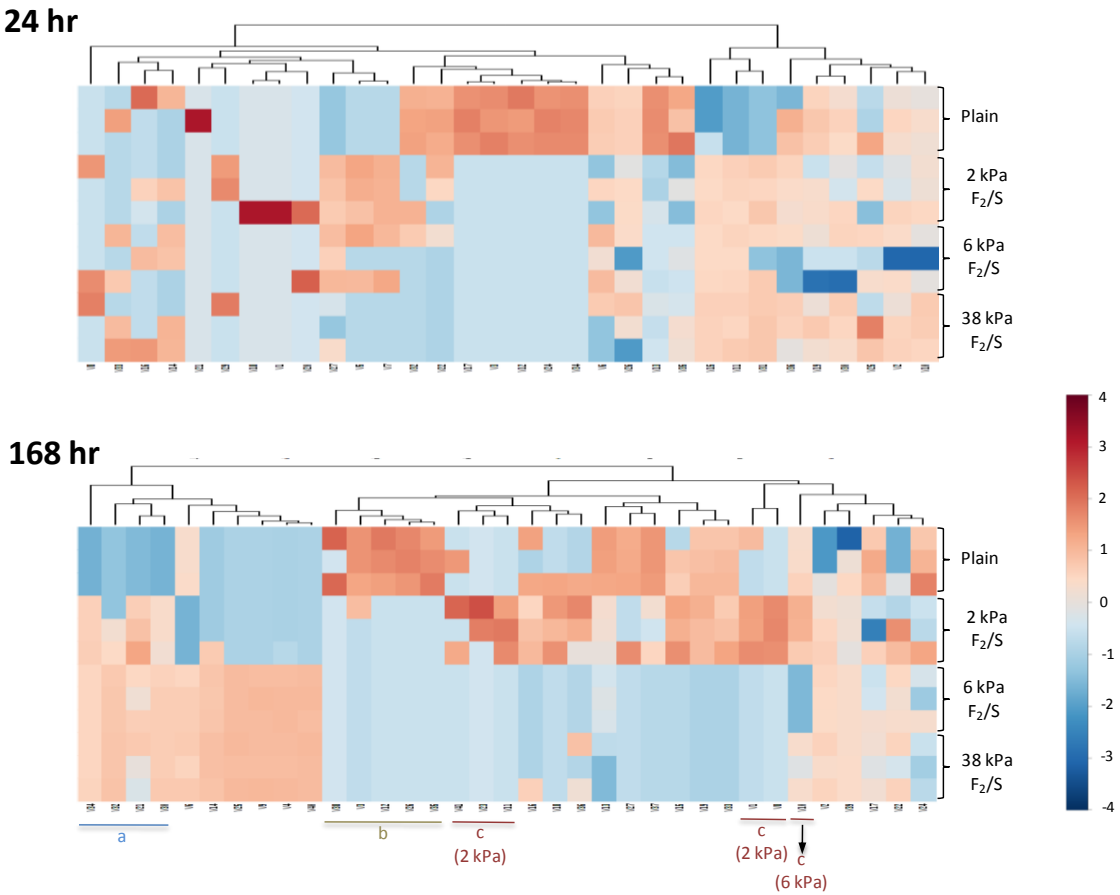

Figure 3-17 Hierarchical cluster analysis performed for cells cultured on plain, 2 kPa, 6 kPa and 38 kPa F_2/S hydrogel substrates. *Data sets were obtained from putative metabolites that were classed within vitamin & cofactor metabolism and analysed at 24 and 168 hours from each substrate set. The image shows the heat maps generated from individual samples (n=3) cultured on each substrate type. At 168 hrs (considered to be the time point where the most divergent activity lies), regions are annotated that show the most contrasting change where metabolites were most up regulated on the F_2/S hydrogels (a) and most up regulated on the plain substrate (b). Together, these both highlight regions of most activity brought on by substrate change. Region (c) is defined by areas that are particular to a certain F_2/S hydrogel type as indicated on the image.*

3.4 Summary

Each sample set was analysed for the total protein content measured using UV (Bradford assay). Peak intensity values measured using LC-MS were then normalised against respective protein content.

Total metabolite abundance was assessed after 24 hrs and 168 hrs (1 week) in culture. The plain (control) substrates did not show any discernible change over the two measured time points. MSCs cultured on the hydrogel surfaces showed a significant decrease in concentrations at 24 hrs and these levels were observed as 'recovered' (comparable to control) after one week. It is thought that when cells are introduced into a microenvironment they undergo a period of adaptation and eventually reach a point of stability where the net change in cell activity is comparatively negligible as observed by day 7. This equilibrated state, however, manifests differently for each of the substrates when the metabolome is analysed as a whole (illustrated using volcano plots) showing unique dispersion patterns for cells cultured on each substrate.

From this, smaller subsets (classified into metabolic pathways – amino acid, lipid, carbohydrate, vitamin & cofactor metabolism) were used to highlight differences that occur on a subtler scale. Cell activity was observed as generally anabolic for amino acid and vitamin metabolism and catabolic for carbohydrate and lipid metabolism.

PCA analysis of each pathway had shown that cell activity of MSCs cultured on the plain substrates were distinct from those on the F_2/S hydrogel substrates. MSCs on the F_2/S hydrogel showed no discernible distinction from one another at 24 hrs but began to differ after 1 week (168 hrs) in culture. Of the three F_2/S substrates, cells cultured on the 2 kPa F_2/S showed the most distinctive metabolic behaviour with cells cultured on the 6 and 38 kPa F_2/S surface having a degree of overlap. Vitamin & cofactor metabolism however, showed unique metabolic patterns for all four substrates independent of one another. Assessment by cluster analysis more or less echoed the sentiments of PCA with cells on the 2 kPa F_2/S showing distinctive metabolic profile from the 6 and the 38 kPa F_2/S which were otherwise very similar to each other.

Assessment by cluster analysis however, enabled pathway mapping of metabolite masses showing the most contrasting differences between the plain and F_2/S substrate and for masses showing differing activity between the F_2/S substrates themselves. Of these, the pentose phosphate pathway was highlighted for NADPH generation for biosynthetic processes as well as arginine & proline metabolism for the observed effect on proline interconversion.

Whilst total amino acid metabolism is observed as steady over 24 hrs in culture (Figure 3-8), the results suggest that the proteinogenic process to affect change is somewhat delayed (later than 24 hrs) as the cells explore their external surrounding and adjust to it

accordingly. The overall biosynthetic process observed at 7 days (168 hrs) requires energy input and catabolism of the required carbohydrate and lipid molecules. Interestingly, in line with this, the precursors needed to drive this process show the most effect after 24 hrs (vitamins & cofactors, carbohydrate metabolism) leading up to phenotypical differences that begin to manifest around 168 hrs in culture.

Mapping metabolite masses for vitamin and cofactor metabolites were of a sporadic nature returning only a few hits per pathway reducing confidence. As such making any plausible assessments proved very difficult. As a collective, it was noted that most of the masses could be attributed to B vitamin metabolism which is responsible for the building blocks of cofactors such as NAD, FAD & ATP, compounds that are responsible for driving many a reaction.

Lipid metabolite masses had presented with the same problem as those for vitamin and cofactor metabolism albeit, for a different reason. Whereas with vitamin and cofactor metabolism most masses were few or not identified, most of the lipid masses could be identified but not mapped due to a lack of general information on the role these compounds play within the cell. This finding is somewhat frustrating given that lipid metabolism was the only pathway that had detected regions on the clusters where change in behaviour particular to a substrate was not restricted for the most part to the 2 kPa F_2/S, but regions of change were also noted for the 6 and 38 kPa substrates also (Figure 3-16).

4 IDENTIFYING ENDOGENOUS SMALL MOLECULES FROM THE METABOLOME THAT DRIVE DIFFERENTIATION

4.1 Introduction

The use of small molecules to direct stem cell fate on differentiation is a practice that has been in place for many years. They have shown particular usefulness as a means of modulating cell behaviour and function through targeting certain cell signaling mechanisms. Phenotypical screening, sometimes involving the use of high throughput processes, has led to the use of singular or combinatorial chemistries for influencing cell behaviour. Of these, purmorphamine, dexamethasone and ascorbic acid have been shown to influence osteogenic and chondrogenic development of cells (Lin et al., 2005, Mirmalek-Sani, 2006, Pittenger et al., 1999, Sekiya et al., 2002, Wu et al., 2004) and are used conventionally as such *in vitro*. Isobutylmethylxanthine (IBMX), indomethacin and rosiglitazone through induced PPAR-γ activation are known to drive adipogenesis of stem cells (Benvenuti et al., 2007, Janderova et al., 2003, Klemm et al., 2001, Mirmalek-Sani, 2006, Zuk et al., 2001). While all trans retinoic acid and β-mercaptoethanol are broadly used in culture systems for neuronal differentiation (Yim et al., 2007, Woodbury et al., 2000).

These compounds tend to have broad acting, non-specific modes of action, modulating a number of pathways that have generic effects on cellular behaviour such as Smad, extracellular signal regulated kinase (ERK) or protein kinase C (PKC). For example, 5-aza-cytidine, a DNA methylating compound, has no direct induction on any specific differentiation pathway but acts by switching the cell into a state whereby it is susceptible to spontaneous differentiation (Ding and Schultz, 2004). As a result, 5-aza-cytidine is implicated in myogenic (Lassar et al., 1986, Taylor and Jones, 1979), adipogenic (Taylor and Jones, 1979) and chondrogenic (Taylor and Jones, 1979) development of stem cells. This characteristic, on one hand, allows the ability to able to induce cells along a primary lineage with careful consideration. And on the other, they are also prone to generate heterogeneous cell populations due to the effects of cross reactivity.

However, the promise of the role of small molecules in pharmacology is considerable given the focus on the generation of research libraries for stem cell therapies. They also provide some distinct advantages over other currently used techniques; such as gene manipulation, lessening the risk associated with viral integrated transcription factors in induced pluripotency of stem cells (Ding and Schultz, 2004). As such, it would be of great advantage to be able to isolate small molecules that have the propensity to reduce population heterogeneity when seeking to either maintain stem cells in an undifferentiated state or looking to drive them toward a particular cell fate by acting through more discrete cell mechanisms.

Metabolite (biological small molecule) profiling of stem cell behaviour during differentiation using a broad metabolomics approach gives information on the plethora of naturally occurring small molecules that exist within the cell as illustrated in the previous chapter. These populations are likely inclusive of small molecules that are vital in influencing signalling transduction pathways such as PKC or mitogen activated protein kinase (MAPK) for example, affecting functions such as DNA transcription, cell differentiation and apoptosis.

The exploration of small compounds generated as a result of innate cell activity may give an insight into metabolites that facilitate stem cell differentiation through more discrete pathways leading to the development of more uniform cell populations *in vitro*, as well as finding application in cellular re-programming methods.

4.1.1 Objective

As illustrated in the previous chapter, an unbiased study of the cells metabolome by LC-MS is able to reflect changes in cellular phenotype as they undergo differentiation. Further scrutiny of the LC-MS data has the potential to give more detail into the activity of the cells beyond illustrating general trends. It was postulated that careful analysis of the obtained data could give information on lesser researched intrinsic molecules that may play a role in influencing stem cell lineage commitment during differentiation.

4.2 Materials & methods

4.2.1 Materials

Materials/Reagents	**Supplier(s)**
Mesenchymal stem cells	Promocell GmBH, Germany.
Fmoc-diphenylalanine	Bachem, UK
Fmoc-serine	Bachem, UK
Sodium hydroxide	Fisher chemicals, UK
Distilled water	Invitrogen, UK
Dulbeccos modified eagle medium (DMEM)	Sigma Aldrich, UK
Foetal bovine serum (FBS)	Sigma Aldrich, UK
Penicillin streptomycin	Sigma Aldrich, UK
Trypsin	Sigma Aldrich, UK

Cholesterol sulphate (sodium salt)	Sigma Aldrich, UK
1-octadecanoyl-sn-glycero-3-phosphate (GP18:0)	Avanti polar lipids Inc., USA
Sphinganine	Sigma Aldrich, UK
Dimethyl sulfoxide (DMSO)	Sigma Aldrich, UK
Human insulin	Sigma Aldrich, UK
Dexamethasone	Sigma Aldrich, UK
Ascorbate-2-phosphate	Sigma Aldrich, UK
Transforming growth factor β1 (TGF-β1)	Sigma Aldrich, UK
Sodium pyruvate	Sigma Aldrich, UK
Phosphate buffered saline (PBS)*	In-house
Fixative*	In-house
Permeability buffer*	In-house
1% BSA in PBS*	In-house
Vectashield-DAPI	Vector laboratories, USA
Rhodamine-phalloidin	Invitrogen, USA
Primary antibodies	Abcam, UK & Santa Cruz biotechnologies, USA
Biotinylated secondary antibodies	Vector laboratories, USA
Streptavidin-FITC	Vector laboratories, USA
0.5% Tween 20 in PBS*	In-house
Alizarin red S	Sigma Aldrich, UK
RNeasy micro kit	Qiagen, UK
Trizol	Life technologies, UK
Chloroform	Sigma Aldrich, UK
Glycoblue	Ambion, UK
Isopropanol	Sigma Aldrich, UK
Ethanol	VWR Chemicals, France
RNase free water	Qiagen, UK
Quantitech reverse transcription kit	Qiagen, UK
Quantifast SYBR green PCR kit	Qiagen, UK

* Preparation procedures for reagents & buffers made in-house are detailed in the appendix.

4.2.2 Test compounds

5mg of cholesterol sulphate and 1-octadecanoyl-sn-glycero-3-phosphate (GP18:0) was dissolved in 0.25 ml of DMSO to give a stock solution of 20 mg/ml. 10mg of sphinganine was dissolved in 0.5 ml of DMSO by sonication at 40°C to give a stock solution of the same concentration.

All stock solutions were subsequently stored at -20°C.

4.2.3 Cell culture

29.4 μl, 18 μl and 26.4 μl of each compound (Cholesterol sulphate, Mw 488.7; sphinganine, Mw 301.51 and GP18:0, Mw 460 respectively) were added to 12 ml of DMEM culture media to give a uniform starting concentration of 100 μM of each compound. Care was taken to ensure that the final DMSO concentration in this solution was less than 0.3% to make certain that cell culture conditions are affected only by the test metabolites.

Starting solutions were then serially diluted 10x to give 10 μM, 1 μM, 100 nM, 10 nM and 1 nM solutions. All 6 solutions were then stored at -20°C until ready for use in cell culture. Cells were cultured in well plates with each compound at each concentration initially for a period of two weeks to assess for toxic effects and subsequently for three weeks with all three test compounds for their ability to influence MSC differentiation lineages.

4.2.3.1 Micromass cell culture

To aid chondrogenic development of MSCs, cells were maintained in culture using a micromass protocol. Micromass cell culture is an adapted version of the pellet culture system generally used for chondrogenic development of bone marrow stromal cells. The micromass culture system maintains the three dimensional support needed to maintain phenotypic integrity of chondrocyte cells, in particular, it also allows *in vitro* monitoring of chondrogenic development to occur at a smaller scale compared to the pellet culture method (Johnstone et al., 1998, Muraglia et al., 2003). Cells are cultured within a confined space and at high density to encourage formation of the spherical phenotype adopted by chondroblast cells as is already attained in pellet culture. This method of cell culture was used to assess the ability of GP18:0 to influence the chondrogenic development of MSCs *in vitro*.

Cell suspension droplets (50 µl) were incubated at 37°C for at least 1½ hours on culture well plates to allow the cells to adhere. Care was taken to ensure that this small volume did not evaporate over the time taken to allow adhesion to occur.

After cells had adhered to the culture well 500 µl of chondrogenic induction media or the required concentration of GP18:0 was gently added to the well and the cells maintained in culture for 10 days.

4.2.3.2 F_2/S hydrogel cell culture

Soft hydrogel substrates (2 kPa) were fabricated and used for culturing MSCs as described earlier in 2.2.3. MSCs cultured on the F_2/S were used to assess the effect of the test compound sphinganine on neuronal differentiation of the MSCs over a two week period. F_2/S culture with sphinganine was carried out as results can conflict when inducing a low tension phenotype on hard and soft biomaterials.

4.2.3.3 Standard differentiation controls

Directed differentiation of MSCs was accomplished by supplementing standard DMEM culture media with tailored cocktailing of inducing agents. These were used as positive controls against the relevant test items.

Chondrogenic differentiation was induced as described elsewhere (Lin et al., 2005, Sekiya et al., 2002) using DMEM containing 10% FBS, insulin (6.25 µg/ml), dexamethasone (100 nM), ascorbate-2-phosphate (50 nM), transforming growth factor (TGF-β1, 10 ng/ml) and sodium pyruvate (110 µg/ml).

Osteogenic differentiation was induced using DMEM containing 10% FBS, dexamethasone (100 nM) and ascorbate-2-phosphate (350 µM).

Cells were then maintained at 37°C in differentiation media and the media changed twice weekly for the duration of the experiment.

4.2.4 Cytotoxicity

Cells were rinsed once in PBS and fixed at 37˚C for 15 minutes. They were then permeabilised and blocked using 1% BSA in PBS. A drop of vectashield-DAPI was placed over the cells and samples stored at 4˚C wrapped with tin foil to protect from light until ready for viewing under a microscope.

Cells visualised by fluorescence staining of their nuclei were counted by observation using a cell counter. An average count was taken from five repeat samples and used to ascertain what concentration ranges were suitable for further experiments.

4.2.5 Immunocytochemistry

Immunocytochemistry and microscopic analysis was carried out as detailed in 2.2.5 and 2.2.6. Details of the primary, secondary and tertiary antibodies used for this chapter are given in Table 4-1.

Table 4-1 Biomarkers used for detection of cellular differentiation

Differentiation lineage	Biomarker	Primary antibody	Secondary antibody	Fluorophore
Osteogenesis	OPN	Mouse monoclonal IgG	Biotinylated anti mouse	Stretavidin conjugated FITC
	OCN			
Chondrogenesis	SOX-9			
	COL2A1			
	Aggrecan			
Cytoskeleton	F-actin			Phalloidin conjugated rhodamine
Nucleus				DAPI

4.2.6 Alizarin red staining of osteogenic cultures

2 grams of alizarin red was weighed and dissolved in 100 ml of distilled water to create a 20mg/ml or 8.3 mM solution. The pH was then adjusted to 4.2 with sodium hydroxide and the solution passed through a 0.2 µm filter.

Culture media was aspirated to waste and the cells washed once with 500 µl of PBS. After washing, 500 µl of 10% formalin (fixative) was added to each well and allowed to incubate at room temperature for 20 minutes after which the cells were then washed twice for 5 minutes on a shaker with water.

Following this, 500µl of alizarin red s solution was added to each culture well and incubated at room temperature for 30 minutes. Cells were then washed four times with 1ml sterile water or repeatedly until the liquid was clear. Samples were stored in PBS solution at 4˚C until ready for viewing under a microscope.

4.2.7 RNA extraction and reverse transcription

RNA extractions of cells cultured in plastic well plates were done using the RNeasy microkit (Qiagen) as per manufacturers protocol and extractions from cells cultured on the 2 kPa hydrogel substrates were done as described in 2.2.7.

Reverse transcription of all samples was carried out using the QuantiTect reverse transcription kit (Qiagen) as per the manufacturer's instructions.
Resultant cDNA samples were then stored at -20°C or used immediately for qRT-PCR experiments.

4.2.8 QRT-PCR

Samples intended for qRT-PCR analyses were handled as described in 2.2.8. Details of the PCR primers used within this chapter are given in Table 4-2.

Table 4-2 PCR primers designed for human genes

Gene		
GLUT-4	Forward	5'-ATG TTG CGG AGG CTA TGGG-3'
	Reverse	5'-AAA GAG AGG GTG TCC GGT GG-3'
OPN	Forward	5'-AGC TGG ATG ACC AGA GTG CT- 3'
	Reverse	5'-TGA AAT TCA TGG CTG TGG AA -3'
Collagen type II (COL2A1)	Forward	5'-GTG AAC CTG GTG TCT CTG GTC-3'
	Reverse	5'-TTT CCA GGT TTT CCA GCT TC-3'
Nestin	Forward	5'-GTG GGA AGA TAC GGT GGA GA-3'
	Reverse	5'-ACC TGT TGT GAT TGC CCT TC-3'
β3-tubulin	Forward	5'-CAG ATG TTC GAT GCC AAG AA -3'
	Reverse	5'-GGG ATC CAC TCC ACG AAG TA-3'
GFAP	Forward	5'-GCT TCC TGG AAC AGC AAA AC-3'
	Reverse	5'-AGG TCC TGT GCC AGA TTG TC-3'
GAPDH	Forward	5'-ACC CAG AAG ACT GTG GAT GG-3'
	Reverse	5'-TTC TAG ACG GCA GGT CAG GT-3'

4.2.9 Statistical Analysis

Suitable statistical tests were applied where warranted. Unpaired student t-tests were carried out using Microsoft excel for comparisons between two test groups. Analysis of variance (ANOVA) and Bonferroni post hoc tests were performed using GraphPad prism software to compare more than two study groups. One-way ANOVA was used when tests present with a single variant and two-way ANOVA for sample sets with more than

one variable. Statistical significance is noted where the calculated probability that the null hypothesis is true (p-value) is less than 5% confident (0.05) using four biological replicates unless otherwise stated.

Mean values for replicate experiments, standard deviations (StDev) and standard error from the mean (SEM) were calculated using Microsoft excel.

4.3 Results & Discussion

4.3.1 Isolating compounds of interest from the metabolome

In the previous chapter, numerical data obtained by mass spectrometric analyses were translated into heat maps to easily visualise regions or metabolites that show differential behaviour when cells were cultured on each substrate (plain, 2 kPa F_2/S, 6 kPa F_2/S and 38 kPa F_2/S). The heat maps and volcano plots were investigated in conjunction with one another in order to choose metabolites that may be of further interest, that is, metabolites that showed unique behaviour to a particular substrate. Although the heat maps give an insight into the abundance of metabolites the volcano plots serve as an added confidence, singling out molecules that are also of statistical significance (Figure 4-1). To reduce the search size, selected metabolites were taken from those identified as being involved with lipid metabolism.

While it is acknowledged that metabolomics carried out for assessment of the lipid population using HILIC is far from ideal, indeed a lipidomics approach optimising methods toward lipid detection is advisable were it the only facet of interest. The presently used HILIC technique however, is not necessarily a method that is considered entirely devoid of information on cellular lipids. In this vein, metabolite masses putatively identified as being involved in lipid metabolism were chosen for further investigation for a number of reasons. Samples within the lipid metabolism pathway showed the most amount of change on differentiation compared to the other investigated pathways. It also gave the most visible differential change between the F_2/S substrates when compared to the other pathways for which the most contrasting change was noted only for the 2 kPa F_2/S hydrogel. Lastly, within cell biology generally, functional changes are widely researched with regards to the genomic and proteomic changes. Relative to these, limited information is available about the role of lipids as regulators of cell behaviour and function as is highlighted in the previous chapter.

It therefore stands to reason that this facet of cell biology be explored further as the metabolomics study allows the means for doing so.

Due to the limitations associated with performing a global metabolomics study as discussed in the previous chapter, a number of precautions were taken when selecting metabolites for further study which also contributed to downsizing the search field:

a) The confidence value: the measure of confidence makes use of an arbitrary value between 1 and 10 (10 indicating the highest confidence) based on the retention time drift of the measured mass from the calculated/predicted retention when performing metabolite identification in Ideom. Selection was restricted to metabolites with a confidence factor of 6 and above.

b) The number of putative metabolites identified for a chosen mass from database cross-referencing is kept as low as possible. This reduces the risk of choosing false positives from metabolites with similar masses that could not be distinguished through chromatographic separation. It is acknowledged however, that this condition applies to the confines of the analytical tools used in this thesis. That is, metabolite identification of noted isomers is restricted to the scope of the databases that Ideom uses for identification.

c) Metabolite(s) that showed a significant decrease in abundance that was unique to a particular substrate. It also had to be detectable on the plain surfaces (control sample) indicating its presence within the cells when it is in a 'resting' state and showing depletion when the substrate properties are changed, i.e, cultured on hydrogel surfaces.

d) Other factors out with metabolite mass detection and behaviour such as commercial availability and current research done on each compound, which may give an inclination on the likelihood to affect cell behaviour (supporting the hypothesis), were also taken into consideration.

Using the aforementioned criteria, the metabolites cholesterol sulphate (CS), 1-octadecanoyl-sn-glycero-3-phosphate (GP18:0) and sphinganine were singled out for further investigation (Figure 4-2).

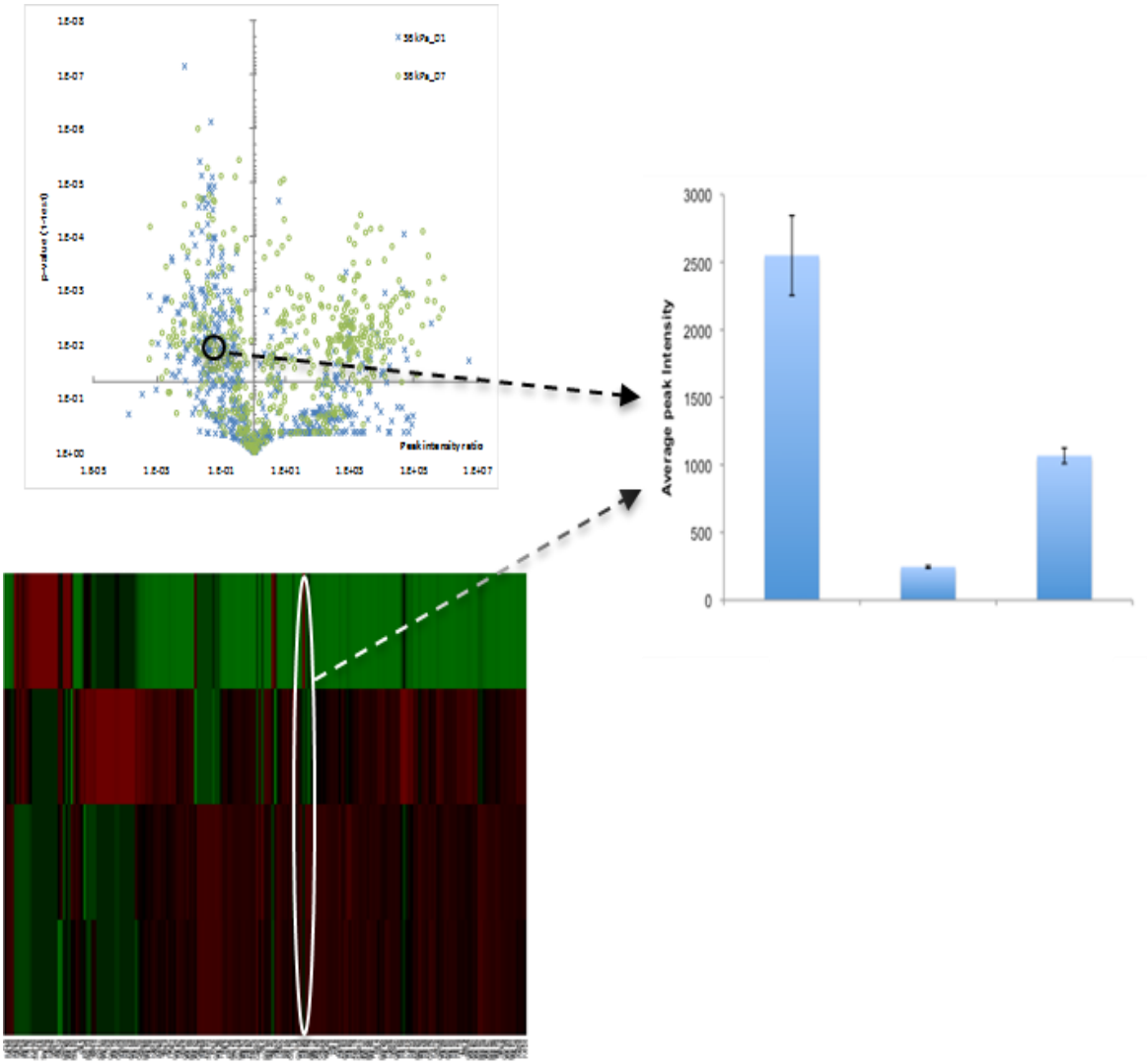

Figure 4-1 Simplified schematic illustrating metabolite selection process. *Metabolite chosen for further investigation were LC-MS metabolites that had been putatively identified as being involved in lipid metabolism. Selections were whittled down based on a number of defined criterion inclusive of measured abundances singled out by cluster analysis and statistical significance as determined from the volcano plots.*

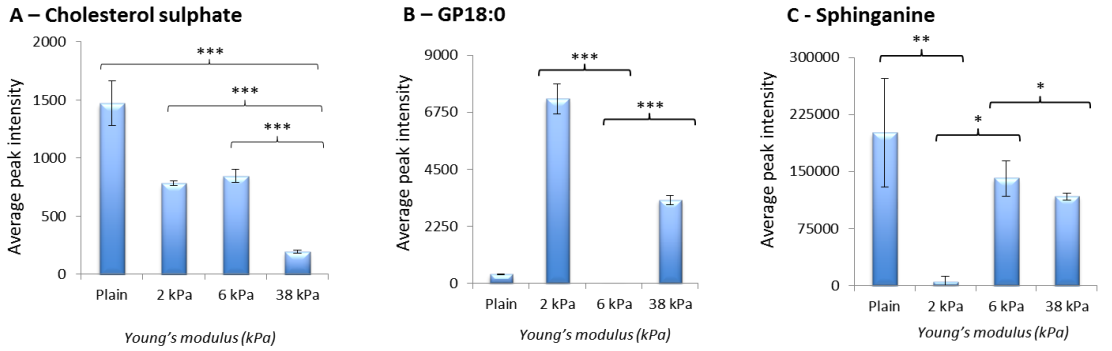

	Cholesterol sulphate	GP18:0	Sphinganine
Confidence value	6	6	8
Molecular mass	466.31	438.28	301.51
Number of identified isomers	1	3	1
Retention time (RT)	4.17 mins	8.00 mins	11.51 mins

Figure 4-2 Average peak intensities of metabolites isolated for further investigation. *Metabolites were chosen from those identified as being involved with lipid metabolism. An initial condition for selection was that each metabolite showed considerable depletion on a singular substrate compared to the remaining three biomaterials suggesting it may play a functional role that occurs uniquely in cells cultured on that particular substrate. Error bars denote standard deviations from the mean; n = 3 replicates; * notes statistical significance to the total population where p < 0.05, ** where p < 0.01 and *** where p < 0.001 calculated using one way ANOVA.*

4.3.2 Metabolite cytotoxicity and screening for differentiation

The metabolites were serially diluted 1 in 10 with DMEM culture media over the concentration range 1nM to 100μM. MSCs were then cultured in increasing concentrations of each metabolite and the cells observed over two weeks for any visible adverse effects. Cell counts were carried out after 1, 7 and 14 days in culture. Cells were fixed, permeabilised and their nuclei stained with DAPI. Cells were counted by observation under a fluorescence microscope. Numbers were then averaged (n = 5 replicates) and standard deviations calculated.

Cells were tolerant of cholesterol sulphate and GP18:0 for 2 weeks up to 10 μM where no significant change from the totalled average cell number was noted. A drop in the cell populations at 1 μM after 7 days was noted when cells were cultured with GP18:0. However, cell populations were observed to be stable for the duration in culture. Cells cultured with sphinganine showed less tolerance to this compound as sphinganine was found to be toxic at the 10 and 100 μM (Figure 4-3). Subsequent experiments were therefore performed using the range 1 nM – 10 μM for cholesterol sulphate and GP18:0 and 1 nM – 1 μM for sphinganine.

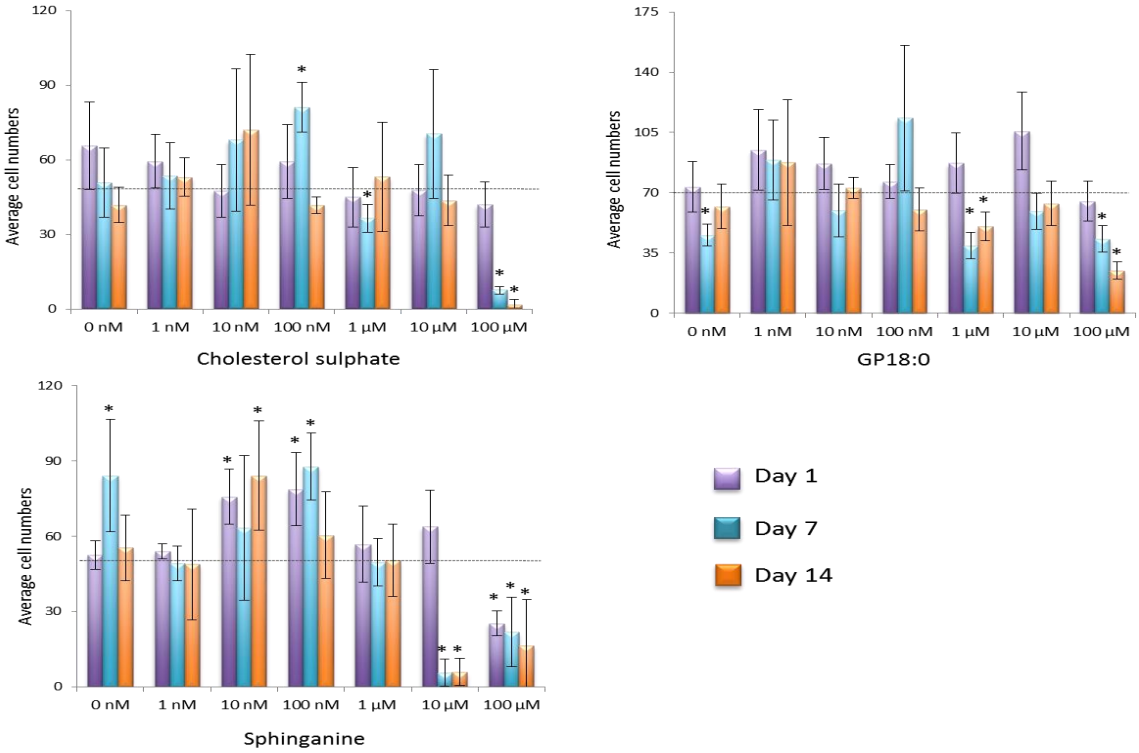

Figure 4-3 Cytotoxicity profiles of the metabolites cholesterol sulphate, GP18:0 and sphinganine. *Mesenchymal stem cells were cultured with increasing concentrations of endogenous metabolite for a two week period. Cell nuclei were stained with DAPI and counted after 1, 7 and 14 days in culture to ascertain populations of adherent cells. Cells were shown to be to cholesterol sulphate and GP18:0 up to 10 µM, while tolerance to sphinganine was observed up to 1 µM. Dashed line represents the average number of cells over the total population; Error bars denote standard deviations from the mean; n = 5 replicates; * notes statistical significance to the total population where p < 0.05 calculated using unpaired student t-test.*

Having determined cell tolerance levels to each of the chosen metabolites, MSCs were then cultured with these increasing concentrations of sphinganine, GP18:0 and cholesterol sulphate for a total of 3 weeks. Cell samples were then analysed for expression of differentiation biomarkers using a qRT-PCR screen. Cell samples were assessed for the production of nestin as indication of neuronal differentiation, Glut-4 for adipose differentiation, type II collagen and osteopontin for chondrogenic and osteogenic development respectively. Gene expression was compared to non-supplemented media sample set as well as being assessed for a dose dependent up-regulation in average gene expression (Figure 4-4).

Cholesterol sulphate showed strong induction of the osteogenic biomarker osteopontin. The same dose dependent up-regulation was not observed for nestin, GLUT-4 and type II collagen, suggesting that cholesterol sulphate is an osteoinductive metabolite.

Incubation of MSCs with GP18:0 showed a dose dependent increase in osteopontin but also for gene expression of type II collagen, a marker of chondrogenic development. Both genes showed a 6-fold increase at their optimum when cultured with 0.1 and 1 μM concentrations. These observations suggest that GP18:0 plays a role in both chondrogenic and osteogenic development of MSCs during differentiation.

Sphinganine did not show influence on the up-regulation of any of the tested lineages when cultured with MSCs. The effect of sphinganine on MSC behaviour was investigated in more detail and is discussed at a later point within this chapter.

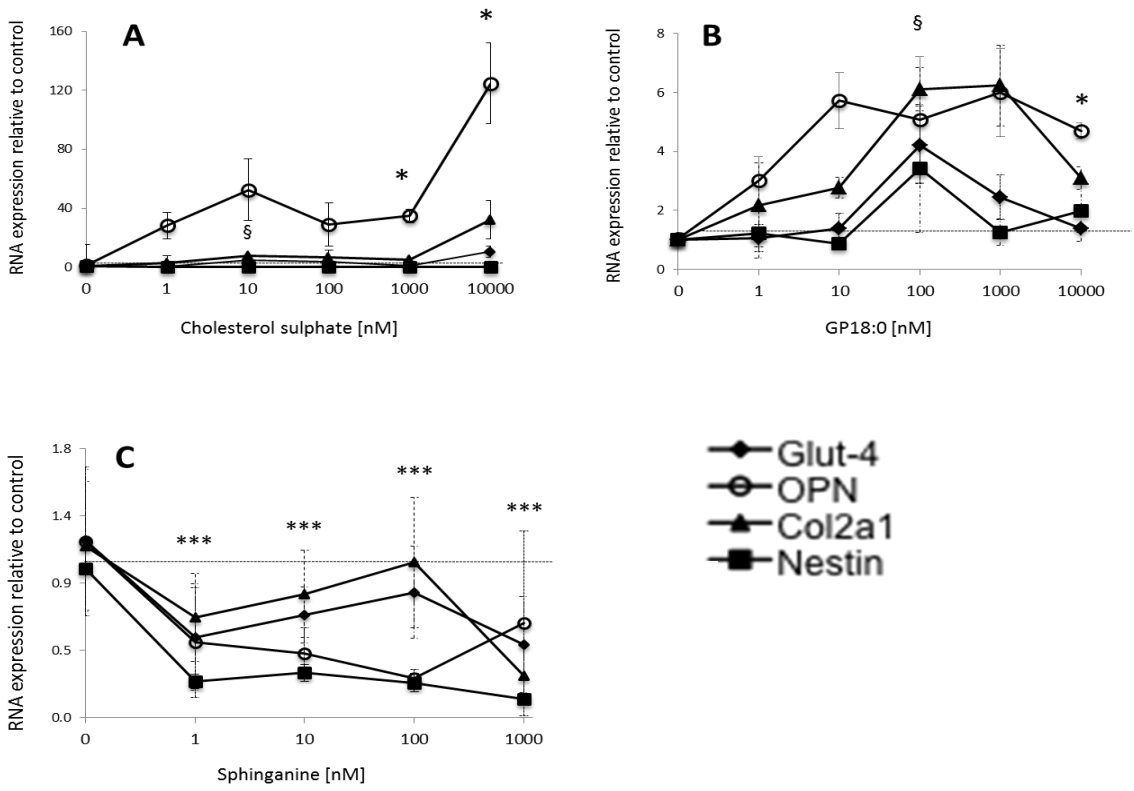

Figure 4-4 PCR screening to detect expression of specific differentiation biomarkers. *Mesenchymal stem cells were cultured with increasing concentrations of cholesterol sulphate, 1-octadecanoyl-sn-glycero-3-phosphate (GP18:0) and sphinganine. Samples were evaluated for production of the differentiation markers nestin, Glut-4, type II collagen (COL2A1) and osteopontin (OPN). Cells cultured with cholesterol sulphate (A), showed a dose dependent increase in OPN expression, while cells cultured with GP18:0 showed up regulation of both OPN and COL2A1. Cells cultured with sphinganine (C) did not show up regulation of any of the tested lineages. Negative control is held nominally at 1 (dashed line). Error bars denote standard error from the mean; n = 4 replicates; * notes statistical significance to the control where p < 0.05 for osteopontin; § notes statistical significance to the control where p < 0.05 for type II collagen; *** notes statistical significance to the control where p < 0.001 for nestin calculated using one way ANOVA.*

4.3.2.1 Cholesterol sulphate

Cholesterol sulphate is a metabolite formed from its more ubiquitous precursor cholesterol. It is found widely in most tissue types but is particularly noted for its abundance in skin where it facilitates the differentiation of keratinocytes (Kuroki et al., 2000). Cholesterol sulphate is also known to induce phosphorylation of high mobility group protein 1(HMG1) via casein protein I (CK-I) (Okano et al., 2001). HMG1 belongs to a larger family of high mobility group proteins that are associated with chromatin and play important roles in the regulation of gene transcription (Boonyaratanakornkit et al., 1998), suggesting an affecting role of cholesterol sulphate in gene expression.

Although cholesterol sulphate has attracted due interest in research, little is known about its ability to influence cell lineage commitment during stem cell differentiation. To confirm the results observed in Figure 4-4, MSCs were again cultured with cholesterol sulphate and fluorescently stained for osteopontin and osteocalcin expression, after 21 days in culture, both were observed to be up regulated (Figure 4-5). Extracellular calcium deposits, as evidence of mineralisation were also observed when cells were stained with alizarin red (Figure 4-6).

Although not as potent as the synthetic glucocorticoid dexamethasone, cholesterol sulphate, which is also a glucocorticoid (Figure 4-7), demonstrated a strong influence in promoting the production of osteogenic markers; dexamethasone is conventionally used in the nM concentration in osteoinductive media compared to cholesterol sulphate, which was tested at 1 μM).

While it is known that glucocorticoids play an integral role in the initial differentiation of MSCs along the osteogenic lineage (Bellows et al., 1987, Cooper et al., 1999, Mirmalek-Sani, 2006, Pittenger et al., 1999), over exposure to glucocorticoids can lead to the inhibition of osteogenesis (and on a larger scale osteoporosis (Manelli and Giustina, 2000)). This increase or over exposure in glucocorticoid levels is known to cause a shift in function, instead promoting adipogenesis (Bujalska et al., 2008, Justesen et al., 2004, Mirmalek-Sani, 2006, Zuk et al., 2001). For this reason, the widespread use of dexamethasone as a media supplement for differentiating cells *in vitro* requires, in addition to careful concentration management, the presence of other compounds that bias the system towards the desired lineage. Typically, nM concentrations of dexamethasone are used for osteogenic differentiation while μM amounts of dexamethasone or cortisol has been used for adipogenesis (Bujalska et al., 2008, Janderova et al., 2003, Klemm et al., 2001, Zuk et al., 2001). The lack of an exact “cut off” point between dexamethasone as an osteo- or adipo- inductive agent can render formation of a heterogenous cell population when MSCs are differentiated *in vitro*.

Cholesterol sulphate on the other hand, was used at concentrations at which dexamethasone and cortisol are known to induce adipogenesis (1 μM). Analysis of cholesterol sulphate effects by qRT-PCR (Figure 4-4A) indicated that at this concentration, GLUT-4 expression was negligible (1.2 fold change) compared to OPN expression (34 fold increase) suggesting that cholesterol sulphate is less likely to produce the heterogeneity effect that can be observed when using dexamethasone in *in vitro* culture.

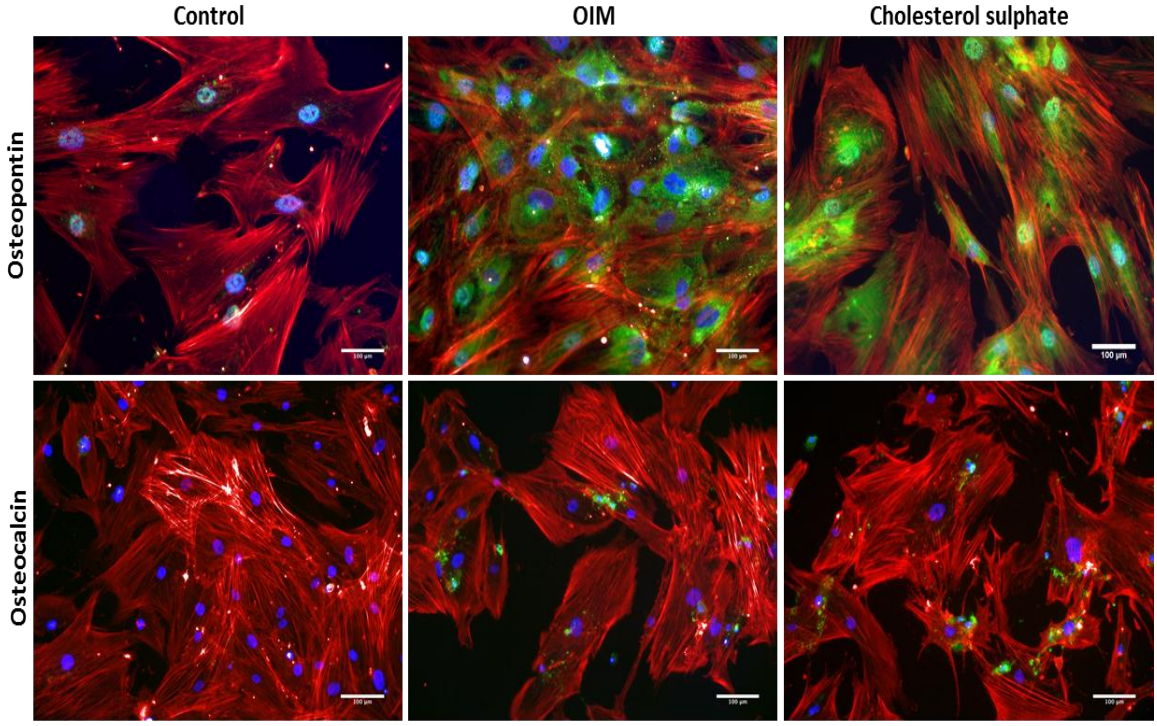

Figure 4-5 Immunofluorescence images of MSCs cultured in non-supplemented media, osteogenic induction media (OIM) and 1 μM cholesterol sulphate (CS). *Cells were maintained in culture for 3 weeks prior to staining. Cells cultured with cholesterol sulphate stained positively for differentiation biomarkers osteopontin and osteocalcin, indicating that cholesterol sulphate induced osteogenic development in MSCs. Fluorescence images show actin cytoskeleton (red), cell nuclei (blue) and either osteopontin or osteocalcin (green). Scale bar - 100μm.*

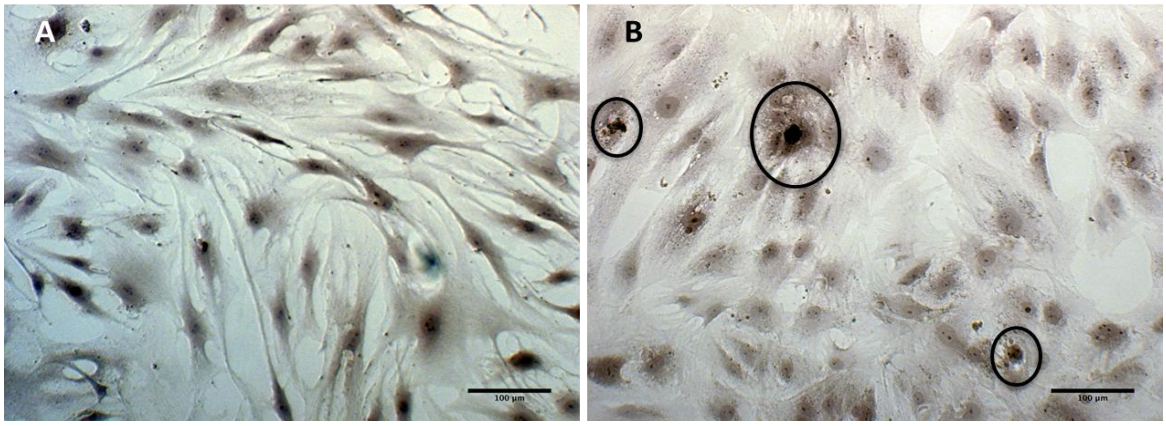

Figure 4-6 Light microscopy images of cells stained with alizarin red for calcium deposition. *Cells were cultured without (A) and with 1 µM cholesterol sulphate (B) for three weeks and then stained with alizarin red to assess for calcium mineralisation as MSCs differentiate into osteoblasts. Cells in (A) have only their intracellular calcium content stained by alizarin red while those in (B) have both intracellular and extracellular (circled) calcium deposits stained. Scale bar - 100µm.*

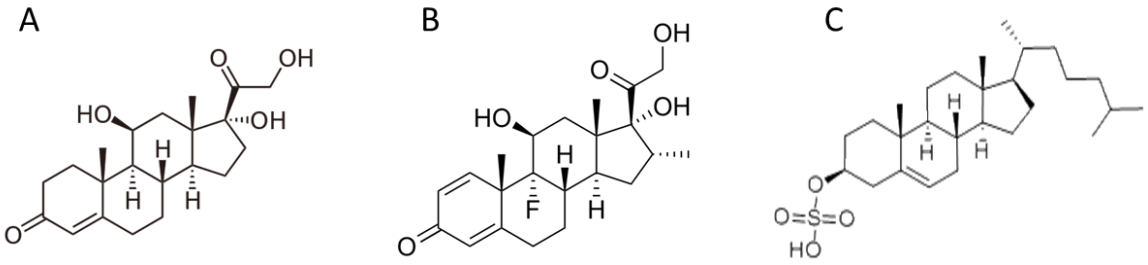

Figure 4-7 Chemical structures of the naturally occurring glucocorticoid cortisol (A), the synthetic counterpart dexamethasone (B) and cholesterol sulphate (C). *All three compounds are cholesterol derivatives, which may account for their common effect in inducing differentiation. Cortisol is known to induce both osteogenic and adipogenic effects. Dexamethasone also induces osteo- and adipogenic fates in MSCs and is routinely used in conjunction with other reagents in in vitro differentiation protocols. Cholesterol sulphate however, shows an osteogenic effect on MSCs as the sole inducing agent and was not shown to affect adipogenesis.*

Analysis using ingenuity pathways (IPA) to integrate metabolomic data with known genomic and proteomic activity shows that cholesterol sulphate is implicated in TGF-β mediated cell activity.

The TGF-β family comprises a set of related proteins inclusive of activins, bone morphogenic proteins (BMP) and growth differentiating factors (GDF). In broad terms, these proteins transmit signals from the cell membrane where they are located to the nucleus via the Smad signalling cascade resulting in a number of cell functions inclusive of differentiation. A number of steroidal compounds such as cortisol and

dehydroepiandrosterone sulfate (DHAS) have been shown to influence the activity of TGF-β (Lebrethon et al., 1994) and it may be that the structurally similar cholesterol sulphate also acts via this signalling route. Whether this interaction empathically leads to differentiation in MSCs however, is a hypothesis that still needs to be confirmed.

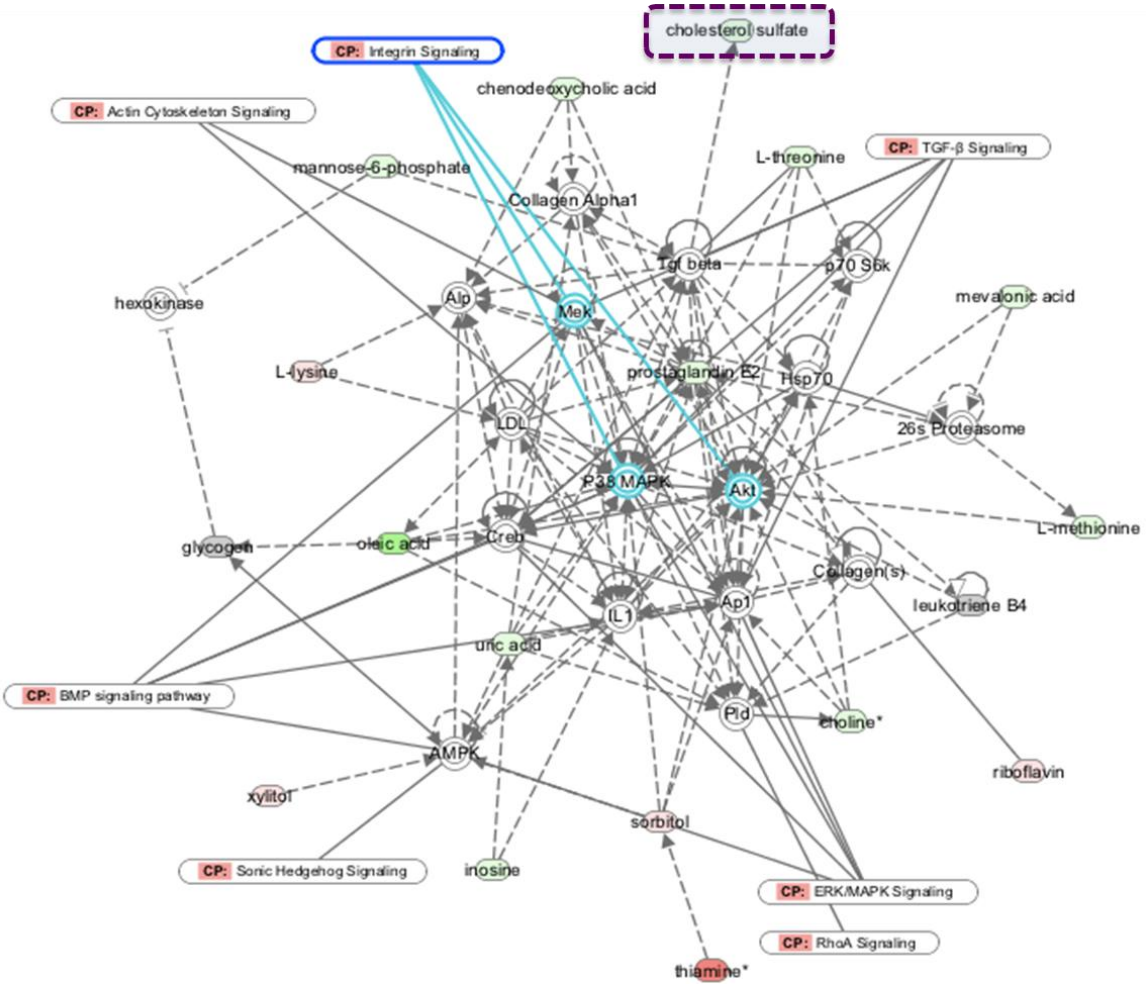

Figure 4-8 Ingenuity interaction pathway depicting direct (unbroken arrow) or indirect (broken arrow) molecular interactions for MSCs cultured on 38 kPa F_2/S hydrogels. *The assembled network illustrates the link between cholesterol sulphate (purple dashed outline), TGF-β and the wider influencing MAPK, which is activated in response to external stimuli via integrin signalling (blue outline). Hubs for detected down regulated metabolites are shown in green, up regulated in red and unchanged in gray. CP denotes systems involved in canonical pathways*

4.3.2.2 1-octadecanoyl-sn-glycero-3-phosphate (GP18:0)

Lysophosphatidic acids (LPAs) comprise a glycerol phosphate backbone attached to a fatty acyl chain. The structures of LPAs differ due to variations in the length and saturation of the acyl chain. They are known to act as regulators of the MAPK and ERK

pathways (Kim et al., 2005) both of which play central signalling roles in a number of cell functions inclusive of differentiation, acting via membrane bound G-protein coupled receptors (LPA_1 – LPA_6 inclusive). 1-octadecanoyl-sn-glycero-3-phosphate (GP18:0), the metabolite identified putatively by LC-MS and used within this study belongs to this class of compounds.

The PCR experiments performed prior (Figure 4-4B) had shown a parallel influence of GP18:0 on both osteogenic and chondrogenic development of MSCs *in vitro*. The results observed for osteogenesis is in line with previous studies also reporting the osteoinductive nature of LPAs (Blackburn and Mansell, 2012, Lapierre et al., 2010, Mansell and Blackburn, 2013, Mansell et al., 2011, Sims et al., 2013). Less is known about the chondrogenic effect on stem cells, however, there are a number of studies that research the effect of LPAs on chondrocyte cells, which is shown to affect their proliferation and migratory behaviour (Facchini et al., 2005, Hurst-Kennedy et al., 2009, Kim et al., 2005, Koolpe et al., 1998).

In light of this, further experiments were carried out to confirm chondrogenic potential of GP18:0. MSCs were maintained in micromass culture for 10 days with 0.1 µM GP18:0 and checked for chondrogenic development by fluorescently staining for the early biomarker SOX-9 and the subsequently expressed aggrecan protein. Expression of the early biomarker SOX-9 was seen for cells cultured with GP18:0 indicative of early chondrogenic differentiation but later development indicated by aggrecan expression was less abundant compared to MSCs cultured using chondrogenic induction media (Figure 4-9); however, it was notable compared to control. The results indicate that GP18:0 potentially plays a role in early signalling for chondrogenesis but perhaps plays a lesser role in the subsequent maturation during cell development. It could also indicate however, that development is simply delayed compare to the use of chondrogenic induction media

The comparable expression of osteo- and chondroinductive markers instigated by the presence of GP18:0 suggests multifunctional roles of the metabolite with regards to cellular development. This occurrence highlights a reason for the observed similarity observed in the cluster analysis heat maps and PCA analysis generated from the metabolomics data set discussed in the previous chapter. While it may very well reflect the heterogeneous population, it is also likely from the experiments done with GP18:0 that metabolites produced during stem cell differentiation play more than a singular function leading to different outcomes. In this instance, the interplay between osteo- and chondrogenic development is something that finds application for development of the osteochondral interface where these two tissue types are intricately linked.

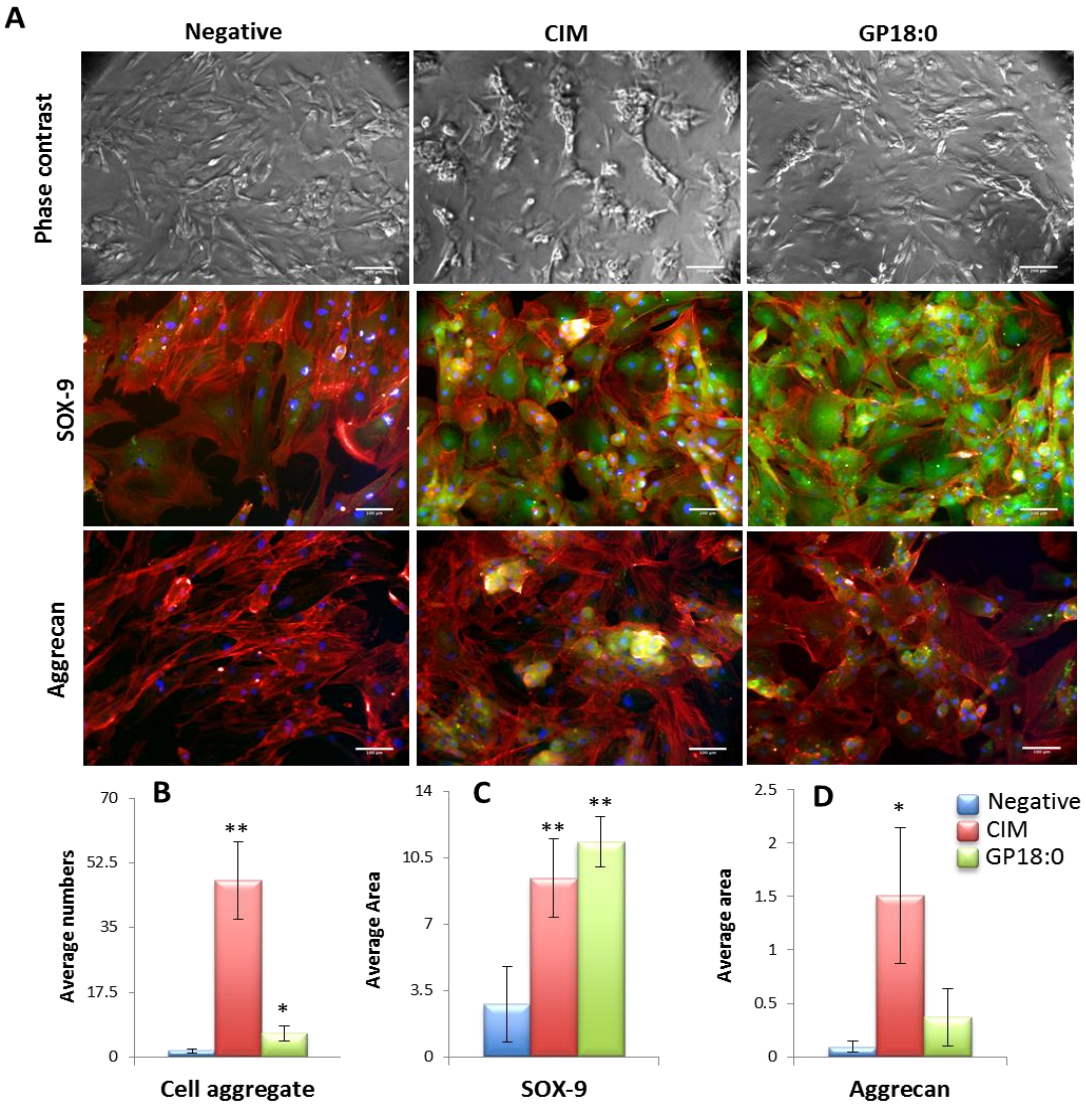

Figure 4-9 Immunofluorescence images of MSCs cultured in non-supplemented media (negative), chondrogenic induction media (CIM) and 0.1 µM GP18:0. *Cells were maintained in culture for 10 days prior to staining. (A) Phase contrast images show the formation of cell aggregates in chondrogenic inductive media (CIM) which was not extensively observed when cells were cultured with GP18:0. Although cell aggregates were not present in as high numbers, the distinct rounded cell morphology adopted by chondroblasts were observed. Aggrecan expression was also considerably less for cells cultured with GP18:0 and could only just be detected by immunofluorescence. (B – D) are graphical representations of the images shown in (A) showing aggregate count (B), area covered by biomarker fluorescence of SOX-9 (C) and aggrecan (D). Fluorescence images show actin cytoskeleton (red), cell nuclei (blue) and either sox-9 or aggrecan (green). Images were taken at 10x magnification; Scale bar - 100µm. Phase contrast images were taken at 4x magnification; Scale bar - 200 µm. Error bars denote standard deviations from the mean; n > 3; * & ** notes statistical significance compared to the negative control where p < 0.05 and 0.01 respectively as calculated using unpaired students t-test.*

4.3.2.3 Sphinganine

It was postulated that the putatively identified sphinganine may have an important role to play with regards to neuronal differentiation, as the primary differentiation route adopted on the 2 kPa hydrogel substrate was determined to be as such (Figure 2-10) and considerable depletion in relative amounts which was unique to the soft (2 kPa) substrate was observed by LC-MS (Figure 4-2).

However, PCR screening for differentiation lineages showed that sphinganine had no positive effect on neuronal development. Analysis of additional neuronal markers β3-tubulin and glial fibrillary acidic protein (GFAP) also showed the same trend.

In light of this, the original experimental format from which the metabolite was identified was returned to and the effect of sphinganine investigated with MSCs cultured on the soft hydrogel substrates. Cells were cultured on the 2kPa hydrogel in the presence and absence of 1 μM sphinganine for a 2 week duration. MSCs were then harvested and RNA expression of nestin, GFAP and β3-tubulin ascertained at 1 and 2 weeks respectively (Figure 4-10B - D).

Gene expression of all three neuronal markers were observed to be elevated in cell samples cultured in the presence of sphinganine (SP+) as compared to the unsupplemented hydrogel substrate (SP-).

These results highlight the extent to which biomaterial properties have an influence in guiding cellular activity. The physical and mechanical differences between the planar culture plastic surface and the relatively soft hydrogel surface affects the overall cell morphology or shape adopted on each surface, which is known to have a profound effect on lineage commitment when stem cells are cultured on substrates that induce these changes (Bhadriraju et al., 2007, Kilian et al., 2010, McBeath et al., 2004). In addition, relative cell elasticity is known to manifest as a consequence of substrate rigidity (Discher et al., 2005, Hoerning et al., 2012) brought about through remodelling of the cytoskeleton or actin polymerisation in cohort with rhoGTPase activity (Patel et al., 2012). As such, these remodelling activities are known to have profound effects on overall cell function, transcription and metabolism (Engler et al., 2006, Hoerning et al., 2012, Patel et al., 2012, Tilghman et al., 2012) and as a result, modulate processes that are deemed permissible to the cell dependent of its microenvironment. It therefore can be postulated that sphinganine is a molecule that acts both as a negative and positive regulator, either enhancing or modulating the differentiation process when the conditions are favourable.

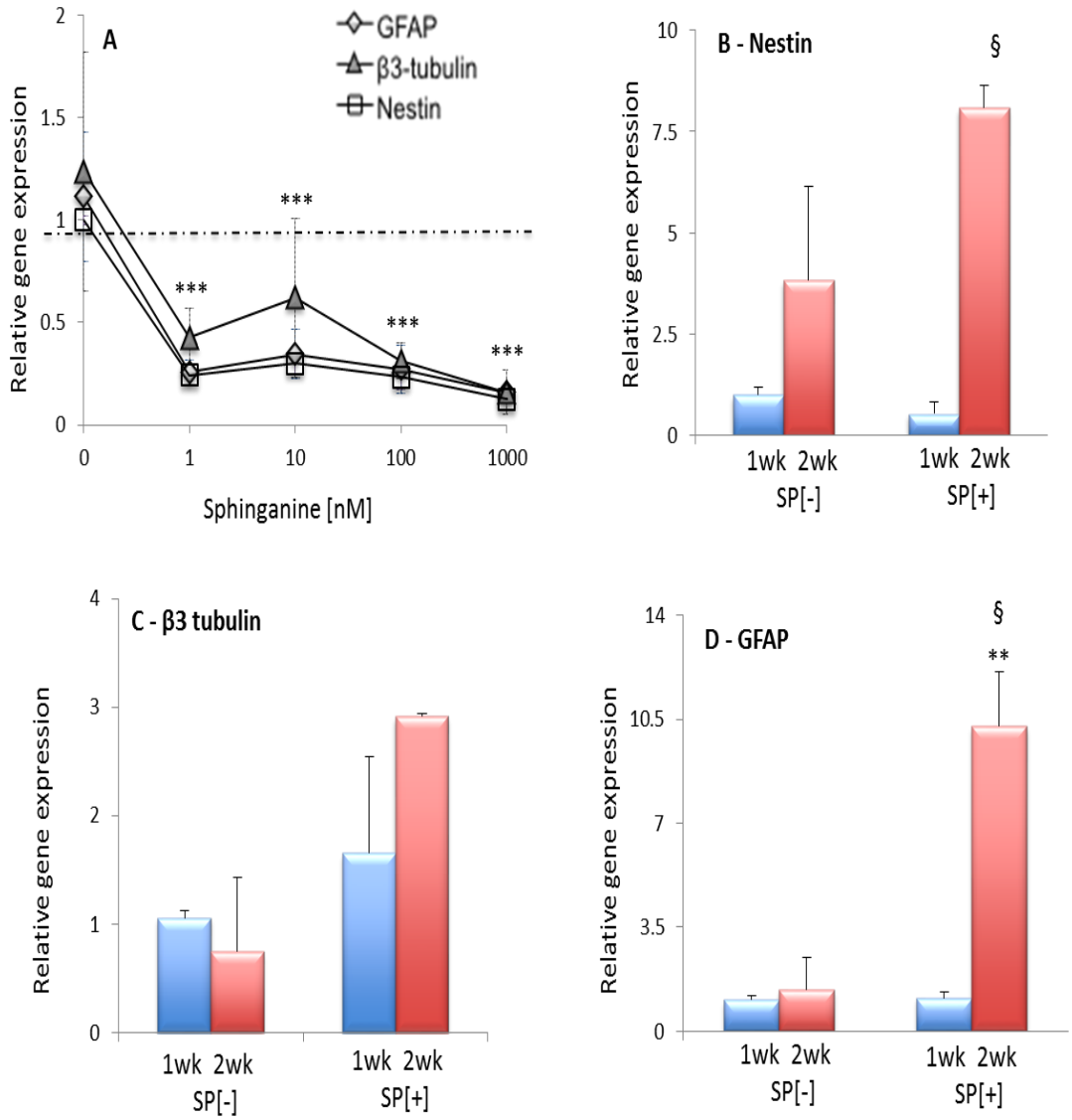

Figure 4-10 PCR analysis of neuronal development of MSCs cultured with 1 μM sphinganine [SP+] and without [SP-]. *(A) MSCs were cultured in well plates with increasing concentrations of sphinganine and samples were evaluated for production neuronal markers, nestin, GFAP & β_3-tubulin. Expression levels for all three biomarkers were considerably lower than those detected for the negative control. Negative control is held nominally at 1 (dashed line). *** notes statistical significance to the control where $p < 0.001$ for nestin calculated using one way ANOVA. The same neuronal markers where again assessed when MSCs were cultured on the 2 kPa F_2/S hydrogel substrate in the presence and absence of sphinganine (B - D). Expression of all biomarkers were observed to have increased over time when treated with sphinganine showing the opposite effect from the cells on the relatively stiff culture well plate. § notes statistical significance ($p < 0.05$) calculated using two way ANOVA in relation to time in culture and ** ($p < 0.01$) in relation to comparisons between treated [SP+] and non-treated groups [SP-]. Error bars denote standard deviations; n = 4 replicates.*

4.4 Summary

Data mining was carried out to isolate metabolites that showed substantial depletion unique to a particular biomaterial compared to the control sample and other hydrogel substrates. From this, the metabolites cholesterol sulphate (CS), 1-octadecanoyl-sn-glycero-3-phosphate (GP18:0) and sphinganine were identified putatively and singled out for further scrutiny on the roles they play in influencing targeted differentiation. Cholesterol sulphate had shown depletion on the rigid (38 kPa) hydrogel of which the primary differentiation lineage was osteogenesis. GP18:0 was observed for the stiff (6 kPa) substrate, which promoted chondrogenesis and sphinganine from the soft (2 kPa) substrate where neurogenesis was observed.

MSCs cultured with cholesterol sulphate had shown a strong propensity for osteogenic development. PCR analysis had shown a dose dependent increase in osteopontin production. Immunostaining for both OPN and OCN were positive suggesting that CS plays a primary role in directing bone development and formation. GP18:0 is a lysophosphatidic acid (LPA), a compound that has been shown in extensive research to play a role in the osteogenic development of stem cells. This finding was also supported in PCR experiments carried out when MSCs were incubated with GP18:0. Interestingly, GP18:0 also showed a dose dependent elevation of the chondrogenic biomarker COL2A1. Immunostaining for the chondrogenic biomarkers SOX-9 and aggrecan showed high level expression of SOX-9 and to a lesser extent aggrecan. This implies that GP18:0 likely has an influential role on initial development of chondroblasts.

MSCs cultured with sphinganine on the culture well plastic showed no increased expression of any of the differentiation markers tested for. Instead, nestin expression (neurogenic biomarker of which the hypothesis predicted cell line development) was observed as actively repressed. However, when cells were then cultured again in the presence and absence of sphinganine on the hydrogel surface, the treated group showed increased expression of a number of neurogenic markers.

The result highlights the importance biomaterial influence can have in guiding cellular activity and the extent to which they are permissive to cell development.

Whether these observed effects on stem cell behaviour due to careful manipulation of biomaterial mechanics can instigate differentiation in cell lines other than bone marrow stem cells and whether the effect is sustained over the longer term are questions that are further investigated in the following chapter.

5 MECHANICALLY TUNED F_2/S HYDROGELS & PERICYTES FOR CARTILAGE ENGINEERING

5.1 Introduction

The principal function of biomaterial design is to replicate *in vitro* the innate physical characteristics of tissue types *in vivo*. The idea being that they are well designed to support adhesion, migration, proliferation and differentiation as close possible to the ideal environment for the desired function.

The Fmoc-F_2/S hydrogel biomaterials were observed in particular to have a high propensity to support initial differentiation of mesenchymal stem cells into chondrocytes, which may also be due in part to the cell morphology adopted on the biomaterial which supports chondrocyte development (Kilian et al., 2010, McBeath et al., 2004). As such, this lineage was focussed on for further investigation. This section pools together the practices explored in the previous chapters and focuses on a particular discipline in order to understand how biomaterial properties affects cellular development during differentiation

5.1.1 Cartilage: structure, function & limitations

Cartilage is a viscoelastic connective tissue that is found mainly in load bearing joints in mammals. It is classed broadly into 3 categories: 1) elastic cartilage, found mainly in the external ear and epiglottis. 2) fibrocartilage, which comprises the pubic symphisis, tendon and ligaments and 3) hyaline cartilage, present at the sternum-rib interface, nucleus pulposus of intervertebral discs and at the articulating ends of long bones where it is referred to as articular cartilage. Hyaline cartilage is the most widespread of all three cartilage forms.

The dry weight of cartilage consists of collagen, proteoglycans and chondrocytes (as the singular cell type present within cartilage tissue). From the articular surface to the bone interface, cartilage tissue exists in a number of distinct zonal regions; these are typified by the differences in their cell and extracellular matrix morphology and organisation (Hunziker et al., 1997, Hunziker et al., 2002, Hwang et al., 1992).

The superficial tangential zone is that closest to the synovial fluid in the joint and therefore at the forefront of changes in mechanistic dynamics. Although, comprising a relative small spatial claim to cartilage (10 – 20%), it houses the largest population of chondrocytes. Chondrocytes within this region are flatter and stiffer compared to those located in the inner zones (Darling et al., 2006, Shieh and Athanasiou, 2006). Collagen content in this zone is highest and proteoglycan content is lowest (Responte et al., 2007) imparting more tensile strength to this zone. The arrangement of collagen fibrils in this zone is almost exclusively perpendicular to the bone rather than parallel as is observed in the remaining zones.

The middle or radial zone has the most spatial occupation of articular cartilage. The chondrocyte population is sparse and the orientation of collagen fibrils and the chondrocytes themselves run parallel. Chondrocytes within this region are highly active compared to the superficial zone (Wong et al., 1996).

The deep zone is located closest to subchondral bone and earmarks the transition of cartilage tissue into bone. Within this zone chondrocytes begin to undergo hypertrophy, signifying terminal differentiation in cell development. Cell activity in this zone is markedly altered as the cells have increased alkaline phosphatase activity and begin to deposit calcium resulting in a calcified layer.

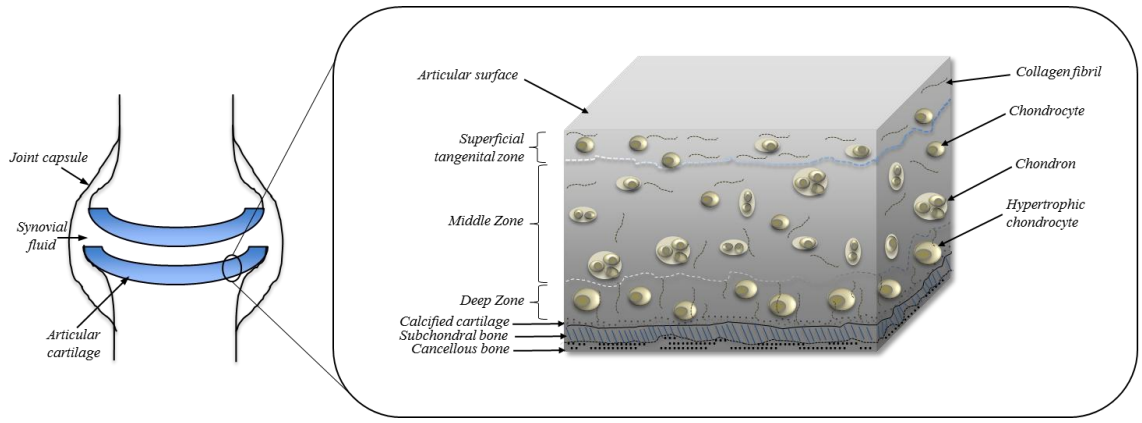

Figure 5-1 Depiction of the structure of hyaline cartilage from the articular end of a knee joint. *The diagram illustrates the zonal organisation of cartilage tissue from the articular surface to the interface with bone tissue.*

The fibrillar element of cartilage extracellular matrix comprises the collagen types II, VI, IX, X and XI. Of these, the most abundant is type II collagen, it is also specific to hyaline cartilage and is therefore considered a primary indication of successful cartilage development. Type IX and type XI collagen form cross-links with type II collagen and together they form the meshwork of fibres that lend cartilage its tensile strength.

The proteoglycan content imparts to cartilage the tissues ability to resist compressive loads. Whilst cartilage holds a number of proteoglycans and non-collagenous proteins: biglycan, decorin, tenascin, cartilage oligomeric matrix protein (COMP) being a few examples. The most abundant proteoglycan, however, is aggrecan. Structurally, aggrecan constitutes a protein core to which a series of glycosaminoglycans (GAG) are attached. The GAG content of aggrecan molecules; keratin sulphate and chondroitin sulphate, are negatively charged causing repulsion between the GAG branches and allowing interaction with water molecules (Roughley et al., 2006, Urban et al., 2000, Walsh and Lotz, 2004). Aggrecan has no covalent links to the collagen mesh and is

stabilised within the fibrillar network due to this interaction with water and the inclination of aggrecan molecules to form dense aggregates.

Type II collagen, structurally, has a high number of hexose groups which facilitate interaction with water better than the other collagen types that have been mentioned (Trelstad et al., 1976). The high propensity of type II collagen and aggrecan for association with water molecules attributes cartilage with its high hydration property. This fluid content makes up approximately 80% of the total tissue weight (Temenoff and Mikos, 2000) and plays an important role in sustaining tissue integrity and survival. As an avascular tissue, nutrient and oxygen exchange occurs mainly via diffusion through the fluid phase of cartilage, which is facilitated by the force dynamics experienced by cartilage tissue.

The low chondrocyte population and avascular nature of cartilage poses as an impairment to the regeneration of tissue injuries that are beyond a superficial nature (Temenoff and Mikos, 2000). Critical defects require the synthesis of large amounts of ECM required to bridge the defect, which is not met by chondrocyte populations. Furthermore, there is a lack of repopulation by progenitor cells that is usually supplied by the vasculature. In addition, the nature of the ECM is such that it can act as an impediment to inherent cellular repair by resident chondrocytes (Temenoff and Mikos, 2000, Responte et al., 2007). For reasons unknown, cartilage that suffers trauma and is repaired naturally does not recover the original ECM make up, synthesising fibrocartilage which characteristically contains type I collagen, and is thus not typical of hyaline cartilage structure (Poole, 1997, Volpato et al., 2013). To this end, a suitable means of repairing or replacing damaged cartilage is an area of intense research in tissue engineering.

The unsuitability of allogenic and autogenic implants means that it is preferable to try to heal damage to cartilage instead of employing replacement therapies. Cartilage injuries can be repaired using tissue grafts. However, this means of regeneration is limited by the low number of chondrocyte cells within the graft able to facilitate integration with the native tissue (Poole, 1997, Responte et al., 2007). Therefore, the use of scaffolds is particularly attractive for engineering cartilage tissue. Cells can be populated as required within the scaffold, it also acts as a major support for the cells promoting retention of chondrocyte morphology thus discouraging dedifferentiation while encouraging cell adhesion and migration (Estes and Guilak, 2011, Ma et al., 2003, vanSusante et al., 1995). Cell types housed within the constructs themselves can be fully differentiated chondrocytes but also includes the use of stem cells encouraged to develop into chondrocytes. The use of MSCs within constructs over mature chondrocytes is thought to be particularly advantageous as MSCs exhibit the ability to produce cartilage tissue as

well as enhance development of the subchondral plate when implanted *in vivo* used to heal osteochondral defects (Vonschroeder et al., 1991). These results suggest that the use of MSCs enables continual development of from naïve chondrocyte through to terminal differentiation.

5.1.2 Emulating the chondrocyte ECM

In order to promote differentiation of stem cells and to maintain functional activity of chondrocyte cells *in vitro*, an ability to maintain the chondrocyte morphology is of particular importance. Chondrocytes maintained in monolayer culture rapidly dedifferentiate, this is triggered by the loss of the rounded morphology typical of chondrocyte cells. As the cell spread on adhesion in monolayer, they create type I collagen with diminished production of the cartilage specific type II collagen (Solchaga et al., 2005, Wang et al., 2005). To abate this, routine culturing of chondrocytes and differentiation of MSCs along the chondrogenic lineage employs the use of pellet or micromass cultures to preserve the rounded shape of chondrocytes (Cooke et al., 2011, Jung et al., 2009, Sekiya et al., 2002, Wang et al., 2005). Although studies have shown chondrocytes to have been cultured *in vitro* in monolayer, it still requires restriction of the cell morphology using functionally patterned substrate surfaces (Curran et al., 2005). Micromass and pellet culture methods require that the cells are spatially arranged in three dimensions, as such, most studies that undertake research with chondrogenesis make use of three dimensional constructs, in particular, alginate hydrogels (Jung et al., 2009, Sekiya et al., 2002).

Chondrocytes reside within the tissue in structures known as chondrons. Chondrons comprise one or more chondrocyte cells and its surrounding pericellular matrix. They are known to be stiffer than chondrocytes in isolation (Nguyen et al., 2010) and their mechanical properties differ from the ECM of cartilage itself (Alexopoulos et al., 2005). The pericellular matrix is distinct from the extracellular matrix in that they are particularly high in proteoglycan and type VI collagen content. The exact function of the pericellular matrix remains unknown but studies have put forward a number of functions that the PCM is involved in. It is thought to play an important role in the cells ability to make structural cartilage. Chondrocytes maintained in pellet culture over time tend to produce an overabundance of type I collagen leading to the formation of an ECM that is likened to fibrocartilage rather than hyaline cartilage (Larson et al., 2002, Vonk et al., 2010). Furthermore, studies comparing cell behaviour of singular chondrocytes with chondrons observed that chondrons had higher levels of type II collagen content compared to type I

collagen. Also, cross linking of type II collagen fibrils occurs with cultured chondrons but was not observed with just chondrocytes in culture (Vonk et al., 2010).

The high proteoglycan content of the chondron pericellular matrix may act to resist the compressive load on cartilage and lessen direct loading onto the cells' themselves. Studies performed on the pericellular matrix using embedded chondrons (either within constructs or tissue) shows an elasticity gradient from chondron periphery to the cell-matrix interface, measuring over a broad modulus range from 20 – 60 kPa suggesting that they are readily deformable and therefore viscoelastic (Alexopoulos et al., 2005). In support to this, the makeup of the pericellular matrix varies between cartilage regions to compensate for the dynamic nature of mechanical loads imposed on the cells. The ability of chondrocytes to tailor the pericellular matrix accordingly within cartilage tissue results in uniform chondron stiffness through tissue zones (Alexopoulos et al., 2003, Wilusz et al., 2012). Indicating that the mechanical integrity of the chondron is of particular importance to the cell niche, imparting both a protective and mechanotransductive role to the contained chondrocyte (Guilak et al., 2006, Poole et al., 1992, Poole et al., 1987)

To promote chondrogenic development of pericyte cells in F_2/S hydrogels, it was therefore hypothesized that cells should be cultured within a three dimensional construct to simulate chondrocyte morphology but also to have the F_2/S hydrogels emulate the mechanical properties of chondrons specifically over neo-cartilaginous tissue. As has been described, cartilage inherently is avascular and therefore is not subject to the level of cytokine signalling that occurs in vascular tissue, relying mainly on diffusion as the foremost source of nutrients. It is thus postulated that biochemical signalling is interpreted mostly through mechanotransductive effects. For this, the elastic modulus of F_2/S hydrogels was tuned to approximately 20 kPa. This figure is in line with studies that show the elastic modulus of free chondrons (cultured in suspension) to be within this elasticity range (Nguyen et al., 2010). It also modulates the production of ECM of chondrocyte cells cultured within substrates of this stiffness to compensate for the imbalance when cultured in softer substrates (Chen et al., 2012).

5.1.3 Cell line (moving from MSCs to pericytes)

Pericytes, also known as Rouget or mural cells, are polymorphic cells that encircle endothelial cells associated with micro-vessel and capillary walls (Figure 5-2). Along with adventitial cells (located in the tunica adventitia of blood vessels), both are collectively referred to as perivascular stem cells (PSCs). These are two distinct populations; pericytes are characterised using the surface markers CD146+, CD34- and adventitial cell as CD146-, CD34+, which make them readily isolatable by fluorescence activated

cell sorting. They are known to perform a number of functions inclusive of the regulation of vasoconstriction and maintaining stability of the vessel walls (Chen, 2012, Diaz-Flores et al., 2009). This section, however, will focus on the role they play as progenitor cells.

Multipotent capabilities of pericyte cells have been shown in a number of studies, illustrating their ability to differentiate along osteogenic, chondrogenic, myogenic and adipogenic lineages (Brighton et al., 1992, Crisan et al., 2009, Diefenderfer and Brighton, 2000); characteristics that are traditionally borne by MSCs (Caplan, 1991, Pittenger et al., 1999).

Although most research with the periosteum is associated with the development and integration of bone cells (Arnsdorf et al., 2009), studies investigating chondrogenic properties have also been done (Gallay et al., 1994). They are also known to be particularly adept at healing critical sized defects in bone (Yu et al., 2010), an application which is of particular usefulness to potential application of this research project.

While not all pericytes are MSCs, current identification methods render MSCs indistinguishable from pericyte cells (Crisan et al., 2008). This trait, taken with the extensive presence of pericytes throughout the vasculature, has led to the idea of pericytes being the ancestral origin of the MSC (Corselli et al., 2010, Crisan et al., 2011) and questioning whether all MSCs inherently are pericytes (Caplan, 2008). Pericytes close association with the vasculature make these cells highly abundant compared to other stem cell sources and provides the possibility of vascular stem cells that 'supply' the various MSC niches around the body (da Silva Meirelles et al., 2006).

Was it the case that MSCs are inherently pericyte cells, and within the boundaries of current research there is nothing to as yet say they are not. This study shows for the first time that use of mechanically tuned F_2/S hydrogels can influence even more 'primitive' stem cells with chondrogenic potential. It also shows that the materials are able to coax differentiation along the chondrogenic route using more than one cell type, i.e., it is able to show enough flexibility to incorporate for the small nuances with regards to differentiating stem cells from different sources as occurs when using chemical means.

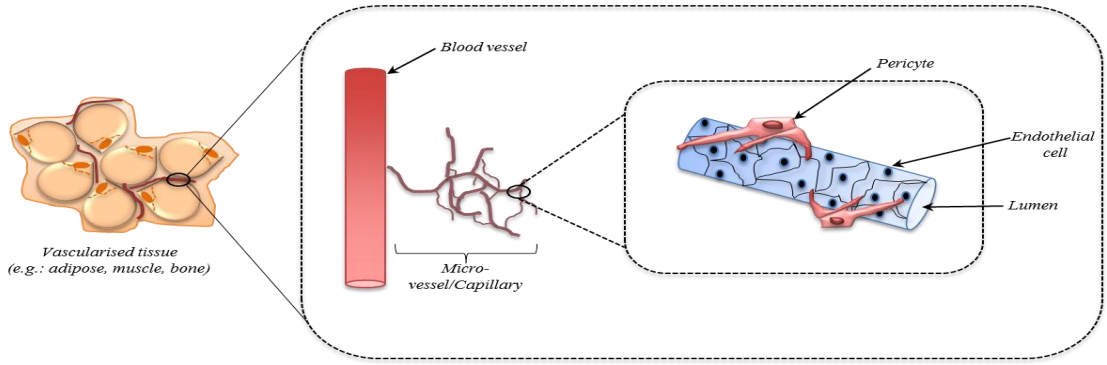

Figure 5-2 Diagram illustrating the pericyte niche. *Pericytes originate from the vasculature where they encircle the endothelial wall of blood micro-vessels and capillaries where they regulate vasoconstriction.*

5.1.4 Objectives/Rationale

Within this chapter, the chondrogenic capabilities of pericytes are explored using the F_2/S hydrogels tuned to mimic the mechanical properties of chondrons (20 kPa) as this is hypothesised to be optimal for chondrogenic development.

The F_2/S biomaterials are designed as such that cells undergo differentiation with little influence out with the biomaterial physical properties (elasticity). Although instigating differentiation using changes in substrate elasticity has been shown extensively within this project, it has not yet been investigated whether cellular interpretation of biomaterial properties is transient or whether it is able to sustain cell development over a period of time.

5.2 Materials & methods

5.2.1 Materials

Materials/Reagents	**Supplier(s)**
Human pericytes	University of Edinburgh, UK
Fmoc-diphenylalanine	University of Strathclyde, UK
Fmoc-serine	Bachem, UK
Sodium hydroxide	Fisher chemicals, UK
Distilled water	Invitrogen, UK
Alginate	Sigma Aldrich, UK
Calcium chloride	BDH Laboratories, UK

Dulbeccos modified eagle medium (DMEM)	Sigma Aldrich, UK
Foetal bovine serum (FBS)	Sigma Aldrich, UK
Penicillin streptomycin	Sigma Aldrich, UK
Trypsin	Sigma Aldrich, UK
Dexamethasone	Sigma Aldrich, UK
Ascorbate-2-phosphate	Sigma Aldrich, UK
Transforming growth factor β1 (TGF-β1)	Peprotech, UK
Sodium pyruvate	Sigma Aldrich, UK
Phosphate buffered saline (PBS)*	In-house
Fixative*	In-house
Permeability buffer*	In-house
1% BSA in PBS*	In-house
Vectashield-DAPI	Vector laboratories, USA
Rhodamine-phalloidin	Invitrogen, USA
Primary antibodies	Abcam, UK & Santa Cruz biotechnologies, USA
Biotinylated secondary antibodies	Vector laboratories, USA
Streptavidin-FITC	Vector laboratories, USA
0.5% Tween 20 in PBS*	In-house
RNeasy micro kit	Qiagen, UK
Trizol	Life technologies, UK
Chloroform	Sigma Aldrich, UK
Glycoblue	Ambion, UK
Isopropanol	Sigma Aldrich, UK
Ethanol	VWR Chemicals, France
RNase free water	Qiagen, UK
Quantitech reverse transcription kit	Qiagen, UK
Quantifast SYBR green PCR kit	Qiagen, UK

* Preparation procedures for reagents & buffers made in-house are detailed in the appendix.

5.2.2 Hydrogel preparation

0.0321 g of Fmoc-F_2 and 0.0207 g of Fmoc-S powders were weighed, placed into 14 ml glass vials and sterilized under UV light for 45 mins prior to use. Powders were then suspended in 4 ml of sterile water to a total peptide concentration of 30 mM. To this mixture, 240 µl of sterile 0.5 M sodium hydroxide solution was added to give the finished peptide solution used for hydrogel fabrication as described in 2.2.3 and for 3D cell culture.

5.2.3 Cell culture

Human adipose derived pericyte cells were kindly provided by Dr Christopher West at the Scottish Centre for Regenerative Medicine, University of Edinburgh. UK. The cells were transferred on dry ice as cryopreserved cell pellets and stored in liquid nitrogen until ready for use.

5.2.3.1 Cultivation of cryopreserved cells

Prior to cell seeding, culture well flasks were first filled with culture medium and incubated at 37°C for 30 minutes. Following this, pericyte cells were thawed in a water bath set to 37°C for 1½ minutes or until the suspension was completely thawed. The cell suspension was transferred to a clean centrifuge tube and an equal amount of culture media added. The cells were then centrifuged for 5 minutes at 1400 rpm to sediment cells and remove the supernatant; which generally contains DMSO.

Cells were resuspended in an appropriate amount of culture media and aliquots transferred to the prepped culture flasks. Cells were then maintained at 37°C, 5% CO_2 and sub-cultured when 90% confluent.

5.2.3.2 Micromass culture

Pericytes were differentiated into chondrocytes using supplemented DMEM and the micromass culture technique as described in 4.2.3.

5.2.3.3 3D culture in F_2/S and alginate hydrogels

F_2/S

Prior to use, F_2/S peptide solutions were placed into an incubator for 30 – 45 minutes to allow the solution to reach physiological temperature. The peptide solutions were then mixed gently with a pipette tip to create a homogenous solution. Detached cells, which

had been centrifuged to form a pellet, were then resuspended in the appropriate amount of the F_2/S peptide solution.

400 µl of the cell suspension mixture was then added to 500 µl of DMEM culture media (unsupplemented). The well plate was then incubated at 37°C for one hour to allow the gels to cure. After this, the media was replaced with fresh medium and twice more after 2 and 24 hours. Cells were then maintained in culture as previously described until ready for harvest.

Alginate

A 1.2% (w/v) alginate solution was made by dissolving 0.360 g of alginate powder (Sigma) slowly in 30 ml of phosphate buffered saline containing a magnetic stirrer. The solution was then autoclaved at 120°C for 20 minutes.

Pericytes were tripsinised from the culture well flasks where they were expanded as described in 2.2.2, pelleted by centrifugation and resuspended in the alginate solution.

Alginate beads were made by pipetting 100 µl of the alginate solution into a 100mM calcium chloride solution. Hydrogels were allowed to cure at room temperature for 5 minutes before removing the calcium chloride solution. Hydrogels were then washed twice with PBS solution and 500 µl of culture media added to each well.

5.2.4 Cell staining & imaging

Immunocytochemistry and microscopic analysis were carried out as detailed in 2.2.5 and 2.2.6. Details of the primary, secondary and tertiary antibodies used for this chapter are given in Table 5-1. F_2/S substrates investigated using confocal microscopy was imaged using a LSM510 META confocal laser-scanning microscope (Carl Zeiss, Jena, Germany). Images were collected and optimised for brightness and contrast using the associated software (LSM510). Images were collected at 1024 by 1024 resolution and compiled in 3 x 3 image tiles.

Table 5-1 Biomarkers used for detection of cellular differentiation

Differentiation lineage	Biomarker	Primary antibody	Secondary antibody	Fluorophore
Chondrogenesis	SOX-9	Mouse monoclonal IgG	Biotinylated anti mouse	Streptavidin conjugated FITC
	COL2A1			
	Aggrecan			
Cytoskeleton	F-actin			Phalloidin conjugated rhodamine
Nucleus				DAPI

5.2.5 Cell viability (Live/Dead assay)

Culture media surrounding the biomaterials were aspirated to waste and washed once with warm PBS solution. A working solution containing both Syto 10 and ethidium homodimer-2 dyes was made in PBS (1:500 v/v). 500 µl of the dye solution was added to the hydrogels and the samples incubated in the dark at room temperature for 15 minutes. Following this, the hydrogels were then fixed at room temperature with 4% formaldehyde solution for at least 15 minutes before viewing under a microscope.

5.2.6 RNA extraction and reverse transcription

F_2/S hydrogels were transferred from culture well plates into clean eppendorf tubes containing 0.5 ml of trizol reagent. Samples were then incubated at room temperature for approximately 10 minutes or until the hydrogels had fully degraded.

Alginate hydrogels were ground finely in 0.5 ml trizol using a mortar and pestle, as they did not degrade when incubated in trizol as occurred with the F_2/S hydrogels. Samples were then transferred into clean eppendorfs for RNA extraction.

Reverse transcription of all samples was carried out using the QuantiTect reverse transcription kit (Qiagen) as per the manufacturer's instructions and the resultant cDNA samples were then stored at -20°C or used immediately for qRT-PCR experiments.

5.2.7 QRT-PCR

Samples intended for qRT-PCR analyses were handled as described in 2.2.8. Details of the PCR primers used within this chapter are given in Table 5-2.

Table 5-2 PCR primers designed for human genes

Gene		
SOX-9	Forward	5'-AGA CAG CCC CCT ATC GAC TT-3'
	Reverse	5'-CGG CAG GTA CTG GTC AAA CT-3'
Aggrecan (ACAN)	Forward	5'-TAC ACT GGC GAG CAC TGT AAC-3'
	Reverse	5'-CAG TGG CCC TGG TAC TTG TT-3'
Collagen type II (COL2A1)	Forward	5'-GTG AAC CTG GTG TCT CTG GTC-3'
	Reverse	5'-TTT CCA GGT TTT CCA GCT TC-3'
Collagen type X (COL10A1)	Forward	5'-CAC CTT CTG CAC TGC TCA TC-3'
	Reverse	5'-GGC AGC ATA TTC TCA GAT GGA-3'
RUNX-2	Forward	5'-GGT CAG ATG CAG GCG GCC-3'
	Reverse	5'-TAC GTG TGG TAG CGC GTC-3'
Osteopontin (OPN)	Forward	5'-AGC TGG ATG ACC AGA GTG CT- 3'
	Reverse	5'-TGA AAT TCA TGG CTG TGG AA -3'
Osteocalcin (OCN)	Forward	5'-CAG CGA GGT AGT GAA GAG ACC-3'
	Reverse	5'-TCT GGA GTT TAT TTG GGA GCA G-3'
GAPDH	Forward	5'-ACC CAG AAG ACT GTG GAT GG-3'
	Reverse	5'-TTC TAG ACG GCA GGT CAG GT-3'

5.2.8 Metabolomics

Samples intended for metabolomic analyses were handled as described in 3.2.4.

Pellets obtained from the metabolite extraction assay were resuspended in 0.2 ml of 0.01% sodium dodecyl sulfate (SDS) solution. Samples were then placed on a heating block (55°C) for 10 minutes to dissolve proteins and subsequently centrifuged at 13000 g for 10 minutes to sediment any insoluble material. The supernatant was transferred into clean eppendorf tubes and used for protein assay.

Relative amounts of protein used to normalise LC-MS data were determined using the Bio-Rad microassay procedure according to the manufacturers protocol.

5.3 Results & discussion

5.3.1 Pericyte differentiation

Pericytes were induced to develop into naive chondrocytes in micromass culture with chondrogenic inductive media. Samples were maintained in culture for two weeks then fluorescently stained with antibodies to SOX-9, type II collagen and aggrecan to assess for chondrogenic development.

At 2 weeks, the number of spread cells had decreased as they adopted the rounded morphology of chondrocytes. Cells that were rounded formed aggregates and had begun to express type II collagen and aggrecan. The aggregates are still visible under the microscope most likely due to preserved cell-cell adhesions with spread cells still on the culture well plastic (Figure 5-3).

The results, in line with other studies, show that pericytes are capable of undergoing differentiation along the chondrogenic lineage

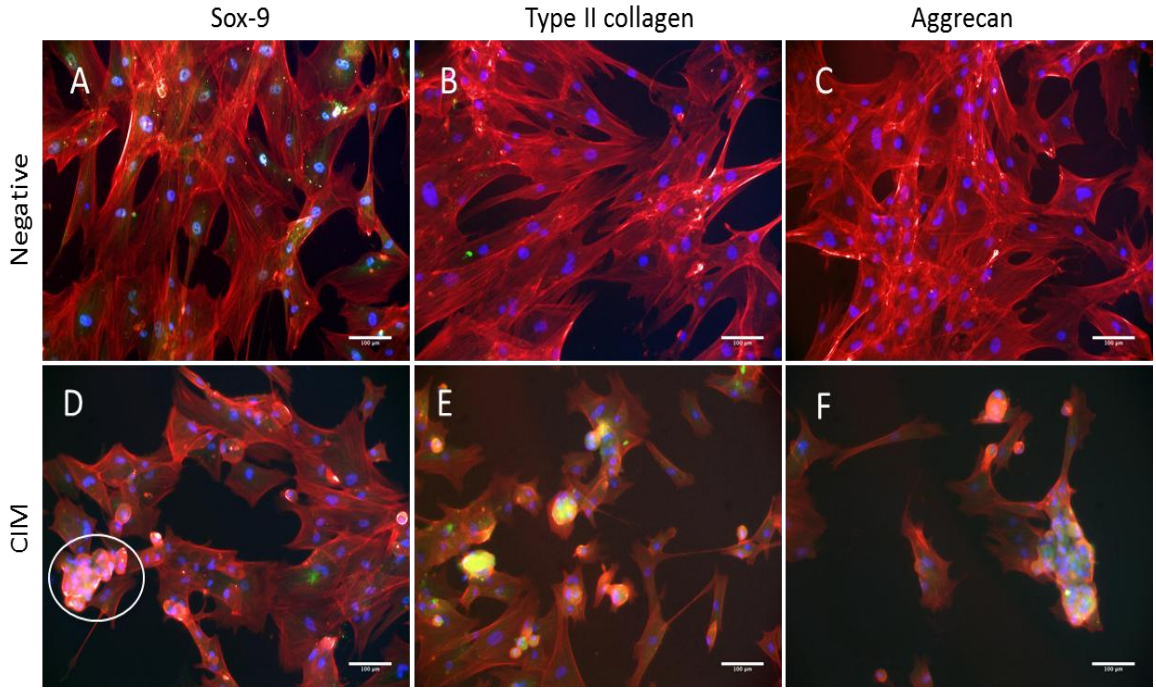

Figure 5-3 Fluorescence images of pericytes cultured in chondrogenic induction media (CIM) for 2 weeks. *Pericyte cells in micromass culture were maintained in the absence (top plane) and presence (bottom plane) of chondrogenic induction media. Cells were stained for early chondrogenic biomarker SOX-9 (A & D) and the latterly expressed biomarkers type II collagen (B & E) and aggrecan (C & F). Chondrocyte adopt a rounded morphology and begin to form aggregates (circled), which then express type II collagen and aggrecan. Undifferentiated pericytes maintain their spread morphology and have no discernible expression of SOX-9, type II collagen or aggrecan. Scale bars – 100 µm.*

5.3.2 Cell viability & initial differentiation in F_2/S substrates

Having determined the ability of pericytes to develop into chondrocytes, the next stage was to affirm that this cell type is also viable when cultured on the F_2/S hydrogel biomaterial. This was done using fluorescent detection of syto10 dye (green fluorescence) for live cells and ethidium-homodimer-2 (red fluorescence) for dead cells (Figure 5-4).

Cells were cultured both in monolayer (two dimensional) and encapsulated (three dimensional) within the hydrogel substrate. Cells were observed as viable both on and within the hydrogels. It was also noted that cells had better viability when cultured within the hydrogel as very little or no red fluorescence was observed when cells were cultured in this manner compared to when cultured in monolayer.

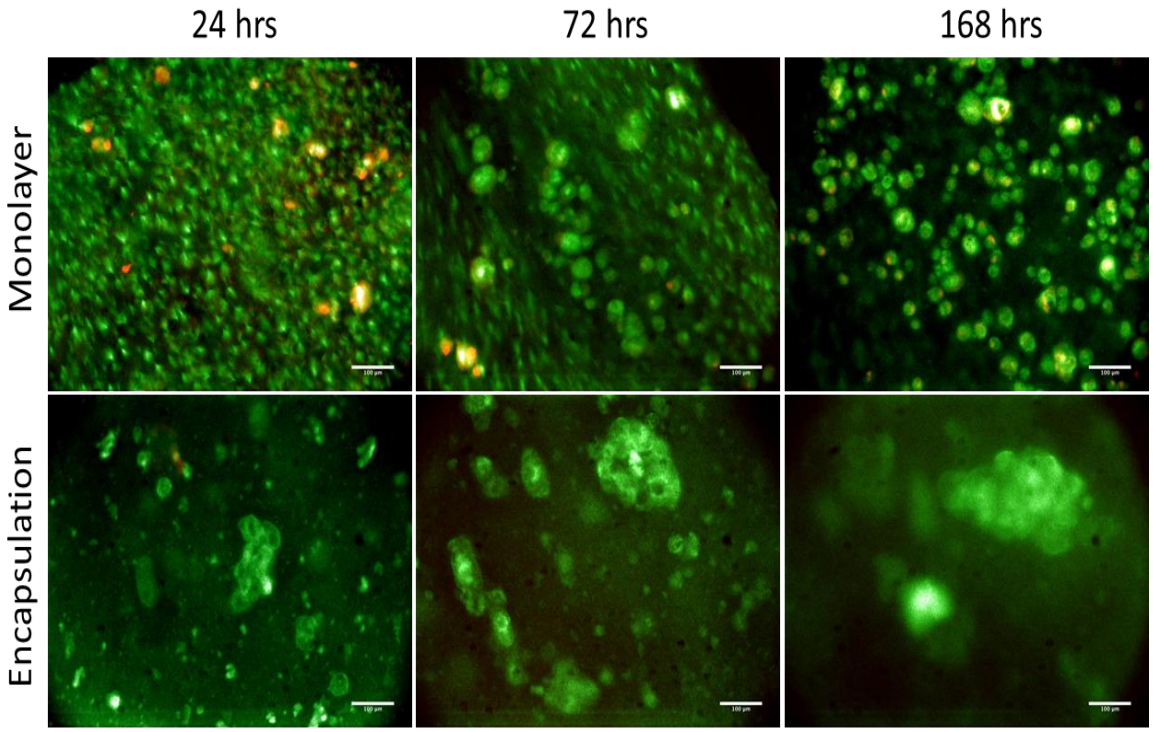

Figure 5-4 Viability of pericyte cells cultured on and within 20 kPa F_2/S hydrogels. *Cells cultured in monolayer and encapsulated within the hydrogels were assessed using live (green) dead (red) viability staining. Fluorescence staining was carried out after 24, 72 & 168 hours in culture. Pericytes exhibited good viability both on and within F_2/S hydrogels. Cell viability was improved when cultured within the hydrogels as no dead cells were observed in the hydrogels. The cells also formed aggregates when encapsulated within the hydrogels, indicative of chondrocyte morphology. Scale bars – 100 µm*

Cells were cultured for 1 week in F_2/S hydrogels and cell behaviour assessed for differentiation along the chondrogenic lineage. Cells were quantified for expression of RUNX-2, SOX-9 and type II collagen. These were compared against pericytes that were maintained in an undifferentiated state on culture well plastic. Cells cultured within the hydrogels in general, showed increased expression of all three protein markers (Figure 5-5), indicating development into chondrocytes.

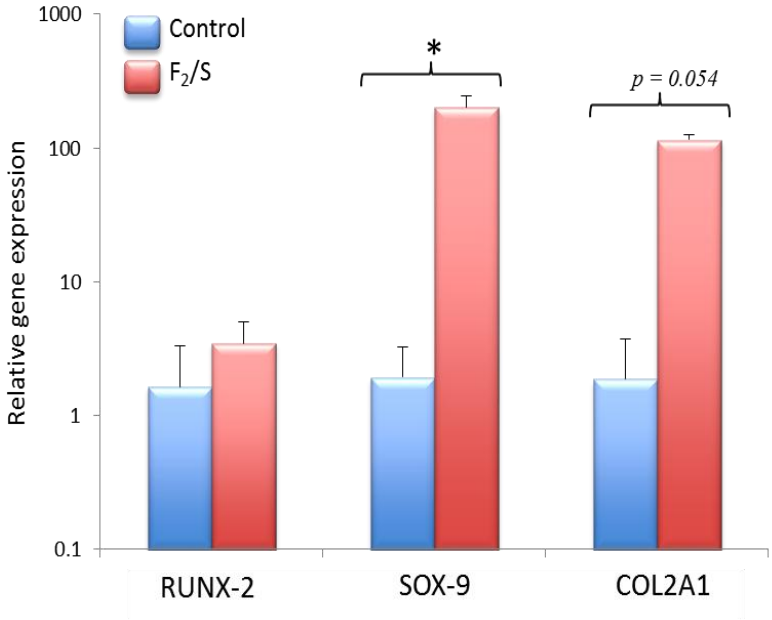

Figure 5-5 QRT-PCR analysis for gene expression of pericyte cells cultured within 20 kPa F_2/S hydrogels. *Cells were assessed for the production of chondrogenic biomarkers RUNX-2, SOX-9 & type II collagen (COL2A1) after one week in culture. Cells showed an increased production of all three biomarkers when cultured within F_2/S hydrogels compared to pericytes maintained on plain substrates (control). Error bars denote standard error from the mean; n = 6 replicates; * notes statistical significance to the control where $p < 0.05$ as calculated using unpaired student t-test.*

5.3.3 Assessing long term development of pericytes into mature chondrocytes

To ascertain biomaterial performance, pericytes differentiated using the F_2/S substrate were compared against chondrocyte development in alginate hydrogels. This section monitors the development of pericytes from initial phenotypic change through to maturity by profiling the gene expression of a number of biomarkers known to be associated with the formation of cartilaginous tissue. To determine the sole effect of F_2/S, differentiation capabilities were also assessed in the presence and absence of chondrogenic induction media.

5.3.3.1 Early development: SOX-9

Initial differentiation of stem cells into chondrocytes is characterised by the expression of the transcription factor SOX-9, both in progenitor cells as well as in differentiated chondrocytes (Ng et al., 1997, Zhao et al., 1997). It plays an essential role in the expression of its co-expressed transcription factors SOX-5 and SOX-6 (Akiyama et al., 2002) and in the latterly expressed, and cartilage specific, type II collagen (Bell & Lefebvre). Inhibition of SOX-9 activity has been shown to lead to the lack of both cartilage and bone formation in chick embryo limb buds (Akiyama et al., 2002) highlighting SOX-9 as a crucial element in chondrogenesis.

SOX-9 expression for pericytes cultured in all substrate types was observed as up regulated with the exception of pericytes maintained on the flat culture well surface (plain) as the defined control set (Figure 5-6). Expression increased steadily over the initial time points and had begun to plateau after 1 week in culture (168 hrs). Pericytes cultured within the F_2/S hydrogels supplemented with induction media (F_2/S+), however, showed the most rapid up-regulation of SOX-9 with its peak occurring after 3 days (72 hrs) in culture, earlier than F_2/S- and the alginate substrates. Continuous production of SOX-9 over the time in culture also suggests the sustained presence of a functional chondrocyte population as it is also considered integral to maintaining homeostasis, suppressing cell apoptosis (Akiyama et al., 2002, Henry et al., 2012) and inhibiting vascularisation of mature cartilage tissue (Hattori et al., 2010).

Although SOX-9 production is induced by dexamethasone, expression was also observed in substrates that were cultured in the absence of induction media (F_2/S- and ALG-). This up regulation is thought to be due to the cells being held spatially within a three dimensional matrix, facilitating the formation of a typical chondrocyte phenotype which is an important factor in being able to encourage chondrogenic development *in vitro* (Johnstone et al., 1998, McBeath et al., 2004, Muraglia et al., 2003).

Cells cultured in alginate hydrogels without chondrogenic induction media (ALG-) had shown good production of SOX-9 but did not show up regulation of any of the remaining chondrogenic biomarkers tested for in later development. For this reason, it was concluded that subsequent chondrocyte development did not occur within this sample set and ALG- was excluded from further analyses. ALG- however, is included in all the acquired gene expression profiles analysed by PCR for completeness.

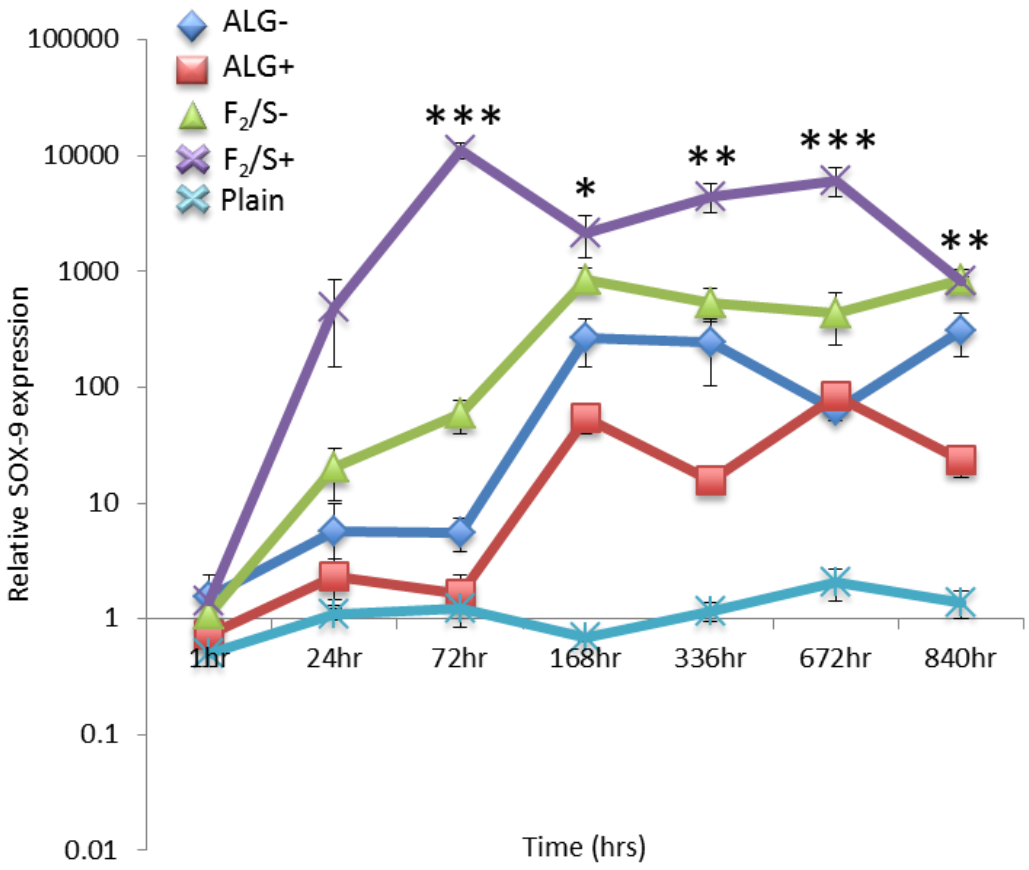

Figure 5-6 Gene expression profile of SOX-9 by pericyte cells cultured within hydrogel biomaterials undergoing chondrogenesis. *Cells were assessed for the production of the early chondrogenic biomarker on plain substrate (control) and in F_2/S and alginate (ALG) hydrogels over 5 weeks in culture. Cells cultured within the hydrogels were assessed for development in the presence (+) and absence (-) of chondrogenic induction media. Error bars denote standard error from the mean; n = 4 replicates; * notes statistical significance between substrates where $p < 0.05$, ** $p < 0.01$ & *** $p < 0.001$ calculated using one way ANOVA.*

5.3.3.2 Structural development: ACAN & COL2A1

Monitoring production of the two main components of hyaline cartilage assessed structural properties of neo-cartilagenous development in the F_2/S hydrogel biomaterials. Cartilage extracellular matrix comprises a high collagen content of which type II collagen is the most abundant and specific to hyaline cartilage. Along with type II collagen, aggrecan also forms the major constituents of cartilage structure (Responte et al., 2007). Their expression by differentiating pericytes therefore provides a good indication of how the cells have developed structurally.

Time dependent increase in type II collagen and aggrecan (ACAN) were observed in the supplemented alginate substrate (ALG+) and in both supplemented (+) and non-

supplemented (-) F_2/S hydrogels (Figure 5-7). Up-regulation of COL2A1 and ACAN were both highest in the F_2/S hydrogels with COL2A1 production in F_2/S+ observed as significantly higher than F_2/S-. In all cases, production of COL2A1 and ACAN had reached saturation by 1 week. The expression of one in respect to another, however, varied between substrate types (Figure 5-8). COL2A1 production in alginate hydrogels (ALG+) was observed to be relatively low compared to aggrecan expression (approximately 1.5 fold increase at its peak compared to 2.6 for aggrecan) while F_2/S+ showed the opposite effect; having on average 2.6x higher concentrations of COL2A1 compared to aggrecan. F_2/S in the absence of induction media however showed no difference between COL2A1 and aggrecan production (0.89x). The implications of balancing the abundance of COL2A1 and ACAN in developing cartilage tissue are something that has not drawn much attention in cartilage developmental research. Albeit, it is likely that the interplay between these two have important consequences on the relative compressive resistance and flexibility of cartilage (Hwang et al., 1992, Responte et al., 2007, Wong and Carter, 2003).

Expression of ACAN, like COL2A1, is also promoted by SOX-9 (Han and Lefebvre, 2008, Sekiya, 2000) via the coupled activation by SOX5 and SOX6. While SOX-9 is expressed relatively early in chondrogenic development and expressed continually until hypertrophy, SOX5 and SOX-6 are expressed at a later stage aiding maturation of chondrocytes through significant expression of ACAN and COL2A1 (Han and Lefebvre, 2008). The differential expression between these two proteins in the alginate and F_2/S hydrogels with and without induction may be due to the nature of the enhancing effect SOX-5 and SOX-6 has on their relative expression pattern.

Confocal microscopy was carried out for pericytes cultured within the F_2/S- hydrogel after five weeks to confirm visually the results obtained by qRT-PCR. The constant level of expression seen after one week in culture by qRT-PCR analysis is thought to stem from having a relatively stable cell population. However, constant production of extracellular COL2A1 and ACAN should have sequestered over time and be well represented throughout the hydrogel. The F_2/S- hydrogel was investigated particularly as it is the main focus biomaterial for inducing phenotypic change in pericyte cells solely using biomaterial mechanics. Hydrogels were stained for the presence of COL2A1 and ACAN had shown good presence throughout the F_2/S biomaterials (Figure 5-9) indicating that pericytes had undergone differentiation in response to biomaterial properties as the sole effector. Cells in the alginate and F_2/S+ hydrogel were not imaged by confocal microscopy as the chondrogenic capabilities of pericytes using inductive media had been demonstrated earlier (Figure 5-3).

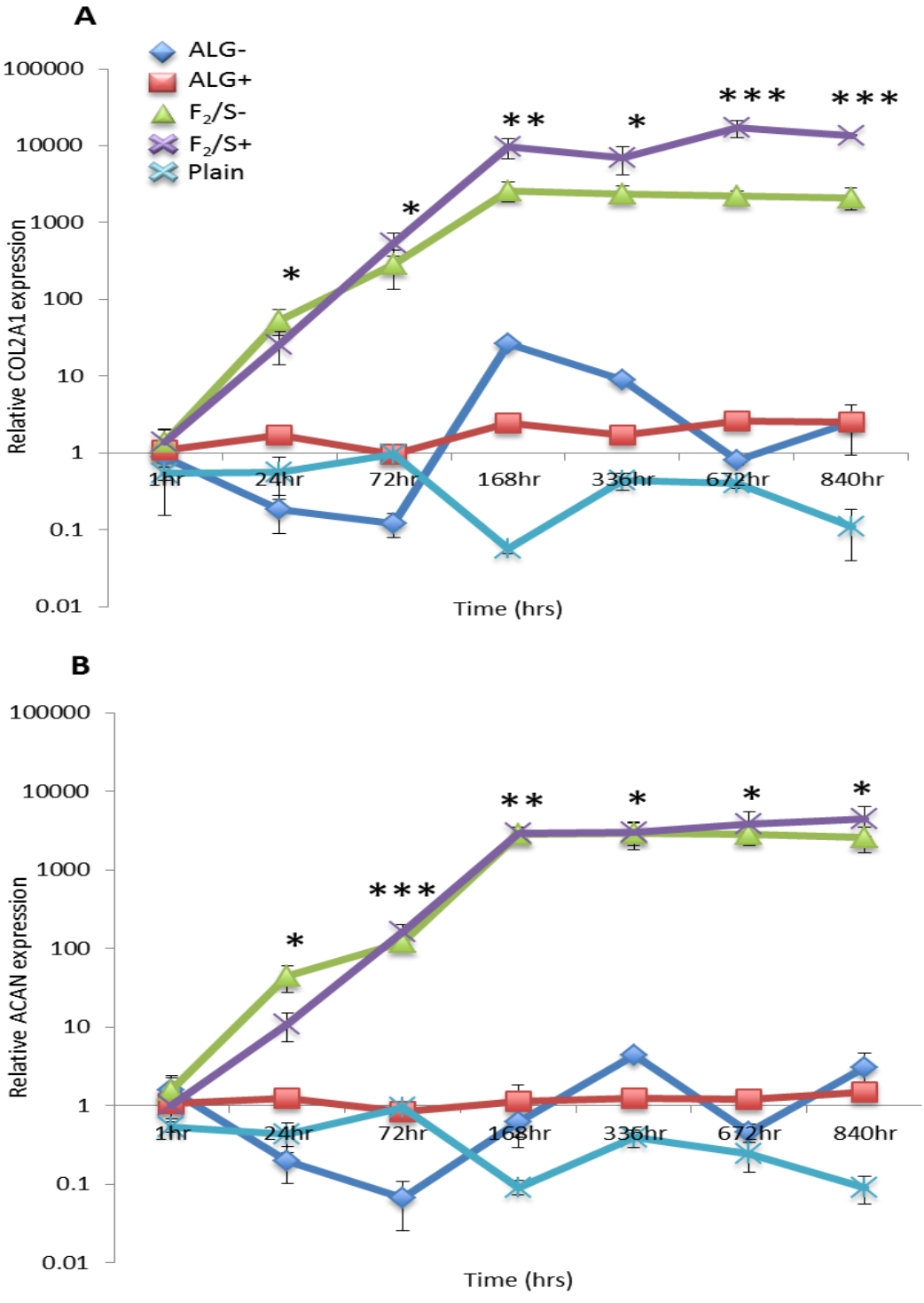

Figure 5-7 Gene expression profile of A) type II collagen (COL2A1) and B) aggrecan (ACAN) by pericyte cells cultured within hydrogel biomaterials undergoing chondrogenesis. *Cells were assessed for the production of the chondrogenic biomarkers on plain substrate (control) and in F_2/S and alginate (ALG) hydrogels over 5 weeks in culture. Cells cultured within the hydrogels were assessed for development in the presence (+) and absence (-) of chondrogenic induction media. Error bars denote standard error from the mean; n = 4 replicates; * notes statistical significance between substrates where $p < 0.05$, ** $p < 0.01$ & *** $p < 0.001$ calculated using one way ANOVA.*

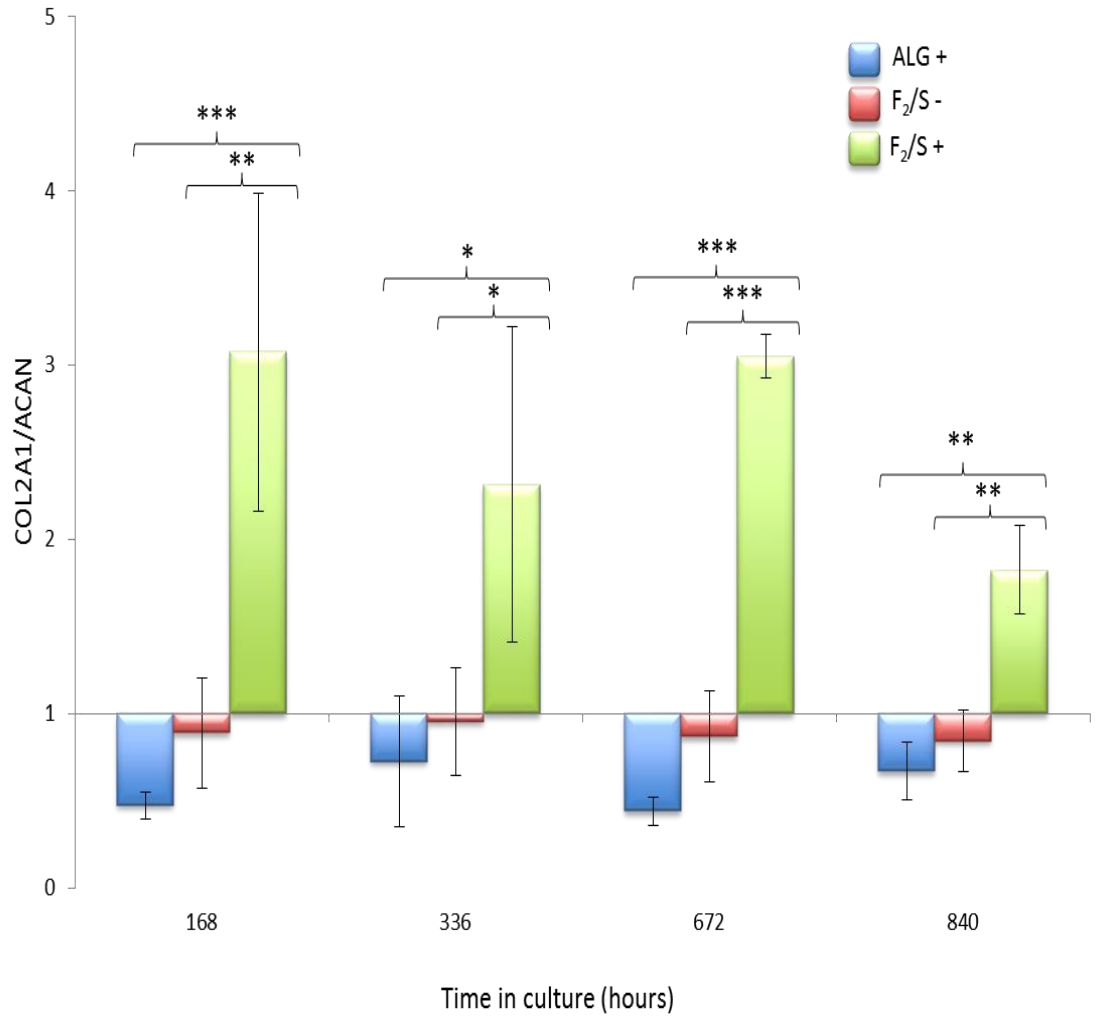

Figure 5-8 Gene expression ratios of type II collagen (COL2A1) and aggrecan (ACAN) by pericyte cells cultured within hydrogel biomaterials undergoing chondrogenesis. *Cells were assessed for production relative to one another over 5 weeks in culture and found that cells behaved differently within each substrate type. Cells cultured in alginate hydrogels (ALG+) exhibited higher ACAN content while those in F_2/S+ showed the opposite effect with COL2A1 content observed as the more abundant. No difference in COL2A1 abundance relative to ACAN was noted in F_2/S- hydrogels. Error bars denote standard error from the mean; n = 4 replicates; * notes statistical significance between substrates where $p < 0.05$, ** $p < 0.01$ & *** $p < 0.001$ calculated using one way ANOVA.*

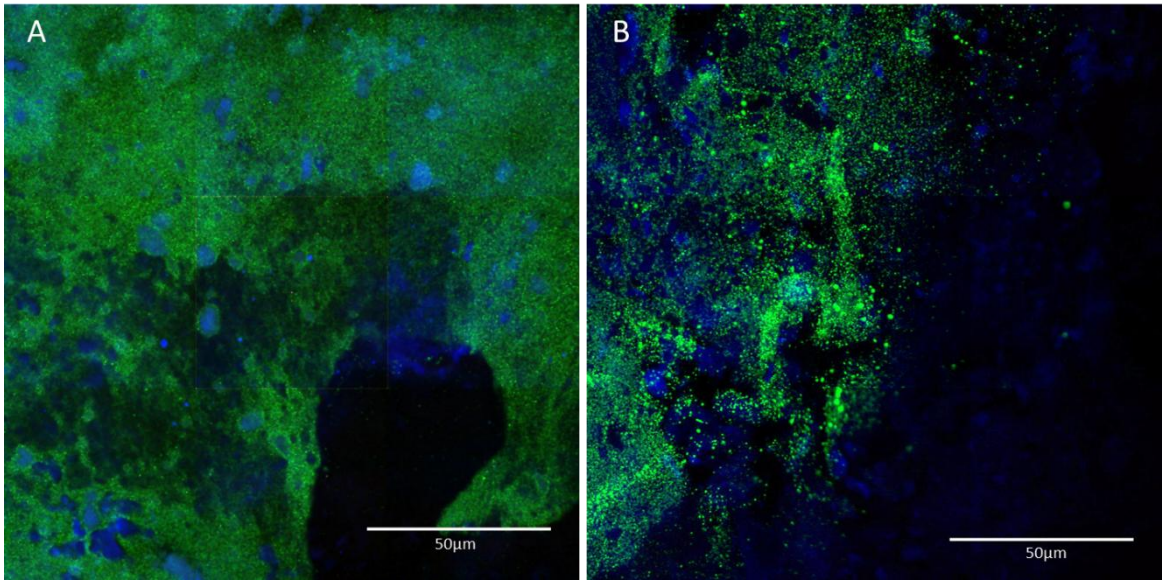

Figure 5-9 Confocal microscopy images of pericyte cells cultured within 20 kPa F_2/S hydrogels. *Cells cultured within the hydrogels were assessed for aggrecan production (A) and type II collagen production (B) after five weeks in culture as indication of cellular differentiation into chondrocytes. Cell nuclei were stained with DAPI, shown in blue and each biomarker with FITC, shown in green. Scale bar – 50 µm.*

5.3.3.3 Maturity: COL10A1

Type X collagen (COL10A1) typically is expressed specifically in non-mitotic hypertrophic chondrocytes *in vivo* (Schmid et al., 1985) and as such is used in some cases as an indicator of terminal differentiation of chondrocytes.

A number of studies investigating stem cell chondrogenesis *in vitro*, however, have noted the widespread expression of type X collagen in culture alongside type II (Cooke et al., 2011, Cui et al., 2012, Karlsson et al., 2007, Perrier et al., 2011) resulting in a mixed chondrocyte phenotype. The relatively early expression of type X collagen for pericytes cultured in the alginate and F_2/S substrates is also observed within this study (Figure 5-10) suggesting that a mixed phenotype is also produced in this case.

Although the production of type X collagen expression form part of a natural cycle in cell progression rather than an exacerbation by culture conditions (Gibson et al., 1997), the state of differentiation does not remain unaffected by microenvironmental conditions (Morimoto et al., 2013, Wang et al., 2010). The observed early expression of type X collagen, in some part, is thought to occur due to an over exposure to transforming growth factor-β1 (TGF-β1) (Cooke et al., 2011, Perrier et al., 2011). A phenomenon that is also echoed in this study as cells cultured in the presence of chondrogenic induction media containing TGF-β1 (ALG+ and F_2/S+) showed higher expression of type X

collagen compared to F_2/S-, which sustained higher type II collagen levels in the extracellular matrix over a longer period (Figure 5-11).

Comparisons between the F_2/S substrates showed that differences between the pericytes cultured in the F_2/S- and F_2/S+ hydrogels occurred mainly with respect to collagen reproduction. Both type II and type X collagen where higher in F_2/S substrates supplemented with chondrogenic media. This increase was also noted as being preceded by higher expression of SOX-9 in F_2/S+, which promotes the formation of type II collagen (Bell et al., 1997, Lefebvre et al., 1997). The presence of induction media, however, had no discernible effect on aggrecan expression suggesting induction media may not intensify GAG formation (Figure 5-7B).

While type II collagen production is induced by SOX-9 activity, type X, however, is induced by the activation of RUNX-2 expression in the cells (Higashikawa et al., 2009). If the F_2/S hydrogels also instigate the expression of RUNX-2 during early stage differentiation, it therefore goes some way to explaining the premature expression of type X collagen in the culture system. The presence of RUNX-2 however, would also suggest that the F_2/S biomaterials go some way to promoting osteogenic development of the pericytes in culture. To test this, samples were checked using qRT-PCR analysis for the osteogenic markers RUNX-2, OPN and OCN in each of the substrates. All three biomarkers were found to be present and elevated in both F_2/S substrates compared to the plain substrate (Figure 5-12A). Assessment of total osteogenic or chondrogenic activity within each of the substrates showed that the F_2/S substrates had, in general, higher chondrogenic activity (2.76x and 2.85x in F_2/S- and F_2/S+ respectively) compared to overall osteogenic activity (Figure 5-12B).

The development of osteoblasts and premature expression of type X collagen in the F_2/S substrates could to some extent be improved by the use of a co-culture system. Experiments performed by Cooke *et al* had shown that chondrogenic differentiation of MSCs with a lessened COL10A1 production could be achieved by using a bilaminar cell pellet culture system (MSC pellet encased in juvenile chondrocytes). Cui *et al* also showed that culturing MSCs with meniscal cells at varying ratios in general, performed better at minimising COL10A1 expression than when MSC were cultured alone. These two systems described by Cooke and Cui, invariably make use of TGF-β to induce differentiation. Pericytes cultured in the F_2/S hydrogels in the absence of TGF-β already exhibited less COL10A1 expression compared to its TGF-β supplemented counterpart (Figure 5-11), but it is worth of note that the chondrogenic development of pericytes in F_2/S may well be further enhanced with the use of co-culture.

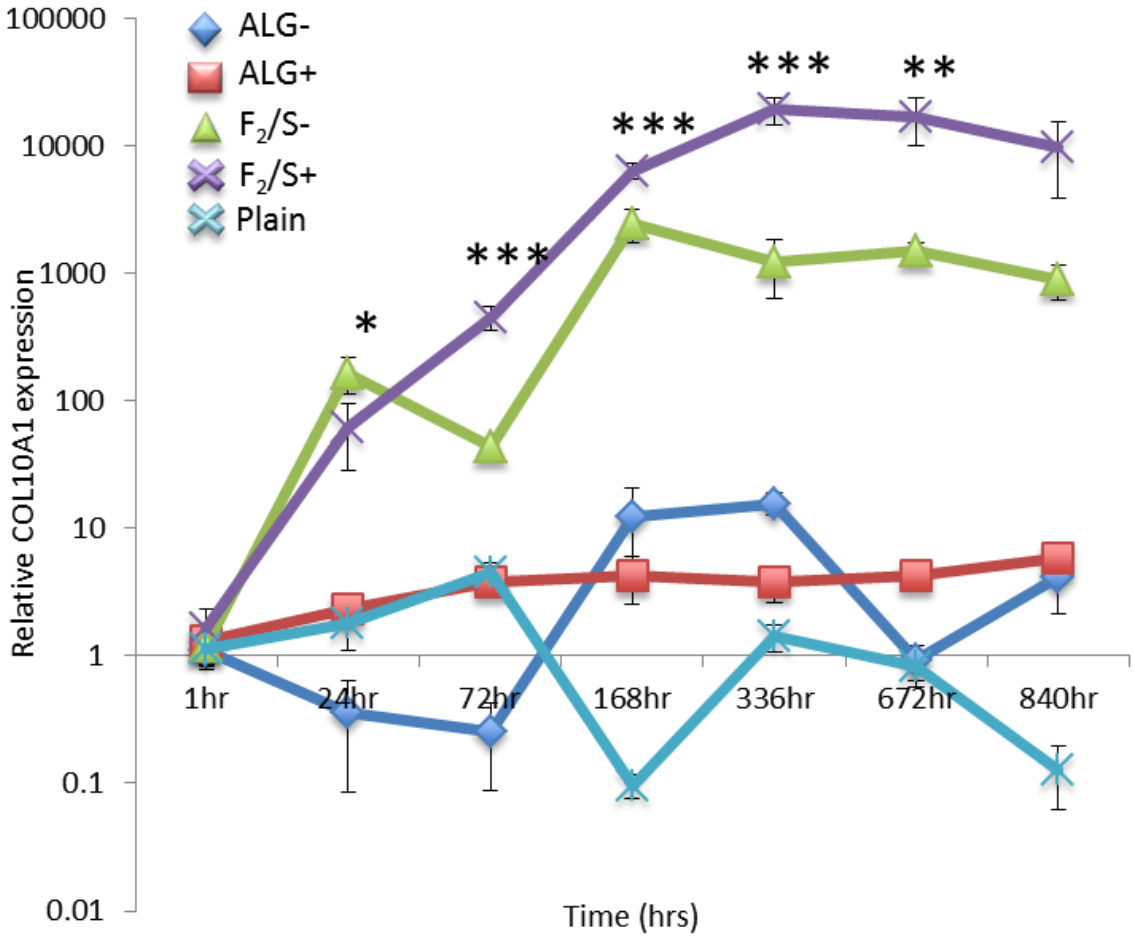

Figure 5-10 Gene expression profile of type X collagen (COL10A1) by pericyte cells cultured within hydrogel biomaterials undergoing chondrogenesis. *Cells were assessed for the production of the chondrogenic biomarker on plain substrate (control) and in F_2/S and alginate (ALG) hydrogels over 5 weeks in culture. Cells cultured within the hydrogels were assessed for development in the presence (+) and absence (-) of chondrogenic induction media. Error bars denote standard error from the mean; n = 4 replicates; * notes statistical significance between substrates where $p < 0.05$, ** $p < 0.01$ & *** $p < 0.001$ calculated using one way ANOVA.*

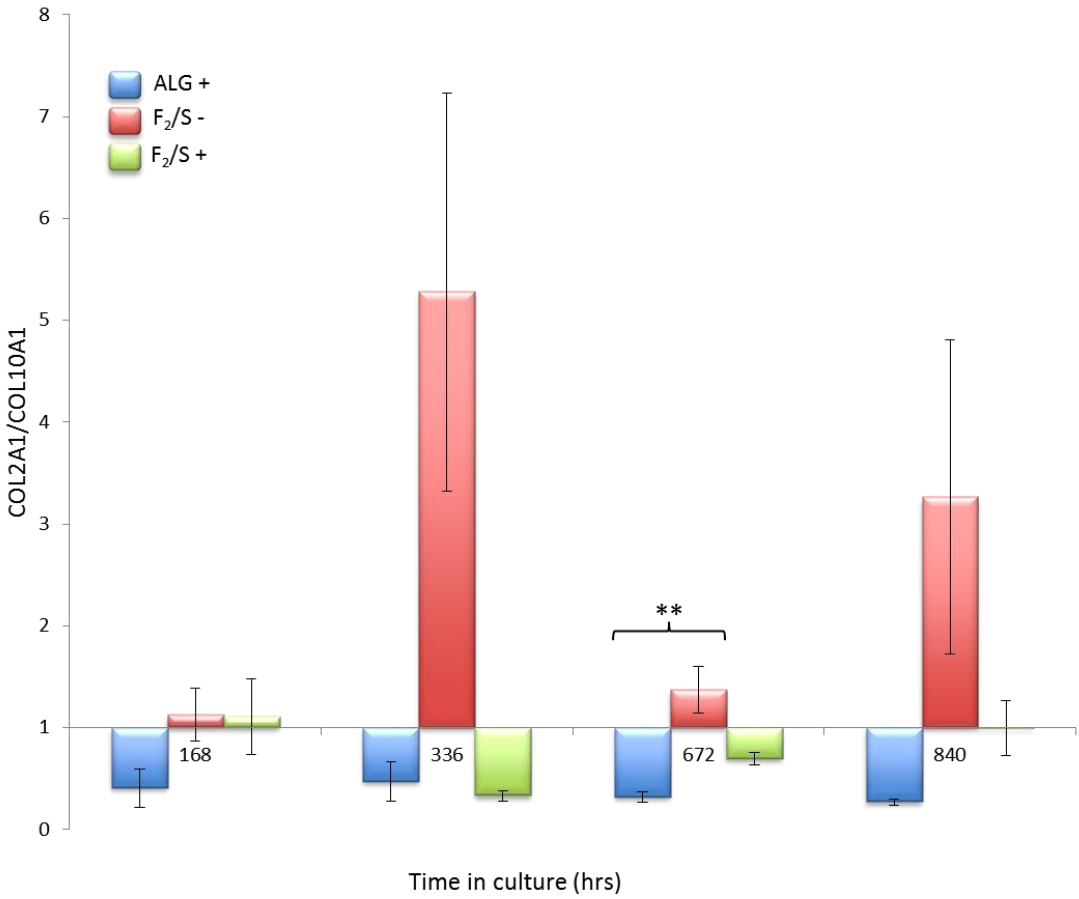

Figure 5-11 Gene expression ratios of type II collagen (COL2A1) and type X collagen (COL10A1) by pericyte cells cultured within hydrogel biomaterials undergoing chondrogenesis. *Cells were assessed for production relative to one another over 5 weeks in culture to ascertain the phenotypic variance of differentiating pericytes. Cells cultured in the presence of chondrogenic induction media (ALG+ and F_2/S+) showed higher amounts of COL10A1 relative to COL2A1 expression. F_2/S-, however, showed higher COL2A1 expression relative to COL10A1. Error bars denote standard error from the mean; n = 4 replicates; * notes statistical significance between substrates where $p < 0.05$, ** $p < 0.01$ & *** $p < 0.001$ calculated using one way ANOVA.*

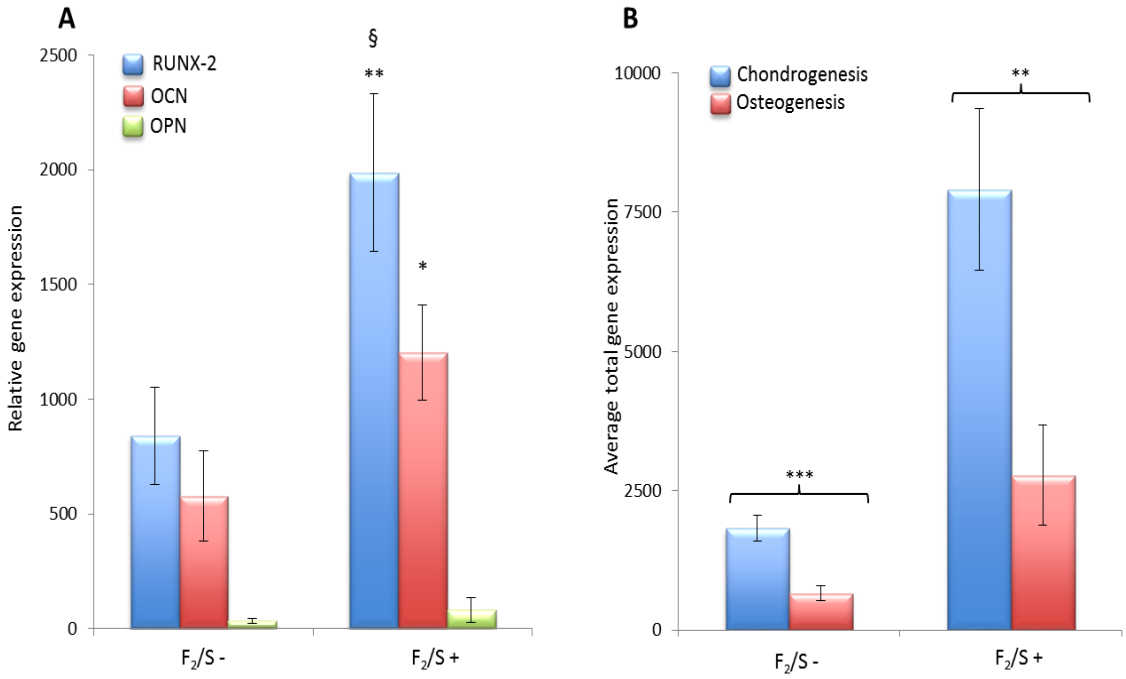

Figure 5-12 Assessing osteogenic development of pericytes within F_2/S hydrogels. *A – Cells cultured in F_2/S hydrogel in the absence (-) and presence (+) of chondrogenic induction media were assessed for production of osteogenic biomarkers RUNX-2, osteopontin (OPN) and osteocalcin (OCN). Expression levels were elevated for all three compared to cells cultured on the plain substrate (held nominally at 1) indicating that the pericytes are also induced to undergo osteogenesis. B – The extent to which osteogenic development occurs was compared to that observed for chondrogenesis. Values were obtained by measuring fold changes from the plain substrate as a control and averaging the value obtained for all tested genes within each lineage, i.e., osteogenesis measured combined average fold change for RUNX-2, OPN and OCN and chondrogenesis from SOX-9, COL2A1, ACAN and COL10A1 expression. On average, chondrogenic development of pericytes was 3 fold higher than levels observed for osteogenic development. Error bars denote standard error from the mean; n > 6 replicates; * notes statistical significance between substrates where $p < 0.05$ and ** $p < 0.01$ compared to plain substrate, § where $p < 0.05$ compared to F_2/S- using one way ANOVA in A. Statistical significance between F_2/S substrates are indicated with ** where $p < 0.01$ and *** where $p < 0.001$ calculated using unpaired students t-test in B.*

5.3.4 Metabolite expression profiling of *in vitro* chondrogenesis

5.3.4.1 Protein expression profiles

Cell pellets obtained from metabolite extraction assay used in metabolomics experiments were used to assess the total amount of protein present in each sample set. These were calculated as fold change from the originating biomaterial (labelled as ‘zero sample’), which was used as a baseline for measurement. Calculated fold change was then used to normalise identified metabolite peak abundance as detected by LC-MS.

Protein concentrations within hydrogel substrates begin to increase within 24 hours of seeding and increase continually over the 5 weeks in cultures. Cells at 5 weeks showed a 4 to 5 fold increase in protein abundance with the highest detected in the F_2/S+ sample set (5.06x). Pericytes maintained on culture well plastic showed modest increase over time compared to the hydrogel biomaterials. Cells were observed as showing a 2-fold increase in protein content as they expand in culture (Figure 5-13).

The comparable protein amounts between the alginate and F_2/S hydrogels infer that the effect seen in gene expression by PCR analysis is not due to differences in cell population but may be due to differences in activity levels adopted in alginate and F_2/S hydrogels.

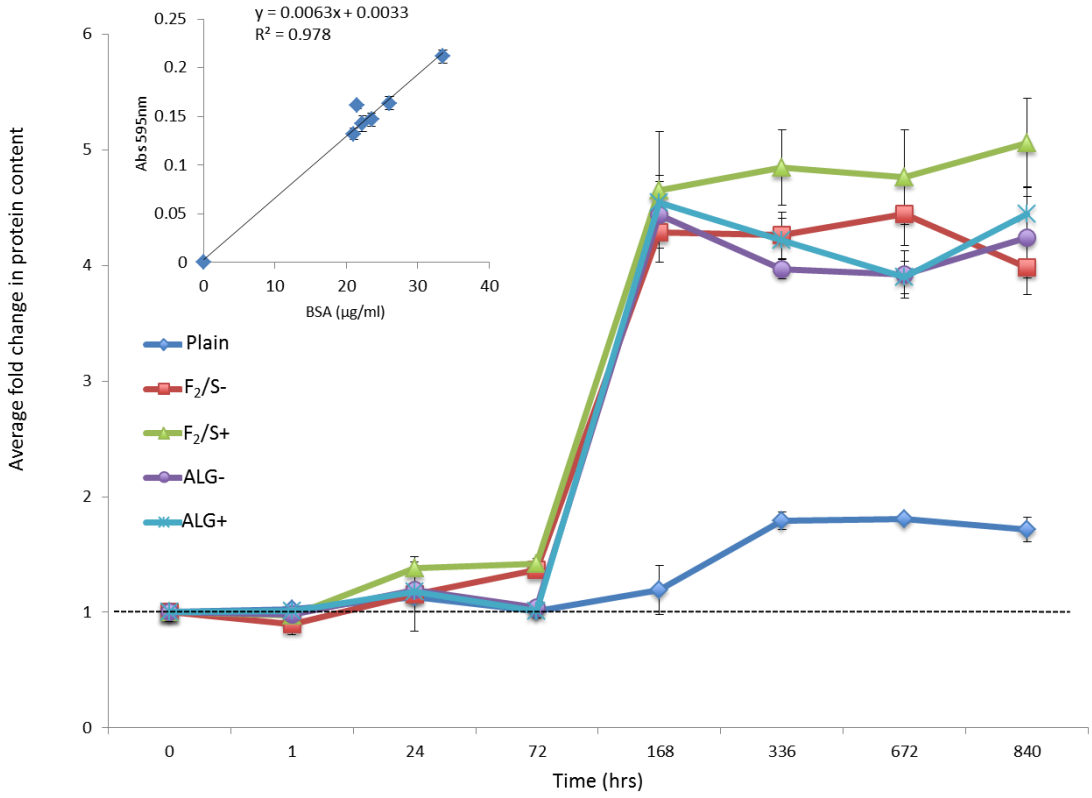

Figure 5-13 Protein content analysis for pericyte cells cultured within F_2/S and alginate hydrogels in the presence (+) and absence (-) of chondrogenic induction media. *Fold change in protein content was normalised against the zero time point, set nominally at 1 (dashed line). Samples at time zero are defined as biomaterials that did not house any cell population. Negative control set is annotated as 'Plain'; these are pericytes that are maintained normally on planar culture well plastic. Inset is a representative graph of BSA standards used to measure protein abundance in each sample. Error bars denote standard deviation; n = 4 replicates.*

5.3.4.2 Assessing chondrocyte metabolome

To assess the chondrocyte metabolome, comparisons were made between pericytes cultured on the plain substrate (culture well plastic) as a negative control against pericytes cultured in F_2/S hydrogels with and without added chondrogenic induction media. The cells cultured within the F_2/S biomaterials did not show a gradual time dependent change towards maturity as originally hypothesised, instead they developed a mixed phenotype expressing both COL2A1 and COL10A1 biomarkers in parallel. This observation however is not unlike the chondrocyte niche, which contains both types of collagens at any one point in time, albeit with zonal organisation. As such, the metabolome expression is therefore likely to give an averaged visual representation of what metabolic processes occur within cartilage tissue as a generalised whole.

Calculations were performed using data acquired over the latter half of the experimental duration (168 – 840 hrs), which were averaged and normalised for total metabolic activity. Samples were treated in this manner because observation from qRT-PCR analyses and protein expression analysis had shown that cell activity post 168 hrs had plateaued for all substrates (Figure 5-6, Figure 5-7, Figure 5-10 and Figure 5-13) indicating stable activity. To confirm this statistically, PCA analysis was carried out on each data subset (Figure 5-14).

Principal component plots show that the pericytes cultured on the plain and F_2/S substrates adopted distinct overall behaviours, with cells cultured in the presence (F_2/S+) and absence (F_2/S-) of inductive media forming a close but distinguishing relationship from one another. Replicate samples assessed for cells cultured on the F_2/S hydrogels from 168 – 840 hrs had clustered together tightly indicating similar or otherwise stable metabolic behaviour over this time in culture. Pericytes maintained on culture well plastic, however, had shown a number of outliers divergent from the general sample cluster. These outliers were determined as the four replicate samples obtained at 168 hrs in culture indicating that cell behaviour was relatively different at this time point. Sample replicates obtained afterwards, however, (336 – 840 hrs) were clustered closely indicating similarity. From this, samples averaged for further analysis were 168 – 840 hrs for F_2/S (n =16) and 336 – 840 hrs for the plain substrate (n = 12). By pooling the samples together into a single averaged time point, statistical confidence and analysis is further improved by the representation from a larger sample population.

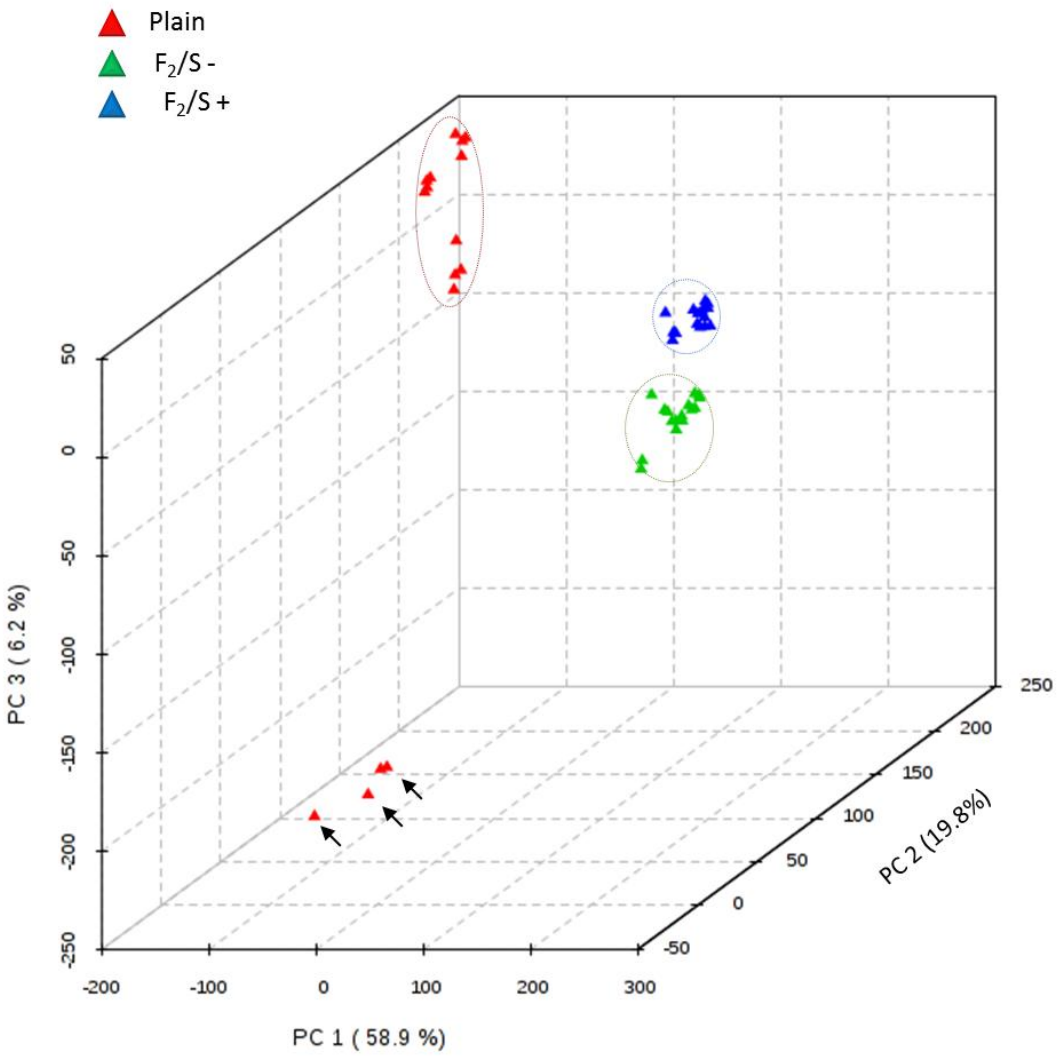

Figure 5-14 Principal component analysis of pericytes cultured on plain and F_2/S substrates in the presence (+) and absence (-) of chondrogenic induction media between 1 and 5 weeks*. The plot shows differences between cells on all three substrates with the F_2/S being particularly distinct from the plain substrate. While cell activity over the assessed duration was observed to be constant for the F_2/S substrates, cell on the plain substrate had some outlier points (arrows) which were samples measured at 1 week, indicating that cell behaviour was dissimilar from the cohort at this time point.*

The time points up to five weeks in culture (840 hrs) represent a steady state metabolism adopted by cells on each substrate. To compare total activity states, metabolite abundance measured by LC-MS were approximated from each total ion chromatogram and represented as fold change relative to the plain substrate. Metabolite abundance was found to be approximately two fold for cells cultured in the F_2/S- hydrogels compared to the plain substrate with the F_2/S+ slightly higher (2.68x), representing a general increase in metabolite abundance and population from pericytes cultured in F_2/S

hydrogels (Figure 5-15). The results also confirm and illustrate the difference in behaviour noted at the transcriptional level, which filters down to cell metabolism aiding changing phenotype. Both sets, however, do not confer necessarily direct correlation as is often noted in studies that integrate gene expression with cell behaviour due to non-gene dependent activity. As it is assumed that non-differentiating pericytes adopt a quiescent metabolic state, then the cells in the F_2/S hydrogels can be considered relatively active in comparison, even though it is noted that these cells have achieved their own 'steady state' over time. This higher steady state, however, is suggestive of continuous turn over activity taken on by cells cultured in the F_2/S substrate that are not observed in cells on the plain substrate, such as the expression of SOX-9 and RUNX-2 leading to the deposition of collagens II, X and aggrecan into the ECM.

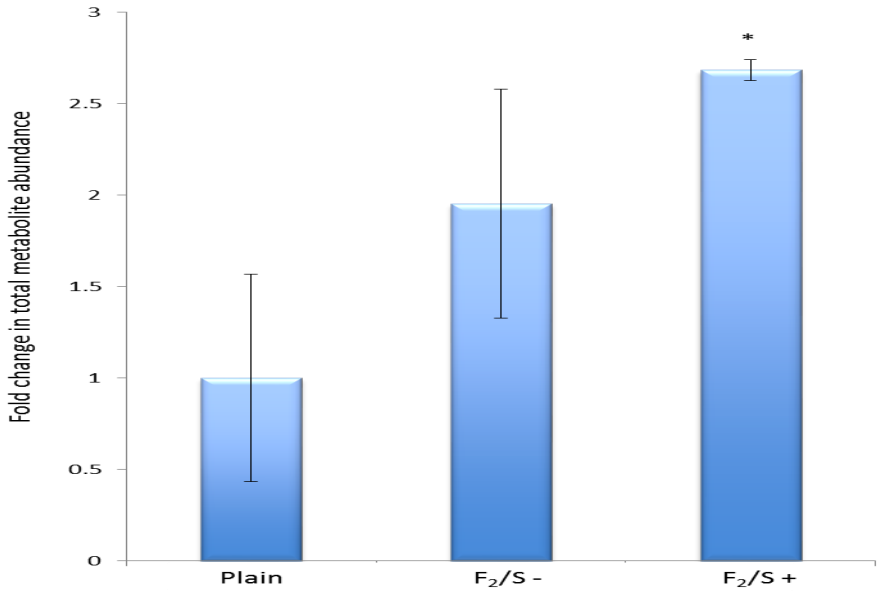

Figure 5-15 Averaged peak intensities of identified metabolite masses detected in pericytes cultured on plain and F_2/S hydrogel substrates in the absence (-) and presence (+) of chondrogenic induction media. *Cells cultured in both F_2/S hydrogel substrates show an increase in metabolite peak intensities compared to the plain substrate with the highest amount of change occurring on the media supplemented substrate (F_2/S+). Error bars denote standard deviation from the mean; n ≥ 12 replicates; * notes statistical significance between substrates where p < 0.05 calculated using one way ANOVA.*

Cluster analysis performed for all three substrate showed that, on the whole, the metabolite profiles of both F_2/S substrates were inadvertently similar with higher abundances detected on the F_2/S+ substrate (Figure 5-16A). Metabolite masses were mapped to known metabolic pathways to ascertain which cell processes experienced the most change compared to the plain substrate. Most of these pathways were primarily

concerned with amino acid metabolism but metabolites involved in energy generating processes such as the TCA cycle had also shown significant change (Figure 5-16B). Interestingly, the pathway showing the most significant change - arginine & proline metabolism, is responsible for driving the synthesis of polyamines from ornithine (Pegg, 2009). Polyamines, while ubiquitous with regards to influencing a number of cell functions inclusive of proliferation and differentiation (Childs et al., 2003, Igarashi and Kashiwagi, 2010), also have particular effect in driving the continued development of chondrocytes (Facchini et al., 2012).

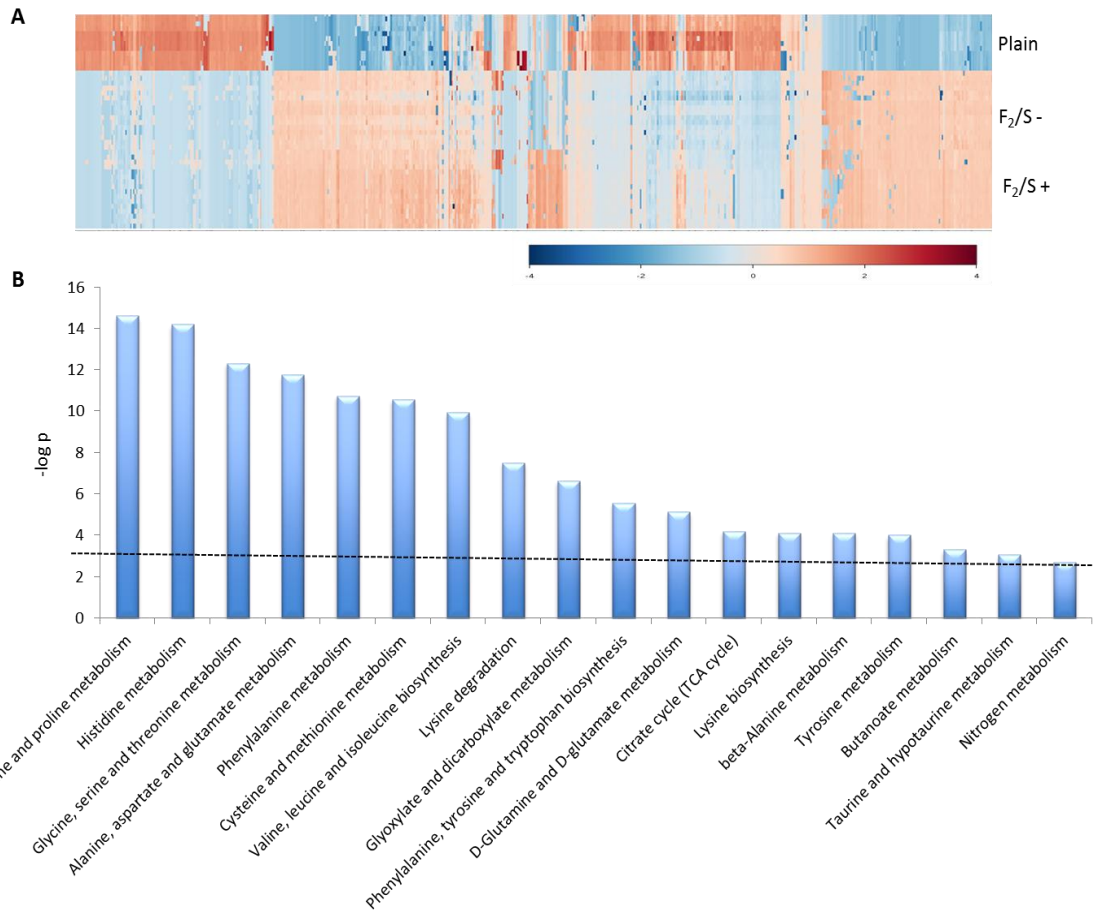

Figure 5-16 Pathway analysis for general chondrogenic activity. *Identified metabolites from pericytes cultured in F_2/S hydrogels in the presence (+) and absence (-) of induction media were compared against pericytes cultured on plain surfaces as a control and their activity assessed using hierarchical cluster analysis (A). Metabolites were then mapped to known metabolic pathways (B) and differences in cell activity from the plain substrate ascertained. Pathways showing the most significant change were primarily involved in amino acid metabolism inclusive of nitrogen metabolism but also processes involved in energy generation such as the TCA cycle are noted to be significantly different from the control sample indicative of a more active cell phenotype in the F_2/S substrates. Dashed in (B) indicates statistically significant the threshold, where $p < 0.05$ as calculated using node centrality statistics in metaboanalyst.*

There are, however, several pockets where there are distinct differences between the F_2/S- and F_2/S+ substrates. These may point toward cell activity that is responsible for the observed differences in chondrogenic phenotype between F_2/S- and F_2/S+ such as the elevated expression of COL10A1 over COL2A1 in F_2/S+ as exacerbated by the use of induction media (Figure 5-11). To assess these further and isolate a pathway(s) that may be affected, discriminatory analysis was done using excel to calculate the ratio of detected metabolite in F_2/S- relative to F_2/S+. These were subsequently depicted as a scatter plot in order to isolate where these distinctions occur. A threshold value of 2 was set as a cut off point for metabolite selection (Figure 5-17A) and all metabolites showing greater than two-fold difference were then used for pathway analysis. From a total of 734 identified masses, 172 were isolated as showing a higher than two-fold difference between both substrates (23.4%). Masses mapped to metabolic pathways, showed that the majority of these differences are also predominantly centred around amino acid metabolic pathways observed in Figure 5-16 with the exception of a few such as tyrosine metabolism and arginine & proline metabolism for which activity had no significant change. Metabolites involved in generating energy, such as those involved in the TCA cycle, which showed significant activity when compared to pericytes maintained on the plain surface, did not show any distinction between F_2/S- and F_2/S+ as both were considered to be particularly active.

As an initial phase, the prerequisite for inducing stem cell differentiation into chondrocytes is the detection of cell type specific behaviour that is uncharacteristic of its predecessor. Confirming the production of the chondrogenic markers COL2A1, aggrecan and low or negligible expression COL10A1 and COL1A1 primarily do this (Yamasaki et al., 2001). Studies generally look into accomplishing these requisites but rarely look into the consequences that small discrepancies in expression levels may have on the quality of cartilaginous development. While there is a degree of overlap in metabolic cell processes as ascertained through the metabolome of pericytes cultured in F_2/S- and F_2/S+ substrates (likely correlating with parallel positive expression of chondrocyte markers), features of distinctive cell processes are adopted through the use of induction media not observed with the biomaterial only (Figure 5-17A). These differences, although sufficient to positively drive chondrogenesis, reflect the more subtle nuances regarding the imbalance in phenotype expression. In this case, the distinct difference observed in collagen expression but not reflected in GAG production (Figure 5-7 and Figure 5-10).

The results obtained in this chapter suggest that directed differentiation of pericytes into mature chondrocytes is better achieved using F_2/S biomaterial instruction solely over co-use with induction media as it supports lessened expression of COL10A1 in chondrocytes (Figure 5-11).

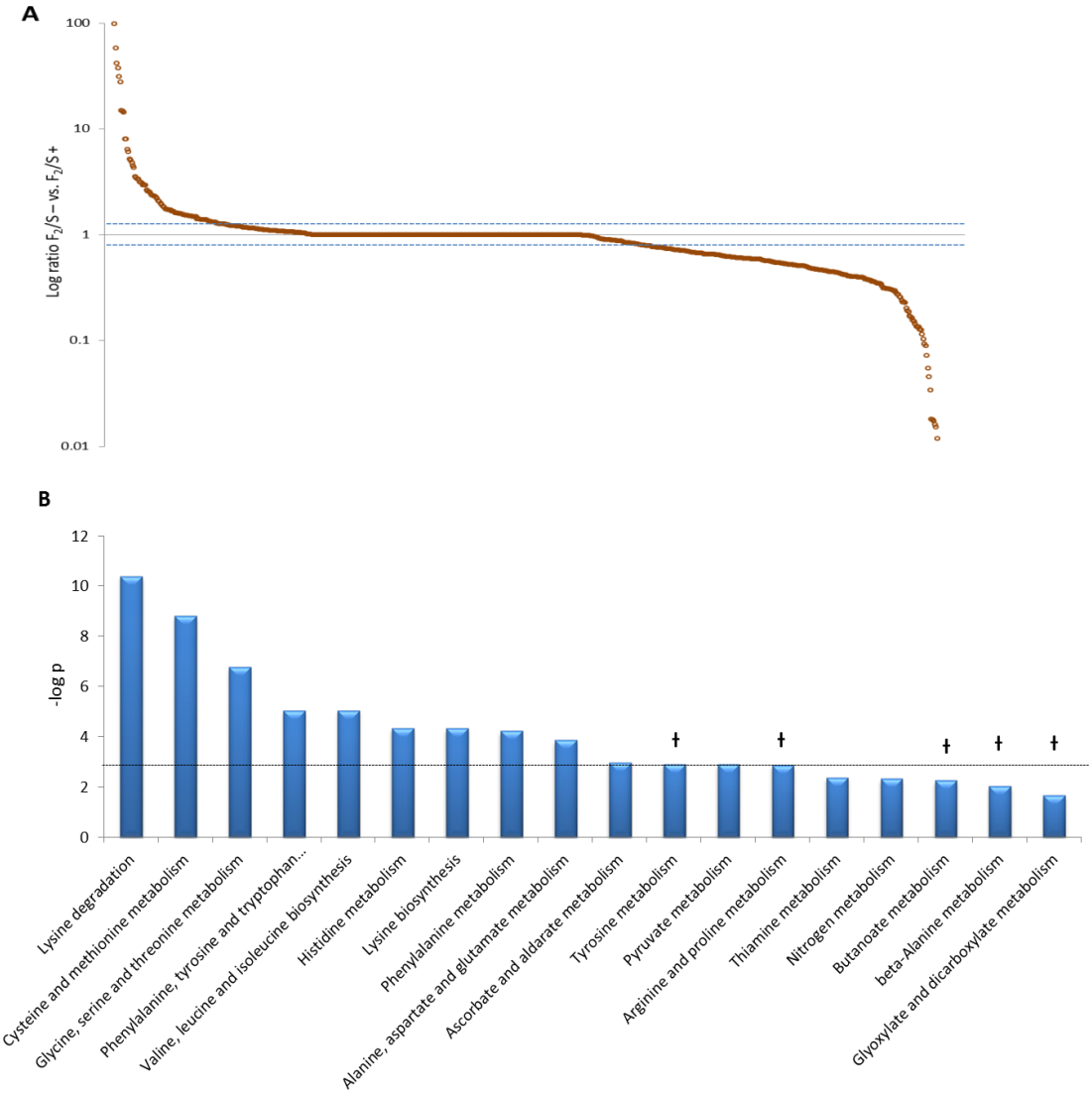

Figure 5-17 Pathway analysis for F_2/S- vs. F_2/S+ activity. *Ratios of identified metabolites from pericytes cultured in F_2/S hydrogels in the presence (+) and absence (-) of induction media depicted in a scatter plot to ascertain differences between the two (A). Metabolites that measured above or below the defined threshold (two fold difference as indicated by the dashed line) were isolated and mapped to known metabolic pathways (B). Pathways where the most significant changes occurred were primarily associated with amino acid metabolism. Interestingly, some pathways (†), while significantly different from the plain substrate remain unchanged between F_2/S substrates indicating selectivity in cell behaviour due to the presence or absence of induction media. Dashed in (B) indicates statistically significant the threshold, where $p < 0.05$ as calculated using node centrality statistics in metaboanalyst.*

5.4 Summary

This chapter has explored the use of finely tuned F_2/S hydrogels (~ 20 kPa) as a means of directing pericyte differentiation into mature chondrocytes and whether the biomaterial was able to sustain this over an extended period of time in cell culture.

Cell lines were moved from bone marrow MSCs to pericytes to show that mechanical stimulus is able to influence more primitive cell lines with chondrogenic potential. Pericytes, like MSCs, were shown to have good viability when cultured using F_2/S biomaterials as well as having an ability to undergo differentiation into chondrogenic phenotypes through material and chemical instruction (Figure 5-3, Figure 5-4 and Figure 5-5).

Cells were maintained in culture with F_2/S in the presence and absence of chondrogenic media for a period of five weeks. Over this time, cells were checked for expression levels of chondrocyte biomarkers SOX-9, aggrecan, COL2A1 and COL10A1. Expression levels of all proteins inclusive of the mentioned markers were observed to increase over time with levels reaching saturation by 1 week in culture as cell attained not only a constant transcription level but also constant metabolic turn over (Figure 5-6, Figure 5-7, Figure 5-10, Figure 5-13 and Figure 5-14). Chondrogenic development of pericytes in F_2/S substrates, however, did not show gene expression patterns of mature chondrocytes as typified by cells *in vivo* (high COL2A1 and negligible COL10A1 levels) but expression of COL10A1 at very early time points (24hrs) suggest that the cultures adopted a mixed phenotype of mature and hypertrophic chondrocytes, which is often observed in *in vitro* systems (Karlsson et al., 2007, Mwale et al., 2006, Perrier et al., 2011). This is thought to occur, in part, due to the indication of some osteogenic activity that occurred in the culture system confirmed by positive detection of the bone marker RUNX-2 (known to promote COL10A1 expression) and others (Figure 5-12). COL10A1 expression is also an effect that may further be exacerbated by the presence of induction media, of which some of its constituents promote rapid chondrocyte maturation (Figure 5-11 (Cooke et al., 2011, Perrier et al., 2011)). This is also likely the case here as the extent to which osteogenesis and chondrogenesis occurs in both F_2/S- and F_2/S+ was not affected despite the F_2/S+ system showing higher levels of COL10A1 (Figure 5-12).

Both cell systems, one just the biomaterial (F_2/S-) and the other in conjunction with differentiating media (F_2/S+) are sufficient enough to allow chondrogenic development. The alternate routes instigate subtle differences in how the cells process these cues, which are reflected in their metabolome (Figure 5-17); they adapt generally similar patterns with very fine divergence likely to account for the differences that manifest in their resultant phenotypes.

The assessment is intended as an exploratory analysis of total pericyte behaviour when differentiating in response to chondrogenic induction media or free from biased chemical interference. As such, the data was analysed as a whole. It is worthy of note however, that for purposes of looking into cell activity in more intricate detail, the selection process could be further refined by using strict isolation criteria in addition to setting a threshold such as coupling the defined threshold with statistical confidence between measured abundance levels of F_2/S - and F_2/S +.

6 DISCUSSION

This project investigated the influence that short chain peptide hydrogel material (F_2/S) properties, specifically matrix stiffness, had on guiding stem cell differentiation. While employing some established methodologies for doing so (immunocytochemistry and qRT-PCR for example), the project also investigated whether adopted changes in phenotype during early stages of differentiation can be tracked by looking into the presence and relative amounts of small molecules that the cell produces as a whole (the metabolome). Perceiving cell phenotype in this way was considered particularly favourable as firstly, the use of matrix rigidity as the sole effector of differentiation allows detection and measurements of metabolites to be a reflection of innate cellular chemistries unbiased by the presence or use of molecules supplemented in media to induce differentiation. And secondly, based on the first principle, a broad reaching metabolomics study was able to give enough information to identify metabolites that are lesser known to have a role in promoting different stem cell phenotypes.

While the above points were illustrated in this project, this chapter goes on to scrutinise some of the more intricate outcomes observed in this project by way of design and obtained results. It also explores a number of ideas that may go towards resolving some of the questions raised as a result by way of further study.

6.1 Differentiation resulting from interplay between matrix mechanics and adopted morphology

Adopting a cell lineage requires a certain degree of pattern distinction or geometric constraint with regards to distinguishing between cell types with similar native tissue mechanics (Lee, 2013). The use of self-assembled peptide F_2/S hydrogels in this project will inevitably have a surface topography, which unfortunately was not optimised for exact patterning and dimensions (personal communication with V. Jayawarna). Assessments of the cytoskeletal properties of MSCs cultured on each of the hydrogels show that their organisation are much more akin to cells that are cultured in encapsulation (Figure 2-6, (Huebsch et al., 2010, Parekh et al., 2011, Sugawara et al., 2013)) as opposed to onto a flat surface. These suggest that the cells cultured on the F_2/S surface are constrained in a pseudo three dimensional construct placing restriction on how the cells are spread creating a morphology that is different from cells that are otherwise unrestricted on smoother surfaces or those with smaller dimension (nano) topography as is typically adopted by most two dimensional cultured cells.

Surface embedding of the cells invariably means that they are subject to geometrical constraints as dictated by the substrate. The spatial restriction experienced in this sense is likely to define the overall morphology of the cell but the effects of the substrate

stiffness is still something that is very much influential over cell behaviour as observed from the different lineages adapted on each hydrogel (Chapter 2, (Chen et al., 2012, Discher et al., 2005, Evans et al., 2009, Saha et al., 2008)). This also goes some way to explain why, although observed in other studies, culturing MSCs on F_2/S hydrogels that bear similar mechanical strength with native muscle tissue did not show any myogenic development (Figure 2-7 - Figure 2-9, (Engler et al., 2004b, Engler et al., 2006, Tse and Engler, 2011)).

Topographical detail for aiding myoblast development is known to be of particular importance, especially with regards to aiding fusion and striation (Choi et al., 2012a, Lu and Leng, 2009). It is therefore plausible that loss of this detail displaces myogenesis for chondrocyte development, a lineage that is more favourable with both adopted morphology and substrate elasticity (Chapter 2, (Allen et al., 2012, Glowacki et al., 1983, Guo et al., 1989, Im, 2005, Jung et al., 2009, Trickey et al., 2004, vanSusante et al., 1995, Gao et al., 2010)). In the same vein, adopting a three-dimensional osteocytic morphology in a mechanically relevant (38 kPa) matrix also primarily resulted in osteogenic development.

It is well documented that cell shape has a profound effect in guiding lineage adoption when stem cells differentiate (Kilian et al., 2010, McBeath et al., 2004, Peng et al., 2011). While the mechanics of the F_2/S substrates have a clear influence on MSC behaviour (Chapter 2), the irregularity of the substrate topography (particularly for two dimensional cell culture) very much goes someway to affecting cell behaviour, given that interplay between matrix mechanics and substrate patterning both play an important role when regulating differentiation (Guilak et al., 2009, Higuchi et al., 2013). This interplay, most likely accounts for the observed cell heterogeneity on each of the F_2/S substrates (Figure 2-7 - Figure 2-9).

By using precision imprinting of topographies on soft substrate surfaces, Lee *et al* were able to show that the manner in which a cell was spatially restricted had an effect on whether neuro- or adipogenic development was observed (Lee, 2013). The study has interesting connotations in the sense that cells observed on the soft and stiff F_2/S substrates using fluorescence live/dead microscopy showed that cells on the soft F_2/S hydrogels were better at forming elongated cell morphologies than those on the stiff substrate (Figure 6-1). An occurrence that is likely due to the lessened cross links formed in the soft F_2/S hydrogel allowing the cells to spread better. Adipogenesis of MSCs is evident across all three substrates, a consequence that may be due to the maintained rounded morphology on each of the substrates. Differences in elasticity, however, also encourage the formation of neuronal cells (2 kPa), chondroblasts (6 kPa) and osteoblasts (38 kPa).

In order to reduce this heterogenic effect, further characterisation of the physical characteristics of the F_2/S surface is required. Pliability of the F_2/S peptide solutions means that better definition of the surface features could be achieved through precise control of the mould used to create the hydrogel surface prior to cell seeding. This is likely to provide better control of differentiation outcomes using two dimensional culture methods. The use of bipotential media as done in other studies (Fu et al., 2010, Guvendiren and Burdick, 2012, Kilian et al., 2010, McBeath et al., 2004) for regulating heterogeneity may also be a point for consideration as matrix mechanics is thought to have an influence over differentiation lineage that outweighs chemical induction (Engler et al., 2006). It is noted, however, that this approach would likely restrict differentiation potential and as such could have invariably masked the observed neurogenic and chondrogenic effects.

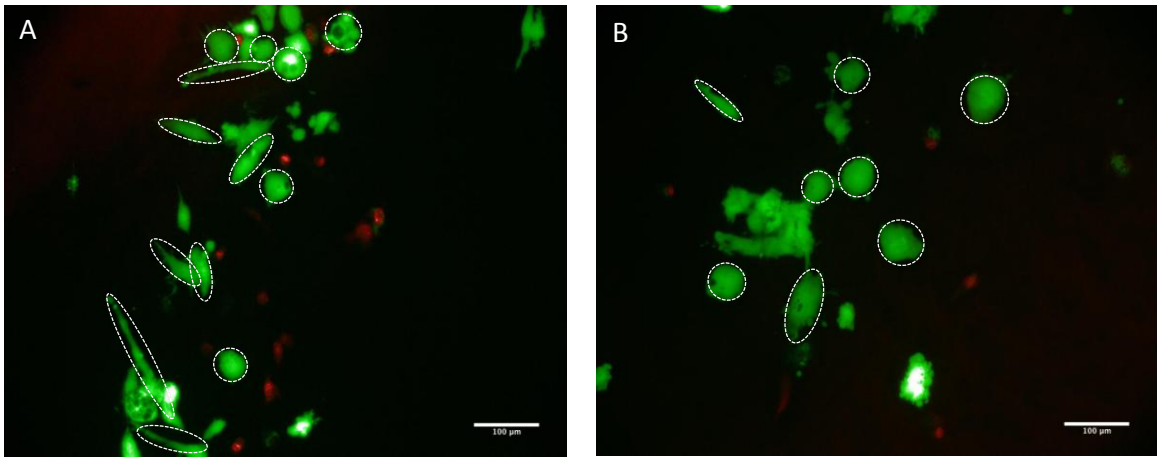

Figure 6-1 Fluorescence live/dead images of MSCs cultured on 2 and 6 kPa F_2/S hydrogels. *Cells cultured on the 2 kPa substrate (A) had shown a number of cells which had adopted an elongated morphology alongside cells with rounded morphology (shape is outlined using dashed ellipses and circles). Cells on the 6 kPa substrate (B) on the other hand, were primarily rounded with few elongated cells. Live cells are shown in green and dead in red; scale bar – 100 µm.*

6.2 F_2/S as a biomaterial for *in vivo* application

Commercially available scaffolds used in tissue engineering are generally animal derived products (Badylak, 2004, Badylak, 2007). While their uses have attained a measure of success, these classes of materials are not wholly ideal due to setbacks such as patient rejection, non-reproducible characteristics and contamination. For this reason, the use of self-assembled peptide scaffolds are particularly attractive prospects as they are able to overcome the limitations of batch variability, reducing unpredictable outcomes on implantation.

The F_2/S hydrogels are a well-placed candidate for regenerative medicine as their peptide scaffolds inherently make them biocompatible, their tunable mechanics enable influence over stem cell differentiation (Chapter 2 and Chapter 5); in particular guiding chondrogenic development and have been shown to be relatively stable long-term in culture (Chapter 5).

The ability of hydrogels to undergo phase shifts from liquid to gel during fabrication is also of added advantage. It potentially allows for delivery to injury sites via microinjection techniques allowing the hydrogel to mould to the shape of the void or injury (Firth et al., 2006, Nisbet et al., 2010, Williams et al., 2011). An area of regenerative medicine where this may find important application is with matrix assisted autologous chondrocyte implantation (MACI). Using this technique, chondrocytes are typically harvested from healthy cartilage, expanded *in vitro* within the implantation scaffold and transplanted back into the injury site of the patient (Demoor et al., 2012, Dunkin and Lattermann, 2013, Ochs et al., 2011). The use of F_2/S biomaterials as an instruction for stem cell differentiation eliminates the need for creating a second injury site to source chondrocytes for autogenic implantation as well as being able to repopulate the defect with a sizeable number of chondrocytes to allow sufficient healing to occur.

The use of Fmoc derived peptide moieties in *in vivo* engineering is something that has recently found use in a number of applications. For example, drug delivery for the reduction of intraocular pressure after glaucoma surgery procedures (Xu et al., 2010) and the development of skeletal muscle in zebrafish (Williams et al., 2011). While *in vitro* experiments do not necessarily predict *in vivo* outcomes, these examples suggest that the use of F_2/S hydrogels for correcting cartilage defects have good potential as an *in vivo* regenerative scaffold. However, studies assessing their compatibility as *in vivo* scaffolds are yet to be explored.

6.3 Incentives for monitoring metabolism as an indication of phenotype

Studying the metabolic activity of cells has of recent given insight into cell behaviour with regards to their plasticity (Yanes et al., 2010) and self-renewal properties (McMurray et al., 2011) for example. While this thesis has shown that distinct metabolic behaviours of stem cells are adopted as they undergo differentiation can be illustrated in the cells overall metabolome, it also highlights a number of facets that are open to consideration when researching cell behaviour.

The first lies in noting the distinctions that the microenvironment type used to persuade differentiation has on cell activity. Differentiation of MSCs *in vitro* can be achieved using

a number of methodologies. Of these, the most commonly used is the supplementation of culture media with a number of small molecules known to instigate stem cell differentiation along a number of cell lineages (Lin et al., 2005, Pittenger et al., 1999, Sekiya et al., 2002). Alternatively, the use of co-culture methods, substrate detailing via surface topography, functionalisation and tailored mechanics have all proved to be instrumental in directing stem cell fate (McMurray et al., 2011, McNamara et al., 2011, Yim et al., 2010). While altered differentiation states can be achieved through each of these means (as a sole instructor or in combination), looking into the broad range metabolic processes that occur highlight these routes have, for the most part, overlapping behaviours resulting in a common outcome. It is also noted, however, that alternate methods do indeed have subtle discrepancies between each other (Chapter 5) that may in part be responsible for minute differences in phenotype, which are not necessarily detected using physical characteristics such as cell shape or the up-regulation of a specific biomarker. Rather, the difference may show up when the 'positive' points are compared in relation to one another (Chapter 5). It is likely that different modes of enforcing differentiation can cause a slight bias of one process over another, exaggerating or lessening expression of one or a class of molecules. This is something that in turn can have an effect on overall cell function and tissue efficacy. Being able to pinpoint where these exaggerations or moderations occur has potential in influencing how biomaterials are refined and designed for cell culture.

Secondly, scrutinising the metabolome enables correlations to be made between smaller building blocks as the constituent parts of a tertiary whole. A good example of this is the observed increase in leucine concentrations from cells cultured on the 38 kPa F_2/S substrate (Chapter 3, (McNamara et al., 2011)) and the role SLRPs play in driving osteogenic development in tissues (Bianco et al., 1990, Kimoto et al., 1994, Xu et al., 1998, Young et al., 2003). Then again, it could be that a leucine rich environment also contributes in alternate ways other than promoting SLRP synthesis towards promoting osteogenesis and it would be of worth researching in what manner this identified amino acid has an effect on bone formation *in vitro*.

Thirdly, a common problem with the use of established induction media cocktails is the production of a heterogeneous cell population. Compounds such as dexamethasone, which is used extensively in most induction media types, is able to instigate the formation of cells into a number of different lineages (Mirmalek-Sani, 2006, Pittenger et al., 1999, Zuk et al., 2001) and as a result, total cell populations are not without a degree of 'contamination'. While the screening of large drug libraries continually recycle this process allowing the discovery of new compounds that affect differentiation (Johnson et al., 2012, Ding and Schultz, 2004), the use of the cellular metabolome to isolate innate

compounds that may play a role in cell differentiation has the potential to generate a new class of compounds which have less of a heterogenic effect when directing cellular differentiation as observed with the use of cholesterol sulphate for osteogenic induction of MSCs (Chapter 4).

These innate compounds also have the potential to be candidate metabolites that act as biomarkers of differentiation at the metabolic level in the same sense that COL2A1 acts as a marker for chondrogenesis, increasing confidence in attaining a desired phenotype. A crude example here would be the use of GP18:0 for monitoring chondrogenesis (Figure 6-2). Depletion of GP18:0 was also noted in pericytes undergoing chondrogenesis in F_2/S substrates, a result that is complementary to that observed in MSCs (Chapter 3). The term crude is used as it is noted that GP18:0 also instigated osteogenic development (Chapter 4), that is, it is not specific to a single lineage. The observed trend, however, does to not necessarily render it negligible as a biomarker candidate. To develop this further, however, a number of optimisation experiments would be required to enhance detection specificity, precision and accuracy when measuring from cell extracts. In particular distinguishing features of metabolite expression between differentiated cell types can be ascertained through quantitation and comparison with mature cell types.

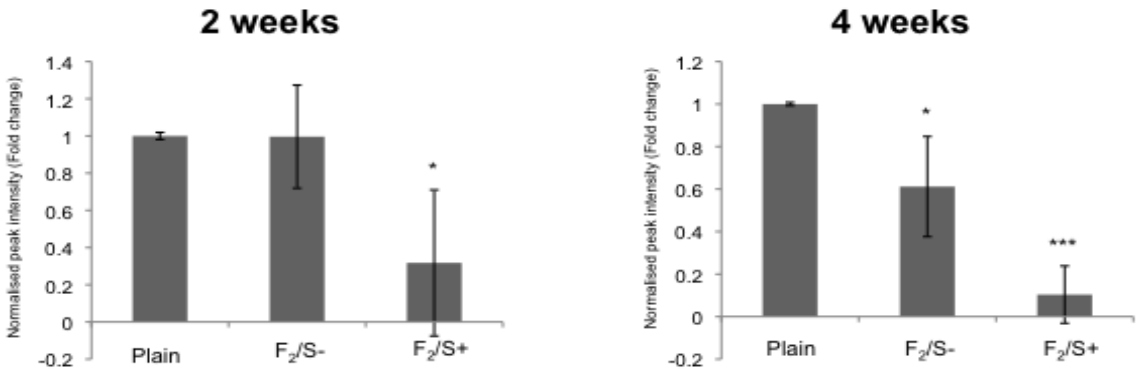

Figure 6-2 Average peak intensities of GP18:0 detected in pericytes cultured on plain and in 20 kPa F_2/S substrates with (+) and without (-) chondrogenic induction media as detected using LC-MS. *Peak intensities are shown as fold change relative to the plain substrate. GP18:0 shows a time dependent decrease for F_2/S substrates. Levels of GP18:0 were also observed to drop much faster for cells cultured in the presence of induction media (F_2/S+). Error bar denote standard deviations from the mean; n = 4; * notes statistical significance compared to the plain substrate where $p < 0.05$ and *** where $p < 0.001$ as calculated using unpaired students t-test*

Lastly, while this project focuses on metabolites with known masses and to an extent function, it is restricted based on known and identified functions held in bioinformatic

databases. Metabolite identification by LC-MS, inclusive of this study, generates a host of detected masses labelled as unknown that may or may not be compounds having an active or passive role in cell kinetics. This study however is confined to compounds that have prior knowledge to their involvement in human metabolic processes. The breadth of unbiased detection experiments reaches beyond this and allows a search for novel compounds of interest to be made. To do this, considerable concern would have to be given to experimental design and confirmatory experiments but this project illustrates that it is a useful starting platform for broadening the inventory of endogenous cell metabolite systems (Chapter 3).

The aforementioned examples illustrate that a metabolomics based study is not only a confirmatory process but also a hypothesis-generating platform that can beg far more questions than give answers. Nonetheless, dependent on the desired objective, it can be viewed inevitably as being part of the process and not necessarily the conclusion.

6.4 Transdifferentiation effects

While MSCs are defined by their ability to differentiate into mesoderm cell types (Dominici et al., 2006), a number of studies have reported their ability to transgress this characterisation, exhibiting an ability to form cells of other germ lines (transdifferentiate). One such in particular is the formation of neuronal cell types (Sanchez-Ramos et al., 2000, Woodbury et al., 2002, Woodbury et al., 2000). Findings within this study echoed this sentiment when MSCs were cultured on relatively soft (2 kPa) F_2/S hydrogel substrates, as ascertained through observed increase in nestin, β3-tubulin and GFAP transcription (Chapter 2 & 4). Observation of this effect seems to require a very precise mode of cell culture, studies showing MSCs which have been successfully cultivated into neuronal cells routinely make use of co-culture with mature neuronal cells (Sanchez-Ramos et al., 2000, Wislet-Gendebien et al., 2005, Zhao et al., 2002) or through fine tuning of the substrate mechanics (Engler et al., 2006, Saha et al., 2008, Teixeira et al., 2009). While attempted differentiation of MSCs into neuronal cells was not successful using supplemented media (Chapter 4 and appendix), experiments by Woodbury *et al* for example, have been able to demonstrate *in vitro* differentiation of MSC into neuronal cells on culture well plastic (Woodbury et al., 2000). While MSCs cultured in the study performed by Woodbury *et al* were positive for the neuronal phenotypic markers; nestin, neuron specific enolase and NeuN, they were not shown to have any excitable activity. A characteristic that has only been shown thus far using co-culture with mature neurons (Wislet-Gendebien et al., 2005).

Conversely, actively blocking generated tension causes the observation of adipogenesis over neurogenesis in studies using relatively hard surfaces (Kilian et al., 2010, McBeath et al., 2004) while those using softer substrates are seemingly still permissible to neuronal development (Engler et al., 2006, Lee, 2013). An indication that substrate mechanics play a vital role in creating this distinction. A single molecule (sphinganine) isolated from the metabolome of MSCs cultured on 2 kPa F_2/S hydrogels showed enhanced productivity of the tested neurogenic biomarkers when the cells were cultured on this substrate but all were actively repressed when cells were placed on culture well plastic (Chapter 4), suggesting active inhibition of neurogenesis on stiff substrates. The results call into question what cell process(es) are permissive when the cells are cultured on compliant/non-compliant surfaces thereby having a direct effect on what lineages are adopted on differentiation.

The observation of adipogenesis on harder substrates on the other hand, is a more common occurrence than neuronal development (Kilian et al., 2010, McBeath et al., 2004). Low contractile states in MSCs that result in adipogenesis either through blocking cytoskeletal contractility (Engler et al., 2006, Guvendiren and Burdick, 2012) or culturing on relatively soft substrates (Lee, 2013, Fu et al., 2010) suggests that adipocyte development is amenable across a stiffness gradient (Guvendiren and Burdick, 2012) and is often observed when other influential factors are biased in its favour. Adipocyte distribution *in vivo* is coupled quite naturally with tissues that span a range of elastic moduli much broader than the ECM coupled with peripheral nerves for example, which has a more uniform association with the viscoelastic epineurium that surrounds neurons (Luque et al., 1983, Salonen et al., 1985). The exacting nature of the surrounding epineurium may go some way to explaining why, when making use of compliant soft substrates *in vitro*, neuronal development is consequently observed.

6.5 Mesenchymal & perivascular stem cells

While MSCs over the last few years have been a focus of much research with stem cells, a number of factors make them restrictive to use, such as low population numbers on extraction, hampering the demands made for progressing tissue engineering *ex vivo*. For this reason, there is a lot of interest in being able to diversify the means by which stem cells are sourced, which are also able to meet research demands. As such, a number of studies that have reported the acquisition of stem cells from a number of sources other than bone marrow such as the pancreas, muscle and kidneys (da Silva Meirelles et al., 2006), giving hope to the creed that stem cells can be sourced in better populations than the bone marrow can give. Pericytes, as one half of the perivascular stem cells, are one

such source currently under scrutiny as they are innately associated with the vasculature and are therefore more extensively available than bone marrow derived stem cells.

Due to the lack of a wholly defined MSC phenotype, the discovery of a number of stem cell types sourced from locations other than the bone marrow means that due consideration must be given to how each of these cells behave with regards to one another and whether fabricated biomaterial substrates are able to influence them in a similar fashion resulting in a more or less uniform outcome.

This thesis explored such an idea starting with the more established MSCs and ascertaining whether differentiation based on substrate mechanics is a translatable quality by testing the theory using pericytes (Chapter 2 and Chapter 5). Furthermore, information obtained from MSCs suggests that these interpretation patterns, at least at the metabolic level, are something that is conveyable across both cell lines. Singular metabolites for influencing differentiation lineages as determined from MSCs in chapter 4 were also tested using pericytes giving the same positive outcomes (Figure 6-3). The results show that these compounds have a prevalent effect, suggesting common interpretation by both MSCs and pericytes, a particularly important point with regards to regulating how cells are differentiated *in vitro*.

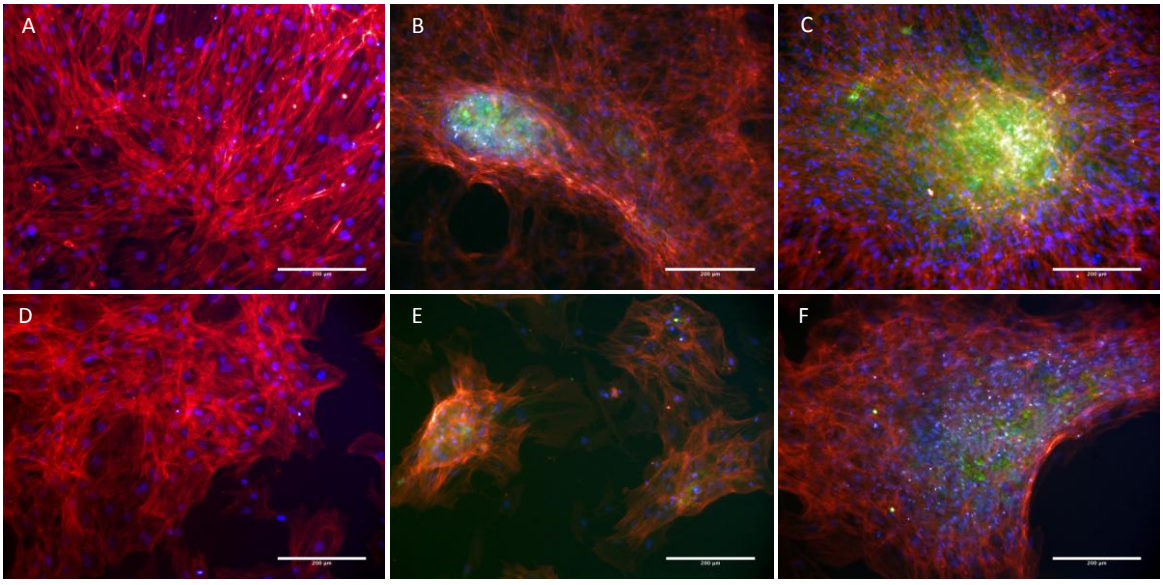

Figure 6-3 Immunofluorescence images of pericytes cultured in non-supplemented media (A & D), osteo- and chondrogenic induction media (B & E) and with 1 µM and 0.1 µM cholesterol sulphate and GP18:0 respectively (C & F). *Cells were assessed for osteogenic development by staining for the production of osteocalcin (A – C) and chondrogenic development by staining for COL2A1 production (D – E). Cells stained positively for each test metabolite confirming the results seen previously using MSCs. Fluorescence images show actin cytoskeleton (red), cell nuclei (blue) and either osteocalcin or COL2A1 (green). Scale bar – 200 µm.*

With the ever-broadening options of stem cell sourcing and means of directing differentiation *in vitro*, it is important that the biomaterial is able to cater for its intent across cell lines. The use of materials with tuned substrate elasticity seems to have a better influence over attaining a cellular phenotype closer to the desired outcome than when compared to using current induction media protocols (Chapter 5). A question that is of particular importance, however, which is not researched in this thesis is the comparative plasticity of both bone marrow derived MSCs and pericyte cells. As pericytes are considered a predecessor of MSCs, it could be postulated that they will exhibit better differentiation potential than MSCs themselves. This, however, is something that has not been tested in this thesis and would warrant further research.

6.6 Conclusions

This thesis in context, firstly illustrates the use of biomaterial mechanics as a sole controlling influence on stem cell differentiation. While this line of research has been used in a number of other studies, the F_2/S substrates comprise the use of peptide moieties over synthetic substrates making them a better suited candidate for use in wound healing applications such as autologous chondrocyte implantation.

Secondly, the project also illustrates how metabolomics, as a powerful tool, is able to highlight phenotypical divergence through the identification and profiling of small molecules that are lesser known to play a role in altering cell states. Being able to influence differentiation using alternate substrate mechanics alone has enabled metabolic processes carried out exclusively by the cells to be profiled using an unbiased metabolomics design. By investigating cell behaviour in this manner, deciphering individual components that drive or support cell differentiation allows identification of classes of molecules that contribute to development of altered or adaptive cell states.

Further research

Questions and particular areas of interest that have arisen during the course of this project that may be of advantage to investigate further have been addressed throughout this thesis as they occurred. These points however, are summarised below.

Optimisation studies to improve desired outcomes and lessen ambiguity.

- Fabrication process of the F_2/S substrate for two-dimensional culture as a means to reduce the observed heterogeneity of cell types formed on MSC differentiation.
- The use of co-culture system to further direct MSC differentiation along a singular lineage as well as to enhance better phenotype development.

New concept and development studies to improve currently used methodologies.

- The use of metabolomics in stem cell research as an aid in assessing cell behaviour and development, monitoring metabolic output as an indicator of efficacy.
- The use of a metabolite profile to as a means of identifying and designing differentiation specific small molecules that are able to reduce or eliminate cross contamination when directing differentiation *in vitro*.

7 REFERENCES

AKIYAMA, H., CHABOISSIER, M. C., MARTIN, J. F., SCHEDL, A. & DE CROMBRUGGHE, B. 2002. The transcrintion factor Sox9 has essential roles in successive steps of the chondrocyte differentiation pathway and is required for expression of Sox5 and Sox6. *Genes & Development,* 16**,** 2813-2828.

AKIYAMA, S. K. & YAMADA, K. M. 1985. The interaction of plasma fibronectin with fibroblastic cells in suspension. *Journal of Biological Chemistry,* 260**,** 4492-4500.

ALANO, C. C., TRAN, A., TAO, R., YING, W., KARLINER, J., S., SWANSON, R., A. 2007. Differences among Cell Types in NAD1 Compartmentalization: A Comparison of Neurons, Astrocytes, and Cardiac Myocytes. *Journal of Neuroscience Research***,** 8.

ALEXANDROVA, A. Y., ARNOLD, K., SCHAUB, S., VASILIEV, J. M., MEISTER, J.-J., BERSHADSKY, A. D. & VERKHOVSKY, A. B. 2008. Comparative Dynamics of Retrograde Actin Flow and Focal Adhesions: Formation of Nascent Adhesions Triggers Transition from Fast to Slow Flow. *Plos One,* 3.

ALEXOPOULOS, L. G., HAIDER, M. A., VAIL, T. P. & GUILAK, F. 2003. Alterations in the mechanical properties of the human chondrocyte pericellular matrix with osteoarthritis. *Journal of Biomechanical Engineering-Transactions of the Asme,* 125**,** 323-333.

ALEXOPOULOS, L. G., SETTON, L. A. & GUILAK, F. 2005. The biomechanical role of the chondrocyte pericellular matrix in articular cartilage. *Acta Biomaterialia,* 1**,** 317-325.

ALLEN, J., DAVEY, H. M., BROADHURST, D., HEALD, J. K., ROWLAND, J. J., OLIVER, S. G. & KELL, D. B. 2003. High-throughput classification of yeast mutants for functional genomics using metabolic footprinting. *Nature Biotechnology,* 21**,** 692-696.

ALLEN, J. L., COOKE, M. E. & ALLISTON, T. 2012. ECM stiffness primes the TGF beta pathway to promote chondrocyte differentiation. *Molecular Biology of the Cell,* 23**,** 3731-3742.

AMANO, M., ITO, M., KIMURA, K., FUKATA, Y., CHIHARA, K., NAKANO, T., MATSUURA, Y. & KAIBUCHI, K. 1996. Phosphorylation and activation of myosin by Rho-associated kinase (Rho-kinase). *Journal of Biological Chemistry,* 271**,** 20246-20249.

ARIAS-SALGADO, E. G., LIZANO, S., SARKAR, S., BRUGGE, J. S., GINSBERG, M. H. & SHATTIL, S. J. 2003. Src kinase activation by direct interaction with the integrin beta cytoplasmic domain. *Proceedings of the National Academy of Sciences of the United States of America,* 100**,** 13298-13302.

ARNSDORF, E. J., JONES, L. M., CARTER, D. R. & JACOBS, C. R. 2009. The Periosteum as a Cellular Source for Functional Tissue Engineering. *Tissue Engineering Part A,* 15.

AZUARA, V., PERRY, P., SAUER, S., SPIVAKOV, M., JORGENSEN, H. F., JOHN, R. M., GOUTI, M., CASANOVA, M., WARNES, G., MERKENSCHLAGER, M. & FISHER, A. G. 2006. Chromatin signatures of pluripotent cell lines. *Nature Cell Biology,* 8**,** 532-U189.

BADYLAK, S. F. 2004. Xenogeneic extracellular matrix as a scaffold for tissue reconstruction. *Transplant Immunology,* 12**,** 367-377.

BADYLAK, S. F. 2007. The extracellular matrix as a biologic scaffold material. *Biomaterials,* 28**,** 3587-3593.

BAI, T. R., COOPER, J., KOELMEYER, T., PARE, P. D. & WEIR, T. D. 2000. The effect of age and duration of disease on airway structure in fatal asthma. *American Journal of Respiratory and Critical Care Medicine,* 162**,** 663-669.

BALABAN, N. Q., SCHWARZ, U. S., RIVELINE, D., GOICHBERG, P., TZUR, G., SABANAY, I., MAHALU, D., SAFRAN, S., BERSHADSKY, A., ADDADI, L. & GEIGER, B. 2001. Force and focal adhesion assembly: a close relationship studied using elastic micropatterned substrates. *Nature Cell Biology,* 3.

BALE, M. D., WOHLFAHRT, L. A., MOSHER, D. F., TOMASINI, B. & SUTTON, R. C. 1989. Identification of vitronectin as a major plasma-protein adsorbed on polymer surfaces of different copolymer composition. *Blood,* 74**,** 2698-2706.

BATEMAN, J. F., BOOT-HANDFORD, R. P. & LAMANDE, S. R. 2009. Genetic diseases of connective tissues: cellular and extracellular effects of ECM mutations. *Nature Reviews Genetics,* 10**,** 173-183.

BEGG, D. A., RODEWALD, R. & REBHUN, L. I. 1978. Visualization of actin filament polarity in thin-sections - evidence for uniform polarity of membrane-associated filaments. *Journal of Cell Biology,* 79**,** 846-852.

BELL, D. M., LEUNG, K. K. H., WHEATLEY, S. C., NG, L. J., ZHOU, S., LING, K. W., SHAM, M. H., KOOPMAN, P., TAM, P. P. L. & CHEAH, K. S. E. 1997. SOX9 directly regulates the type-II collagen gene. *Nature Genetics,* 16**,** 174-178.

BELLOWS, C. G., AUBIN, J. E. & HEERSCHE, J. N. M. 1987. Physiological concentrations of glucocorticoids stimulate formation of bone nodules from isolated rat calvaria cells-invitro. *Endocrinology,* 121**,** 1985-1992.

BENDERS, K. E. M., WEEREN, P. R. V., BADYLAK, S. F., SARIS, D. B. F., DHERT, W. J. A. & MALDA, J. 2013. Extracellular matrix scaffolds for cartilage and bone regeneration. *Trends in Biotechnology,* 31**,** 169-76.

BENINGO, K. A., DEMBO, M., KAVERINA, I., SMALL, J. V. & WANG, Y. L. 2001. Nascent focal adhesions are responsible for the generation of strong propulsive forces in migrating fibroblasts. *Journal of Cell Biology,* 153**,** 881-887.

BENOIT, D. S. W., SCHWARTZ, M. P., DURNEY, A. R. & ANSETH, K. S. 2008. Small functional groups for controlled differentiation of hydrogel-encapsulated human mesenchymal stem cells. *Nature Materials,* 7**,** 816-823.

BENVENUTI, S., CELLAI, I., LUCIANI, P., DELEDDA, C., BAGLIONI, S., GIULIANI, C., SACCARDI, R., MAZZANTI, B., DAL POZZO, S., MANNUCCI, E., PERI, A. & SERIO, M. 2007. Rosiglitazone stimulates adipogenesis and decreases osteoblastogenesis in human mesenchymal stem cells. *Journal of Endocrinological Investigation,* 30**,** RC26-RC30.

BERSHADSKY, A. D., BALABAN, N. Q. & GEIGER, B. 2003. Adhesion-dependent cell mechanosensitivity. *Annual Review of Cell and Developmental Biology,* 19**,** 677-695.

BETTINGER, C. J., LANGER, R. & BORENSTEIN, J. T. 2009. Engineering Substrate Topography at the Micro- and Nanoscale to Control Cell Function. *Angewandte Chemie-International Edition,* 48**,** 5406-5415.

BHADRIRAJU, K. & HANSEN, L. K. 2002. Extracellular matrix- and cytoskeleton-dependent changes in cell shape and stiffness. *Experimental Cell Research,* 278**,** 92-100.

BHADRIRAJU, K., YANG, M., RUIZ, S. A., PIRONE, D., TAN, J. & CHEN, C. S. 2007. Activation of ROCK by RhoA is regulated by cell adhesion, shape, and cytoskeletal tension. *Experimental Cell Research,* 313**,** 3616-3623.

BIANCO, P. 2011. Bone and the hematopoietic niche: a tale of two stem cells. *Blood,* 117**,** 5281-5288.

BIANCO, P., FISHER, L. W., YOUNG, M. F., TERMINE, J. D. & ROBEY, P. G. 1990. Expression and localization of the 2 small proteoglycans biglycan and decorin in developing human skeletal and nonskeletal tissues. *Journal of Histochemistry & Cytochemistry,* 38**,** 1549-1563.

BIGGS, M. J. P., RICHARDS, R. G., GADEGAARD, N., WILKINSON, C. D. W., OREFFO, R. O. C. & DALBY, M. J. 2009. The use of nanoscale topography to modulate the dynamics of adhesion formation in primary osteoblasts and ERK/MAPK signalling in STRO-1+enriched skeletal stem cells. *Biomaterials,* 30**,** 5094-5103.

BJORNSON, C. R. R., RIETZE, R. L., REYNOLDS, B. A., MAGLI, M. C. & VESCOVI, A. L. 1999. Turning brain into blood: A hematopoietic fate adopted by adult neural stem cells in vivo. *Science,* 283**,** 534-537.

BLACKBURN, J. & MANSELL, J. P. 2012. The emerging role of lysophosphatidic acid (LPA) in skeletal biology. *Bone,* 50**,** 756-762.

BOEHM, B., WESTERBERG, H., LESNICAR-PUCKO, G., RAJA, S., RAUTSCHKA, M., COTTERELL, J., SWOGER, J. & SHARPE, J. 2010. The Role of Spatially Controlled Cell Proliferation in Limb Bud Morphogenesis. *Plos Biology,* 8.

BONDER, E. M., FISHKIND, D. J. & MOOSEKER, M. S. 1983. Direct measurement of critical concentrations and assembly rate constants at the 2 ends of an actin filament. *Cell,* 34**,** 491-501.

BOONYARATANAKORNKIT, V., MELVIN, V., PRENDERGAST, P., ALTMANN, M., RONFANI, L., BIANCHI, M. E., TARASEVICIENE, L., NORDEEN, S. K., ALLEGRETTO, E. A. & EDWARDS, D. P. 1998. High-mobility group chromatin proteins 1 and 2 functionally interact with steroid hormone receptors to enhance their DNA binding in vitro and transcriptional activity in mammalian cells. *Molecular and Cellular Biology,* 18**,** 4471-4487.

BRIGHTON, C. T., LORICH, D. G., KUPCHA, R., REILLY, T. M., JONES, A. R. & WOODBURY, R. A. 1992. The pericyte as a possible osteoblast progenitor-cell. *Clinical Orthopaedics and Related Research***,** 287-299.

BUBLITZ, C., GROLLMAN, A. P. & LEHNINGER, A. L. 1958. The enzymic conversion of d-glucuronate to l-ascorbate and l-xylulose in animal tissues. *Biochimica Et Biophysica Acta,* 27**,** 221-222.

BUJALSKA, I. J., GATHERCOLE, L. L., TOMLINSON, J. W., DARIMONT, C., ERMOLIEFF, J., FANJUL, A. N., REJTO, P. A. & STEWART, P. M. 2008. A novel selective 11 beta-hydroxysteroid dehydrogenase type 1 inhibitor prevents human adipogenesis. *Journal of Endocrinology,* 197**,** 297-307.

BURRIDGE, K. & WENNERBERG, K. 2004. Rho and Rac take center stage. *Cell,* 116**,** 167-179.

CALDERWOOD, D. A., HUTTENLOCHER, A., KIOSSES, W. B., ROSE, D. M., WOODSIDE, D. G., SCHWARTZ, M. A. & GINSBERG, M. H. 2001. Increased filamin binding to beta-integrin cytoplasmic domains inhibits cell migration. *Nature Cell Biology,* 3**,** 1060-1068.

CALVI, L. M., ADAMS, G. B., WEIBRECHT, K. W., WEBER, J. M., OLSON, D. P., KNIGHT, M. C., MARTIN, R. P., SCHIPANI, E., DIVIETI, P., BRINGHURST, F. R., MILNER, L. A., KRONENBERG, H. M. & SCADDEN, D. T. 2003. Osteoblastic cells regulate the haematopoietic stem cell niche. *Nature,* 425**,** 841-846.

CAPLAN, A. I. 1991. Mesenchymal stem cells. *Journal of Orthopaedic Research,* 9**,** 641-650.

CAPLAN, A. I. 2008. All MSCs Are Pericytes? *Cell Stem Cell,* 3**,** 2.

CAREY, D. J. 1997. Syndecans: Multifunctional cell-surface co-receptors. *Biochemical Journal,* 327**,** 1-16.

CARY, L. A., KLINGHOFFER, R. A., SACHSENMAIER, C. & COOPER, J. A. 2002. Src catalytic but not scaffolding function is needed for integrin-regulated tyrosine phosphorylation, cell migration, and cell spreading. *Molecular and Cellular Biology,* 22**,** 2427-2440.

CAVALCANTI-ADAM, E. A., AYDIN, D., HIRSCHFELD-WARNEKEN, V. C. & SPATZ, J. P. 2008. Cell adhesion and response to synthetic nanopatterned environments by steering receptor clustering and spatial location. *Hfsp Journal,* 2**,** 276-285.

CAVALCANTI-ADAM, E. A., VOLBERG, T., MICOULET, A., KESSLER, H., GEIGER, B. & SPATZ, J. P. 2007. Cell spreading and focal adhesion dynamics are regulated by spacing of integrin ligands. *Biophysical Journal,* 92**,** 2964-2974.

CHARDIN, P., BOQUET, P., MADAULE, P., POPOFF, M. R., RUBIN, E. J. & GILL, D. M. 1989. The mammalian G-protein RhoC is ADP-ribosylated by clostridium-botulinum exoenzyme C3 and affects actin microfilaments in vero cells. *Embo Journal,* 8**,** 1087-1092.

CHEN, C.-W., CORSELLI, M., PEAULT, B., HUARD J. 2012. Human Blood-Vessel-Derived Stem Cells for Tissue Repair and Regeneration. *Journal of Biomedicine and Biotechnology,* 2012.

CHEN, C. S., MRKSICH, M., HUANG, S., WHITESIDES, G. M. & INGBER, D. E. 1998. Micropatterned surfaces for control of cell shape, position, and function. *Biotechnology Progress,* 14**,** 356-363.

CHEN, J., IRIANTO, J., INAMDAR, S., PRAVINCUMAR, P., LEE, D. A., BADER, D. L. & KNIGHT, M. M. 2012. Cell Mechanics, Structure, and Function Are Regulated by the Stiffness of the Three-Dimensional Microenvironment. *Biophysical Journal,* 103**,** 1188-1197.

CHEN, P. & PARKS, W. C. 2009. Role of Matrix Metalloproteinases in Epithelial Migration. *Journal of Cellular Biochemistry,* 108**,** 1233-1243.

CHEN, W. T., HASEGAWA, E., HASEGAWA, T., WEINSTOCK, C. & YAMADA, K. M. 1985. Development of cell-surface linkage complexes in cultured fibroblasts. *Journal of Cell Biology,* 100**,** 1103-1114.

CHILDS, A. C., MEHTA, D. J. & GERNER, E. W. 2003. Polyamine-dependent gene expression. *Cellular and Molecular Life Sciences,* 60**,** 1394-1406.

CHOI, C. K., VICENTE-MANZANARES, M., ZARENO, J., WHITMORE, L. A., MOGILNER, A. & HORWITZ, A. R. 2008. Actin and alpha-actinin orchestrate the assembly and maturation of nascent adhesions in a myosin II motor-independent manner. *Nature Cell Biology,* 10**,** 1039-U36.

CHOI, Y. S., VINCENT, L. G., LEE, A. R., DOBKE, M. K. & ENGLER, A. J. 2012a. Mechanical derivation of functional myotubes from adipose-derived stem cells. *Biomaterials,* 33.

CHOI, Y. S., VINCENT, L. G., LEE, A. R., KRETCHMER, K. C., CHIRASATITSIN, S., DOBKE, M. K. & ENGLER, A. J. 2012b. The alignment and fusion assembly of adipose-derived stem cells on mechanically patterned matrices. *Biomaterials,* 33.

CHOQUET, D., FELSENFELD, D. P. & SHEETZ, M. P. 1997. Extracellular matrix rigidity causes strengthening of integrin-cytoskeleton linkages. *Cell,* 88.

CHOW, A., LUCAS, D., HIDALGO, A., MÉNDEZ-FERRER, S., HASHIMOTO,D., SCHEIERMANN, C., BATTISTA, M., LEBOEUF, M.,PROPHETE, C., VAN ROOIJEN, N., TANAKA, M., MERAD, M., FRENETTE, P. 2011. Bone marrow CD169+ macrophages promote the retention of hematopoietic stem and progenitor cells in the mesenchymal stem cell niche. *The Journal of Experimental Medicine,* 208**,** 11.

COLIGE, A., SIERON, A. L., LI, S. W., SCHWARZE, U., PETTY, E., WERTELECKI, W., WILCOX, W., KRAKOW, D., COHN, D. H., REARDON, W., BYERS, P. H., LAPIERE, C. M., PROCKOP, D. J. & NUSGENS, B. V. 1999. Human Ehlers-Danlos syndrome type VIIC and bovine dermatosparaxis are caused by mutations in the procollagen IN-proteinase gene. *American Journal of Human Genetics,* 65**,** 308-317.

COOKE, M. E., ALLON, A. A., CHENG, T., KUO, A. C., KIM, H. T., VAIL, T. P., MARCUCIO, R. S., SCHNEIDER, R. A., LOTZ, J. C. & ALLISTON, T. 2011. Structured three-dimensional co-culture of mesenchymal stem cells with chondrocytes promotes chondrogenic differentiation without hypertrophy. *Osteoarthritis and Cartilage,* 19**,** 1210-1218.

COOPER, L. A., SHEN, T. L. & GUAN, J. L. 2003. Regulation of focal adhesion kinase by its amino-terminal domain through an autoinhibitory interaction. *Molecular and Cellular Biology,* 23**,** 8030-8041.

COOPER, M. S., HEWISON, M. & STEWART, P. M. 1999. Glucocorticoid activity, inactivity and the osteoblast. *Journal of Endocrinology,* 163**,** 159-164.

CORSELLI, M., CHEN, C.-W., CRISAN, M., LAZZARI, L. & PEAULT, B. 2010. Perivascular Ancestors of Adult Multipotent Stem Cells. *Arteriosclerosis Thrombosis and Vascular Biology,* 30**,** 1104-1109.

COTSARELIS, G., SUN, T. T. & LAVKER, R. M. 1990. Label-retaining cells reside in the bulge area of pilosebaceous unit - implications for follicular stem-cells, hair cycle, and skin carcinogenesis. *Cell,* 61**,** 1329-1337.

CREEK, D. J., JANKEVICS, A., BREITLING, R., WATSON, D. G., BARRETT, M. P. & BURGESS, K. E. V. 2011. Toward Global Metabolomics Analysis with Hydrophilic Interaction Liquid Chromatography-Mass Spectrometry: Improved Metabolite Identification by Retention Time Prediction. *Analytical Chemistry,* 83**,** 8703-8710.

CREEK, D. J., JANKEVICS, A., BURGESS, K. E. V., BREITLING, R. & BARRETT, M. P. 2012. IDEOM: an Excel interface for analysis of LC-MS-based metabolomics data. *Bioinformatics,* 28**,** 1048-1049.

CRISAN, M., CHEN, C.-W., CORSELLI, M., ANDRIOLO, G., LAZZARI, L. & PEAULT, B. 2009. Perivascular Multipotent Progenitor Cells in Human Organs. *Hematopoietic Stem Cells Vii,* 1176**,** 118-123.

CRISAN, M., CORSELLI, M., CHEN, C.-W. & PEAULT, B. 2011. Multilineage stem cells in the adult A perivascular legacy? *Organogenesis,* 7**,** 101-104.

CRISAN, M., YAP, S., CASTEILLA, L., CHEN, C. W., CORSELLI, M., PARK, T. S., ANDRIOLO, G., SUN, B., ZHENG, B., ZHANG, L., NOROTTE, C., TENG, P. N., TRAAS, J., SCHUGAR, R., DEASY, B. M., BADYLAK, S., BUHRING, H. J., GIACOBINO, J. P., LAZZARI, L., HUARD, J. & PEAULT, B. 2008. A perivascular origin for mesenchymal stem cells in multiple human organs. *Cell Stem Cell,* 3**,** 301-313.

CRISP, M., LIU, Q., ROUX, K., RATTNER, J. B., SHANAHAN, C., BURKE, B., STAHL, P. D. & HODZIC, D. 2006. Coupling of the nucleus and cytoplasm: role of the LINC complex. *Journal of Cell Biology,* 172**,** 41-53.

CUI, X., HASEGAWA, A., LOTZ, M. & D'LIMA, D. 2012. Structured three-dimensional co-culture of mesenchymal stem cells with meniscus cells promotes meniscal phenotype without hypertrophy. *Biotechnology and Bioengineering,* 109**,** 2369-2380.

CURRAN, J. M., CHEN, R. & HUNT, J. A. 2005. Controlling the phenotype and function of mesenchymal stem cells in vitro by adhesion to silane-modified clean glass surfaces. *Biomaterials,* 26**,** 7057-7067.

CURRAN, J. M., STOKES, R., IRVINE, E., GRAHAM, D., AMRO, N. A., SANEDRIN, R. G., JAMIL, H. & HUNT, J. A. 2010. Introducing dip pen nanolithography as a tool for controlling stem cell behaviour: unlocking the potential of the next generation of smart materials in regenerative medicine. *Lab on a Chip,* 10**,** 1662-1670.

CURTIS, A. & WILKINSON, C. 1997. Topographical control of cells. *Biomaterials,* 18**,** 1573-1583.

CURTIS, A. S. G. & SEEHAR, G. M. 1978. Control of cell-division by tension or diffusion. *Nature,* 274**,** 52-53.

DA SILVA MEIRELLES, L., CHAGASTELLES, P. C. & NARDI, N. B. 2006. Mesenchymal stem cells reside in virtually all post-natal organs and tissues. *J Cell Sci,* 119**,** 2204-13.

DALBY, M. J., BIGGS, M. J. P., GADEGAARD, N., KALNA, G., WILKINSON, C. D. W. & CURTIS, A. S. G. 2007a. Nanotopographical stimulation of mechanotransduction and changes in interphase centromere positioning. *Journal of Cellular Biochemistry,* 100**,** 326-338.

DALBY, M. J., GADEGAARD, N., HERZYK, P., SUTHERLAND, D., AGHELI, H., WILKINSON, C. D. W. & CURTIS, A. S. G. 2007b. Nanomechanotransduction and interphase nuclear organization influence on genomic control. *Journal of Cellular Biochemistry,* 102**,** 1234-1244.

DALBY, M. J., GADEGAARD, N., TARE, R., ANDAR, A., RIEHLE, M. O., HERZYK, P., WILKINSON, C. D. W. & OREFFO, R. O. C. 2007c. The control of human mesenchymal cell differentiation using nanoscale symmetry and disorder. *Nature Materials,* 6**,** 997-1003.

DALBY, M. J., RIEHLE, M. O., YARWOOD, S. J., WILKINSON, C. D. W. & CURTIS, A. S. G. 2003. Nucleus alignment and cell signaling in fibroblasts: response to a micro-grooved topography. *Experimental Cell Research,* 284**,** 274-282.

DALEY, W. P., PETERS, S. B. & LARSEN, M. 2008. Extracellular matrix dynamics in development and regenerative medicine. *J Cell Sci,* 121**,** 255-64.

DAMSKY, C. H., KNUDSEN, K. A., BRADLEY, D., BUCK, C. A. & HORWITZ, A. F. 1985. Distribution of the cell substratum attachment (csat) antigen on myogenic and fibroblastic cells in culture. *Journal of Cell Biology,* 100**,** 1528-1539.

DARLING, E. M., ZAUSCHER, S. & GUILAK, F. 2006. Viscoelastic properties of zonal articular chondrocytes measured by atomic force microscopy. *Osteoarthritis and Cartilage,* 14**,** 571-579.

DAWSON, E., MAPILI, G., ERICKSON, K., TAQVI, S. & ROY, K. 2008. Biomaterials for stem cell differentiation. *Advanced Drug Delivery Reviews,* 60**,** 215-228.

DEL RIO, A., PEREZ-JIMENEZ, R., LIU, R., ROCA-CUSACHS, P., FERNANDEZ, J. M. & SHEETZ, M. P. 2009. Stretching Single Talin Rod Molecules Activates Vinculin Binding. *Science,* 323**,** 638-641.

DEMOOR, M., MANEIX, L., OLLITRAULT, D., LEGENDRE, F., DUVAL, E., CLAUS, S., MALLEIN-GERIN, F., MOSLEMI, S., BOUMEDIENE, K. & GALERA, P. 2012. Deciphering chondrocyte behaviour in matrix-induced autologous chondrocyte implantation to undergo accurate cartilage repair with hyaline matrix. *Pathologie Biologie,* 60**,** 199-207.

DEPEINT, F., BRUCE, W. R., SHANGARI, N., MEHTA, R. & O'BRIEN, P. J. 2006a. Mitochondrial function and toxicity: Role of B vitamins on the one-carbon transfer pathways. *Chemico-Biological Interactions,* 163**,** 113-132.

DEPEINT, F., BRUCE, W. R., SHANGARI, N., MEHTA, R. & O'BRIEN, P. J. 2006b. Mitochondrial function and toxicity: Role of the B vitamin family on mitochondrial energy metabolism. *Chemico-Biological Interactions,* 163**,** 94-112.

DIAZ-FLORES, L., GUTIERREZ, R., MADRID, J. F., VARELA, H., VALLADARES, F., ACOSTA, E., MARTIN-VASALLO, P. & DIAZ-FLORES, L., JR. 2009. Pericytes. Morphofunction, interactions and pathology in a quiescent and activated mesenchymal cell niche. *Histology and Histopathology,* 24**,** 909-969.

DIEFENDERFER, D. L. & BRIGHTON, C. T. 2000. Microvascular pericytes express aggrecan message which is regulated by BMP-2. *Biochemical and Biophysical Research Communications,* 269**,** 172-178.

DIETMAIR, S., TIMMINS, N. E., GRAY, P. P., NIELSEN, L. K. & KROEMER, J. O. 2010. Towards quantitative metabolomics of mammalian cells: Development of a metabolite extraction protocol. *Analytical Biochemistry,* 404**,** 155-164.

DING, S. & SCHULTZ, P. G. 2004. A role for chemistry in stem cell biology. *Nature Biotechnology,* 22**,** 833-840.

DISCHER, D. E., JANMEY, P. & WANG, Y. L. 2005. Tissue cells feel and respond to the stiffness of their substrate. *Science,* 310.

DISCHER, D. E., MOONEY, D. J. & ZANDSTRA, P. W. 2009. Growth Factors, Matrices, and Forces Combine and Control Stem Cells. *Science,* 324**,** 1673-1677.

DOMINICI, M., LE BLANC, K., MUELLER, I., SLAPER-CORTENBACH, I., MARINI, F. C., KRAUSE, D. S., DEANS, R. J., KEATING, A., PROCKOP, D. J. & HORWITZ, E. M. 2006. Minimal criteria for defining multipotent mesenchymal stromal cells. The International Society for Cellular Therapy position statement. *Cytotherapy,* 8**,** 315-317.

DRESSEL, U., ALLEN, T. L., PIPPAL, J. B., ROHDE, P. R., LAU, P. & MUSCAT, G. E. O. 2003. The peroxisome proliferator-activated receptor beta/delta agonist, GW501516, regulates the expression of genes involved in lipid catabolism and energy uncoupling in skeletal muscle cells. *Molecular Endocrinology,* 17**,** 2477-2493.

DUNKIN, B. S. & LATTERMANN, C. 2013. New and Emerging Techniques in Cartilage Repair: Matrix-Induced Autologous Chondrocyte Implantation. *Operative Techniques in Sports Medicine,* 21**,** 100-107.

DUNN, W. B., BAILEY, N. J. C. & JOHNSON, H. E. 2005. Measuring the metabolome: current analytical technologies. *Analyst,* 130**,** 606-625.

EHNINGER, A. & TRUMPP, A. 2011. The bone marrow stem cell niche grows up: mesenchymal stem cells and macrophages move in. *Journal of Experimental Medicine,* 208**,** 421-428.

ELEFTHERIADES, E. G., FERGUSON, A. G., SPRAGIA, M. L. & SAMAREL, A. M. 1995. Prolyl hydroxylation regulates intracellular procollagen degradation in cultured rat cardiac fibroblasts. *Journal of Molecular and Cellular Cardiology,* 27**,** 1459-1473.

ELKIN, B. S., AZELOGLU, E. U., COSTA, K. D. & MORRISON, B., III 2007. Mechanical heterogeneity of the rat hippocampus measured by atomic force microscope indentation. *Journal of Neurotrauma,* 24.

ENGLER, A., BACAKOVA, L., NEWMAN, C., HATEGAN, A., GRIFFIN, M. & DISCHER, D. 2004a. Substrate compliance versus ligand density in cell on gel responses. *Biophysical Journal,* 86.

ENGLER, A. J., CARAG-KRIEGER, C., JOHNSON, C. P., RAAB, M., TANG, H.-Y., SPEICHER, D. W., SANGER, J. W., SANGER, J. M. & DISCHER, D. E. 2008. Embryonic cardiomyocytes beat best on a matrix with heart-like elasticity: scar-like rigidity inhibits beating. *Journal of Cell Science,* 121.

ENGLER, A. J., GRIFFIN, M. A., SEN, S., BONNETNANN, C. G., SWEENEY, H. L. & DISCHER, D. E. 2004b. Myotubes differentiate optimally on substrates with tissue-like stiffness: pathological implications for soft or stiff microenvironments. *Journal of Cell Biology,* 166**,** 877-887.

ENGLER, A. J., SEN, S., SWEENEY, H. L. & DISCHER, D. E. 2006. Matrix elasticity directs stem cell lineage specification. *Cell,* 126**,** 677-689.

ENGVALL, E., RUOSLAHTI, E. & MILLER, E. J. 1978. Affinity of fibronectin to collagens of different genetic types and to fibrinogen. *Journal of Experimental Medicine,* 147**,** 1584-1595.

ESTES, B. T. & GUILAK, F. 2011. Three-Dimensional Culture Systems to Induce Chondrogenesis of Adipose-Derived Stem Cells. *Adipose-Derived Stem Cells: Methods and Protocols,* 702**,** 201-217.

EVANS, E. A., WAUGH, R. & MELNIK, L. 1976. Elastic area compressibility modulus of red-cell membrane. *Biophysical Journal,* 16**,** 585-595.

EVANS, N. D., MINELLI, C., GENTLEMAN, E., LAPOINTE, V., PATANKAR, S. N., KALLIVRETAKI, M., CHEN, X., ROBERTS, C. J. & STEVENS, M. M. 2009. Substrate stiffness affects early differentiation events in embryonic stem cells. *European Cells & Materials,* 18.

FACCHINI, A., BORZI, R. M. & FLAMIGNI, F. 2005. Induction of ornithine decarboxylase in T/C-28a2 chondrocytes by lysophosphatidic acid: Signaling pathway and inhibition of cell proliferation. *Febs Letters,* 579**,** 2919-2925.

FACCHINI, A., BORZI, R. M., OLIVOTTO, E., PLATANO, D., PAGANI, S., CETRULLO, S. & FLAMIGNI, F. 2012. Role of polyamines in hypertrophy and terminal differentiation of osteoarthritic chondrocytes. *Amino Acids,* 42**,** 667-678.

FIEHN, O. 2001. Combining genomics, metabolome analysis, and biochemical modelling to understand metabolic networks. *Comparative and Functional Genomics,* 2**,** 155-168.

FIEHN, O. 2002. Metabolomics - the link between genotypes and phenotypes. *Plant Molecular Biology,* 48**,** 155-171.

FIRTH, A., AGGELI, A., BURKE, J. L., YANG, X. & KIRKHAM, J. 2006. Biomimetic self-assembling peptides as injectable scaffolds for hard tissue engineering. *Nanomedicine,* 1**,** 189-199.

FISHER, M. B. & MAUCK, R. L. 2013. Tissue Engineering and Regenerative Medicine: Recent Innovations and the Transition to Translation. *Tissue Engineering Part B-Reviews,* 19**,** 1-13.

FLANAGAN, L. A., JU, Y. E., MARG, B., OSTERFIELD, M. & JANMEY, P. A. 2002. Neurite branching on deformable substrates. *Neuroreport,* 13.

FRANTZ, C., STEWART, K. M. & WEAVER, V. M. 2010. The extracellular matrix at a glance. *Journal of Cell Science,* 123**,** 4195-4200.

FRIEDENSTEIN, A. J., CHAILAKHJAN, R. K. & LALYKINA, K. S. 1970. The development of fibroblast colonies in monolayer cultures of guinea-pig bone marrow and spleen cells. *Cell Tissue Kinet,* 3**,** 393-403.

FRIEDENSTEIN, A. J., CHAILAKHYAN, R. K. & GERASIMOV, U. V. 1987. Bone marrow osteogenic stem cells: in vitro cultivation and transplantation in diffusion chambers. *Cell Tissue Kinet,* 20**,** 263-72.

FRIEDLAND, J. C., LEE, M. H. & BOETTIGER, D. 2009. Mechanically Activated Integrin Switch Controls alpha(5)beta(1) Function. *Science,* 323**,** 642-644.

FU, J., WANG, Y.-K., YANG, M. T., DESAI, R. A., YU, X., LIU, Z. & CHEN, C. S. 2010. Mechanical regulation of cell function with geometrically modulated elastomeric substrates. *Nature Methods,* 7**,** 733-U95.

GALBRAITH, C. G., YAMADA, K. M. & SHEETZ, M. P. 2002. The relationship between force and focal complex development. *Journal of Cell Biology,* 159**,** 695-705.

GALLAY, S. H., MIURA, Y., COMMISSO, C. N., FITZSIMMONS, J. S. & ODRISCOLL, S. W. 1994. Relationship of donor site to chondrogenic potential of periosteum in-vitro. *Journal of Orthopaedic Research,* 12.

GAO, L., MCBEATH, R. & CHEN, C. S. 2010. Stem Cell Shape Regulates a Chondrogenic Versus Myogenic Fate Through Rac1 and N-Cadherin. *Stem Cells,* 28.

GEIGER, B. & BERSHADSKY, A. 2002. Exploring the neighborhood: Adhesion-coupled cell mechanosensors. *Cell,* 110**,** 139-142.

GEIGER, B., SPATZ, J. P. & BERSHADSKY, A. D. 2009. Environmental sensing through focal adhesions. *Nature Reviews Molecular Cell Biology,* 10**,** 21-33.

GERECHT, S., BURDICK, J. A., FERREIRA, L. S., TOWNSEND, S. A., LANGER, R. & VUNJAK-NOVAKOVIC, G. 2007. Hyaluronic acid hydrogen for controlled self-renewal and differentiation of human embryonic stem cells. *Proceedings of the National Academy of Sciences of the United States of America,* 104**,** 11298-11303.

GIANNONE, G., JIANG, G., SUTTON, D. H., CRITCHLEY, D. R. & SHEETZ, M. P. 2003. Talin1 is critical for force-dependent reinforcement of initial integrin-cytoskeleton bonds but not tyrosine kinase activation. *Journal of Cell Biology,* 163**,** 409-419.

GIBSON, G., LIN, D. L. & ROQUE, M. 1997. Apoptosis of terminally differentiated chondrocytes in culture. *Experimental Cell Research,* 233**,** 372-382.

GILBERT, P. M., HAVENSTRITE, K. L., MAGNUSSON, K. E. G., SACCO, A., LEONARDI, N. A., KRAFT, P., NGUYEN, N. K., THRUN, S., LUTOLF, M. P. & BLAU, H. M. 2010. Substrate Elasticity Regulates Skeletal Muscle Stem Cell Self-Renewal in Culture. *Science,* 329**,** 1078-1081.

GILL, S. E. & PARKS, W. C. 2008. Metalloproteinases and their inhibitors: Regulators of wound healing. *International Journal of Biochemistry & Cell Biology,* 40**,** 1334-1347.

GIRY, M., POPOFF, M. R., VONEICHELSTREIBER, C. & BOQUET, P. 1995. Transient expression of RhoA, RhoB, and RhoC GTPases in hela-cells potentiates resistance to clostridium-difficile toxin-A and toxin-B but not to clostridium-sordellii lethal toxin. *Infection and Immunity,* 63**,** 4063-4071.

GLOWACKI, J., TREPMAN, E. & FOLKMAN, J. 1983. Cell-shape and phenotypic-expression in chondrocytes. *Proceedings of the Society for Experimental Biology and Medicine,* 172**,** 93-98.

GORDON, M. K. & HAHN, R. A. 2010. Collagens. *Cell and Tissue Research,* 339**,** 247-257.

GOSLINE, J., LILLIE, M., CARRINGTON, E., GUERETTE, P., ORTLEPP, C. & SAVAGE, K. 2002. Elastic proteins: biological roles and mechanical properties. *Philosophical Transactions of the Royal Society of London Series B-Biological Sciences,* 357**,** 121-132.

GRAUMANN, J., HUBNER, N. C., KIM, J. B., KO, K., MOSER, M., KUMAR, C., COX, J., SCHOELER, H. & MANN, M. 2008. Stable Isotope Labeling by Amino Acids in Cell Culture (SILAC) and proteome quantitation of mouse embryonic stem cells to a depth of 5,111 proteins. *Molecular & Cellular Proteomics,* 7**,** 672-683.

GREENWOOD, J. A., THEIBERT, A. B., PRESTWICH, G. D. & MURPHY-ULLRICH, J. E. 2000. Restructuring of focal adhesion plaques by PI 3-kinase: Regulation by PtdIns (3,4,5)-P-3 binding to alpha-actinin. *Journal of Cell Biology,* 150**,** 627-641.

GRITTI, F., PEREIRA, A. D. S., SANDRA, P. & GUIOCHON, G. 2010. Efficiency of the same neat silica column in hydrophilic interaction chromatography and per aqueous liquid chromatography. *Journal of Chromatography A,* 1217**,** 683-688.

GROLLMAN, A. P. & LEHNIGER, A. L. 1957. Enzymic synthesis of L-ascorbic acid in different animal species. *Arch Biochem and Biophys,* 69**,** 458-467.

GUILAK, F., ALEXOPOULOS, L. G., UPTON, M. L., YOUN, I., CHOI, J. B., CAO, L., SETTON, L. A. & HAIDER, M. A. 2006. The pericellular matrix as a transducer of biomechanical and biochemical signals in articular cartilage. *Skeletal Development and Remodeling in Health, Disease, and Aging,* 1068**,** 498-512.

GUILAK, F., COHEN, D. M., ESTES, B. T., GIMBLE, J. M., LIEDTKE, W. & CHEN, C. S. 2009. Control of Stem Cell Fate by Physical Interactions with the Extracellular Matrix. *Cell Stem Cell,* 5**,** 17-26.

GULLBERG, D. & EKBLOM, P. 1995. Extracellular matrix and its receptors during development. *International Journal of Developmental Biology,* 39**,** 845-854.

GUO, J. F., JOURDIAN, G. W. & MACCALLUM, D. K. 1989. Culture and growth-characteristics of chondrocytes encapsulated in alginate beads. *Connective Tissue Research,* 19**,** 277-297.

GUPTA, S., MARCEL, N., SARIN, A. & SHIVASHANKAR, G. V. 2012. Role of Actin Dependent Nuclear Deformation in Regulating Early Gene Expression. *Plos One,* 7.

GUVENDIREN, M. & BURDICK, J. A. 2012. Stiffening hydrogels to probe short- and long-term cellular responses to dynamic mechanics. *Nature Communications,* 3.

GYGI, S. P., ROCHON, Y., FRANZA, B. R. & AEBERSOLD, R. 1999. Correlation between protein and mRNA abundance in yeast. *Molecular and Cellular Biology,* 19**,** 1720-1730.

HALL, A. 1998. Rho GTPases and the actin cytoskeleton. *Science,* 279**,** 509-514.

HAN, Y. & LEFEBVRE, V. 2008. L-Sox5 and Sox6 drive expression of the aggrecan gene in cartilage by securing binding of Sox9 to a far-upstream enhancer. *Molecular and Cellular Biology,* 28**,** 4999-5013.

HARMA, V., KNUUTTILA, M., VIRTANEN, J., MIRTTI, T., KOHONEN, P., KOVANEN, P., HAPPONEN, A., KAEWPHAN, S., AHONEN, I., KALLIONIEMI, O., GRAFSTROM, R., LOTJONEN, J. & NEES, M. 2012. Lysophosphatidic acid and sphingosine-1-phosphate promote morphogenesis and block invasion of prostate cancer cells in three-dimensional organotypic models. *Oncogene,* 31**,** 2075-2089.

HARRIS, A. K., WILD, P. & STOPAK, D. 1980. Silicone-rubber substrata - new wrinkle in the study of cell locomotion. *Science,* 208.

HATTORI, T., MUELLER, C., GEBHARD, S., BAUER, E., PAUSCH, F., SCHLUND, B., BOESL, M. R., HESS, A., SURMANN-SCHMITT, C., VON DER MARK, H., DE CROMBRUGGHE, B. & VON DER MARK, K. 2010. SOX9 is a major negative regulator of cartilage vascularization, bone marrow formation and endochondral ossification. *Development,* 137**,** 901-911.

HENRY, S. P., LIANG, S., AKDEMIR, K. C. & DE CROMBRUGGHE, B. 2012. The Postnatal Role of Sox9 in Cartilage. *Journal of Bone and Mineral Research,* 27**,** 2511-2525.

HIGASHIKAWA, A., SAITO, T., IKEDA, T., KAMEKURA, S., KAWAMURA, N., KAN, A., OSHIMA, Y., OHBA, S., OGATA, N., TAKESHITA, K., NAKAMURA, K., CHUNG, U.-I. & KAWAGUCHI, H. 2009. Identification of the Core Element Responsive to Runt-Related Transcription Factor 2 in the Promoter of Human Type X Collagen Gene. *Arthritis and Rheumatism,* 60**,** 166-178.

HIGUCHI, A., LING, Q.-D., CHANG, Y., HSU, S.-T. & UMEZAWA, A. 2013. Physical Cues of Biomaterials Guide Stem Cell Differentiation Fate. *Chemical Reviews,* 113**,** 3297-3328.

HIGUERA, G. A., VAN BOXTEL, A., VAN BLITTERSWIJK, C. A. & MORONI, L. 2012. The physics of tissue formation with mesenchymal stem cells. *Trends in Biotechnology,* 30**,** 583-590.

HOERNING, M., KIDOAKI, S., KAWANO, T. & YOSHIKAWA, K. 2012. Rigidity Matching between Cells and the Extracellular Matrix Leads to the Stabilization of Cardiac Conduction. *Biophysical Journal,* 102**,** 379-387.

HOGEWEG, P. 2011. The Roots of Bioinformatics in Theoretical Biology. *Plos Computational Biology,* 7.

HOJER-PEDERSEN, J., SMEDSGAARD, J. & NIELSEN, J. 2008. The yeast metabolome addressed by electrospray ionization mass spectrometry: Initiation of a mass spectral library and its applications for metabolic footprinting by direct infusion mass spectrometry. *Metabolomics,* 4**,** 393-405.

HOLLYWOOD, K., BRISON, D. R. & GOODACRE, R. 2006. Metabolomics: Current technologies and future trends. *Proteomics,* 6**,** 4716-4723.

HU, S. H., CHEN, J. X., BUTLER, J. P. & WANG, N. 2005. Prestress mediates force propagation into the nucleus. *Biochemical and Biophysical Research Communications,* 329**,** 423-428.

HUANG, J., GRATER, S. V., CORBELLINL, F., RINCK, S., BOCK, E., KEMKEMER, R., KESSLER, H., DING, J. & SPATZ, J. P. 2009. Impact of Order and Disorder in RGD Nanopatterns on Cell Adhesion. *Nano Letters,* 9**,** 1111-1116.

HUEBSCH, N., ARANY, P. R., MAO, A. S., SHVARTSMAN, D., ALI, O. A., BENCHERIF, S. A., RIVERA-FELICIANO, J. & MOONEY, D. J. 2010. Harnessing traction-mediated manipulation of the cell/matrix interface to control stem-cell fate. *Nature Materials,* 9**,** 518-526.

HUNZIKER, E. B., MICHEL, M. & STUDER, D. 1997. Ultrastructure of adult human articular cartilage matrix after cryotechnical processing. *Microscopy Research and Technique,* 37**,** 271-284.

HUNZIKER, E. B., QUINN, T. M. & HAUSELMANN, H. J. 2002. Quantitative structural organization of normal adult human articular cartilage. *Osteoarthritis and Cartilage,* 10**,** 564-572.

HURST-KENNEDY, J., BOYAN, B. D. & SCHWARTZ, Z. 2009. Lysophosphatidic acid signaling promotes proliferation, differentiation, and cell survival in rat growth plate chondrocytes. *Biochimica Et Biophysica Acta-Molecular Cell Research,* 1793**,** 836-846.

HWANG, W. S., LI, B., JIN, L. H., NGO, K., SCHACHAR, N. S. & HUGHES, G. N. F. 1992. Collagen fibril structure of normal, aging, and osteoarthritic cartilage. *Journal of Pathology,* 167**,** 425-433.

HYNES, R. O. 2002. Integrins: Bidirectional, allosteric signaling machines. *Cell,* 110**,** 673-687.

HYNES, R. O. & NABA, A. 2012. Overview of the Matrisome-An Inventory of Extracellular Matrix Constituents and Functions. *Cold Spring Harbor Perspectives in Biology,* 4.

IGARASHI, K. & KASHIWAGI, K. 2010. Modulation of cellular function by polyamines. *The international journal of biochemistry & cell biology,* 42**,** 39-51.

ILIC, D., FURUTA, T., KANAZAWA, S., TAKEDA, N., SOBUE, K., NAKATSUJI, N., NOMURA, S., FUJIMOTO, J., OKADA, M., YAMAMOTO, T. & AIZAWA, S. 1995. Reduced cell motility and enhanced focal adhesion contact formation in cells from FAK-deficient mice. *Nature (London),* 377**,** 539-544.

IM, G.-I. 2005. Chondrogenesis from mesenchymal stem cells derived from adipose tissue on the fibrin scaffold. *Current Applied Physics,* 5**,** 438-443.

INGBER, D. 1991. Extracellular-matrix and cell shape - potential control points for inhibition of angiogenesis. *Journal of Cellular Biochemistry,* 47**,** 236-241.

INGBER, D. E. 2006. Cellular mechanotransduction: putting all the pieces together again. *Faseb Journal,* 20**,** 811-827.

ISHII, I., IKEGUCHI, Y., MANO, H., WADA, M., PEGG, A. E. & SHIRAHATA, A. 2012. Polyamine metabolism is involved in adipogenesis of 3T3-L1 cells. *Amino Acids,* 42**,** 619-626.

IVASKA, J., PALLARI, H.-M., NEVO, J. & ERIKSSON, J. E. 2007. Novel functions of vimentin in cell adhesion, migration, and signaling. *Experimental Cell Research,* 313**,** 2050-2062.

IYER, K. V., PULFORD, S., MOGILNER, A. & SHIVASHANKAR, G. V. 2012. Mechanical Activation of Cells Induces Chromatin Remodeling Preceding MKL Nuclear Transport. *Biophysical Journal,* 103**,** 1416-1428.

IZARD, T., EVANS, G., BORGON, R. A., RUSH, C. L., BRICOGNE, G. & BOIS, P. R. J. 2004. Vinculin activation by talin through helical bundle conversion. *Nature,* 427**,** 171-175.

IZU, Y., SUN, M., ZWOLANEK, D., VEIT, G., WILLIAMS, V., CHA, B., JEPSEN, K. J., KOCH, M. & BIRK, D. E. 2011. Type XII collagen regulates osteoblast polarity and communication during bone formation. *Journal of Cell Biology,* 193**,** 1115-1130.

JANDEROVA, L., MCNEIL, M., MURRELL, A. N., MYNATT, R. L. & SMITH, S. R. 2003. Human mesenchymal stem cells as an in vitro model for human adipogenesis. *Obesity Research,* 11**,** 65-74.

JANMEY, P. A. & LINDBERG, U. 2004. Cytoskeletal regulation: Rich in lipids. *Nature Reviews Molecular Cell Biology,* 5**,** 658-666.

JAYAWARNA, V., ALI, M., JOWITT, T. A., MILLER, A. E., SAIANI, A., GOUGH, J. E. & ULIJN, R. V. 2006. Nanostructured hydrogels for three-dimensional cell culture through self-assembly of fluorenylmethoxycarbonyl-dipeptides. *Advanced Materials,* 18**,** 611-+.

JAYAWARNA, V., RICHARDSON, S. M., HIRST, A. R., HODSON, N. W., SAIANI, A., GOUGH, J. E. & ULIJN, R. V. 2009. Introducing chemical functionality in Fmoc-peptide gels for cell culture. *Acta Biomaterialia,* 5**,** 934-943.

JIANG, G. Y., HUANG, A. H., CAI, Y. F., TANASE, M. & SHEETZ, M. P. 2006. Rigidity sensing at the leading edge through alpha(v)beta(3) Integrins and RPTP alpha. *Biophysical Journal,* 90**,** 1804-1809.

JOHNSON, K., ZHU, S., TREMBLAY, M. S., PAYETTE, J. N., WANG, J., BOUCHEZ, L. C., MEEUSEN, S., ALTHAGE, A., CHO, C. Y., WU, X. & SCHULTZ, P. G. 2012. A Stem Cell-Based Approach to Cartilage Repair. *Science,* 336**,** 717-721.

JOHNSTONE, B., HERING, T. M., CAPLAN, A. I., GOLDBERG, V. M. & YOO, J. U. 1998. In vitro chondrogenesis of bone marrow-derived mesenchymal progenitor cells. *Experimental Cell Research,* 238**,** 265-272.

JUNG, Y., KIM, S. H. & KIM, Y. H. 2009. The effects of dynamic and three-dimensional environments on chondrogenic differentiation of bone marrow stromal cells. *Biomedical Materials,* 4.

JUSTESEN, J., MOSEKILDE, L., HOLMES, M., STENDERUP, K., GASSER, J., MULLINS, J. J., SECKL, J. R. & KASSEM, M. 2004. Mice deficient in 11 beta-hydroxysteroid dehydrogenase type 1 lack bone marrow adipocytes, but maintain normal bone formation. *Endocrinology,* 145**,** 1916-1925.

KAMOLZ, L. P., KOCH, H. & KASPER, C. 2013. Tissue engineering and its potential use in surgery. *European Surgery-Acta Chirurgica Austriaca,* 45**,** 120-121.

KANCHANAWONG, P., SHTENGEL, G., PASAPERA, A. M., RAMKO, E. B., DAVIDSON, M. W., HESS, H. F. & WATERMAN, C. M. 2010. Nanoscale architecture of integrin-based cell adhesions. *Nature,* 468**,** 580-U262.

KANEHISA, M. & GOTO, S. 2000. KEGG: Kyoto Encyclopedia of Genes and Genomes. *Nucleic Acids Research,* 28**,** 27-30.

KARLSSON, C., BRANTSING, C., SVENSSON, T., BRISBY, H., ASP, J., TALLHEDEN, T. & LINDAHL, A. 2007. Differentiation of human mesenchymal stem cells and articular chondrocytes: Analysis of chondrogenic potential and expression pattern of differentiation-related transcription factors. *Journal of Orthopaedic Research,* 25**,** 152-163.

KATAYAMA, Y., BATTISTA, M., KAO, W. M., HIDALGO, A., PEIRED, A. J., THOMAS, S. A. & FRENETTE, P. S. 2006. Signals from the sympathetic nervous system regulate hematopoietic stem cell egress from bone marrow. *Cell,* 124**,** 407-421.

KATOH, K., KANO, Y., AMANO, M., ONISHI, H., KAIBUCHI, K. & FUJIWARA, K. 2001. Rho-kinase-mediated contraction of isolated stress fibers. *Journal of Cell Biology,* 153**,** 569-583.

KATZ, B. Z., ROMER, L., MIYAMOTO, S., VOLBERG, T., MATSUMOTO, K., CUKIERMAN, E., GEIGER, B. & YAMADA, K. M. 2003. Targeting membrane-localized focal adhesion kinase to focal adhesions - Roles of tyrosine phosphorylation and Src family kinases. *Journal of Biological Chemistry,* 278**,** 29115-29120.

KATZ, B. Z., ZAMIR, E., BERSHADSKY, A., KAM, Z., YAMADA, K. M. & GEIGER, B. 2000. Physical state of the extracellular matrix regulates the structure and molecular composition of cell-matrix adhesions. *Molecular Biology of the Cell,* 11**,** 1047-1060.

KELLAM, B., DE BANK, P. A. & SHAKESHEFF, K. M. 2003. Chemical modification of mammalian cell surfaces. *Chemical Society Reviews,* 32**,** 327-337.

KELLEY, R. O. & FALLON, J. F. 1978. Identification and distribution of gap junctions in mesoderm of developing chick limb bud. *Journal of Embryology and Experimental Morphology,* 46**,** 99-110.

KHAN, S. & SHEETZ, M. P. 1997. Force effects on biochemical kinetics. *Annual Review of Biochemistry,* 66**,** 785-805.

KILIAN, K. A., BUGARIJA, B., LAHN, B. T. & MRKSICH, M. 2010. Geometric cues for directing the differentiation of mesenchymal stem cells. *Proceedings of the National Academy of Sciences of the United States of America,* 107**,** 4872-4877.

KILPINEN, L., TIGISTU-SAHLE, F., OJA, S., GRECO, D., PARMAR, A., SAAVALAINEN, P., NIKKILA, J., KORHONEN, M., LEHENKARI, P., KAKELA, R. & LAITINEN, S. 2013. Aging bone marrow mesenchymal stromal cells have altered membrane glycerophospholipid composition and functionality. *Journal of Lipid Research,* 54**,** 622-635.

KIM, M., CARMAN, C. V. & SPRINGER, T. A. 2003. Bidirectional transmembrane signaling by cytoplasmic domain separation in integrins. *Science,* 301**,** 1720-1725.

KIM, M. K., LEE, H. Y., PARK, K. S., SHIN, E. H., JO, S. H., YUN, J., LEE, S. W., YOO, Y. H., LEE, Y. S., BAEK, S. H. & BAE, Y. S. 2005. Lysophosphatidic acid stimulates cell proliferation in rat chondrocytes. *Biochemical Pharmacology,* 70**,** 1764-1771.

KIMOTO, S., CHENG, S. L., ZHANG, S. F. & AVIOLI, L. V. 1994. The effect of glucocorticoid on the synthesis of biglycan and decorin in human osteoblasts and bone-marrow stromal cells. *Endocrinology,* 135**,** 2423-2431.

KINGDON, K. H. 1923. A method for the neutralization of electron space charge by positive ionization at very low gas pressures. *Physical Review,* 21**,** 408-418.

KIRCHNER, J., KAM, Z., TZUR, G., BERSHADSKY, A. D. & GEIGER, B. 2003. Live-cell monitoring of tyrosine phosphorylation in focal adhesions following microtubule disruption. *Journal of Cell Science,* 116**,** 975-986.

KLEIN-NULEND, J., BAKKER, A. D., BACABAC, R. G., VATSA, A. & WEINBAUM, S. 2013. Mechanosensation and transduction in osteocytes. *Bone,* 54**,** 182-190.

KLEINMAN, H. K., MCGARVEY, M. L., LIOTTA, L. A., ROBEY, P. G., TRYGGVASON, K. & MARTIN, G. R. 1982. Isolation and characterization of type-iv procollagen, laminin, and heparan-sulfate proteoglycan from the ehs sarcoma. *Biochemistry,* 21**,** 6188-6193.

KLEMM, D. J., LEITNER, J. W., WATSON, P., NESTEROVA, A., REUSCH, J. E. B., GOALSTONE, M. L. & DRAZNIN, B. 2001. Insulin-induced adipocyte differentiation - Activation of CREB rescues adipogenesis from the arrest caused by inhibition of prenylation. *Journal of Biological Chemistry,* 276**,** 28430-28435.

KOESTER, S., LIN, Y.-C., HERRMANN, H. & WEITZ, D. A. 2010. Nanomechanics of vimentin intermediate filament networks. *Soft Matter,* 6**,** 1910-1914.

KOOLPE, M., RODRIGO, J. J. & BENTON, H. P. 1998. Adenosine 5 '-triphosphate, uridine 5 '-triphosphate, bradykinin, and lysophosphatidic acid induce different patterns of calcium responses by human articular chondrocytes. *Journal of Orthopaedic Research,* 16**,** 217-226.

KOPEN, G. C., PROCKOP, D. J. & PHINNEY, D. G. 1999. Marrow stromal cells migrate throughout forebrain and cerebellum, and they differentiate into astrocytes after injection into neonatal mouse brains. *Proc Natl Acad Sci U S A,* 96**,** 10711-6.

KORPOS, E., WU, C., SONG, J., HALLMANN, R. & SOROKIN, L. 2010. Role of the extracellular matrix in lymphocyte migration. *Cell and Tissue Research,* 339**,** 47-57.

KOYAMA, M., ITO, M., FENG, J. H., SEKO, T., SHIRAKI, K., TAKASE, K., HARTSHORNE, D. J. & NAKANO, T. 2000. Phosphorylation of CPI-17, an inhibitory phosphoprotein of smooth muscle myosin phosphatase, by Rho-kinase. *Febs Letters,* 475**,** 197-200.

KRIEG, M., ARBOLEDA-ESTUDILLO, Y., PUECH, P. H., KAEFER, J., GRANER, F., MUELLER, D. J. & HEISENBERG, C. P. 2008. Tensile forces govern germ-layer organization in zebrafish. *Nature Cell Biology,* 10.

KUHN, T. B., BROWN, M. D. & BAMBURG, J. R. 1998. Rac1-dependent actin filament organization in growth cones is necessary for beta 1-integrin-mediated advance but not for growth on poly-D-lysine. *Journal of Neurobiology,* 37**,** 524-540.

KUO, J.-C. 2013. Mechanotransduction at focal adhesions: integrating cytoskeletal mechanics in migrating cells. *Journal of Cellular and Molecular Medicine,* 17**,** 704-712.

KUROKI, T., IKUTA, T., KASHIWAGI, M., KAWABE, S., OHBA, M., HUH, N., MIZUNO, K., OHNO, S., YAMADA, E. & CHIDA, K. 2000. Cholesterol sulfate, an activator of protein kinase C mediating squamous cell differentiation: a review. *Mutation Research-Reviews in Mutation Research,* 462**,** 189-195.

KWONG, L., WOZNIAK, M. A., COLLINS, A. S., WILSON, S. D. & KEELY, P. J. 2003. R-Ras promotes focal adhesion formation through focal kinase and p130(Cas) by a novel mechanism that differs from integrins. *Molecular and Cellular Biology,* 23**,** 933-949.

LAMORTE, L., RODRIGUES, S., SANGWAN, V., TURNER, C. E. & PARK, M. 2003. Crk associates with a multimolecular Paxillin/GIT2/beta-PIX complex and promotes Rac-dependent relocalization of Paxillin to focal contacts. *Molecular Biology of the Cell,* 14**,** 2818-2831.

LAPIERRE, D. M., TANABE, N., PEREVERZEV, A., SPENCER, M., SHUGG, R. P. P., DIXON, S. J. & SIMS, S. M. 2010. Lysophosphatidic Acid Signals through Multiple Receptors in Osteoclasts to Elevate Cytosolic Calcium Concentration, Evoke Retraction, and Promote Cell Survival. *Journal of Biological Chemistry,* 285**,** 25792-25801.

LARSON, C. M., KELLEY, S. S., BLACKWOOD, A. D., BANES, A. J. & LEE, G. M. 2002. Retention of the native chondrocyte pericellular matrix results in significantly improved matrix production. *Matrix Biology,* 21.

LASSAR, A. B., PATERSON, B. M. & WEINTRAUB, H. 1986. Transfection of a DNA locus that mediates the conversion of 10t1/2 fibroblasts to myoblasts. *Cell,* 47**,** 649-656.

LEADER, D. P., BURGESS, K., CREEK, D. & BARRETT, M. P. 2011. Pathos: A web facility that uses metabolic maps to display experimental changes in metabolites identified by mass spectrometry. *Rapid Communications in Mass Spectrometry,* 25**,** 3422-3426.

LEBRETHON, M. C., JAILLARD, C., NAVILLE, D., BEGEOT, M. & SAEZ, J. M. 1994. Regulation of corticotropin and steroidogenic enzyme messenger-rnas in human fetal adrenal-cells by corticotropin, angiotensin-ii and transforming growth-factor beta(1). *Molecular and Cellular Endocrinology,* 106**,** 137-143.

LEE, J., ABDEEN, A., A., ZHANG, D., KILIAN, K. 2013. Directing stem cell fate on hydrogel substrates by controlling cell geometry, matrix mechanics and adhesion ligand composition. *Biomaterials,* 34**,** 9.

LEFEBVRE, V., HUANG, W. D., HARLEY, V. R., GOODFELLOW, P. N. & DECROMBRUGGHE, B. 1997. SOX9 is a potent activator of the chondrocyte-specific enhancer of the pro alpha 1(II) collagen gene. *Molecular and Cellular Biology,* 17**,** 2336-2346.

LEVENTAL, K. R., YU, H., KASS, L., LAKINS, J. N., EGEBLAD, M., ERLER, J. T., FONG, S. F. T., CSISZAR, K., GIACCIA, A., WENINGER, W., YAMAUCHI, M., GASSER, D. L. & WEAVER, V. M. 2009. Matrix Crosslinking Forces Tumor Progression by Enhancing Integrin Signaling. *Cell,* 139**,** 891-906.

LEWANDOWSKA, K., PERGAMENT, E., SUKENIK, C. N. & CULP, L. A. 1992. Cell-type-specific adhesion mechanisms mediated by fibronectin adsorbed to chemically derivatized substrata. *Journal of Biomedical Materials Research,* 26**,** 1343-1363.

LI, J., CUI, Z., ZHAO, S. & SIDMAN, R. L. 2007. Unique glycerophospholipid signature in retinal stem cells correlates with enzymatic functions of diverse long-chain Acyl-CoA synthetases. *Stem Cells,* 25**,** 2864-2873.

LIN, Y. F., LUO, E., CHEN, X. Z., LIU, L., QIAO, J., YAN, Z. B., LI, Z. Y., TANG, W., ZHENG, X. H. & TIAN, W. D. 2005. Molecular and cellular characterization during chondrogenic differentiation of adipose tissue-derived stromal cells in vitro and cartilage formation in vivo. *Journal of Cellular and Molecular Medicine,* 9**,** 929-939.

LIU, S. C., KIOSSES, W. B., ROSE, D. M., SLEPAK, M., SALGIA, R., GRIFFIN, J. D., TURNER, C. E., SCHWARTZ, M. A. & GINSBERG, M. H. 2002. A fragment of paxillin binds the alpha(4) integrin cytoplasmic domain (tail) and selectively inhibits alpha(4)-mediated cell migration. *Journal of Biological Chemistry,* 277**,** 20887-20894.

LOMBARDI, M. L., JAALOUK, D. E., SHANAHAN, C. M., BURKE, B., ROUX, K. J. & LAMMERDING, J. 2011. The Interaction between Nesprins and Sun Proteins at the Nuclear Envelope Is Critical for Force Transmission between the Nucleus and Cytoskeleton. *Journal of Biological Chemistry,* 286**,** 26743-26753.

LU, X. & LENG, Y. 2009. Comparison of the Osteoblast and Myoblast Behavior on Hydroxyapatite Microgrooves. *Journal of Biomedical Materials Research Part B-Applied Biomaterials,* 90B**,** 438-445.

LUNT, S. Y. & VANDER HEIDEN, M. G. 2011. Aerobic Glycolysis: Meeting the Metabolic Requirements of Cell Proliferation. *Annual Review of Cell and Developmental Biology, Vol 27,* 27**,** 441-464.

LUQUE, E. H., ANGULO, E. & MONTES, G. S. 1983. A histochemical and electron-microscopic study on the collagen of nerves in the domestic-fowl. *Journal of Anatomy,* 137**,** 171-176.

MA, H. L., HUNG, S. C., LIN, S. Y., CHEN, Y. L. & LO, W. H. 2003. Chondrogenesis of human mesenchymal stem cells encapsulated in alginate beads. *Journal of Biomedical Materials Research Part A,* 64A**,** 273-281.

MACDONALD, J. A., ETO, M., BORMAN, M. A., BRAUTIGAN, D. L. & HAYSTEAD, T. A. J. 2001. Dual Ser and Thr phosphorylation of CPI-17, an inhibitor of myosin phosphatase, by MYPT-associated kinase. *Febs Letters,* 493**,** 91-94.

MAHARJAN, R. P. & FERENCI, T. 2003. Global metabolite analysis: the influence of extraction methodology on metabolome profiles of Escherichia coli. *Analytical Biochemistry,* 313**,** 145-154.

MAHESHWARI, G., BROWN, G., LAUFFENBURGER, D. A., WELLS, A. & GRIFFITH, L. G. 2000. Cell adhesion and motility depend on nanoscale RGD clustering. *Journal of Cell Science,* 113**,** 1677-1686.

MAKAROV, A., DENISOV, E., LANGE, O. & HORNING, S. 2006. Dynamic range of mass accuracy in LTQ Orbitrap hybrid mass spectrometer. *Journal of the American Society for Mass Spectrometry,* 17**,** 977-982.

MANELLI, F. & GIUSTINA, A. 2000. Glucocorticoid-induced osteoporosis. *Trends in Endocrinology and Metabolism,* 11**,** 79-85.

MANIOTIS, A. J., CHEN, C. S. & INGBER, D. E. 1997. Demonstration of mechanical connections between integrins cytoskeletal filaments, and nucleoplasm that stabilize nuclear structure. *Proceedings of the National Academy of Sciences of the United States of America,* 94**,** 849-854.

MANSELL, J. P. & BLACKBURN, J. 2013. Lysophosphatidic acid, human osteoblast formation, maturation and the role of 1 alpha,25-Dihydroxyvitamin D3 (calcitriol). *Biochimica Et Biophysica Acta-Molecular and Cell Biology of Lipids,* 1831**,** 105-108.

MANSELL, J. P., NOWGHANI, M., PABBRUWE, M., PATERSON, I. C., SMITH, A. J. & BLOM, A. W. 2011. Lysophosphatidic acid and calcitriol co-operate to promote human osteoblastogenesis: Requirement of albumin-bound LPA. *Prostaglandins & Other Lipid Mediators,* 95**,** 45-52.

MARESCHI, K., NOVARA, M., RUSTICHELLI, D., FERRERO, I., GUIDO, D., CARBONE, E., MEDICO, E., MADON, E., VERCELLI, A. & FAGIOLI, F. 2006. Neural differentiation of human mesenchymal stem cells: evidence for expression of neural markers and eag K+ channel types. *Experimental Hematology,* 34**,** 1563-1572.

MARTINAC, B. & HAMILL, O. P. 2002. Gramicidin A channels switch between stretch activation and stretch inactivation depending on bilayer thickness. *Proceedings of the National Academy of Sciences of the United States of America,* 99**,** 4308-4312.

MCBEATH, R., PIRONE, D. M., NELSON, C. M., BHADRIRAJU, K. & CHEN, C. S. 2004. Cell shape, cytoskeletal tension, and RhoA regulate stem cell lineage commitment. *Developmental Cell,* 6**,** 483-495.

MCMURRAY, R. J., GADEGAARD, N., TSIMBOURI, P. M., BURGESS, K. V., MCNAMARA, L. E., TARE, R., MURAWSKI, K., KINGHAM, E., OREFFO, R. O. C. & DALBY, M. J. 2011. Nanoscale surfaces for the long-term maintenance of mesenchymal stem cell phenotype and multipotency. *Nature Materials,* 10**,** 637-644.

MCNAMARA, L. E., SJOESTROEM, T., BURGESS, K. E. V., KIM, J. J. W., LIU, E., GORDONOV, S., MOGHE, P. V., MEEK, R. M. D., OREFFO, R. O. C., SU, B. & DALBY, M. J. 2011. Skeletal stem cell physiology on functionally distinct titania nanotopographies. *Biomaterials,* 32**,** 7403-7410.

MEIRELLES, L. D. S., CAPLAN, A. I. & NARDI, N. B. 2008. In search of the in vivo identity of mesenchymal stem cells. *Stem Cells,* 26**,** 2287-2299.

MERRILL, A. H. & SCHROEDER, J. J. 1993. Lipid modulation of cell function. *Annual Review of Nutrition,* 13**,** 539-559.

MIMEAULT, M. & BATRA, S. K. 2008. Recent progress on tissue-resident adult stem cell biology and their therapeutic implications. *Stem Cell Reviews,* 4**,** 27-49.

MINGUELL, J. J., ERICES, A. & CONGET, P. 2001. Mesenchymal stem cells. *Exp Biol Med (Maywood),* 226**,** 507-20.

MIRMALEK-SANI, S., TARE, R., MORGAN, S., M., ROACH H., WILSON, D., HANLEY, N. AND OREFFO R., C. 2006. Characterization and Multipotentiality of Human Fetal Femur–Derived Cells: Implications for Skeletal Tissue Regeneration. *Stem Cells,* 24**,** 12.

MITHIEUX, S. M., WISE, S. G. & WEISS, A. S. 2013. Tropoelastin - A multifaceted naturally smart material. *Advanced Drug Delivery Reviews,* 65**,** 421-428.

MORIMOTO, H., BABA, R., HANEJI, T. & DOI, Y. 2013. Double-stranded RNA-dependent protein kinase regulates insulin-stimulated chondrogenesis in mouse clonal chondrogenic cells, ATDC-5. *Cell and Tissue Research,* 351**,** 41-47.

MURAGLIA, A., CORSI, A., RIMINUCCI, M., MASTROGIACOMO, M., CANCEDDA, R., BIANCO, P. & QUARTO, R. 2003. Formation of a chondro-osseous rudiment in micromass cultures of human bone-marrow stromal cells. *Journal of Cell Science,* 116**,** 2949-2955.

MURATA-HORI, M., SUIZU, F., IWASAKI, T., KIKUCHI, A. & HOSOYA, H. 1999. ZIP kinase identified as a novel myosin regulatory light chain kinase in HeLa cells. *Febs Letters,* 451**,** 81-84.

MWALE, F., STACHURA, D., ROUGHLEY, P. & ANTONIOU, J. 2006. Limitations of using aggrecan and type X collagen as markers of chondrogenesis in mesenchymal stem cell differentiation. *Journal of Orthopaedic Research,* 24.

MYLLYHARJU, J. & KIVIRIKKO, K. I. 2004. Collagens, modifying enzymes and their mutations in humans, flies and worms. *Trends in Genetics,* 20**,** 33-43.

MYTHREYE, K. & BLOBE, G. C. 2009. Proteoglycan signaling co-receptors: Roles in cell adhesion, migration and invasion. *Cellular Signalling,* 21**,** 1548-1558.

NASTASE, M. V., YOUNG, M. F. & SCHAEFER, L. 2012. Biglycan: A Multivalent Proteoglycan Providing Structure and Signals. *Journal of Histochemistry & Cytochemistry,* 60**,** 963-975.

NG, L. J., WHEATLEY, S., MUSCAT, G. E. O., CONWAYCAMPBELL, J., BOWLES, J., WRIGHT, E., BELL, D. M., TAM, P. P. L., CHEAH, K. S. E. & KOOPMAN, P. 1997. SOX9 binds DNA, activates transcription, and coexpresses with type II collagen during chondrogenesis in the mouse. *Developmental Biology,* 183**,** 108-121.

NGUYEN, B. V., WANG, Q. G., KUIPER, N. J., EL HAJ, A. J., THOMAS, C. R. & ZHANG, Z. 2010. Biomechanical properties of single chondrocytes and chondrons determined by micromanipulation and finite-element modelling. *Journal of the Royal Society Interface,* 7.

NIELSEN, J. & OLIVER, S. 2005. The next wave in metabolome analysis. *Trends in Biotechnology,* 23**,** 544-546.

NISBET, D. R., RODDA, A. E., HORNE, M. K., FORSYTHE, J. S. & FINKELSTEIN, D. I. 2010. Implantation of Functionalized Thermally Gelling Xyloglucan Hydrogel Within the Brain: Associated Neurite Infiltration and Inflammatory Response. *Tissue Engineering Part A,* 16**,** 2833-2842.

OAKES, P. W., BECKHAM, Y., STRICKER, J. & GARDEL, M. L. 2012. Tension is required but not sufficient for focal adhesion maturation without a stress fiber template. *Journal of Cell Biology,* 196**,** 363-374.

OCHS, B. G., MUELLER-HORVAT, C., ALBRECHT, D., SCHEWE, B., WEISE, K., AICHER, W. K. & ROLAUFFS, B. 2011. Remodeling of Articular Cartilage and Subchondral Bone After Bone Grafting and Matrix-Associated Autologous Chondrocyte Implantation for Osteochondritis Dissecans of the Knee. *American Journal of Sports Medicine,* 39**,** 764-773.

ODA, T., IWASA, M., AIHARA, T., MAEDA, Y. & NARITA, A. 2009. The nature of the globular- to fibrous-actin transition (vol 457, pg 441, 2009). *Nature,* 461**,** 550-550.

OHASHI, T., KIEHART, D. P. & ERICKSON, H. P. 1999. Dynamics and elasticity of the fibronectin matrix in living cell culture visualized by fibronectin-green fluorescent protein. *Proceedings of the National Academy of Sciences of the United States of America,* 96**,** 2153-2158.

OKANO, M., KANO, S., MUNAKATA, H. & OHTSUKI, K. 2001. Biochemical characterization of cholesterol-3-sulfate as the sole effector for the phosphorylation of HMG1 by casein kinase I in vitro. *Biochemical and Biophysical Research Communications,* 281**,** 1325-1330.

OLDIGES, M., LUTZ, S., PFLUG, S., SCHROER, K., STEIN, N. & WIENDAHL, C. 2007. Metabolomics: current state and evolving methodologies and tools. *Applied Microbiology and Biotechnology,* 76**,** 495-511.

ORBACH, R., ADLER-ABRAMOVICH, L., ZIGERSON, S., MIRONI-HARPAZ, I., SELIKTAR, D. & GAZIT, E. 2009. Self-Assembled Fmoc-Peptides as a Platform for the Formation of Nanostructures and Hydrogels. *Biomacromolecules,* 10**,** 2646-2651.

PADMAKUMAR, V. C., LIBOTTE, T., LU, W. S., ZAIM, H., ABRAHAM, S., NOEGEL, A. A., GOTZMANN, J., FOISNER, R. & KARAKESISOGLOU, L. 2005. The inner nuclear membrane protein Sun1 mediates the anchorage of Nesprin-2 to the nuclear envelope. *Journal of Cell Science,* 118**,** 3419-3430.

PAGLIA, G., MAGNUSDOTTIR, M., THORLACIUS, S., SIGURJONSSON, O. E., GUDMUNDSSON, S., PALSSON, B. O. & THIELE, I. 2012. Intracellular metabolite profiling of platelets: Evaluation of extraction processes and chromatographic strategies. *Journal of Chromatography B-Analytical Technologies in the Biomedical and Life Sciences,* 898**,** 111-120.

PAPAKONSTANTI, E. A., VARDAKI, E. A. & STOURNARAS, C. 2000. Actin cytoskeleton: A signaling sensor in cell volume regulation. *Cellular Physiology and Biochemistry,* 10**,** 257-264.

PAREKH, S. H., CHATTERJEE, K., LIN-GIBSON, S., MOORE, N. M., CICERONE, M. T., YOUNG, M. F. & SIMON, C. G., JR. 2011. Modulus-driven differentiation of marrow stromal cells in 3D scaffolds that is independent of myosin-based cytoskeletal tension. *Biomaterials,* 32**,** 2256-2264.

PATEL, N. R., BOLE, M., CHEN, C., HARDIN, C. C., KHO, A. T., MIH, J., DENG, L., BUTLER, J., TSCHUMPERLIN, D., FREDBERG, J. J., KRISHNAN, R. & KOZIEL, H. 2012. Cell Elasticity Determines Macrophage Function. *Plos One,* 7.

PATERSON, H. F., SELF, A. J., GARRETT, M. D., JUST, I., AKTORIES, K. & HALL, A. 1990. Microinjection of recombinant-p21Rho induces rapid changes in cell morphology. *Journal of Cell Biology,* 111**,** 1001-1007.

PEGG, A. E. 2009. Mammalian Polyamine Metabolism and Function. *Iubmb Life,* 61**,** 880-894.

PENG, R., YAO, X. & DING, J. 2011. Effect of cell anisotropy on differentiation of stem cells on micropatterned surfaces through the controlled single cell adhesion. *Biomaterials,* 32**,** 8048-8057.

PERRIER, E., RONZIERE, M.-C., BAREILLE, R., PINZANO, A., MALLEIN-GERIN, F. & FREYRIA, A.-M. 2011. Analysis of collagen expression during chondrogenic induction of human bone marrow mesenchymal stem cells. *Biotechnology Letters,* 33**,** 2091-2101.

PETERSEN, B. E., BOWEN, W. C., PATRENE, K. D., MARS, W. M., SULLIVAN, A. K., MURASE, N., BOGGS, S. S., GREENBERGER, J. S. & GOFF, J. P. 1999. Bone marrow as a potential source of hepatic oval cells. *Science,* 284**,** 1168-1170.

PFAFF, M., LIU, S. C., ERLE, D. J. & GINSBERG, M. H. 1998. Integrin beta cytoplasmic domains differentially cytoskeletal proteins. *Journal of Biological Chemistry,* 273**,** 6104-6109.

PITTENGER, M. F., MACKAY, A. M., BECK, S. C., JAISWAL, R. K., DOUGLAS, R., MOSCA, J. D., MOORMAN, M. A., SIMONETTI, D. W., CRAIG, S. & MARSHAK,

D. R. 1999. Multilineage potential of adult human mesenchymal stem cells. *Science,* 284**,** 143-147.

PLACE, E. S., EVANS, N. D. & STEVENS, M. M. 2009. Complexity in biomaterials for tissue engineering. *Nature Materials,* 8.

POLLARD, T. D. & BORISY, G. G. 2003. Cellular motility driven by assembly and disassembly of actin filaments. *Cell,* 112**,** 453-465.

POOLE, C. A. 1997. Articular cartilage chondrons: Form, function and failure. *Journal of Anatomy,* 191.

POOLE, C. A., AYAD, S. & GILBERT, R. T. 1992. Chondrons from articular-cartilage .5. immunohistochemical evaluation of type-vi collagen organization in isolated chondrons by light, confocal and electron-microscopy. *Journal of Cell Science,* 103.

POOLE, C. A., FLINT, M. H. & BEAUMONT, B. W. 1987. Chondrons in cartilage - ultrastructural analysis of the pericellular microenvironment in adult human articular cartilages. *Journal of Orthopaedic Research,* 5**,** 509-522.

PRAGER-KHOUTORSKY, M., LICHTENSTEIN, A., KRISHNAN, R., RAJENDRAN, K., MAYO, A., KAM, Z., GEIGER, B. & BERSHADSKY, A. D. 2011. Fibroblast polarization is a matrix-rigidity-dependent process controlled by focal adhesion mechanosensing. *Nature Cell Biology,* 13**,** 1457-U178.

PRAJAPATI, R. T., CHAVALLY-MIS, B., HERBAGE, D., EASTWOOD, M. & BROWN, R. A. 2000. Mechanical loading regulates protease production by fibroblasts in three-dimensional collagen substrates. *Wound Repair and Regeneration,* 8**,** 226-237.

PYNE, S. & PYNE, N. J. 2000. Sphingosine 1-phosphate signalling in mammalian cells. *Biochemical Journal,* 349**,** 385-402.

QIN, Z., KREPLAK, L. & BUEHLER, M. J. 2009a. Hierarchical Structure Controls Nanomechanical Properties of Vimentin Intermediate Filaments. *Plos One,* 4.

QIN, Z., KREPLAK, L. & BUEHLER, M. J. 2009b. Nanomechanical properties of vimentin intermediate filament dimers. *Nanotechnology,* 20.

RAAMSDONK, L. M., TEUSINK, B., BROADHURST, D., ZHANG, N. S., HAYES, A., WALSH, M. C., BERDEN, J. A., BRINDLE, K. M., KELL, D. B., ROWLAND, J. J., WESTERHOFF, H. V., VAN DAM, K. & OLIVER, S. G. 2001. A functional genomics strategy that uses metabolome data to reveal the phenotype of silent mutations. *Nature Biotechnology,* 19**,** 45-50.

REILLY, D. T. & BURSTEIN, A. H. 1974. Review article - mechanical-properties of cortical bone. *Journal of Bone and Joint Surgery-American Volume,* A 56.

RESPONTE, D. J., NATOLI, R. M. & ATHANASIOU, K. A. 2007. Collagens of Articular Cartilage: Structure, Function, and Importance in Tissue Engineering. *Critical Reviews in Biomedical Engineering,* 35.

REZANIA, A. & HEALY, K. E. 1999. Biomimetic peptide surfaces that regulate adhesion, spreading, cytoskeletal organization, and mineralization of the matrix deposited by osteoblast-like cells. *Biotechnology Progress,* 15**,** 19-32.

RIVELINE, D., ZAMIR, E., BALABAN, N. Q., SCHWARZ, U. S., ISHIZAKI, T., NARUMIYA, S., KAM, Z., GEIGER, B. & BERSHADSKY, A. D. 2001. Focal contacts as mechanosensors: Externally applied local mechanical force induces growth of focal contacts by an mDia1-dependent and ROCK-independent mechanism. *Journal of Cell Biology,* 153**,** 1175-1185.

ROBINSON, A. R., GHENEIM, R., KOZAK, R. A., ELLIS, D. D. & MANSFIELD, S. D. 2005. The potential of metabolite profiling as a selection tool for genotype discrimination in Populus. *Journal of Experimental Botany,* 56**,** 2807-2819.

ROCHEAPPLIEDSCIENCES Universal Probe Library Assay Design Centre. *https://qpcr.probefinder.com/roche3.html*.

RODGERS, U. R. & WEISS, A. S. 2004. Integrin alpha(v)beta(3) binds a unique non-RGD site near the C-terminus of human tropoelastin. *Biochimie,* 86**,** 173-178.

ROESSNER, U. & BOWNE, J. 2009. What is metabolomics all about? *Biotechniques,* 46**,** 363-365.

ROSENBLAT, G., WILLEY, A., ZHU, Y. N., JONAS, A., DIEGELMANN, R. F., NEEMAN, I. & GRAHAM, M. F. 1999. Palmitoyl ascorbate: Selective augmentation of procollagen mRNA expression compared with L-ascorbate in human intestinal smooth muscle cells. *Journal of Cellular Biochemistry,* 73**,** 312-320.

ROUGHLEY, P., MARTENS, D., RANTAKOKKO, J., ALINI, M., MWALE, F. & ANTONIOU, J. 2006. The involvement of aggrecan polymorphism in degeneration of human intervertebral disc and articular cartilage. *European Cells & Materials,* 11**,** 1-7.

ROWLANDS A., G. P., A., COOPER-WHITE J., J. 2008. Directing osteogenic and myogenic differentiation of MSCs: interplay of stiffness and adhesive ligand presentation. *Am J Physiol Cell Physiol* 295**,** 7.

ROZARIO, T., DZAMBA, B., WEBER, G. F., DAVIDSON, L. A. & DESIMONE, D. W. 2009. The physical state of fibronectin matrix differentially regulates morphogenetic movements in vivo. *Developmental Biology,* 327.

RUANGPANIT, N., PRICE, J. T., HOLMBECK, K., BIRKEDAL-HANSEN, H., GUENZLER, V., HUANG, X. F., CHAN, D., BATEMAN, J. F. & THOMPSON, E. W. 2002. MT1-MMP-dependent and -independent regulation of gelatinase a activation in long-term, ascorbate-treated fibroblast cultures: Regulation by fibrillar collagen. *Experimental Cell Research,* 272**,** 109-118.

SAHA, K., KEUNG, A. J., IRWIN, E. F., LI, Y., LITTLE, L., SCHAFFER, D. V. & HEALY, K. E. 2008. Substrate Modulus Directs Neural Stem Cell Behavior. *Biophysical Journal,* 95**,** 4426-4438.

SALONEN, V., LEHTO, M., VAHERI, A., ARO, H. & PELTONEN, J. 1985. Endoneurial fibrosis following nerve transection - an immunohistological study of collagen types and fibronectin in the rat. *Acta Neuropathologica,* 67**,** 315-321.

SALTI, A., NAT, R., NETO, S., PUSCHBAN, Z., WENNING, G. & DECHANT, G. 2013. Expression of Early Developmental Markers Predicts the Efficiency of Embryonic Stem Cell Differentiation into Midbrain Dopaminergic Neurons. *Stem Cells and Development,* 22**,** 397-411.

SANCHEZ-RAMOS, J., SONG, S., CARDOZO-PELAEZ, F., HAZZI, C., STEDEFORD, T., WILLING, A., FREEMAN, T. B., SAPORTA, S., JANSSEN, W., PATEL, N., COOPER, D. R. & SANBERG, P. R. 2000. Adult bone marrow stromal cells differentiate into neural cells in vitro. *Experimental Neurology,* 164**,** 247-256.

SANCHO, E., BATLLE, E. & CLEVERS, H. 2004. Signaling pathways in intestinal development and cancer. *Annual Review of Cell and Developmental Biology,* 20**,** 695-723.

SANDER, E. E., TEN KLOOSTER, J. P., VAN DELFT, S., VAN DER KAMMEN, R. A. & COLLARD, J. G. 1999. Rac downregulates Rho activity: Reciprocal balance between both GTPases determines cellular morphology and migratory behavior. *Journal of Cell Biology,* 147**,** 1009-1021.

SANDERS, T., A., LLAGOSTERA, E., BARNA, M. 2013. Specialized filopodia direct long-range transport of SHH during vertebrate tissue patterning. *Nature,* 497**,** 7.

SAWADA, Y. & SHEETZ, M. P. 2002. Force transduction by Triton cytoskeletons. *Journal of Cell Biology,* 156**,** 609-615.

SAWADA, Y., TAMADA, M., DUBIN-THALER, B. J., CHERNIAVSKAYA, O., SAKAI, R., TANAKA, S. & SHEETZ, M. P. 2006. Force sensing by mechanical extension of the Src family kinase substrate p130Cas. *Cell,* 127**,** 1015-1026.

SAWKINS, M. J., BOWEN, W., DHADDA, P., MARKIDES, H., SIDNEY, L. E., TAYLOR, A. J., ROSE, F. R. A. J., BADYLAK, S. F., SHAKESHEHH, K. M. & WHITE, L. J. 2013. Hydrogels derived from demineralized and decellularized bone extracellular matrix. *Acta Biomaterialia,* 9**,** 7865-7873.

SCHEFE, J. H., LEHMANN, K. E., BUSCHMANN, I. R., UNGER, T. & FUNKE-KAISER, H. 2006. Quantitative real-time RT-PCR data analysis: current concepts and the novel "gene expression's C-T difference" formula. *Journal of Molecular Medicine-Jmm,* 84.

SCHELTEMA, R. A., JANKEVICS, A., JANSEN, R. C., SWERTZ, M. A. & BREITLING, R. 2011. PeakML/mzMatch: A File Format, Java Library, R Library, and Tool-Chain for Mass Spectrometry Data Analysis. *Analytical Chemistry,* 83**,** 2786-2793.

SCHILLER, H., B., HERMANN, M., POLLEUX, J., VIGNAUD, T., ZANIVAN, S., FRIEDEL, C., C., SUN, Z., RADUCANU, A., GOTTSCHALK, K., THÉRY, M., MANN, M., FÄSSLER, R. 2013. β1- and αv-class integrins cooperate to regulate myosin II during rigidity sensing of fibronectin-based microenvironments. *Nature cell biology,* 15**,** 12.

SCHMID, T. M., GIBNEY, E. & LINSENMAYER, T. F. 1985. Type-X collagen within the embryonic chick sternum - immunohistochemical localization with a monoclonal-antibody. *Annals of the New York Academy of Sciences,* 460**,** 497-499.

SCHOFIELD, R. 1978. Relationship between spleen colony-forming cell and hematopoietic stem-cell - hypothesis. *Blood Cells,* 4**,** 7-25.

SEKIYA, I., TSUJI, K., KOOPMAN, P., WATANABE, H., YAMADA, Y., SHINOMIYA, K., NIFUJI, A., NODA, M. 2000. SOX9 enhances aggrecan gene promoter/enhancer activity and Is up-regulated by retinoic acid in a cartilage-derived cell Line, TC6. *Journal of Biological chemistry,* 275**,** 8.

SEKIYA, I., VUORISTO, J. T., LARSON, B. L. & PROCKOP, D. J. 2002. In vitro cartilage formation by human adult stem cells from bone marrow stroma defines the sequence of cellular and molecular events during chondrogenesis. *Proceedings of the National Academy of Sciences of the United States of America,* 99**,** 4397-4402.

SHIEH, A. C. & ATHANASIOU, K. A. 2006. Biomechanics of single zonal chondrocytes. *Journal of Biomechanics,* 39**,** 1595-1602.

SILVA, G. A., CZEISLER, C., NIECE, K. L., BENIASH, E., HARRINGTON, D. A., KESSLER, J. A. & STUPP, S. I. 2004. Selective differentiation of neural progenitor cells by high-epitope density nanofibers. *Science,* 303**,** 1352-1355.

SIMMONS, P. J., LEVESQUE, J. P. & ZANNETTINO, A. C. W. 1997. Adhesion molecules in haemopoiesis. *Baillieres Clinical Haematology,* 10**,** 485-505.

SIMS, S. M., PANUPINTHU, N., LAPIERRE, D. M., PEREVERZEV, A. & DIXON, S. J. 2013. Lysophosphatidic acid: A potential mediator of osteoblast-osteoclast signaling in bone. *Biochimica Et Biophysica Acta-Molecular and Cell Biology of Lipids,* 1831**,** 109-116.

SINHA, R. K. & TUAN, R. S. 1996. Regulation of human osteoblast integrin expression by orthopedic implant materials. *Bone,* 18**,** 451-457.

SMITH, A. M., WILLIAMS, R. J., TANG, C., COPPO, P., COLLINS, R. F., TURNER, M. L., SAIANI, A. & ULIJN, R. V. 2008. Fmoc-Diphenylalanine self assembles to a hydrogel via a novel architecture based on pi-pi interlocked beta-sheets. *Advanced Materials,* 20**,** 37-+.

SOLCHAGA, L. A., TEMENOFF, J. S., GAO, J. Z., MIKOS, A. G., CAPLAN, A. I. & GOLDBERG, V. M. 2005. Repair of osteochondral defects with hyaluronan- and polyester-based scaffolds. *Osteoarthritis and Cartilage,* 13**,** 297-309.

SOMLYO, A. P. & SOMLYO, A. V. 2003. Ca2+ sensitivity of smooth muscle and nonmuscle myosin II: Modulated by G proteins, kinases, and myosin phosphatase. *Physiological Reviews,* 83**,** 1325-1358.

SORDELLA, R., JIANG, W., CHEN, G. C., CURTO, M. & SETTLEMAN, J. 2003. Modulation of rho GTPase signaling regulates a switch between adipogenesis and myogenesis. *Cell,* 113**,** 147-158.

SPIEGEL, S. & MILSTIEN, S. 2002. Sphingosine 1-phosphate, a key cell signaling molecule. *Journal of Biological Chemistry,* 277**,** 25851-25854.

STEIN, L. R. & IMAI, S.-I. 2012. The dynamic regulation of NAD metabolism in mitochondria. *Trends in Endocrinology and Metabolism,* 23**,** 420-428.

STOSSEL, T. P. 1984. Contribution of actin to the structure of the cytoplasmic matrix. *Journal of Cell Biology,* 99**,** S15-S21.

SUGAWARA, Y., KAMIOKA, H., ISHIHARA, Y., FUJISAWA, N., KAWANABE, N. & YAMASHIRO, T. 2013. The early mouse 3D osteocyte network in the presence and absence of mechanical loading. *Bone,* 52**,** 189-196.

SULLIVAN, T. A., USCHMANN, B., HOUGH, R. & LEBOY, P. S. 1994. Ascorbate modulation of chondrocyte gene-expression is independent of its role in collagen secretion. *Journal of Biological Chemistry,* 269**,** 22500-22506.

SWETMAN, C. A., LEVERRIER, Y., GARG, R., GAN, C. H. V., RIDLEY, A. J., KATZ, D. R. & CHAIN, B. M. 2002. Extension, retraction and contraction in the formation of a dendritic cell dendrite: distinct roles for Rho GTPases. *European Journal of Immunology,* 32**,** 2074-2083.

SYAMALADEVI, D., P., SPUDICH J., A., SOWDHAMINI, R. 2012. Structural and Functional Insights on the Myosin Superfamily. *Bioinformatics and Biology Insights,* 6**,** 11.

TAKAGI, J., PETRE, B. M., WALZ, T. & SPRINGER, T. A. 2002. Global conformational rearrangements in integrin extracellular domains in outside-in and inside-out signaling. *Cell,* 110**,** 599-611.

TANG, C., SMITH, A. M., COLLINS, R. F., ULIJN, R. V. & SAIANI, A. 2009. Fmoc-Diphenylalanine Self-Assembly Mechanism Induces Apparent pK(a) Shifts. *Langmuir,* 25.

TARE, R. S., BABISTER, J. C., KANCZLER, J. & OREFFO, R. O. C. 2008. Skeletal stem cells: Phenotype, biology and environmental niches informing tissue regeneration. *Molecular and Cellular Endocrinology,* 288**,** 11-21.

TAYLOR, S. M. & JONES, P. A. 1979. Multiple new phenotypes induced in 10t1/2-cells and 3t3-cells treated with 5-azacytidine. *Cell,* 17**,** 771-779.

TEIXEIRA, A. I., ILKHANIZADEH, S., WIGENIUS, J. A., DUCKWORTH, J. K., INGANAS, O. & HERMANSON, O. 2009. The promotion of neuronal maturation on soft substrates. *Biomaterials,* 30.

TEMENOFF, J. S. & MIKOS, A. G. 2000. Review: tissue engineering for regeneration of articular cartilage. *Biomaterials,* 21**,** 431-440.

THERY, M., RACINE, V., PIEL, M., PEPIN, A., DIMITROV, A., CHEN, Y., SIBARITA, J.-B. & BORNENS, M. 2006. Anisotropy of cell adhesive microenvironment governs cell internal organization and orientation of polarity. *Proceedings of the National Academy of Sciences of the United States of America,* 103**,** 19771-19776.

TILGHMAN, R. W., BLAIS, E. M., COWAN, C. R., SHERMAN, N. E., GRIGERA, P. R., JEFFERY, E. D., FOX, J. W., BLACKMAN, B. R., TSCHUMPERLIN, D. J., PAPIN, J. A. & PARSONS, J. T. 2012. Matrix Rigidity Regulates Cancer Cell Growth by Modulating Cellular Metabolism and Protein Synthesis. *Plos One,* 7.

TJABRINGA, G. S., ZANDIEH-DOULABI, B., HELDER, M. N., KNIPPENBERG, M., WUISMAN, P. I. J. M. & KLEIN-NULEND, J. 2008. The polymine spermine regulates osteogenic differentiation in adipose stem cells. *Journal of Cellular and Molecular Medicine,* 12**,** 1710-1717.

TOCCHI, A. & PARKS, W. C. 2013. Functional interactions between matrix metalloproteinases and glycosaminoglycans. *Febs Journal,* 280**,** 2332-2341.

TOKUOKA, M., SAWAMURA, N., KOBAYASHI, K. & MIZUNO, A. 2010. Simple metabolite extraction method for metabolic profiling of the solid-state fermentation of Aspergillus oryzae. *Journal of Bioscience and Bioengineering,* 110**,** 665-669.

TORTORELLA, M. D., BURN, T. C., PRATTA, M. A., ABBASZADE, I., HOLLIS, J. M., LIU, R., ROSENFELD, S. A., COPELAND, R. A., DECICCO, C. P., WYNN, R., ROCKWELL, A., YANG, F., DUKE, J. L., SOLOMON, K., GEORGE, H., BRUCKNER, R., NAGASE, H., ITOH, Y., ELLIS, D. M., ROSS, H., WISWALL, B. H., MURPHY, K., HILLMAN, M. C., HOLLIS, G. F., NEWTON, R. C., MAGOLDA, R. L., TRZASKOS, J. M. & ARNER, E. C. 1999. Purification and cloning of aggrecanase-1: A member of the ADAMTS family of proteins. *Science,* 284**,** 1664-1666.

TOZZI, M. G., CAMICI, M., MASCIA, L., SGARRELLA, F. & IPATA, P. L. 2006. Pentose phosphates in nucleoside interconversion and catabolism. *Febs Journal,* 273**,** 1089-1101.

TRAPPMANN, B., GAUTROT, J. E., CONNELLY, J. T., STRANGE, D. G. T., LI, Y., OYEN, M. L., STUART, M. A. C., BOEHM, H., LI, B., VOGEL, V., SPATZ, J. P., WATT, F. M. & HUCK, W. T. S. 2012. Extracellular-matrix tethering regulates stem-cell fate. *Nature Materials,* 11.

TRELSTAD, R. L., CATANESE, V. M. & RUBIN, D. F. 1976. Collagen fractionation - separation of native type-i, type-ii and type-iii by differential precipitation. *Analytical Biochemistry,* 71**,** 114-118.

TRICKEY, W. R., VAIL, T. P. & GUILAK, F. 2004. The role of the cytoskeleton in the viscoelastic properties of human articular chondrocytes. *Journal of Orthopaedic Research,* 22**,** 131-139.

TSE, J. R. & ENGLER, A. J. 2011. Stiffness Gradients Mimicking In Vivo Tissue Variation Regulate Mesenchymal Stem Cell Fate. *Plos One,* 6.

TSIMBOURI, P. M., MCMURRAY, R. J., BURGESS, K. V., ALAKPA, E. V., REYNOLDS, P. M., MURAWSKI, K., KINGHAM, E., OREFFO, R. O. C., GADEGAARD, N. & DALBY, M. J. 2012. Using nanotopography and metabolomics to identify biochemical effectors of multipotency. *ACS nano,* 6.

UNDERWOOD, P. A. & BENNETT, F. A. 1989. A comparison of the biological-activities of the cell-adhesive proteins vitronectin and fibronectin. *Journal of Cell Science,* 93**,** 641-649.

URBAN, J. P. G., ROBERTS, S. & RALPHS, J. R. 2000. The nucleus of the intervertebral disc from development to degeneration. *American Zoologist,* 40**,** 53-61.

VAN HORSSEN, J., DIJKSTRA, C. D. & DE VRIES, H. E. 2007. The extracellular matrix in multiple sclerosis pathology. *Journal of Neurochemistry,* 103**,** 1293-1301.

VANSUSANTE, J. L. C., BUMA, P., VANOSCH, G., VERSLEYEN, D., VANDERKRAAN, P. M., VANDERBERG, W. B. & HOMMINGA, G. N. 1995. Culture of chondrocytes in alginate and collagen carrier gels. *Acta Orthopaedica Scandinavica,* 66**,** 549-556.

VAUPEL, J. W. 2010. Biodemography of human ageing. *Nature,* 464**,** 536-542.

VEGNERS, R., SHESTAKOVA, I., KALVINSH, I., EZZELL, R. M. & JANMEY, P. A. 1995. Use of a gel-forming dipeptide derivative as a carrier for antigen presentation. *Journal of peptide science : an official publication of the European Peptide Society,* 1**,** 371-8.

VICENTE-MANZANARES, M., CHOI, C. K. & HORWITZ, A. R. 2009. Integrins in cell migration - the actin connection. *Journal of Cell Science,* 122**,** 199-206.

VICENTE-MANZANARES, M., XUEFEI, M., ADELSTEIN, R., S., HORWITZ, A., R. 2009. Non-muscle myosin II takes centre stage in cell adhesion and migration. *Nature Reviews Molecular Cell Biology,* 10**,** 13.

VILLAS-BOAS, S. G., RASMUSSEN, S. & LANE, G. A. 2005. Metabolomics or metabolite profiles? *Trends in Biotechnology,* 23**,** 385-386.

VOLPATO, F. Z., FUEHRMANN, T., MIGLIARESI, C., HUTMACHER, D. W. & DALTON, P. D. 2013. Using extracellular matrix for regenerative medicine in the spinal cord. *Biomaterials,* 34**,** 4945-4955.

VON WICHERT, G., HAIMOVICH, B., FENG, G. S. & SHEETZ, M. P. 2003. Force-dependent integrin-cytoskeleton linkage formation requires downregulation of focal complex dynamics by Shp2. *Embo Journal,* 22**,** 5023-5035.

VONK, L. A., DOULABI, B. Z., HUANG, C., HELDER, M. N., EVERTS, V. & BANK, R. A. 2010. Preservation of the Chondrocyte's Pericellular Matrix Improves Cell-Induced Cartilage Formation. *Journal of Cellular Biochemistry,* 110.

VONSCHROEDER, H. P., KWAN, M., AMIEL, D. & COUTTS, R. D. 1991. The use of polylactic acid matrix and periosteal grafts for the reconstruction of rabbit knee articular defects. *Journal of Biomedical Materials Research,* 25**,** 329-339.

WALSH, A. J. L. & LOTZ, J. C. 2004. Biological response of the intervertebral disc to dynamic loading. *Journal of Biomechanics,* 37**,** 329-337.

WANG, C.-Y., CHEN, L.-L., KUO, P.-Y., CHANG, J.-L., WANG, Y.-J. & HUNG, S.-C. 2010. Apoptosis in chondrogenesis of human mesenchymal stem cells: effect of serum and medium supplements. *Apoptosis,* 15**,** 439-449.

WANG, N. & INGBER, D. E. 1994. Control of cytoskeletal mechanics by extracellular-matrix, cell-shape, and mechanical tension. *Biophysical Journal,* 66**,** 2181-2189.

WANG, N. & INGBER, D. E. 1995. Probing transmembrane mechanical coupling and cytomechanics using magnetic twisting cytometry. *Biochemistry and Cell Biology-Biochimie Et Biologie Cellulaire,* 73**,** 327-335.

WANG, P.-Y., TSAI, W.-B. & VOELCKER, N. H. 2012. Screening of rat mesenchymal stem cell behaviour on polydimethylsiloxane stiffness gradients. *Acta Biomaterialia,* 8**,** 519-530.

WANG, Y. Z., KIM, U. J., BLASIOLI, D. J., KIM, H. J. & KAPLAN, D. L. 2005. In vitro cartilage tissue engineering with 3D porous aqueous-derived silk scaffolds and mesenchymal stem cells. *Biomaterials,* 26**,** 7082-7094.

WEDEMEYER, W. J., WELKER, E. & SCHERAGA, H. A. 2002. Proline cis-trans isomerization and protein folding. *Biochemistry,* 41**,** 14637-14644.

WILLIAMS, R. J., HALL, T. E., GLATTAUER, V., WHITE, J., PASIC, P. J., SORENSEN, A. B., WADDINGTON, L., MCLEAN, K. M., CURRIE, P. D. & HARTLEY, P. G. 2011. The in vivo performance of an enzyme-assisted self-assembled peptide/protein hydrogel. *Biomaterials,* 32**,** 5304-5310.

WILUSZ, R. E., DEFRATE, L. E. & GUILAK, F. 2012. Immunofluorescence-guided atomic force microscopy to measure the micromechanical properties of the pericellular matrix of porcine articular cartilage. *Journal of the Royal Society Interface,* 9**,** 2997-3007.

WISE, S. G. & WEISS, A. S. 2009. Tropoelastin. *International Journal of Biochemistry & Cell Biology,* 41**,** 494-497.

WISHART, D. S., KNOX, C., GUO, A. C., EISNER, R., YOUNG, N., GAUTAM, B., HAU, D. D., PSYCHOGIOS, N., DONG, E., BOUATRA, S., MANDAL, R., SINELNIKOV, I., XIA, J., JIA, L., CRUZ, J. A., LIM, E., SOBSEY, C. A., SHRIVASTAVA, S., HUANG, P., LIU, P., FANG, L., PENG, J., FRADETTE, R., CHENG, D., TZUR, D., CLEMENTS, M., LEWIS, A., DE SOUZA, A., ZUNIGA, A., DAWE, M., XIONG, Y., CLIVE, D., GREINER, R., NAZYROVA, A., SHAYKHUTDINOV, R., LI, L., VOGEL, H. J. & FORSYTHE, I. 2009. HMDB: a knowledgebase for the human metabolome. *Nucleic Acids Research,* 37**,** D603-D610.

WISLET-GENDEBIEN, S., HANS, G., LEPRINCE, P., RIGO, J. M., MOONEN, G. & ROGISTER, B. 2005. Plasticity of cultured mesenchymal stem cells: Switch from nestin-positive to excitable neuron-like phenotype. *Stem Cells,* 23**,** 392-402.

WOLFENSON, H., LAVELIN, I. & GEIGER, B. 2013. Dynamic Regulation of the Structure and Functions of Integrin Adhesions. *Developmental Cell,* 24**,** 447-458.

WOLFENSON, H., LUBELSKI, A., REGEV, T., KLAFTER, J., HENIS, Y., I., GEIGER, B. 2009a. A role for the juxtamembrane cytoplasm in the molecular dynamics of focal adhesions. *PLos ONE,* 4**,** 12.

WOLFENSON, H., YOAV, I., H., GEIGER, B., BERSHADSKY, A., D. 2009b. The heel and toe of the cell's foot: A multifaceted approach for understanding the structure and dynamics of focal adhesions. *Cytoskeleton,* 66**,** 13.

WOLFENSON, H. W. H., BERSHADSKY, A., HENIS, Y. I. & GEIGER, B. 2011. Actomyosin-generated tension controls the molecular kinetics of focal adhesions. *Journal of Cell Science,* 124**,** 1425-1432.

WONG, A. P., DUTLY, A. E., SACHER, A., LEE, H., HWANG, D. M., LIU, M., KESHAVJEE, S., HU, J. & WADDELL, T. K. 2007. Targeted cell replacement with bone marrow cells for airway epithelial regeneration. *American Journal of Physiology-Lung Cellular and Molecular Physiology,* 293**,** L740-L752.

WONG, M. & CARTER, D. R. 2003. Articular cartilage functional histomorphology and mechanobiology: a research perspective. *Bone,* 33.

WONG, M., WUETHRICH, P., EGGLI, P. & HUNZIKER, E. 1996. Zone-specific cell biosynthetic activity in mature bovine articular cartilage: A new method using confocal microscopic stereology and quantitative autoradiography. *Journal of Orthopaedic Research,* 14**,** 424-432.

WOOD, A. 1988. Contact guidance on microfabricated substrata the response of teleost fin mesenchyme cells to repeating topographical patterns. *Journal of Cell Science,* 90**,** 67-682.

WOODBURY, D., REYNOLDS, K. & BLACK, I. B. 2002. Adult bone marrow stromal stem cells express germline, ectodermal, endodermal, and mesodermal genes prior to neurogenesis. *Journal of Neuroscience Research,* 69**,** 908-917.

WOODBURY, D., SCHWARZ, E. J., PROCKOP, D. J. & BLACK, I. B. 2000. Adult rat and human bone marrow stromal cells differentiate into neurons. *Journal of Neuroscience Research,* 61**,** 364-370.

WOZNIAK, M. A., DESAI, R., SOLSKI, P. A., DER, C. J. & KEELY, P. J. 2003. ROCK-generated contractility regulates breast epithelial cell differentiation in response to the physical properties of a three-dimensional collagen matrix. *Journal of Cell Biology,* 163**,** 583-595.

WOZNIAK, M. A., MODZELEWSKA, K., KWONG, L. & KEELY, P. J. 2004. Focal adhesion regulation of cell behavior. *Biochimica Et Biophysica Acta-Molecular Cell Research,* 1692**,** 103-119.

WU, X., WALKER, J., ZHANG, J., DING, S. & SCHULTZ, P. G. 2004. Purmorphamine induces osteogenesis by activation of the hedgehog signaling pathway. *Chemistry & Biology,* 11**,** 1229-1238.

XIA, J., PSYCHOGIOS, N., YOUNG, N. & WISHART, D. S. 2009. MetaboAnalyst: a web server for metabolomic data analysis and interpretation. *Nucleic Acids Research,* 37**,** W652-W660.

XIA, J. & WISHART, D. S. 2010. MSEA: a web-based tool to identify biologically meaningful patterns in quantitative metabolomic data. *Nucleic Acids Research,* 38.

XIAO, T., TAKAGI, J., COLLER, B. S., WANG, J. H. & SPRINGER, T. A. 2004. Structural basis for allostery in integrins and binding to fibrinogen-mimetic therapeutics. *Nature,* 432**,** 59-67.

XIE, T. & SPRADLING, A. C. 2000. A niche maintaining germ line stem cells in the Drosophila ovary. *Science,* 290**,** 328-330.

XIONG, J. P., STEHLE, T., DIEFENBACH, B., ZHANG, R. G., DUNKER, R., SCOTT, D. L., JOACHIMIAK, A., GOODMAN, S. L. & ARNAOUT, M. A. 2001. Crystal structure of the extracellular segment of integrin alpha V beta 3. *Science,* 294**,** 339-345.

XIONG, J. P., STEHLE, T., ZHANG, R. G., JOACHIMIAK, A., FRECH, M., GOODMAN, S. L. & ARNAOUT, M. A. 2002. Crystal structure of the extracellular segment of integrin alpha V beta 3 in complex with an Arg-Gly-Asp ligand. *Science,* 296**,** 151-155.

XU, T. S., BIANCO, P., FISHER, L. W., LONGENECKER, G., SMITH, E., GOLDSTEIN, S., BONADIO, J., BOSKEY, A., HEEGAARD, A. M., SOMMER, B., SATOMURA, K., DOMINGUEZ, P., ZHAO, C. Y., KULKARNI, A. B., ROBEY, P. G. & YOUNG, M. F. 1998. Targeted disruption of the biglycan gene leads to an osteoporosis-like phenotype in mice. *Nature Genetics,* 20**,** 78-82.

XU, X.-D., LIANG, L., CHEN, C.-S., LU, B., WANG, N.-L., JIANG, F.-G., ZHANG, X.-Z. & ZHUO, R.-X. 2010. Peptide Hydrogel as an Intraocular Drug Delivery System for Inhibition of Postoperative Scarring Formation. *Acs Applied Materials & Interfaces,* 2**,** 2663-2671.

YAMADA, K. M. & GEIGER, B. 1997. Molecular interactions in cell adhesion complexes. *Current Opinion in Cell Biology,* 9.

YAMASAKI, A., ITABASHI, M., SAKAI, Y., ITO, H., ISHIWARI, Y., NAGATSUKA, H. & NAGAI, N. 2001. Expression of type I, type II, and type X collagen genes during altered endochondral ossification in the femoral epiphysis of osteosclerotic (oc/oc) mice. *Calcified Tissue International,* 68**,** 53-60.

YAMAZAKI, M., FURUIKE, S. & ITO, T. 2002. Mechanical response of single filamin A (ABP-280) molecules and its role in the actin cytoskeleton. *Journal of Muscle Research and Cell Motility,* 23**,** 525-534.

YANES, O., CLARK, J., WONG, D. M., PATTI, G. J., SANCHEZ-RUIZ, A., BENTON, H. P., TRAUGER, S. A., DESPONTS, C., DING, S. & SIUZDAK, G. 2010. Metabolic oxidation regulates embryonic stem cell differentiation. *Nature Chemical Biology,* 6**,** 411-417.

YIM, E. K. F., DARLING, E. M., KULANGARA, K., GUILAK, F. & LEONG, K. W. 2010. Nanotopography-induced changes in focal adhesions, cytoskeletal organization, and mechanical properties of human mesenchymal stem cells. *Biomaterials,* 31**,** 1299-1306.

YIM, E. K. F., PANG, S. W. & LEONG, K. W. 2007. Synthetic nanostructures inducing differentiation of human mesenchymal stem cells into neuronal lineage. *Experimental Cell Research,* 313**,** 1820-1829.

YOUNG, M. F., BI, Y. M., AMEYE, L. & CHEN, X. D. 2003. Biglycan knockout mice: New models for musculoskeletal diseases. *Glycoconjugate Journal,* 19**,** 257-262.

YU, C.-H., LAW, J. B. K., SURYANA, M., LOW, H. Y. & SHEETZ, M. P. 2011. Early integrin binding to Arg-Gly-Asp peptide activates actin polymerization and contractile movement that stimulates outward translocation. *Proceedings of the National Academy of Sciences of the United States of America,* 108**,** 20585-20590.

YU, Y. Y., LIEU, S., LU, C. & COLNOT, C. 2010. Bone morphogenetic protein 2 stimulates endochondral ossification by regulating periosteal cell fate during bone repair. *Bone,* 47.

ZAIDEL-BAR, R. 2009. Evolution of complexity in the integrin adhesome. *Journal of Cell Biology,* 186**,** 317-321.

ZAIDEL-BAR, R., BALLESTREM, C., KAM, Z. & GEIGER, B. 2003. Early molecular events in the assembly of matrix adhesions at the leading edge of migrating cells. *Journal of Cell Science,* 116**,** 4605-4613.

ZAIDEL-BAR, R., ITZKOVITZ, S., MA'AYAN, A., IYENGAR, R. & GEIGER, B. 2007. Functional atlas of the integrin adhesome. *Nature Cell Biology,* 9**,** 858-868.

ZHANG, W. M., KAPYLA, J., PURANEN, J. S., KNIGHT, C. G., TIGER, C. F., PENTIKAINEN, O. T., JOHNSON, M. S., FARNDALE, R. W., HEINO, J. & GULLBERG, D. 2003a. alpha(11)beta(1) integrin recognizes the GFOGER sequence in interstitial collagens. *Journal of Biological Chemistry,* 278**,** 7270-7277.

ZHANG, Y., GU, H. W., YANG, Z. M. & XU, B. 2003b. Supramolecular hydrogels respond to ligand-receptor interaction. *Journal of the American Chemical Society,* 125**,** 13680-13681.

ZHAO, L. R., DUAN, W. M., REYES, M., KEENE, C. D., VERFAILLIE, C. M. & LOW, W. C. 2002. Human bone marrow stem cells exhibit neural phenotypes and ameliorate neurological deficits after grafting into the ischemic brain of rats. *Experimental Neurology,* 174**,** 11-20.

ZHAO, Q., EBERSPAECHER, H., LEFEBVRE, V. & DECROMBRUGGHE, B. 1997. Parallel expression of Sox9 and Col2a1 in cells undergoing chondrogenesis. *Developmental Dynamics,* 209**,** 377-386.

ZHAO, T., GOH, K. J., NG, H. H. & VARDY, L. A. 2012. A role for polyamine regulators in ESC self-renewal. *Cell Cycle,* 11**,** 4517-4523.

ZHOU, M., SMITH, A. M., DAS, A. K., HODSON, N. W., COLLINS, R. F., ULIJN, R. V. & GOUGH, J. E. 2009. Self-assembled peptide-based hydrogels as scaffolds for anchorage-dependent cells. *Biomaterials,* 30**,** 2523-2530.

ZUELA, N., BAR, D. Z. & GRUENBAUM, Y. 2012. Lamins in development, tissue maintenance and stress. *Embo Reports,* 13**,** 1070-1078.

ZUK, P. A., ZHU, M., MIZUNO, H., HUANG, J., FUTRELL, J. W., KATZ, A. J., BENHAIM, P., LORENZ, H. P. & HEDRICK, M. H. 2001. Multilineage cells from human adipose tissue: implications for cell-based therapies. *Tissue Eng,* 7**,** 211-28.

APPENDIX

I. Buffers made in-house

a) Phosphate buffered saline (PBS)

Single phosphate buffered saline tablets (Sigma-Aldrich, UK) were diluted to 250ml in distilled water as per manufacturers' instructions. PBS solutions were then autoclaved at 200°C for 20 minutes and stored at room temperature

b) Fixative

Fixative solutions constituted 10% formaldehyde-40 (Sigma-Aldrich, UK) in PBS. Solutions were typically made using 10 ml formaldehyde added to 90 ml PBS. Solutions were stored at 4°C until ready for use.

c) Permeability buffer

Permeability buffers constituted 10.3 g sucrose, 0.292 g sodium chloride, 0.06 g magnesium chloride and 0.476 g HEPES dissolved in 100 ml of PBS solution using a magnetic stirrer. The solution pH was then adjusted to 7.2 and 0.5 ml of triton X added. . Solutions were stored at 4°C until ready for use.

All reagents were purchased from Sigma-Aldrich, UK.

d) 1% BSA in PBS

1 gram of BSA (Sigma-Aldrich, UK) was dissolved in 100 ml PBS. Solutions were stored at 4°C for the short term or at -20°C for longer periods (> 2 weeks).

e) 0.5% Tween-20

0.5 ml of Tween-20 (Sigma-Aldrich, UK) was diluted in 100 ml PBS. Solutions were stored at 4°C until ready for use.

II. Statistics calculated using two-way ANOVA followed by Bonferroni multiple comparison post-tests for measured protein abundances in MSCs cultured on plain, 2 kPa F_2/S, 6 kPa F_2/S and 38 kPa F_2/S substrates.

Statistically significant comparisons are denoted with an asterix where the calculated p value is < 0.05, *; <0.01, ** and < 0.001 ***.

Source of variation	Substrate	**
	Time	*
	Interaction between both variables	

Day 1				
	Plain	2 kPa	6 kPa	38 kPa
Plain	-			
2 kPa		-		
6 kPa			-	
38 kPa				-

Day 2				
	Plain	2 kPa	6 kPa	38 kPa
Plain	-			
2 kPa		-		
6 kPa			-	
38 kPa				-

Day 3				
	Plain	2 kPa	6 kPa	38 kPa
Plain	-			
2 kPa		-		
6 kPa			-	
38 kPa				-

Day 5				
	Plain	2 kPa	6 kPa	38 kPa
Plain	-			
2 kPa		-		
6 kPa			-	
38 kPa				-

Day 7				
	Plain	2 kPa	6 kPa	38 kPa
Plain	-		*	*
2 kPa		-		
6 kPa	*		-	
38 kPa	*			-

III. Metabolic pathway; Steroid biosynthesis

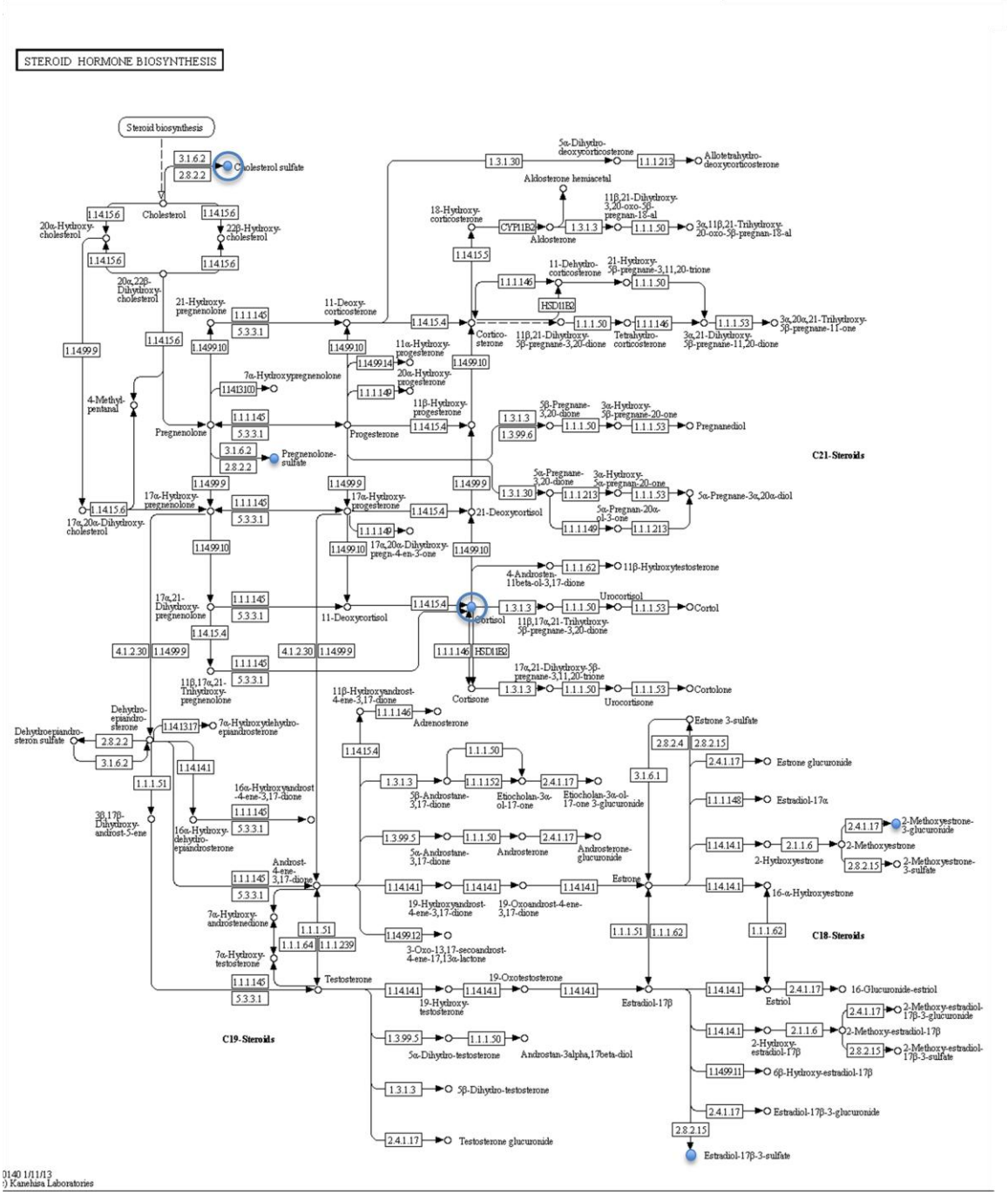

KEGG metabolic pathway shows synthesis of the glucorticoids cholesterol sulphate and cortisol (circled). Both compounds are derivatives of cholesterol and have been implicated in osteogenic development. Cortisol, known mainly for its involvement in early development (Cooper et al., 1999, Manelli and Giustina, 2000), and cholesterol sulphate in *in vitro* osteogenesis of MSCs and pericytes (Chapter 4 and chapter 6).

IV. DMSO controls

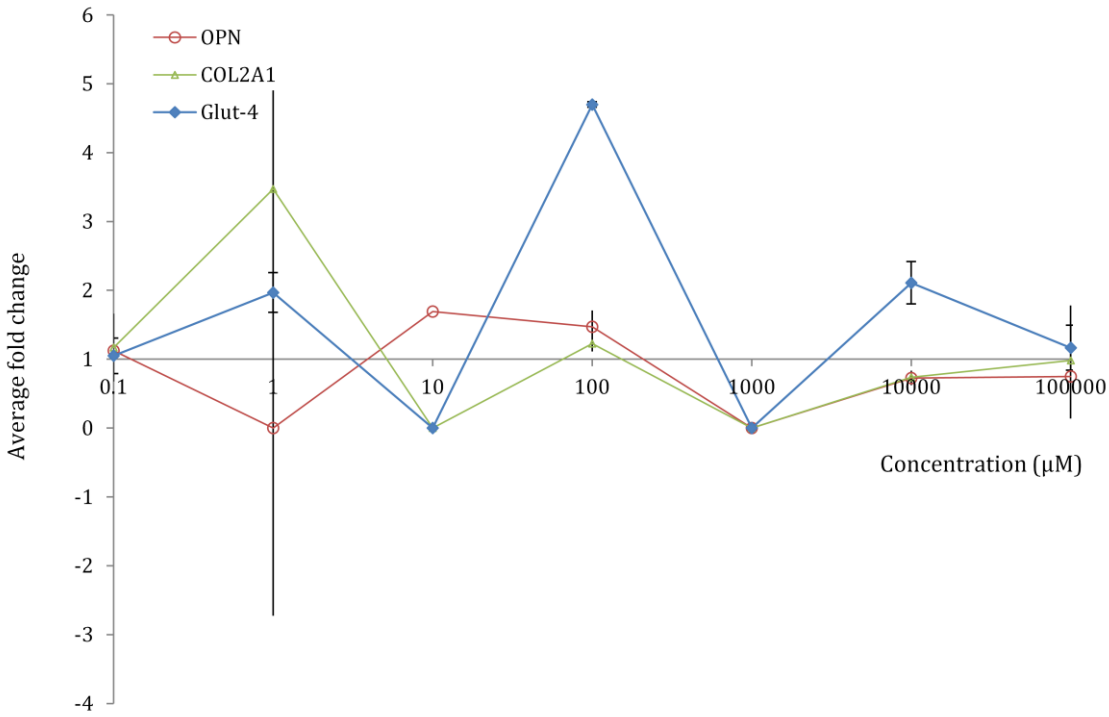

The above graph shows the results obtained from PCR experiments done with MSCs incubated with serially diluted concentrations of DMSO.

DMSO was used to create solutions of the test items used in Chapter 4 - cholesterol sulphate, GP18:0 and sphinganine. Each test compound was made with a starting concentration of 100 µM containing 0.2% DMSO in the final volume. To ensure that DMSO concentrations had no bias on MSC differentiation, cells were cultured with equivalent levels of DMSO in the media only and transcription levels of OPN,GLUT-4 and COL2A1 ascertained. It was concluded that the DMSO levels were low enough not to cause any discernible effects.

Error bars denote standard errors; n = 4 replicates.

V. Statistics calculated using one-way ANOVA followed by Bonferroni multiple comparison post-tests for SOX-9 gene expression by pericyte cells cultured up to 5 weeks in different substrates.

Statistically significant comparisons are denoted with an asterix where the calculated p value is < 0.05, *; <0.01, ** and < 0.001 ***.

SOX-9: 1 hr in culture					
	Plain	ALG-	ALG+	F_2/S-	F_2/S+
Plain	-				
ALG-		-			
ALG+			-		
F_2/S-				-	
F_2/S+					-

SOX-9: 24 hr in culture					
	Plain	ALG-	ALG+	F_2/S-	F_2/S+
Plain	-				
ALG-		-			
ALG+			-		
F_2/S-				-	
F_2/S+					-

SOX-9: 72 hr in culture					
	Plain	ALG-	ALG+	F_2/S-	F_2/S+
Plain	-				***
ALG-		-			***
ALG+			-	***	
F_2/S-			***	-	***
F_2/S+	***			***	-

SOX-9: 168 hr in culture					
	Plain	ALG-	ALG+	F_2/S-	F_2/S+
Plain	-				
ALG-		-			
ALG+			-		
F_2/S-				-	
F_2/S+					-

SOX-9: 336 hr in culture					
	Plain	ALG-	ALG+	F_2/S-	F_2/S+
Plain	-				**
ALG-		-			*
ALG+			-		
F_2/S-				-	*
F_2/S+	**	*		*	-

SOX-9: 672 hr in culture					
	Plain	ALG-	ALG+	F_2/S-	F_2/S+
Plain	-				**
ALG-		-			**
ALG+			-		**
F_2/S-				-	**
F_2/S+	**	**	**	**	-

SOX-9: 840 hr in culture					
	Plain	ALG-	ALG+	F_2/S-	F_2/S+
Plain	-				*
ALG-		-			
ALG+			-	*	*
F_2/S-			*	-	
F_2/S+	*		*		-

VI. Statistics calculated using one-way ANOVA followed by Bonferroni multiple comparison post-tests for type II collagen (COL2A1) gene expression by pericyte cells cultured up to 5 weeks in different substrates.

Statistically significant comparisons are denoted with an asterix where the calculated p value is < 0.05, *; <0.01, ** and < 0.001 ***.

COL2A1: 1 hr in culture					
	Plain	ALG-	ALG+	F_2/S-	F_2/S+
Plain	-				
ALG-		-			
ALG+			-		
F_2/S-				-	
F_2/S+					-

COL2A1: 24 hr in culture					
	Plain	ALG-	ALG+	F_2/S-	F_2/S+
Plain	-			*	
ALG-		-		*	
ALG+			-	*	
F_2/S-	*	*	*	-	
F_2/S+					-

COL2A1: 72 hr in culture					
	Plain	ALG-	ALG+	F_2/S-	F_2/S+
Plain	-				
ALG-		-			
ALG+			-		
F_2/S-				-	
F_2/S+					-

COL2A1: 168 hr in culture					
	Plain	ALG-	ALG+	F_2/S-	F_2/S+
Plain	-				**
ALG-		-			**
ALG+			-		**
F_2/S-				-	*
F_2/S+	**	**	**	*	-

COL2A1: 336 hr in culture					
	Plain	ALG-	ALG+	F_2/S-	F_2/S+
Plain	-				*
ALG-		-			
ALG+			-		
F_2/S-				-	
F_2/S+	*				-

COL2A1: 672 hr in culture					
	Plain	ALG-	ALG+	F_2/S-	F_2/S+
Plain	-				***
ALG-		-			***
ALG+			-		***
F_2/S-				-	***
F_2/S+	***	***	***	***	-

COL2A1: 840 hr in culture					
	Plain	ALG-	ALG+	F_2/S-	F_2/S+
Plain	-			*	***
ALG-		-		*	***
ALG+			-	*	***
F_2/S-	*	*	*	-	***
F_2/S+	***	***	***	***	-

VII. Statistics calculated using one-way ANOVA followed by Bonferroni multiple comparison post-tests for aggrecan (ACAN) gene expression by pericyte cells cultured up to 5 weeks in different substrates.

Statistically significant comparisons are denoted with an asterix where the calculated p value is < 0.05, *; <0.01, ** and < 0.001 ***.

Aggrecan: 1 hr in culture					
	Plain	ALG-	ALG+	F_2/S-	F_2/S+
Plain	-				
ALG-		-			
ALG+			-		
F_2/S-				-	
F_2/S+					-

Aggrecan: 24 hr in culture					
	Plain	ALG-	ALG+	F_2/S-	F_2/S+
Plain	-			*	
ALG-		-		*	
ALG+			-	*	
F_2/S-	*	*	*	-	
F_2/S+					-

Aggrecan: 72 hr in culture					
	Plain	ALG-	ALG+	F_2/S-	F_2/S+
Plain	-			**	**
ALG-		-		*	**
ALG+			-	**	**
F_2/S-	**	*	**	-	
F_2/S+	**	**	**		-

Aggrecan: 168 hr in culture					
	Plain	ALG-	ALG+	F_2/S-	F_2/S+
Plain	-			*	*
ALG-		-		*	*
ALG+			-	**	*
F_2/S-	*	*	**	-	
F_2/S+	*	*	*		-

Aggrecan: 336 hr in culture					
	Plain	ALG-	ALG+	F_2/S-	F_2/S+
Plain	-				
ALG-		-			
ALG+			-		
F_2/S-				-	
F_2/S+					-

Aggrecan: 672 hr in culture					
	Plain	ALG-	ALG+	F_2/S-	F_2/S+
Plain	-				
ALG-		-			
ALG+			-		
F_2/S-				-	
F_2/S+					-

Aggrecan: 840 hr in culture					
	Plain	ALG-	ALG+	F_2/S-	F_2/S+
Plain	-				
ALG-		-			
ALG+			-		
F_2/S-				-	
F_2/S+					-

VIII. Statistics calculated using one-way ANOVA followed by Bonferroni multiple comparison post-tests for type X collagen (COL10A1) gene expression by pericyte cells cultured up to 5 weeks in different substrates.

Statistically significant comparisons are denoted with an asterix where the calculated p value is < 0.05, *; <0.01, ** and < 0.001 ***.

COL10A1: 1 hr in culture					
	Plain	ALG-	ALG+	F_2/S-	F_2/S+
Plain	-				
ALG-		-			
ALG+			-		
F_2/S-				-	
F_2/S+					-

COL10A1: 24 hr in culture					
	Plain	ALG-	ALG+	F_2/S-	F_2/S+
Plain	-			*	
ALG-		-		*	
ALG+			-	*	
F_2/S-	*	*	*	-	
F_2/S+					-

COL10A1: 72 hr in culture					
	Plain	ALG-	ALG+	F_2/S-	F_2/S+
Plain	-				***
ALG-		-			**
ALG+			-		***
F_2/S-				-	**
F_2/S+	***	**	***	**	-

COL10A1: 168 hr in culture					
	Plain	ALG-	ALG+	F_2/S-	F_2/S+
Plain	-				***
ALG-		-			***
ALG+			-	*	***
F_2/S-			*	-	**
F_2/S+	***	***	***	**	-

COL10A1: 336 hr in culture					
	Plain	ALG-	ALG+	F_2/S-	F_2/S+
Plain	-				***
ALG-		-			
ALG+			-		***
F_2/S-				-	***
F_2/S+	***		***	***	-

COL10A1: 672 hr in culture					
	Plain	ALG-	ALG+	F_2/S-	F_2/S+
Plain	-				*
ALG-		-			*
ALG+			-		*
F_2/S-				-	*
F_2/S+	*	*	*	*	-

COL10A1: 840 hr in culture					
	Plain	ALG-	ALG+	F_2/S-	F_2/S+
Plain	-				
ALG-		-			
ALG+			-		
F_2/S-				-	
F_2/S+					-

IX. Statistics calculated using one-way ANOVA followed by Bonferroni multiple comparison post-tests for measured protein abundances in pericytes cultured on plain substrates, 20 kPa F_2/S and alginate hydrogels with and without chondrogenic induction media.

Statistically significant comparisons are denoted with an asterix where the calculated p value is < 0.05, *; <0.01, ** and < 0.001 ***.

1 hr in culture					
	Plain	ALG-	ALG+	F_2/S-	F_2/S+
Plain	-				
ALG-		-			
ALG+			-		
F_2/S-				-	
F_2/S+					-

24 hr in culture					
	Plain	ALG-	ALG+	F_2/S-	F_2/S+
Plain	-				
ALG-		-			
ALG+			-		
F_2/S-				-	
F_2/S+					-

72 hr in culture					
	Plain	ALG-	ALG+	F_2/S-	F_2/S+
Plain	-			***	***
ALG-		-		***	***
ALG+			-	***	***
F_2/S-	***	***	***	-	
F_2/S+	***	***	***		-

168 hr in culture					
	Plain	ALG-	ALG+	F_2/S-	F_2/S+
Plain	-	***	***	***	***
ALG-	***	-			
ALG+	***		-		
F_2/S-	***			-	
F_2/S+	***				-

336 hr in culture					
	Plain	ALG-	ALG+	F_2/S-	F_2/S+
Plain	-	***	***	***	***
ALG-	***	-		*	***
ALG+	***		-	*	**
F_2/S-	***	*	*	-	**
F_2/S+	***	***	**	**	-

672 hr in culture					
	Plain	ALG-	ALG+	F_2/S-	F_2/S+
Plain	-	***	***	***	***
ALG-	***	-			**
ALG+	***		-		**
F_2/S-	***			-	
F_2/S+	***	**	**		-

840 hr in culture					
	Plain	ALG-	ALG+	F_2/S-	F_2/S+
Plain	-	***	***	***	***
ALG-	***	-			**
ALG+	***		-		
F_2/S-	***			-	
F_2/S+	***	**			-

X. Assessing neurogenesis of MSCs

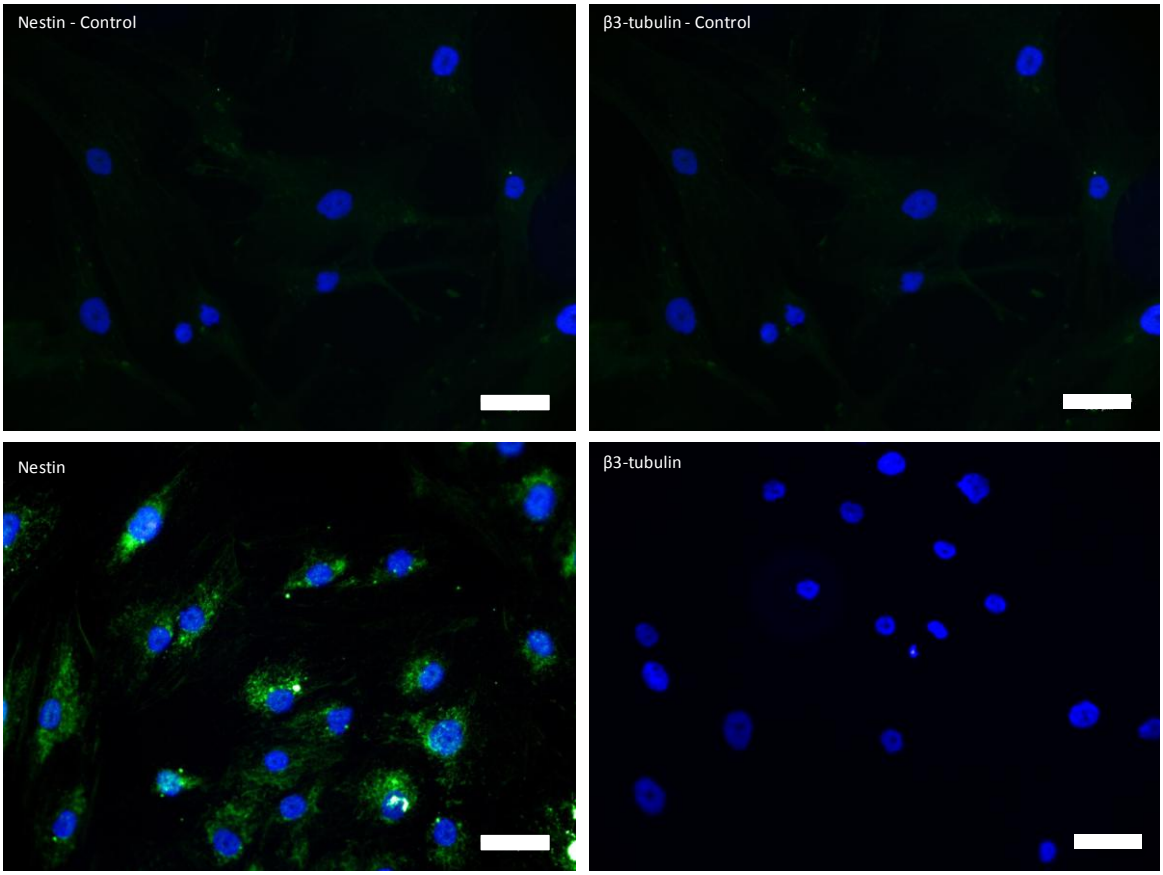

MSCs were cultured on glass cover slips for 7 and 21 days in the absence (top row) and presence (bottom row) of 60 µM retinoic acid to induce neurogenesis (Yim et al., 2007). Cells were subsequently stained for the early biomarker nestin at 7 days and β3-tubulin at 21 days. Cells stained positively for nestin indicating initial stage neurogenesis, but were negative for the latterly expressed β3-tubulin showing that development of MSCs did not progress to formation of mature neuronal cells. Cell nuclei are shown in blue and biomarkers nestin or β3-tubulin in green; scale bar 100 µm.